Method for Remaining Useful Life Prediction of a Light Aircraft Landing Gear Structure

Gerhardinger, David

University of Zagreb

FACULTY OF TRANSPORT AND TRAFFIC SCIENCES

David Gerhardinger

METHOD FOR REMAINING USEFUL LIFE PREDICTION OF A LIGHT AIRCRAFT LANDING GEAR STRUCTURE

DOCTORAL THESIS

Zagreb, 2023

Sveučilište u Zagrebu

FAKULTET PROMETNIH ZNANOSTI

David Gerhardinger

METODA ZA PREDVIĐANJE PREOSTALOGA KORISNOGA ŽIVOTNOGA VIJEKA KONSTRUKCIJE PODVOZJA LAKOGA ZRAKOPLOVA

DOKTORSKI RAD

Zagreb, 2023.

University of Zagreb

FACULTY OF TRANSPORT AND TRAFFIC SCIENCES

David Gerhardinger

METHOD FOR REMAINING USEFUL LIFE PREDICTION OF A LIGHT AIRCRAFT LANDING GEAR STRUCTURE

DOCTORAL DISSERTATION

Supervisors: Anita Domitrović and Darko Ivančević

Zagreb, 2023

Sveučilište u Zagrebu

FAKULTET PROMETNIH ZNANOSTI

David Gerhardinger

METODA ZA PREDVIĐANJE PREOSTALOGA KORISNOGA ŽIVOTNOGA VIJEKA KONSTRUKCIJE PODVOZJA LAKOGA ZRAKOPLOVA

DOKTORSKI RAD

Mentori: Anita Domitrović i Darko Ivančević

Zagreb, 2023.

SUPERVISORS:

Assoc. Prof. Anita Domitrović, PhD

Assoc. Prof. Darko Ivančević, PhD

MENTORI:

Izv. prof. dr. sc. Anita Domitrović

Izv. prof. dr. sc. Darko Ivančević

Biography of the supervisors

Associate Professor Anita Domitrović, PhD, is the Head of the Chair of Aeronautical Engineering at the Department of Aeronautics, Faculty of Traffic Sciences, University of Zagreb, Croatia. She teaches several courses at the undergraduate, graduate, and doctoral levels at the Faculty of Traffic Sciences, University of Zagreb. Her main interests in teaching and scientific work are aircraft propulsion systems and aircraft maintenance. She has worked as a team member and researcher on several scientific projects. As an author or co-author, she has published a number of scientific papers on topics related to aircraft maintenance and aircraft propulsion systems. Additionally, she is involved in quality assurance systems in the training of aviation personnel and in higher education.

Associate Professor Darko Ivančević, PhD, is the Head of the Chair of Aircraft Structures at the Department of Aeronautical Engineering, Faculty of Mechanical Engineering and Naval Architecture, University of Zagreb. His research activities are related to numerical modelling of composite structures, micromechanics and damage modelling in composite structures. As co-author, he has published 42 scientific papers, of which 12 are in CC journals, and the rest are published in the proceedings of international and national conferences. He participates in teaching activities at a group of courses related to aircraft structures and mechanics of composite materials in the undergraduate and graduate studies at the Faculty of Mechanical Engineering and Naval Architecture. Additionally, he is involved in teaching at the undergraduate study Military Engineering of the University of Zagreb.

I. Acknowledgment

First and foremost, I would like to express my profound gratitude to my mentors for their exceptional support and their work ethic throughout my time as a research and teaching assistant, and during the writing of this PhD Thesis. Their unwavering commitment to academic excellence and tireless dedication to fostering an environment of intellectual curiosity for our undergraduate and graduate students, as well as myself, has been a beacon of inspiration. I am deeply appreciative of their invaluable insights, patience, and encouragement.

I would like to express my gratitude to my dear friends and colleagues. Their friendship, lively debates, and thoughtful insights have truly added a richness to this journey. One of the most memorable moments was when they joined me in celebration of the birth of my daughter, a moment I will hold dear forever. Their support in my research pursuits has been invaluable, motivating me to devote time and energy to push the boundaries of this Thesis. The progress I've made is a testament to their encouragement and faith in me.

I am immensely grateful to my family for their steadfast and unwavering support. Their constant encouragement, understanding, and unconditional love, even at the most challenging of times, have been my source of strength. This Thesis would never have seen the light of day without their belief in my potential and their faith in my pursuits.

To my dear wife, words alone cannot express the gratitude I feel. Your belief in me, your unwavering support, and your love have been my anchor. The comforting words and patience during moments of hardship have been the bedrock of this journey. Your love has been my strength and motivation, and for that, I am forever grateful.

Finally, I dedicate this work to our children, Jan and Julia. The joy and love you bring to our lives is the most potent and precious motivation for everything I do. You are my greatest inspiration, and my love for you is the driving force behind all my endeavours. I hope that this Thesis serves as a testament to the power of dedication, perseverance, and love, that may inspire you as you forge your paths in life.

II. Abstract

This Doctoral Thesis focused on developing a method for predicting the remaining useful life (*RUL*) of the landing gear structure of light aircraft based on different operational conditions. The research was based on the hypothesis that the *RUL* of a light aircraft's landing gear structure can be determined from aircraft operation records. Current methods for predicting *RUL* are not commonly applied in the light aircraft maintenance system, with operators mainly relying on experience-based methods and the manufacturer's recommendations, without considering the conditions of the actual aircraft operation. This Thesis consists of seven Chapters. The first Chapter is introductory, stating the research motivation and aims. The research method, hypothesis, scientific contributions, and Thesis structure are presented in this Chapter. The second Chapter involves a thorough review and analysis of literature related to aircraft maintenance concepts. A state-of-the-art introduction to prognostics and health management is given, explaining in detail two main prognostic approaches, the data driven, and physics based prognostic approach. Prognostic and health management applications in aeronautics and related problems are explained. The specifics of prognostics and health management implementation in light aircraft maintenance are discussed. In the third Chapter, the division of general aviation aircraft according to applicable regulations is explained. The specifics of nationally regulated aircraft regulations, maintenance and mandatory records are stated. Light aircraft accident literature is explored to identify main reasons for part failure. The problem with implementing prognostics and health management in light aircraft maintenance is discussed. Prognostic and health management relevant information in mandatory operation records is exposed. The specifics of data acquisition for prognostics and health management of light aircraft structural parts are highlighted, and data acquisition with prognostic and health management implementation steps relevant to the developed method is explained. The fourth Chapter of this Thesis focuses on fundamental concepts in metal fatigue for computational modelling, specifically in the context of aeronautical applications. The Chapter explores various fatigue analysis types, including loading types, mean stress effects, multiaxial stress correction, and fatigue modifications. The fifth Chapter presents the development of a method for predicting *RUL* of aircraft structural parts. The method involves multiple phases, including selecting the observed part, creating a detailed model, developing fatigue-relevant load models, validating the fatigue analysis software, and implementing an expert system approach. The

validation process compares results obtained from literature and software fatigue analysis. It also includes the development of an expert system architecture for information input and result processing. The sixth Chapter presents the numerical strength analysis results obtained in this study. The analysis was conducted to assess the structural strength and performance of the examined structural part. Results are analysed using statistical methods, including correlation, regression, and sensitivity analysis. The impact of the analysis results on maintenance and operational safety was examined. Prediction uncertainty sources were discussed, recognizing the inherent challenges and limitations in predicting light aircraft structural part remaining useful life. The seventh and last Chapter summarizes research findings. Thesis scientific and applicative contributions are stated. Implications for enhancing the current standard of light aircraft landing gear structure parts are highlighted. The research findings have contributed to the understanding of landing gear structural behaviour and performance in relation to material fatigue relevant load variability. Overall, this research offers valuable insights and potential improvements for light aircraft landing gear maintenance while setting the stage for future research in the field.

The implementation of this predictive method could significantly enhance the safety of light aircraft operations by changing the maintenance approach from reactive to proactive.

Keywords: Prognostic and Health Management, Remaining Useful Life, light aircraft, landing gear structure, operational records, light aircraft maintenance

III. Prošireni sažetak

Ovaj doktorski rad opisuje razvoj metode za predviđanje preostalog korisnog životnog vijeka dijela konstrukcije podvozja lakih zrakoplova. Izrađena metoda je primjenjiva na raznim dijelovima konstrukcije, pod uvjetom da se uzmu u obzir specifični podaci koji se odnose na opterećenje, mehanička svojstva i geometriju promatranog dijela.

Uvod i kontekst: Značaj održavanja zrakoplova u svrhu povećanja sigurnosti i pouzdanosti zrakoplovnih operacija je neporeciv. U suvremenim pristupima održavanju, posebice kod velikih zrakoplova, koriste se sofisticirane metode koje uključuju predviđanje i upravljanje stanjem zrakoplova (izvorni naziv: Prognostics and Health Management, skraćeno: PHM). Ove metode omogućuju predviđanje preostalog korisnog životnog vijeka (izvorni naziv: Remaining Useful life, skraćeno: *RUL*) zrakoplovnih dijelova, što je ključno za preventivno održavanje i povećanje sigurnosti operacija zrakoplova. Unatoč napretku u razvoju PHM metoda za velike zrakoplove, postoji nedostatak metoda i njihove primjene kod lakih zrakoplova. Primjena postojećih PHM metoda za prognozu *RUL*-a dijelova konstrukcije lakih zrakoplova otežana je zbog nedostatka potrebnih informacija. Primjerice, Gouriveau et al. [1] navode da moderni veliki komercijalni zrakoplovi imaju oko 300.000 senzora, generirajući pregršt informacija od kojih se neke mogu koristiti za prognozu *RUL*-a. Međutim, laki zrakoplovi nemaju niti približnu količinu senzora, što otežava primjenu postojećih PHM metoda. To zahtijeva razvoj alternativnih pristupa koji mogu adekvatno predviđati *RUL* dijelova, primjerice uporabom zapisa iz zrakoplovnih operacija, što je glavni fokus ove disertacije. Uobičajena praksa održavanja lakih zrakoplova uključuje preventivnu zamjenu dijelova na temelju fiksnih vremenskih intervala. Ovaj pristup ne uzima u obzir varijabilnost operativnih uvjeta kojima su svi zrakoplovi izloženi, što može dovesti do prerane zamjene dijelova, ili u najgorem slučaju, do otkaza, sukladno osobnom iskustvu autora ove disertacije, [2]. Ova je disertacija stoga usmjerena na razvoj metode za predviđanje *RUL*-a, s obzirom na postojeće informacije o stvarnim operativnim uvjetima, sa svrhom povećanja sigurnosti operacija i efikasnosti održavanja lakih zrakoplova.

Problem i motivacija: Ključni problem istaknut u ovoj disertaciji tiče se izazova u predviđanju preostalog korisnog životnog vijeka konstrukcije podvozja lakih zrakoplova. Iako su metode predviđanja *RUL*-a uspostavljene u komercijalnom i vojnom zrakoplovstvu, laki zrakoplovi su zanemareni zbog svoje jedinstvene prirode korištenja i održavanja. Konkretno, nedostatak ugrađenih senzora u ovim zrakoplovima onemogućava primjenu standardnih PHM

metoda koje se oslanjaju na kontinuirano praćenje stanja. Osim toga, održavanje lakih zrakoplova, u određenim okolnostima, može se provesti od osobe koja je istovremeno vlasnik i pilot zrakoplova, bez nužnog iskustva i školovanja potrebnog osobi koja provodi održavanje velikih zrakoplova komercijalne namjene. Nedostatak metoda i njihove primjene u predviđanju *RUL*-a dijelova konstrukcija lakih zrakoplova stvara potencijalne sigurnosne rizike, kao i neefikasnost u održavanju, s obzirom na to da se odluke temelje na generaliziranim intervalima zamjene, a ne na stvarnom stanju dijelova. Održavanje zrakoplova prilagođeno stvarnom stanju zrakoplovnih dijelova može dovesti do smanjenja nepotrebnih zamjena, povećanja raspoloživosti zrakoplova i, što je najvažnije, do sprječavanja otkaza tijekom operacija.

Ciljevi istraživanja i hipoteze: Primarni cilj istraživanja opisanog u ovoj disertaciji je razviti metodu za predviđanje *RUL*-a dijelova konstrukcije podvozja lakih zrakoplova. To uključuje definiranje parametara koji opisuju zrakoplovne operacije i utječu na predviđanje *RUL*-a. Osim toga, cilj je razviti metodu koja će biti primjenjiva u nedostatku senzorskih podataka, čime se prevladavaju ograničenja u primjeni PHM-a nametnuta specifičnošću lakih zrakoplova. Hipoteza istraživanja temelji se na pretpostavci da se koristeći uobičajene i obavezne operativne zapise zrakoplova može predvidjeti *RUL* konstrukcijskih dijelova lakih zrakoplova, konkretno podvozja. Hipoteza proizlazi iz zapažanja da postojeći podaci o operacijama lakih zrakoplova sadrže informacije koje se mogu primijeniti u procjeni *RUL*-a dijelova konstrukcije podvozja lakih zrakoplova.

Pregled literature: Proučavanje prethodno objavljenih radova u području PHM-a, konkretno prognoziranja *RUL*-a dijelova konstrukcije lakih zrakoplova otkrilo je nedostatak metoda prilagođenih specifičnostima lakih zrakoplova, poptu nedostatka senzora. Gotovo sve postojeće metode fokusirane su na komercijalne i vojne zrakoplove, koji nude pregršt senzorskih informacija koje je moguće koristiti u prognozi stanja dijelova konstrukcije. Međutim, laki zrakoplovi usporedno nude vrlo ograničene podatke. Temeljni mehanizam starenja dijelova konstrukcije zrakoplova koji je identificiran tijekom istraživanja opisanog u ovoj disertaciji je zamor materijala i posljedična akumulacija oštećenja. Metoda razvijena u ovom radu oslanja se na pristup određivanja *RUL*-a koristeći uobičajene zapise iz operacija zrakoplova. Razvijena metoda integrira informacije iz obaveznih operativnih zapisa sa izračunom akumuliranog oštećenja u promatranom dijelu koonstrukcije zbog zamora materijala.

Metodološki pristup: Pristup izračunu ukupnog *RUL*-a promatranog dijela konstrukcije u ovom radu se temelji na integraciji operativnih podataka letenja i podataka održavanja lakog zrakoplova, s rezultatima *RUL*-ova izračunatih numeričkim proračunom čvrstoće za specifične operativne uvjete. Metoda uključuje identifikaciju i kvantifikaciju opterećenja koja utječu na zamor materijala tijekom dozvoljenih operacija lakog zrakoplova, koristeći prilagođene procedure za izračun te računalni model promatranog dijela za simulaciju i analizu utjecaja zamora materijala na *RUL* dijela konstrukcije podvozja. Ovaj pristup je inovativan zbog primjene vrlo ograničenih informacija iz operacija lakog zrakoplova u prognozi ukupnog *RUL*-a promatranog dijela konstrukcije. Za razvoj metode, korištena su saznanja iz područja zamora materijala, numeričkog proračuna čvrstoće metodom konačnih elemenata i analitički modeli za izračun akumuliranog oštećenja pod cikličkim opterećenjem. Metoda konačnih elemenata (FEM) upotrijebljena je uz pomoć računalnog programa u izračunu deformacija i naprezanja u promatranom dijelu konstrukcije podvozja lakog zrakoplova. Svrha primjene metode bila je utvrditi akumulirano oštećenje koje je posljedica zamora materijala. Analiza zamora materijala provedena je također u računalnom programu, s ciljem izračuna *RUL*-a promatranog dijela konstrukcije temeljem primjene analitičkog modela za izračun akumuliranog oštećenja na rezultate analize zamora. Ključna metodološka inovacija prikazana u ovoj disertaciji je ekspertni sustav koji integrira operativne podatke s rezultatima simulacije kako bi se izračunao ukupni *RUL* promatranog dijela konstrukcije. Ekspertni sustav omogućava predviđanje *RUL*-a bez potrebe za dodatnim izvorima informacija, poput senzorskih sustava.

Izvori informacija i prikupljanje podataka: Izvore podataka korištenih u ovome radu moguće je podijeliti u tri kategorije. Prva kategorija su podaci čija je svrha bila izračun specifičnih *RUL*-ova koje bi promatrani dio imao da je bio izložen isključivo jednoj vrsti operacija. Zatim podaci koji su korišteni za validaciju vrijednosti korištenih u izračunu spomenutih *RUL*-ova. I zaključno, treća kategorija su podaci korišteni za izračun ukupnog *RUL*-a kojega bi promatrani dio imao da je bio izložen stvarnim (zabilježenim) operativnim uvjetima. Prva kategorija sastoji se od podataka iz uputstava za korištenje zrakoplova [3], podataka iz mjerenja koja su obavljena na promatranom zrakoplovu, [4] i podataka koji su nužni za analizu degradacije promatranog dijela konstrukcije, ([5], [6], [7], [8], [9], [10], [11], [12]). Druga kategorija podataka su podaci iz uputstava za održavanje zrakoplova [13], istraživanja u kojemu je provedeno ispitivanje zamora materijala [14] i istraživanja koja uključuju mjerenja koja su obavljena na velikom broju operacija zrakoplovima istoga tipa, [15]. Treća kategorija

su podaci iz operacija promatranog zrakoplova koji se prikupljaju prema predlošku za izračun mase i težišta u uputstvima za korištenje zrakoplova, [3].

Analiza i razvoj modela i metodologije: Metoda prikazana u ovoj disertaciji integrira dostupne podatke zabilježene tijekom operacija promatranog zrakoplova sa ekspertnim znanjem koje predstavlja specifične *RUL*-ove koje bi promatrani dio imao kada bi bio izložen isključivo opterećenju koje je karakteristično za specifičnu vrstu operacije. Prvi korak u razvoju i primjeni metode bio je identificirati dio konstrukcije podvozja lakog zrakoplova koji je podložan oštećenju uslijed uobičajenih operacija i ključan za normalan rad podvozja. U prilog odabiru išla je činjenica da je za promatrani dio proizviđač propisao najstroži režim održavanja u uputstvima za održavanje zrakoplova. Dio prvoga koraka bio je i određivanje glavnog degradacijskog mehanizma *RUL*-a za promatrani dio. Degradacijski mehanizam podvozja određen je temeljem pretražene literature koja identificira glavni degradacijski mehanizam na podvozjima istog ili sličnog tipa, [16], [17], [18], [19], [20] i [21]. Drugi korak bio je priprema za analizu degradacije promatranog dijela. Priprema je uključila pretragu i analizu literature koja prikazuje metodologiju pri izračunu degradacije dijela konstrukcije, [22], [23], [24], [25], [26], [27], [28], [29], [30], [31], [32], [33], [34], [35] i [36]. Također, prikupljeni su i podaci iz literature koja definira svojstva materijala, potrebna za analizu degradacije promatranog dijela ([5], [6], [7], [8], [9], [10], [11], [12]). Dio drugog koraka bila je i identifikacija raznih faza operacija lakog zrakoplova, sa svrhom utvrđivanja i kvantificiranja veličina koje utječu na degradaciju promatranog dijela, [3] i [13]. U ovome koraku uspostavljena je veza između raznih operacija lakog zrakoplova i posljedičnog opterećenja relevantnog za degradaciju promatranog dijela. Treći korak bio je izrada računalnog modela za numerički proračun čvrstoće sa svrhom izračuna inkrementa degradacije koji se akumulira na promatranom dijelu tijekom dozvoljenih operacija. Promatrani dio modeliran je temeljem geometrijskih značajki koje su izmjerene na zrakoplovu koji je uzet kao primjer za implementaciju metode. Dio trećeg koraka bio je i validacija numeričkog proračuna čvrstoće sa svrhom utvrđivanja vjerodostojnosti rezultata, [14]. Validacija je obavljena prema proceduri koja se u odgovarajućim okolnotima ubičajeno primjenjuje, [37]. U četvrtom koraku izrađen je ekspertni sustav. Svrha ekspertnog sustava bila je povezati ekspertno znanje u obliku *RUL*-ova koje bi promatrani dio imao da je bio izložen isključivo jednoj vrsti operacija i informacija iz uobičajenih zapisa o tim operacijama. Ishod primjene ekspertnog sustava je ukupni *RUL* promatranog dijela obzirom na dostupne informacije iz operacija zrakoplova. Ekspertni sustav se sastoji od četiri modula: Prvi modul

prikuplja znanje iz zabilješki o operacijama promatranog zrakoplova; Drugi modul pohranjuje znanje eksperta u vidu specifičnih *RUL*-ova koje bi promatrani dio imao da je bio izložen isključivo jednoj vrsti operacija; Treći modul je inferencijski, služi izračunu ukupnog *RUL*-a temeljem modificranog pravila za linearnu akumulaciju oštećenja; Posljednji, četvrti modul služi prezentaciji rezultata u obliku ukupnog *RUL*-a i povezivanju toga rezultata s informacijama o održavanju promatranog dijela konstrukcije.

U konačnici, rezultati primjenjene metode validirani su usporedbom s rezultatima drugih metoda.

Faze istraživanja i sažeci poglavlja: Prvo poglavlje sažima motivaciju i cilj istraživanja, način i svrhu pregleda literature, metodologiju istraživanja, cilj i hipotezu, očekivane znanstvene doprinose i pregled strukture ove disertacije. Drugo poglavlje bavi se analizom literature iz održavanja zrakoplova i PHM metoda s posebnim naglaskom na predviđanje *RUL*-a konstrukcija podvozja lakih zrakoplova. Poglavlje započinje prikazom temeljnih strategija održavanja zrakoplova. Slijedi prikaz primjena PHM-a u održavanju zrakoplova. Zatim su identificirani problemi u primjeni PHM metoda u održavanju lakih zrakoplova. Za kraj poglavlja razmatrale su se različite metode i rezultati primjenjene u predviđanju *RUL*-a konstrukcija podvozja. Treće poglavlje Bavi se primjenom zapisa iz operacija lakih zrakoplova u prognozi *RUL*-a. U svrhu identifikacije operacijskih zapisa analizirana je regulatorna podjela civilnih zrakoplova. Nakon toga je predstavljen značaj održavanja za lake zrakoplove i problem impelmentacije PHM metoda u njihovu održavanju. Zaključno, treće poglavlje prikazuje potencijalne izvore informaicja s podacima koji su relevantni za prognozu *RUL*-a te prikazuje korake koje je potrebno poduzeti u primjeni tih podataka u PHM metodi koju je moguće implementirati u održavanje lakog zrakoplova. Četvrto pogavlje prikazuje osnovne koncepte zamora metala koji su relevantni za istraživanje opisano u ovoj disertaciji. Pogavlje započinje detaljnim opisom različitih vrsta analize zamora, nakon čega slijedi pregled vrsta opterećenja u analizi zamora materijala. Poglavlje zatim prikazuje utjecaj usrednjenog naprezanja i važnost korekcija višeosnog naprezanja u analizi zamora. Naposljetku, poglavje raspravlja o modifikacijama zamora, sa svrhom premošćivanja jaza između teorijskih predviđanja i stvarnih događaja koji su posljedica zamora materijala. U petom poglavlju dan je prikaz razvoja metode koja je predmet ovog doktroksog istraživanja. Metoda je primjenjena na dijelu konstrukcije podvozja lakog zrakoplova. Za promatrani dio ustanovljeno je da je zamor materijala dominantan mehanizam degradacije u dozvoljenim operativnim uvjetima. Poglavlje je

razrađeno kroz primjenu metode koja započinje odabirom promatranog dijela konstrukcije, za primjer je uzeta noga glavnog podvozja aviona Cessna 172R. Slijedi uspostavljanje preduvjeta za analizu zamora materijala. Preduvjeti uključuju stvaranje računalnog modela geometrije, pripadajućih svojstava materija i opterećenja koji su nužni za računalnu analizu degradacije promatranog dijela. Opisan je proces modeliranja geometrije, svojstava materijala i identifikacija faza operacija koje za posljedicu imaju različita opterećenja koja su relevantna za degradaciju promatranog dijela. Degradacija dijela analizirana je numeričkim proračunom čvrstoće u računalnom programu, a valjanost proračuna potvrđena je repliciranjem rezultata stvarnih ispitivanja iz literature. Dan je detaljan opis provedene analize zamora za izračun specifičnih *RUL*-ova za različite uvjete opterećenja koji su posljedica dozvoljenih operacija s promatranim zrakoplovom. Nadalje, prikazan je razvoj ekspertnog sustava kroz četiri modula s detaljnim opisom uloga u prognoziranju ukupnog *RUL*-a promatranog dijela. Zaključno, u petom je pogavlju prikazan i postupak za izračun ukupnih *RUL*-ova na primjeru noge glavnog podvozja Cessna 172R u dozvoljenim operacijama. Šesto poglavlje prikazuje rezultate izračuna ukupnih *RUL*-ova dobivenih u petom poglavlju. Šesto pogavlje također prikazuje i komentira statističke analize provedene nad rezultatima i to u vidu korelacijske i regresijske analize te analize senzitivnosti. Svrha analiza bila je utvrđivanje izvora prognostičke nesigurnosti i ostvarenje podloge za diskusiju o značaju i implikacijama ustanovljenih parametara sa utjecajem na *RUL* promatranog dijela. U zaključku disertacije sumirani su glavni doprinosi istraživanja u teorijskom i praktičnom smislu, kao i preporuke te ograničenja koja mogu biti predmet budućih istraživanja u području primjene PHM-a u održavanju lakih zrakoplova.

Rezultati i analiza: Rezultati istraživanja pokazuju da je moguće prognozirati preostali korisni životni vijek (*RUL*) konstrukcije podvozja lakih zrakoplova koristeći podatke koji se obavezno bilježe tijekom operacija. Metoda prikazana u ovoj disertaciji omogućava kvantifikaciju i analizu akumulacije oštećenja uzrokovanih zamorom materijala, u svojstvu ključnog mehanizma degradacije konstrukcijskih dijelova izloženih dozvoljenim operativnim uvjetima. Identificirane su operativne faze lakog zrakoplova koje imaju utjecaj na *RUL* konstrukcije podvozja lakog zrakoplova, uključujući fazu polijetanja, slijetanja i vožnje po tlu. Metoda razvijena u ovom istraživanju može biti temelj za novi pristup održavanja konstrukcijskih dijelova lakih zrakoplova, s obzirom na stvarno stanje promatranog dijela, umjesto na unaprijed utvrđenom intervalu zamjene koji zanemaruje operativne uvjete. Pored toga, ovo istraživanje je pokazalo da je identifikacijom mehanizma degradacije konstrukcijskog

dijela moguće ustanoviti ključne parametre koji utječu na *RUL*, što pruža mogućnost za prilagodbu održavanja specifičnim operativnim uvjetima zrakoplova. Primjena ove metode mogla bi unaprijediti održavanje lakih zrakoplova promjenom paradigme održavanja s reaktivnog u proaktivni pristup, što očekivano ima pozitivne učinke na sigurnost operacija lakih zrakoplova. Predlaže se nastavak istraživanja usmjeren na smanjenje utjecaja identificiranih izvora prognostičke nesigurnosti te proširenje metode na druge dijelove konstrukcije zrakoplova i druge zrakoplove.

Zaključci i smjernice za buduća istraživanja: Metoda prikazana u ovoj disertaciji oslanja se na analizu operativnih podataka bez potrebe za dodatnim prikupljanjem podataka iz izvora poput senzora. Osobito jer senzori kod lakih zrakoplova nisu implementiranih u istoj mjeri kao kod velikih zrakoplova. Prikazano istraživanje dokazuje da se s informacijama koje se uobičajeno bilježe tijekom operacija lakog zrakoplova može prognozirati *RUL* dijela konstrukcije podvozja toga zrakoplova. Korištenje rezultata primjenjene metode omogućava operaterima lakih zrakoplova palniranje održavanja i zamjenu dijelova koji zavise o stvarnom stanju dijelova, umjesto o unaprijed određenom intervalu zamjene. Time se povećava sigurnost operacija lakih zrakoplova, u slučaju da je dio bio izložen uvjetima koji uzrokuju kraći *RUL* dijela, ili povećanje ekonomičnosti održavanja, u slučaju da je dio bio izložen operacijskim uvjetima s povoljnijim učinkom na *RUL* promatranog dijela. Za buduća istraživanja predlaže se: Validacija metode kroz usporedbu s ishodima stvarnih operacija; Proširenje metode s ciljem smanjenja utjecaja prognostičkih nesigurnosti na *RUL*; Primjena metode na drugim dijelovima konstrukcije lakog zrakoplova; Primjena metode na konstrukcijske dijelove drugih tipova zrakoplova.

Izvorni doprinosi: Ova disertacija predstavlja nekoliko izvornih znanstvenih doprinosa. Prvo, definirani su parametari koji opisuju vrstu zrakoplovne operacije i utječu na predviđanje preostalog korisnog životnog vijeka konstrukcije podvozja lakog zrakoplova. Identificirani su i kvantificirani razni čimbenici koji utječu na *RUL* dijela konstrukcije podvozja lakog zrakoplova, relevantan za intenzitet opterećenja, smjer i orijentaciju, kao i operativne faze lakog zrakoplova koje doprinose akumulaciji oštećenja promatranog dijela. Karakterizacijom ovih parametara, produbljeno je razmijevanje preostalog korisnog životnog vijeka konstrukcije podvozja lakog zrakoplova pod opterećenjima koja su relevantna za zamor materijala. Drugo, razvijena je metoda za predviđanje preostalog korisnog životnog vijeka konstrukcije podvozja

lakog zrakoplova prema vrstama zrakoplovnih operacija. Ovaj znanstveni doprinos ostvaren je kroz razvijenu metodu za predviđanje preostalog korisnog životnog vijeka konstrukcije podvozja lakog zrakoplova, ovisno o različitim vrstama zrakoplovnih operacija. Metoda se oslanja na parametre definirane u prvom doprinosu i integrira ih u računalni model koristeći računalne alate. Kao rezultat ovog pristupa, uspostavljena je metoda za procjenu preostalog korisnog životnog vijeka konstrukcije podvozja lakog zrakoplova bez potrebe za dodatnim informacijama o operativnim uvjetima koje je moguće prikupiti, primjerice, implementacijom dodatnih senzora. Ovaj razvoj označava značajan iskorak u području preventivnog pristupa održavanju i povećanju sigurnosti operacija, s obzirom da u trenutku pisanja ove disertacije održavanje lakih zrakoplova ne uključuje nikakve postupke predviđanja preostalog korisnog životnog vijeka konstrukcijskih dijelova. Treće, identificirani su parametri koji utječu na nesigurnost predviđanja preostalog korisnog životnog vijeka konstrukcije podvozja lakog zrakoplova. Ti parametri potencijalno obuhvaćaju greške mjerenja, varijacije u svojstvima materijala i nesigurnosti unutar operativnih uvjeta lakog zrakoplova. Dodatno, ova disertacija prikazuje primjenjive doprinose razvijene metode. Primjenjivi doprinosi su: Mogućnost prognoziranja preostalog korisnog životnog vijeka konstrukcije podvozja zrakoplova Cessna 172R ili Cessna 172N, pod uvjetom da mjerodavan promatrani konstrukcijski dio ima istu geometriju i mehanička svojstva, te da je glavni mehanizam degradacije zamor materijala; Mogućnost primjene metode na bilo koji dio konstrukcije, pod uvjetom da se model za simulaciju degradacije dijela i model opterećenja relevantnog za degradaciju odgovaraju promatranom dijelu, i da je glavni mehanizam degradacije zamor materijala.

Ključne riječi: Prognoza i upravljanje stanjem, preostali korisni životni vijek, laki zrakoplov, konstrukcija podvozja, operativni zapisi, održavanje lakih zrakoplova, zamor materijala, ekspertni sustav, prediktivno održavanje.

IV. Table of Contents

V. List of Abbreviations

Abbreviation	Meaning
ACFS	Aircraft Cumulative Fatigue System
AIS	Aeronautical Information Service
AL	Autonomic Logistics
ATS	Air Traffic Service
CAD	Computer-Aided Design
CAT	Commercial Air Transport
CBM	Condition Based Maintenance
CCAA	Croatian Civil Aviation Agency
CF	Cycle fatigue
CM	Condition Monitoring
CoG	Centre of gravity
cPHM	Chemical Prognostics and Health Management
DoD	Department of Defence
EAA	Experimental Aircraft Association
EASA	European Union Aviation Safety Agency
ELA 1	Manned European Light Aircraft (airplanes, sailplanes, and powered sailplanes under 1200 kg maximum take-off mass (*MTOM*), and balloons which are differentiated by their hot air, gas, and tethered gas volume)
ELA 2	Manned aircraft have a higher *MTOM* ≤ 2000 kg applied to airplanes and sailplanes; they also include balloons not classified as ELA1; and simple very light rotorcraft (*MTOM* ≤ 600 kilograms) having not more than two occupants, not powered by a turbine or rocket engine, and restricted to operations under visual flight rules
EOL	End Of Life
ePHM	Electronic Prognostics and Health Management
EU	European Union
EUROSTAT	Statistical Office of the European Union
FAA	Federal Aviation Administrations
FAR	Federal Aviation Regulations

FEM	Finite Element Method
FLIGHT	Remaining useful life the landing gear structure would experience if operated exclusively under load conditions representing the flight phase of operation
FMECA	Failure Modes, Effects, and Criticality Analysis
GP	Gaussian process
HCF	High Cycle Fatigue
HUMS	Health and Usage Management Systems
ISHM	Integrated Systems Health Management
ISO	International Standardization Organization
JSF	Joint Strike Fighter
LCF	Low Cycle Fatigue
LCM	Life Cycle Management
LP1	Load Profile experienced by the aircraft's landing gear during aircraft taxi-out
LP2	Load Profile experienced by the aircraft's landing gear during the aircraft take-off run
LP3	Load Profile experienced by the aircraft's landing gear during aircraft flight
LP4	Load Profile experienced by the aircraft's landing gear during aircraft landing
LP5	Load Profile experienced by the aircraft's landing gear during aircraft taxi-in
mPHM	Mechanical Prognostics and Health Management
NCC	Non-commercial operations with complex aircraft
NCO	Non-commercial operations with non-complex aircraft
NN	Neural Networks
NOTAM	Notice to Airmen
OC	On Condition (maintenance)
PHM	Prognostics and Health Management
SHM	Structural Health Monitoring
SPO	Special Operations including complex and non-complex aircraft
US	United States (of America)
USUA	United States Ultralight Association
VBA	Visual Basic

XFEM	Extended Finite Element Method

VI. List of symbols

SYMBOL	EXPLANATION
A	Distance between the airplanes firewall and its main landing gear, [m]
$a_1 \dots a_n$	Accelerations measured for the observed load phase, corresponding to the moment in time they were recorded [m/s^2]
D_{accFa}	Accumulated Fatigue Damage
B	Longitudinal distance between the airplanes nose and main landing gear, [m]
BEM	Basic Empty Mass, [kg]
$BGA1$	Baggage Area 1, [kg]
$BGA2$	Baggage Area 2, [kg]
b	Fatigue strength exponent, [-]
c	Fatigue ductility exponent, [-]
D	Distance of the center of gravity from the landing gear nose wheel, [m]
ΔD_i	Damage increment - damage accumulation due to one single operation, [-]
E	Modulus od elasticity, [N/m^2]
E_{CG}	Center of gravity distance from one of the aircraft's main wheels, [m]
$E\%$	Percentage of main wheel distance to the CoG against the sum of all-wheel distances to the CoG, [%]
F	Distance of the main landing gear wheel from the centre of gravity, having the same value as E_{CG}, based on airplane symmetry, [m]
FA	Average value of the measured vertical acceleration component for the flight phase of operation, [m/s^2]
FX	Load acting on the observed landing gear structure part in the direction of the longitudinal aircraft axis, [N]
FY	Load intensity acting in the direction of the aircraft's lateral axis, [N]
FZ	Load intensity acting in the direction of the aircraft's vertical axis, [N]
$FPAX$	Mass in the front pilot seats, [kg]
H	Longitudinal center of gravity distance from the main wheels, [m]

I	Lateral CoG istance from the main wheels, [m]
LANDING	Remaining useful life the landing gear structure would experience if operated exclusively under load conditions representing the landing phase of operation, [-]
LDGA	Average value of the measured vertical acceleration component for the landing phase of operation, [m/s2]
LA1	Aircraft angle of rotation around the longitudinal aircraft axis, [^{o}]
LA2	Aircraft angle of rotation around the lateral aircraft axis, [^{o}]
LA3	Aircraft angle of rotation around the vertical aircraft axis, [^{o}]
m	Share of aircraft total mass causing observed part loading, [-]
m_{TOT}	Total airplane mass, [kg]
m_1	Calculated mass on the observed main landing gear wheel, [kg]
m_{NLG}	Calculated mass that could also be measured by placing a scale under the nose landing gear, [kg]
MTOM	Maximum take-off mass, [kg]
N	fatigue life given in number of cycles to failure, [-]
$n(t)$	sensor noise vector at time t
nx	Load factor relevant to the aircraft's longitudinal axis, [-]
ny	Load factor relevant to the aircraft's lateral axis, [-]
nz	Load factor relevant to the aircraft's vertical axis, [-]
RPAX	Mass in the airplanes rear seats, [kg]
RUL	Remaining Useful Life, [-]
SRUL	Specific Remaining Useful Life, [-]
t	Continuous time, [s]
t_E	Time of the event, [s]
Δt_E	Time increment until the event [s]
t_p	Time of prediction [s]
t_H	End time of prediction [s]
TAKEOFF	Remaining useful life the landing gear structure would experience if operated exclusively under load conditions representing the take-off phase of operation, [-]

TAXI-IN	Remaining useful life the landing gear structure would experience if operated exclusively under load conditions representing the taxi-in phase of operation, [-]
TAXI-OUT	Remaining useful life the landing gear structure would experience if operated exclusively under load conditions representing the taxi-out phase of operation, [-]
TFT	Total Flight Time, [*h*]
TNO	Total Number of Operations, [-]
TOA	Average value of the measured vertical acceleration component for the takeoff phase of operation, [m/s^2]
TXIA	Average value of the measured vertical acceleration component for the takeoff phase of operation, [m/s^2]
TXOA	Average value of the measured vertical acceleration component for the taxi-out phase of operation, [m/s^2]
u(t)	Input vector at time t, [unit varies based on observed quantity]
U.FUEL	Usable Fuel, [kg]
z(t)	Prediction output vector at time t, [unit varies based on observed quantity]
$Z_{t_P}^{t_H}$	Future values of *z(t)* within [t_P, t_H].
X	Airplanes center of gravity arm, [m]
x(t)	State vector at time t, [unit varies based on observed quantity]
y(t)	Measured system output vector at time t, [unit varies based on observed quantity]
α	Angle between the vertical aircraft axis and the load direction acting on the observed structural part, [^{o}]
β	Angle between the lateral aircraft axis and the load direction acting on the observed structural part, [^{o}]
$\Delta\varepsilon/2$	Strain amplitude, [m/m]
ε_{ar}	Combined strain due to its elastic and plastic components, [m/m]
$\Delta\varepsilon_e$	Incremental elastic strain, [m/m]
$\Delta\varepsilon_p$	Incremental plastic strain, [m/m]
ε_f'	Fatigue ductility coefficient, [m/m]

$\Theta(t)$	Unknown parameter vector at time t
$v(t)$	Process noise vector at time t
σ_a	Stress amplitude, [N/m^2]
σ_f'	Fatigue strength coefficient, [N/m^2]
σ_m	Mean stress, [N/m^2]

VII. List of figures

VIII. List of tables

1 INTRODUCTION

This Chapter provides an overview of the structure and key elements of this Doctoral thesis. It begins by articulating the motivation and aims of the underlying research, providing its driving factors and goals. This is followed by a description of the research method. The Chapter then outlines the research objective and hypothesis. Subsequently, the Chapter discusses the scientific contributions of the research. Lastly, the Chapter presents the research structure, providing an organized outline of the components of the research and how they are interconnected, facilitating a comprehensive understanding of the Thesis structure.

1.1 Research Motivation and Aims

Maintenance is an essential part of the aviation industry, ensuring aircraft safety and reliability. Regular maintenance checks are carried out on aircraft to detect and fix any issues before they become a safety hazard. However, maintenance methods have evolved, and modern transport aircraft maintenance concepts now include aircraft condition prediction and health management methods. These methods use sensors to monitor and record in-flight data, predicting the remaining useful life (*RUL*) of aircraft parts. In the context of this research, the *RUL* is a concept used to estimate how long before an aircraft part, subject to material fatigue, can perform its intended function. The *RUL* is typically calculated based on various factors, such as the part's manufacturing date, its history of use, the results of regular inspections, and computational models that predict the rate of fatigue growth. It is a critical factor in ensuring aircraft safety and efficiency, as it helps determine when parts should be repaired or replaced. Maintenance based on predicted future conditions is a proactive approach that involves monitoring the current condition and predicting a future condition using prognostic methods. Elattar et al. [38] describe prognostics and health management (PHM) as a process in which the *RUL* of an aircraft part, component, or system is predicted. There are different levels of *RUL* prediction, ranging from providing information about the remaining useful life of a part to failure to characterizing the *RUL* reliability interval. Prognostic and health management (PHM) methods can be divided into physics-based methods, data-based methods, and hybrid methods. Determining the *RUL* is possible by physics-based methods, data-based methods, or hybrid methods.

However, the application of PHM methods is limited in light aircraft maintenance condition prediction because light aircraft are not equipped with sensors to monitor and record in-flight data. Therefore, maintenance methods for light aircraft are mainly based on models

that mimic the physical properties of the observed aircraft part, component, or system. For example, in this Thesis material fatigue analysis of landing gear of a light aircraft landing gear strut is carried out using the Finite Element Method (FEM). In other research, crack propagation in the spar of a light aircraft wing is investigated in different phases, where the methodology often involves integrating the Paris-Erdogan equation ([39], [40]) and comparing the results for different cross-sectional shapes of the wing spar of a light aircraft.

Several examples of PHM methods have been identified in aircraft parts, components, and systems by analysing scientific works focused on aeronautics. For instance, aircraft high-pressure engine valves and hydraulic pumps' *RUL* are predicted using PHM methods. Aircraft engines are diagnosed based on measured parameters and predicting the evolution of these parameters. Prediction of the *RUL* of electronic systems (for example: [41] and [42]), aircraft generators (for example: [43]), and landing gear ([22], [27], [44] and others) is also done using PHM methods. According to Hess et al. [45], The U.S. Air Force has included PHM in the Joint Strike Fighter program, and the Procurement Directive issued by the U.S. Department of Defence requires that any new system includes adequate PHM.

Despite the advancements in PHM methods for large aircraft, light aircraft maintenance still lacks a defined method for condition prediction. No method for predicting the remaining useful life of light aircraft landing gear structures based on information from the operational records of these aircraft in a manner suitable for maintenance processes is defined in the observed literature. Therefore, the prediction of the condition of light aircraft structural parts is mainly made by applying physical PHM models that mimic the physical properties of the observed aircraft part.

Current light aircraft maintenance approaches largely depend on fixed and predetermined time-frames for part replacement, known as "hard time replacement intervals." These intervals are part of a preventive maintenance strategy aimed at averting future faults through maintenance actions executed at predetermined intervals or according to prescribed criteria. Light aircraft maintenance is also subject to corrective and condition-based maintenance strategies. Corrective maintenance is applied after a fault detection, while condition-based maintenance relies on Condition Monitoring (CM) based on sensor data, occurrence reports, or inspection reports. The landing gear strut, the subject of this research, is designed with a safe life design approach in mind, acknowledging the need for preventive maintenance. The safe-life design approach aims to prevent fatigue damage from progressing to a catastrophic condition within its predicted operational lifetime, considering static and dynamic loads [5]. The primary issue with preventive maintenance and "hard time replacement intervals" is the

difficulty in accurately predicting the useful life of light aircraft parts during the design phase due to the various load and environmental conditions they experience. Despite incorporating safety factors, certain load and environmental conditions can lead to a shorter operational life than prescribed, potentially resulting in catastrophic failure. A simple, reliable, and robust method for Remaining Useful Life prediction, dependent on operational conditions, could help to prevent sudden light aircraft accidents due to fatigue failure.

Fatigue failure in light aircraft landing gear structures is a significant concern due to the potentially catastrophic consequences as determined by Campbell and Lahey [16]. Metallic aircraft parts, particularly those in light aircraft, are subjected to a wide range of stresses and strains during operation. Material fatigue, defined as the cycle-by-cycle accumulation of damage in a material experiencing fluctuating stresses and strains [46], is a significant concern for these parts, especially considering part fatigue life. Fatigue life is described as the number of loading cycles a structural member or part can sustain before a fracture occurs (Yuan [47]). Various methods are employed to prevent fatigue failure, including design, testing, load monitoring, inspection, and the replacement of parts at scheduled intervals (Schijve [48]). Light aircraft design is commonly approached through a safe-life design approach.

Maintenance strategies for light aircraft often involve fixed "hard time replacement intervals," which are preventive measures carried out at predetermined intervals to avoid future faults. Although corrective and condition-based maintenance strategies are also employed, they are less prevalent. The current maintenance approach, relying on fixed "hard time“ replacement intervals may not adequately account for the diverse operational conditions experienced by light aircraft, leading to premature or delayed part replacement and consequent part failure. This research aims to develop a simple, reliable, and robust method for predicting the Remaining Useful Life of light aircraft landing gear structure parts, based on operational conditions. The proposed method will help avoid light aircraft operational failures and enable a more efficient and cost-effective maintenance approach. Such a method can enable operators to make more informed decisions about maintenance intervals, potentially reducing costs and improving safety.

1.2 Literature review

To better understand the critical aspects and complexities of aircraft maintenance, specifically light aircraft, a detailed literature review was performed in the second Chapter of this Thesis. This review will encompass an in-depth analysis of existing research, methods, and

practices in the field, thus providing a comprehensive theoretical foundation for developing a new method for remaining useful life prediction of light aircraft landing gear structures.

1.3 Research Method

To confirm the research hypothesis, the research was conducted in five phases, as displayed in Figure 1.

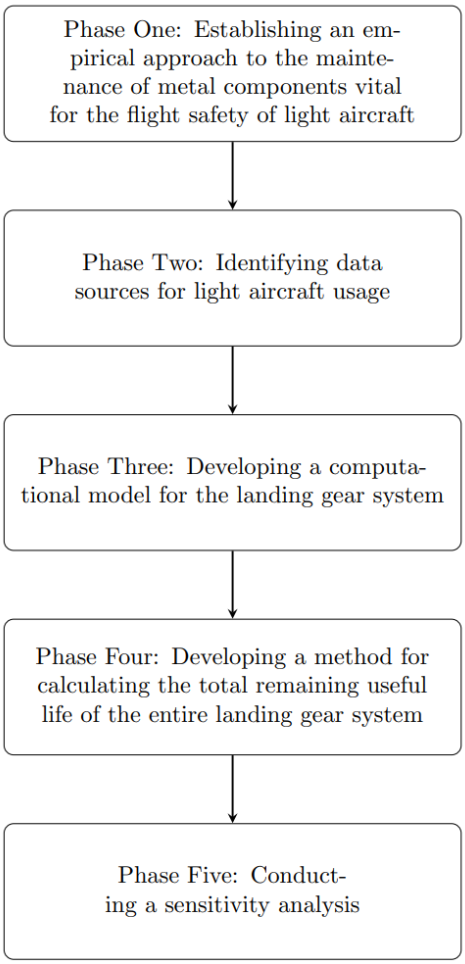

Figure 1. Research methodology.

Phase One: Establishing an empirical approach to maintaining metal components essential for the operational safety of light aircraft. This was achieved by analysing both professional and academic literature. The professional literature includes light aircraft maintenance regulations, manufacturers' maintenance instructions, and maintenance manuals. The scientific literature focuses on predicting the remaining useful life of metal components susceptible to damage during regular use. Once the literature has been reviewed, the extent to which existing methods for predicting the remaining useful life of metal components in light aircraft maintenance systems are implemented was determined. The literature review also helped identify the advantages and disadvantages of various methods for predicting the remaining

useful life of metal aircraft parts and their suitability for predicting the remaining useful life of light aircraft parts.

Phase Two: Discovering data sources related to light aircraft usage. This involves identifying appropriate data sources for determining the remaining useful life of light aircraft landing gear during regular operation. Additionally, common usage profiles for light aircraft and the characteristic loads acting on the landing gear system were determined. Finally, characteristic loads that influence the useful life of the observed system were identified.

Phase Three: Constructing a computational model for the landing gear system. This entails creating a numerical model that includes the geometry and material composition of a light aircraft's landing gear structure. The model was subjected to loading conditions outlined in Phase Two. The useful life of the landing gear system was determined based on the simulation results for each characteristic load, allowing for the identification of critical operation conditions that result in the shortest remaining useful life under individual characteristic loads.

Phase Four: Formulating a method to calculate the remaining useful life of the landing gear structural parts. This involves establishing a relationship between usage data, load profiles, and the remaining useful life for each individual load profile. By employing a damage accumulation rule, the total accumulated damage was calculated. Subsequently, the remaining useful life of the landing gear structure was determined based on the provided usage data.

Phase Five: Carrying out a sensitivity analysis. This includes evaluating the effects of alterations in specific variables employed in the remaining useful life determination method on the prognostic outcomes. The influence of mass change within defined usage profiles on the remaining useful life of the landing gear system structure was analysed. A comparison was made between the results and usual maintenance intervals for the corresponding aircraft type utilized for each individual regular usage profile. The impact of the developed method on aircraft maintenance and safety was assessed, considering the maintenance intervals estimated based on the remaining useful life determined by the developed method and the intervals prescribed in the original documentation for light aircraft maintenance. Lastly, sources of prediction uncertainty and their impact on the developed method results were discussed.

1.4 Research Objective and Hypothesis

The main objective of this research is to develop a method for predicting the remaining useful life of light aircraft landing gear structure parts under typical operating conditions. In line with this objective, the following hypothesis was stated:

- Based on the analysis of typical operating conditions, it is possible to determine the remaining useful life of a light aircraft's structural parts.

The research will focus on metal parts of light aircraft that are vital for flight safety and prone to damage due to regular usage. To achieve the research objectives and validate the hypothesis, a comprehensive research plan encompassing data collection, computational modelling, simulation, and method development was followed.

1.5 Scientific Contribution

The scientific contributions of the Doctoral thesis are:

- Defining the parameters that describe the type of aeronautical operation and affect the prediction of the remaining useful life of a light aircraft's landing gear structure.

This contribution aims to identify and quantify the various factors associated with different aeronautical operations that could influence the remaining useful life of a light aircraft's landing gear structure. These factors may include load intensities, mass distribution, flight hours, and operational environments. By defining these parameters, a better understanding of their impact on the landing gear's lifespan can be achieved, which is essential for accurate remaining useful life predictions.

- Developing a method for predicting the remaining useful life of a light aircraft's landing gear structure according to the types of aeronautical operations.

This contribution involves creating a method for estimating the remaining useful life of a light aircraft's landing gear structure, considering various aeronautical operation types. The method would consider the defined parameters from contribution 1 and integrate them into a predictive model, using computational techniques and software tools. This method allows for more accurate estimations of the remaining useful life, ultimately contributing to enhanced maintenance planning and aircraft safety.

- Identifying the parameters that affect the uncertainty of predicting the remaining useful life of a light aircraft's landing gear structure.

In any prediction model, uncertainty plays a crucial role in determining the reliability and accuracy of the predictions. This contribution aims to identify the parameters that significantly contribute to the uncertainty in predicting the remaining useful life of a light aircraft's landing gear structure. These parameters might include measurement errors, material properties variations, and uncertainties in operational conditions. By understanding and quantifying the impact of these parameters on the uncertainty of the predictions, the prediction method can be

refined, and accuracy increased, leading to more reliable maintenance scheduling and improved aircraft safety.

1.6 Thesis structure

This Doctoral thesis consists of seven Chapters that collectively contribute to the development of a method for predicting the remaining useful life (*RUL*) of light aircraft landing gear structures. The research is driven by the hypothesis that the *RUL* of these structures can be determined from aircraft operation records.

The Thesis begins with an introductory Chapter, which establishes the motivation and aims of the research. The research method, hypothesis, scientific contributions, and Thesis structure are presented in detail. The second Chapter delves into a comprehensive literature review, focusing on aircraft maintenance concepts. It also provides an in-depth introduction to prognostics and health management, discussing two main prognostic approaches: data-driven and physics-based. Applications of prognostics and health management in aeronautics are explored, along with the specific challenges of implementing these approaches in light aircraft maintenance. In the third Chapter, the division of general aviation aircraft according to applicable regulations is explained, emphasizing the specifics of nationally regulated aircraft regulations, maintenance procedures, and mandatory records. The Chapter further examines light aircraft accident literature to identify the main reasons for part failure and discusses the challenges of implementing prognostics and health management in light aircraft maintenance. It also highlights the relevance of information in mandatory operation records for prognostics and health management and sheds light on data acquisition procedures for light aircraft structural parts. The fourth Chapter focuses on fundamental concepts in metal fatigue for computational modeling, particularly within the context of aeronautical applications. Various fatigue analysis types are explored, including loading types, mean stress effects, multiaxial stress correction, and fatigue modifications. Moving forward, the fifth Chapter presents the development of a method for predicting the *RUL* of aircraft structural parts. This method encompasses several phases, such as selecting the observed part, creating a detailed model, developing fatigue-relevant load models, validating the fatigue analysis software, and implementing an expert system approach. Validation involves comparing results from literature and software fatigue analysis, while the development of an expert system architecture aids in information input and result processing. The sixth Chapter reveals the numerical strength analysis results obtained from the study, assessing the structural strength and performance of

the examined parts. Statistical methods, including correlation, regression, and sensitivity analysis, are utilized for result analysis. The impact of these analysis results on maintenance and operational safety is thoroughly examined, alongside a discussion of prediction uncertainty sources and limitations. Lastly, the seventh and final Chapter concludes the Thesis by summarizing the research findings and presenting possibilities for future research. The scientific and applicative contributions of this Thesis are highlighted, specifically in terms of enhancing the current standard of light aircraft landing gear structure maintenance. The research findings offer valuable insights and potential improvements for light aircraft landing gear maintenance, ultimately aiming to enhance the safety of light aircraft operations.

2 LITERATURE REVIEW AND STATE OF THE ART IN *RUL* PREDICTION

The second Chapter offers an extensive exploration of aircraft maintenance and prognostics, with a particular emphasis on *RUL* prediction for light aircraft landing gear structures. It begins with laying out the foundational concepts of aircraft maintenance strategies. This is followed by an examination of Prognostics and Health Management modelling approaches. PHM Applications in Aeronautics with the corresponding challenges and limitations are laid out next, discussing the problem of PHM implementation in light aircraft maintenance. Various applied *RUL* prediction methods of landing gear structures are observed, following an overview of their *RUL* results, fit for comparison with results produced by this research.

2.1 Aircraft maintenance concepts

Aircraft maintenance can be defined as a combination of all technical, administrative, and managerial actions during the aircraft life cycle, intended to retain or restore it to a state in which it can perform its required function, as stated by Insley and Turkoglu [49]. The purpose of aircraft maintenance is to keep the aircraft in a serviceable and reliable condition to generate revenue while maintaining the current and future value of the aircraft by minimizing the physical deterioration throughout its life, as stated by Rodrigues et al. [50]. Aircraft maintenance is an indispensable aspect of ensuring flight safety. Without proper maintenance, aircraft parts can degrade over time, leading to malfunctions or even catastrophic failures. Degradation of aircraft structural integrity during operation is inevitable, causing performance to deviate from the original specifications defined and guaranteed by the manufacturer. The characteristics of a used aircraft differ from those of a new aircraft due to this degradation. Maintenance procedures are carried out to restore aircraft characteristics and are linked to high operational and logistical costs. In fact, according to Pan et al. [51], 72 % of the total aircraft operating cost is spent on operational and logistical processes. Regular aircraft maintenance not only prolongs the service life of the aircraft but also helps to prevent accidents. It is the responsibility of the aircraft operator or maintenance organization to adhere to strict maintenance schedules and procedures to ensure that every aircraft is in optimal condition. Maintenance procedures are determined by the aircraft operator who is required to carry out maintenance in accordance with the aircraft's maintenance program [13] approved by the competent authority [52]. The maintenance program defines maintenance activities and

intervals for the aircraft. Most aircraft maintenance programs are defined by three maintenance strategies. Those maintenance strategies are corrective maintenance, preventive maintenance, and Condition Based Maintenance (CBM). Corrective maintenance is applied after fault detection. Preventive maintenance aims at avoiding future faults by carrying out maintenance actions at predetermined intervals or according to prescribed criteria. Finally, condition-based maintenance relies on Condition Monitoring (CM) which is based on sensor data, occurrence reports and/or inspection reports. CBM however, recognizes only present aircraft state information. Predicting the future and adapting CBM accordingly is called predictive maintenance or in more general terms, applicable to any kind of activity, Prognostics and Health Management (PHM).

Tinga and Loendersloot [53] describe three maintenance strategies, Condition Based Maintenance (CBM), Structural Health Monitoring (SHM), and the aforementioned PHM. They focus on different maintenance aspects but have a common aim of improving maintenance decision-making. Aircraft health management is an activity related to Life Cycle Management (LCM), which tries to optimize all maintenance activities during the complete life cycle of the aircraft. Selection of an appropriate maintenance policy, defining the maintenance interval length, and deciding when an aircraft or its component should be discarded are steps for that kind of optimization. The relationship, regarding maturity level, between CBM, SHM, and PHM is shown in Figure 2.

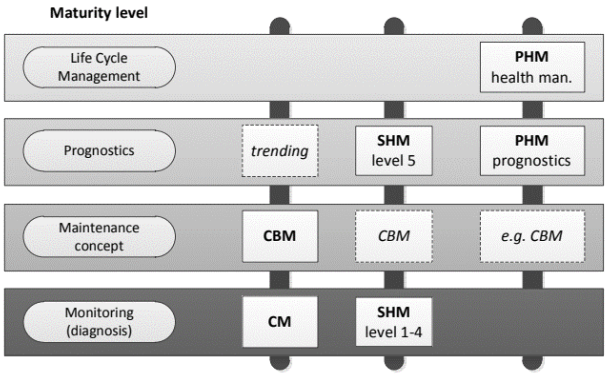

Figure 2. Relationship between CBM, SHM, and PHM, [53].

Tinga et al. [53] propose an integral approach to aircraft maintenance, starting from defining an appropriate monitoring strategy (CM and SHM), applying the appropriate maintenance policy (CBM), performing prognostics (PHM), and eventually supporting the decision-making that leads to an optimal maintenance process throughout the life cycle of the aircraft.

2.2 Prognostics and Health Management (PHM)

Prognostics and Health Management (PHM) of aircraft is a process with the outcome of identifying the Remaining Useful Life (*RUL*). Fornlöf et al. [54] list a definition of the International Standardization Organization (ISO) according to which the prognosis of a future state estimates the time until the occurrence of a failure and the risk of the existence or emergence of an undisclosed failure in the future. PHM is considered part of Integrated Systems Health Management (ISHM), according to Elattar [38]. ISHM consists of the following phases: fault search, diagnosis of failure (or failure isolation), and *RUL* prognosis, as stated by Saxena et al. [55]. Accurate assessment of aircraft *RUL*, or some of its components, has an impact on all phases of ISHM.

Elattar et al. [38] state that PHM reduces operation prices and increases safety. The US military evaluates aircraft operation quality, in which PHM is implemented within the Joint Strike Fighter Program (JSF program), as given by Hess et al. [45]. Contribution is expected in the Autonomic Logistics (AL) concept through increasing safety in aircraft operation, improving sortie generation rate, reduction of the logistic footprint, and significant reduction of operation and support costs. Janasak et al. [56] state a procurement directive issued by the Department of Defence (DoD), number directive 5000.2, 2002, [57], which instructs that each new integrated DoD system must contain PHM.

After a comprehensive literature review, it can be concluded that PHM includes different subjects. According to Saxena et al. [55], these are mechanical PHM (mPHM), electronic PHM (ePHM), and chemical PHM (cPHM). mPHM deals with prognostics and health management of mechanical parts, bearings, beams, and others. ePHM deals with electronic parts, circuit boards, etc. cPHM focuses on chemical interactions, battery chemistry, corrosion, etc.

Prognostics and health management methods allow for the prediction of future system health behaviour and the determination of *RUL* for appropriate maintenance action scheduling. According to Kim et al. [58], prognostic methods can be categorized into two: physics-based and data-driven approaches. The authors state three main differences between the two approaches; (1) the availability of a physical model that describes the behaviour of damage, (2) the availability of field operating conditions, and (3) damage degradation data from similar systems. There is, however, a third approach, the hybrid approach, a combination of the two, all shown in Figure 3.

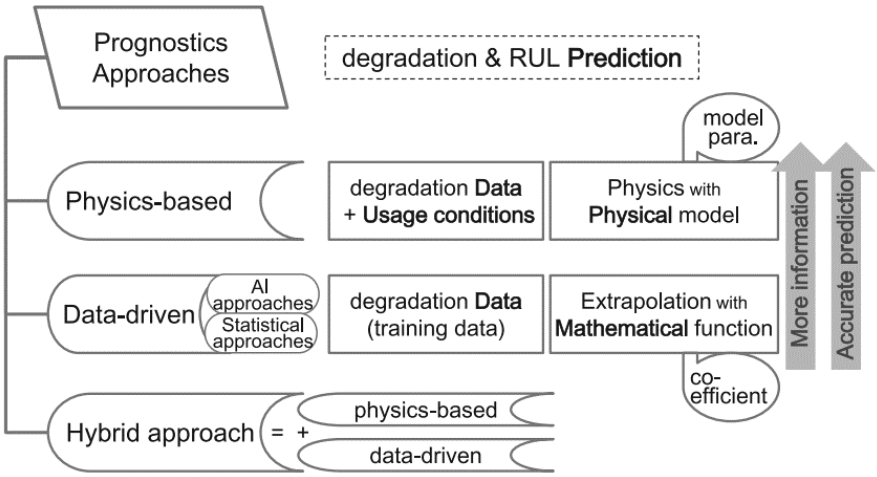

Figure 3. Categorization and definition of prognostics methods, [58].

According to Goebel et al. [59], prognostic models, algorithms, and architectures require a mathematical definition of the prognostic problem. The task of prognostic modelling is to map the connection between a set of inputs and a set of outputs for a given system. In that context, mapping means computing the time of the event of interest and/or released system variables. The task of prognostic modelling is therefore to identify as much of the model structure and parameters as possible before utilizing prognostic algorithms. According to Bretscher, unknown parameters (or coefficients) may be found with the least squares method, by minimizing the sum of square errors between measured data and simulation outputs from the model/function.

Goebel et al. [59] also discuss other uses of the prognostic model, for example, in simulation test beds. This can help in algorithm development and testing, as well as performance comparison. Models also have explanatory power. Damage models can explain a failure prediction, which then may be linked back to component usage.

Prognostic models need to satisfy a variety of constraints, as stated by Goebel et al. [59]. Model complexity and simplicity need to be well balanced to obtain accurate predictions but also enable restricted computation capability, as is the case in online computation. Modelling efforts, model complexity, computational requirements, and prediction accuracy must all be balanced to satisfy the requirements of the given prognostics problem. Having all these constraints in mind, model development is typically initiated by selecting the appropriate modelling scope. This is determined by the variable that needs to be predicted. A general mathematical framework applicable to prognostic model development requires the introduction of common notation, as described by Goebel et al. [59]. This notation allows framework application regardless of it being based on empirical laws, known physical principles, learned from data, or any such combination and is commonly represented as follows:

- t is continuous time (when appropriate, k was used for discrete time),
- $x(t)$ is the state vector at time t,
- $u(t)$ is the input vector at time t,
- $y(t)$ is the (measured) system output vector at time t,
- $z(t)$ is the prediction output vector at time t (system variables that are to be predicted, i.e., here, these are outputs in the context of the prediction, not of the system sensors),
- E_{vent} is the event to be predicted,
- t_E (resp. k_E) is the time of the event E_{vent},
- Δt_E (resp. Δk_E) is the time increment until the event E_{vent},
- t_P (resp. k_P) is the time of prediction,
- $\underline{t_H} > t_p$ is the end time of prediction,
- and $Z_{t_P}^{t_H}$ is the future values of $z(t)$ within $[t_P, t_H]$.
- $\Theta(t)$ is the unknown parameter vector at time t (explicit model parameters that may be time-varying, but evolving in an unknown way),
- $v(t)$ is the process noise vector at time t,
- and $n(t)$ is the sensor noise vector at time t.

According to Goebel et al. [59], a set of equations relates all these variables. State evolution as a function of time, state, unknown parameters, inputs, and process noise is described by the state equation *(1)*:

$$\dot{x}(t) = f(t, x(t), \theta(t), u(t), v(t)) \qquad (1)$$

where: f - represents the state function.

Both the measured and predicted outputs are functions of time, state, parameters, and inputs:

$$\begin{gathered} y(t) = h\big(t, x(t), \theta(t), u(t), n(t)\big), \\ z(t) = g(t, x(t), \theta(t), u(t)) \end{gathered} \qquad (2)$$

where:

h - Is the system output function;

g - Is the prediction output function.

It must be noted that the system output is also a function of the sensor noise vector.

When some predefined system condition is satisfied, event E_{vent} occurs. A threshold function determines whether the condition is satisfied, depending on the states, parameters, and inputs:

$$c_E = T_E(t, x(t), \theta(t), u(t)\ ) \tag{3}$$

where:

$c_E \in \mathcal{B}$ - is a Boolean variable, true (1) when the condition is satisfied (E_{vent} has occurred), and false (0) otherwise.

Then, t_E, at some time of prediction, denoted as t_P, is defined as:

$$t_E(t_P) \triangleq inf\{t \in \mathbb{R}: t \geq t_P \wedge T_E\big(x(t), \theta(t), u(t)\big) = 1\} \tag{4}$$

And the time remaining until that event, Δt_E, is defined as:

$$\Delta t_E(t_P) \triangleq t_E(t_P) - t_P \tag{5}$$

Two regions are defined by the threshold function of the joint-state parameter input space, one where E_{vent} has not yet occurred, and one where it has. The former region, denoted as A, can be expressed using:

$$A = \left\{\Big(x(t), \theta(t), u(t), : T_E\big(x(t), \theta(t), u(t)\big)\Big) = 0\right\} \tag{6}$$

Simple structures are possible. They map u and y to t_E. For example, given sufficient data through several examples of t_E, such a model can be learned, and, internally, it need not explicitly include the state, system output, and threshold equations. More basic representations of the above models are possible. However, the relationship between system inputs and outputs, and the quantities that must be predicted must be captured.

2.2.1 Data-driven prognostic modelling

Measured operation data allows for the prognosis of damage degradation. According to Kim et al. [58], data-driven prognostic approaches are usually considered when physical degradation models are not available, or the failure phenomenon is too complex to be expressed as a model.

Provided they are based on the same degradation data, physics-based methods can give more accurate prediction results than data-driven methods. This could be explained by the additional information that physics-based models require: a physical model of the degradation process and loading conditions. However, Goebel et al. [59] state that data-driven modelling can be just as accurate or even more so, given un-modelled dynamics, measurement variability, and environment factor information. Also, physical degradation models are not always easy to develop, hence the practicality of data-driven approaches.

Data-driven approaches can prognose a future state by extrapolating existing data, schematically depicted in Figure 4.

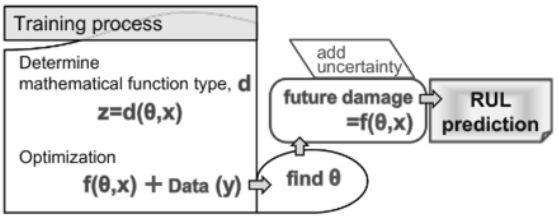

Figure 4. Data-driven prognostics example, [58].

The mathematical model output *(z)* is a function of input variables *(x)* and parameters *(Θ)* associated with the mathematical model.

Kim et al. [58] state that data-driven prognostics use various extrapolation methods. Those methods, also called data-driven prognostic approaches, are generally divided into two categories, machine learning, and statistical approaches. Machine learning approaches were categorized as neural networks (NN) ([60], [61], and [62]) and fuzzy logic ([63], [64]). Statistical approaches include the Gaussian process (GP) regression ([65] and [66]), relevance/support vector machine ([67] and [68]), least squares regression ([69] and [70]), the gamma process [71], the Wiener processes [72], hidden Markov model [73], and others. A review of various data-driven algorithms is provided by Si et al. [74].

According to Goebel et al. [59], neural networks, decision trees, and support vector machines constitute tools that generate a static mapping from input to output, meaning that there is a dynamical state change over time. This contrasts with Gaussian process regression techniques which are centred around the concept of a stochastic change for which state time dependence is implicit.

The problem of selecting a suitable algorithm was tackled by Zhang [75], via cross-validation. By comparing the testing error across multiple data-driven algorithms, it is possible to ease the algorithm selection process.

Regardless of the used method, in data-driven prognostics, data is extrapolated by using "training data". The term training data represents degradation data up to the end of life of the observed object, as well as current system data (mostly various operation variables) used to identify the degradation characteristics. Regardless of the lack of need for a physical model, data-driven predictions still require a functional relationship between input variables and output degradation. However, the functional relationship does not need to have any physical meaning. An example of training data function fitting is given in Figure 5.

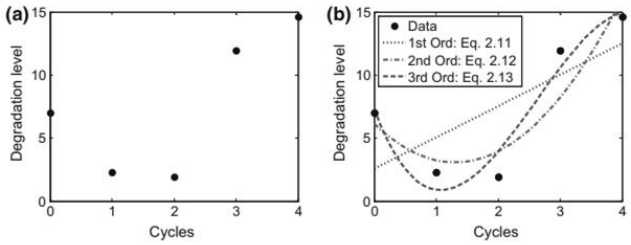

Figure 5. a) training data b) training data function fitting, [58].

Data-driven prediction accuracy can be improved if a degradation history of identical systems is available, meaning that several sets of runs-to-failure data exist. Training data is best collected from identical systems under identical conditions. However, data-driven approaches can also utilize data from similar systems under different usage conditions.

It is usually expected that there is more training data than unknown coefficients. According to Kim et al. [58] the least squares method tends to follow the mean trend of the function. However, when the number of unknown coefficients increases, the least squares method tends to fit noise, instead of the degradation trend. This phenomenon is called overfitting. Overfitting is a modelling error that generally occurs when the proposed function is overly complex so that it fits noisy data (as shown in Figure 5 b)), and when the function has no conformability with the data shape (Hawkins [76]). Kim et al. [58] state that overfitting is usually prevented by two approaches (in data-driven prognostics): (1) the behaviour of degradation is expressed with a simple function and (2) more information, such as more training data and usage conditions, is used for reliable prognostics results.

Data-driven prediction quality is according to Goebel et al. [59] identified by three relevant factors. Those factors are functional relationship description, quantity of data, and noise level.

2.2.2 Physics-based prognostic modelling

Physics-based prognostic modelling is based on a physical model to describe the evolution of damage or degradation. Therefore, it is common to refer to the physical model as a degradation model while physics-based prognostics are referred to as model-based prognostics. According to Kim et al. [58], an accurate physical model describing damage degradation as a function of time completes prognostics because of the ability to predict damage behaviour. However, practice shows prediction inaccuracies because of model imperfections. Those inaccuracies require the introduction of prognostic result uncertainty. The key issue of physics-based prognostics is how to improve the accuracy of the degradation model and how to include uncertainty in the future.

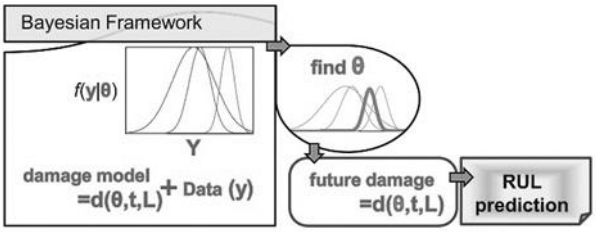

Figure 6. Illustration of physics-based prognostics, [58].

In Figure 6 (L) represents prognostic model usage (or loading) conditions, (t) represents the elapsed time or cycle, and (Θ) represents the prognostic model parameters.

Physics-based methods can produce long-term predictions. The main prerequisite for that is accurate model parameter identification. Accurate model parameters allow for *RUL* prediction by degradation progression through model propagation. The model is being propagated until its output value reaches a predetermined threshold. According to Goebel et al. [59], model development requires consideration of quantities, accuracy, and precision to which the quantities must be predicted, as well as the speed and available memory for prediction. Those considerations must fit the modelling scope, level of model abstraction, model fidelity, and computational efficiency. The behaviours the model needs to express are defined by the quantities that must be predicted. An important modelling decision is the level of abstraction. According to Daigle et al. [77], abstraction is the process of simplification. Zeigler et al. [78] state common abstractions, they include aggregation, omission, linearization, deterministic/stochastic replacement, and formalism transformation (differential equations to discrete-event systems). The correlation between abstraction and the questions the model must address was explored by Frantz [79], Lee et al. [80], and Zeigler et al. [78].

The physics-based approach requires a smaller amount of data in comparison to data-driven models. The number of model parameters must at least equal the number of available data. However, actual operation conditions introduce numerous factors which contribute to prognostic model result uncertainty. This can be mitigated by increasing the number of included data. The distinction between physics-based and data-driven methods is not as clear as the first impression would lead to believe. Goebel et al. [59] present an example of that statement. The popular Paris model and its modifications serve as damage progression models and are being used to predict crack propagation as a function of loading amount, measured in terms of stress, and the number of loading cycles. The damage variable is crack size, and fatigue loading increases this variable. Crack size prediction is the subject of interest. Paris's model is based on fitting against observed data; thus, it should be classified as a data-driven approach, however, it includes the stress intensity factor whose determination is based on the physics of fracture

mechanics. The degradation model is, therefore, a unique combination of a data-driven model and a physics-based modelling approach.

Physics-based failure prediction is often done with two models. One model is the representation of nominal system operation, enabling system state prediction in the absence of faults. The other is a damage progression model. Some prediction cases are focused only on damage propagation, without the need for a nominal model. Model adequacy is a common physics-based prognostic approach issue. It addresses the model's ability to predict behaviour, mostly degradation.

An important step in physics-based prognostic model development is model validation. Models usually contain assumptions and approximations. Much research has been done on statistical model validation approaches, for example, the hypothesis test and Bayesian approach (Oden et al. [81], Rebba et al. [82], Sargent [83], Ling and Mahadevan [84]). There is also an approach made by Coppe et al. [85] that aims at identifying equivalent parameters from a simple Paris model. That approach assumes the stress intensity factor to predict crack growth of complex geometries, the model parameters were adjusted to compensate for the error in the stress intensity factor.

2.3 PHM applications in aeronautics

A prognostic approach based on knowledge of the physical properties of the observed process is particularly suitable when insight into process parameters is difficult. An example of such a situation is a prognostic model of gas turbine performance, where the parameters of the thermodynamic cycle (for example combustion chamber temperature and pressure, transmitted heat) are unknown, and only operational parameters (shaft rotation speed, exhaust gas temperature) are known, according to Hanachi et al. [86]. PHM literature has other physics-based examples of the use of PHM on specific aircraft, aircraft systems, parts of systems, and components. Shen [87] gives an example of the application of the PHM method in a simple aviation fuel supply system and explains the steps for establishing such a system. The necessary steps are the analysis of possible failures and parameters by which individual failures are identified as well as the model establishment. In the observed case, the relevant faults were at the fuel pipe connection points, pipeline rupture, obstruction of the injector, and fuel tank leakage. The parameters by which these failures are identified are pressure and fuel flow.

Batzel et al. [43] describe the development of the PHM system on an example of an aeronautical electric generator to recognize failure and predict *RUL*. Current approaches to limited lifetime parts and “on condition” maintenance was described. Such approaches result

in the frequent elimination of parts with a usable *RUL*, investment in PHM development for such components is considered cost-effective. According to Batzel et al. [43], there exist aircraft parts that can be generally considered economically and safely justified areas of PHM development, such as aircraft structure, actuators, avionics, and mechanical generator bearings. Additionally, Batzel et al. [43] introduce the concept of recognition of the type and consequences of failure and the analysis of the criticality of its impact on the operation of the aircraft failure mode, effects, and criticality analysis (FMECA). FMECA is a procedure of fault identification and classification of its influence on aircraft operation. It is a tool for critical component recognition with PHM development playing a significant role. After the identification of these components, there follows the search for a measurable characteristic that contains a recognizable parameter whose measured value changes depending on the status of the component. Monitoring the status of this parameter is performed with the help of algorithms predicting the future development of the observed parameter based on the embedded hypothesis. The outcome of this procedure is *RUL*, along with the probability of such an outcome.

Prognostics and Health Management contain some major application challenges. Model parameters define degradation behaviour in physics-based prognostics. Model parameter definition is difficult due to the influence of data noise and bias. This, however, does not always exclude the possibility of accurate predictions. Noise also affects data-driven approaches. Data-driven approaches require a larger amount of data than physics-based approaches. Obtaining data is costly and requires a certain amount of time. When there are difficulties obtaining data directly related to damage, variables related indirectly can be considered. An example of this is vibration intensity which can be related to crack size. Again, noise plays a significant role while correlating vibration intensity and crack size, the signal-to-noise ratio is crucial for separating signal from noise.

Having these problems in mind, it is interesting to note that the development of prognostics and health management was pioneered by the aerospace and defence industry. Top performance requirements, as well as a high-risk margin, have impacted PHM development at a greater pace in this field.

The Health and Usage Management Systems (HUMS) patented by Rozak and Cycon [88] is an example of a PHM approach for rotorcraft that detects several problems from shaft unbalance to gear and bearing deterioration. Hess et al. [45] depict PHM as a key enabler for the JSF autonomic logistics concept. They emphasize its capabilities and aim to improve aircraft safety, improve sortie generation rate, decrease logistics footprint, and significantly reduce

operation and support costs. Brown et al. [89] provide an overview of the PHM data-driven concept, design and architecture, general capability description, and overall program status in the Joint Strike Fighter program. They describe on-board and off-board systems for fault detection and isolation, as well as fleet information sharing. The Future Combat Systems program was designed with PHM as an integral element of the system architecture, as shown by Barton [90]. McMollon et al. [91] provide an overview of the PHM concept, architecture, and incremental design approach.

The prognostic approach was applied to gas turbine engines, such as Rolls-Royce industrial AVON 1535, by Li and Nilkitsaranont [92]. Gupta et al. [93] consider the lifecycle of a PHM function, having in mind the drift from initial function assumptions which can lead to a loss of prediction performance. General Electric Aviation monitors aircraft engines for years, it is providing diagnostic services for early problem detection. Sun et al. [94] show survey PHM practices and case studies covering defence, aerospace, wind power, civil infrastructure, manufacturing, and electronics. PHM advanced in various fields, from rotating machinery, Marble, and Tow [95] to batteries Saha et al. [96], printed circuit boards [42], and solid rocket motors [97]. Further PHM technology maturing can lead to an increasingly important role in commercial systems, from design to operation.

2.4 The problems of PHM in aeronautics

When preparing data for prognostic model selection, especially when dealing with degradation data, bias needs to be taken into consideration. Noise or measurement error is a random fluctuation in measured data or signal. Bias is a static deviation from correct measurements due to calibration errors. Noise aggravates degradation signal identification and bias can introduce errors in prediction. According to Kim et al. [58], filtering noise and compensating bias has been major research issue for prognostics. Gu et al. [41] presented a prognostic approach that detects the performance degradation of multilayer ceramic capacitors under temperature humidity-bias conditions. Coppe et al. [98] showed that the uncertainty in structure-specific damage growth parameters can be progressively reduced, despite noise and bias in sensor measurements. Guan et al. [99] considered various uncertainties from measurements, modelling, and parameter estimations to describe the stochastic process of fatigue damage accumulation based on a maximum entropy-based general framework. The research found that noise induces slow convergence, and bias shifts parameter distribution. De-noising research was done by Zhang et al. [100]. In that research, the authors showed a de-

noising scheme that improves the signal-to-noise ratio and applied it to vibration signals from a helicopter gearbox test bed.

Prediction accuracy is influenced by prediction uncertainty, which primarily arises from future usage conditions. Additionally, materials can have properties that are highly sensitive to minor variations in composition, microstructure, and defects. Even small differences in these factors can significantly impact the material's performance. Uncertainty in degradation model parameters can be mitigated by incorporating measurements within a Bayesian framework. Consequently, physics-based methods often rely on Bayesian inference, as asserted by Kim et al. [58].

2.5 PHM in light aircraft maintenance

Unlike large aircraft, light aircraft are not equipped with many sensors to monitor and record in-flight data. For this reason, methods for monitoring parameters recorded by sensors are not applicable in the context of light aircraft maintenance condition prediction but are mainly methods based on models that mimic the physical properties of the observed aircraft part, component, or system. Chen et al. [27] analysed the effects of material fatigue on the landing gear of light aircraft using the Finite Element Method (FEM), comparing the fatigue characteristics of lightweight aluminium and composite landing gear structural parts for cross-sections round and square-shaped profiles. The authors verify the accuracy of the numerical analysis settings by comparing the stress ratio and the number of load cycles to the failure of a standardized test model with experimental values from the literature at different stress amplitude ratios. Grbović and Rašuo [101] researched crack propagation in the spar of a light aircraft wing. The research was carried out in three characteristic phases. In the first phase, the authors perform an experiment in which the wing spar is subjected to a cyclic load of constant amplitude and frequency and a cyclic load of variable amplitude and constant frequency. In the second research phase, the authors adjust numerical stress analysis settings by comparing the calculated strain and stress results with the recorded results from the experiment. In the third phase, the authors perform fatigue analysis using the computer programs Ansys and FRANC2D. The methodology in Ansys includes fatigue analysis based on measured load and fatigue analysis based on measured deflections in the test. The analysis methodology of the program FRANC2D involves integrating the modified Forman-Net NASGRO equation to calculate the change in crack length with the number of load cycles. In [102], Grbović et al. determines the cross-sectional area of the light aircraft wing spar for which fatigue analysis shows the largest number of load cycles to failure. The paper's methodology involves

integrating the Paris-Erdogan equation and comparing the results for two different cross-sectional shapes of the wing spar of a light aircraft. The authors determined the stress intensity factor at the crack tip using the Extended Finite Element Method (XFEM). Gowda and Basha [26] analysed material fatigue of tricycle nose-gear parts using the Finite Element Method.

In contrast to previous studies that refer to the parts which allow crack initiation and propagation, Gowda and Basha consider material fatigue only up to the point of crack initiation. This approach is explained by the unacceptable existence of cracks on parts of the aircraft landing gear. Lok et al. [44] consider the multiaxial stress state of tricycle-type landing gear to predict its remaining useful life. In the paper, the authors identify a landing with lateral drift as an event that causes a multiaxial stress state of the landing gear. Based on the components of the resulting landing gear landing load obtained by sensors in the Cartesian coordinate system, the authors perform numerical stress analysis and determine the stresses in parts of the landing gear structure, after which they calculate the equivalent stress using the Sines and Crossland theory. The equivalent stress was then used to determine the number of cycles to failure using S-N curves from the literature. The authors then use the Palmgren-Miner equation to calculate the cumulative *RUL* of the landing gear structure. Tao et al. [103] emphasize the role of material fatigue in aircraft accidents due to landing gear failure. The paper deals with the influence of landing gear overload on the service life of aircraft landing gear parts because of material fatigue. The research starts with calculating stresses and strains within the material's elastic properties using the Finite Element Method. They then perform corrections due to previously neglected properties in the plastic region of material deformation to calculate the amplitudes of elastoplastic stresses and strains using the Neuber equation. The authors use the "Rainflow" method for counting load cycles to calculate fatigue through calculated strain, with correction due to the multiaxiality of the load. The total accumulated fatigue was then calculated using the Palmgren-Miner equation.

From the above examples, the prediction of the condition of light aircraft is made by applying models that mimic the physical properties of the observed aircraft part, component, or system.

After systematic research, it can be concluded that no method for predicting the remaining useful life of light aircraft landing gear structures based on information from the operational records of these aircraft in a manner suitable for maintenance processes is defined in existing literature.

2.6 Overview of Methodologies in Landing Gear *RUL* Prediction

This Chapter reviews various research studies aimed at understanding methods used to predict the remaining useful life of aircraft landing gear structural parts. Special attention is given to research observing parameters relevant for remaining useful life estimation based on numerical strength calculation, such as loads acting on the landing gear structure. Initially, a brief summary for each considered research will introduce the research question, the types, components, or parts studied, and the key findings. Following each summary, the specific methodology is briefly presented. Lastly, Table 7 consisting of five columns is displayed. The first column serves to identify the observed research, consisting of the sub-Chapter number containing the corresponding review. The second column defines the object of observation, be it the complete aircraft landing gear, a structural part or other. The third column states the *RUL* indicator defined in the particular research for *RUL* prediction. The fourth column presents the *RUL* unit of measure (for example, the number of cycles or time until failure and others). The last column states the actual value of the *RUL* from the observed article.

The reviews are presented in a specific order intended to enhance the understanding of prediction methods, *RUL* relevant parameters and the resulting quantifiable data fit for comparison with results from this Thesis.

2.6.1 PHM Integration for landing gear *RUL* prediction

In paper [22] Hsu et al. delve into the critical role of landing gear in aircraft and the challenges it faces due to operational degradation, which can result in issues like the shimmy effect during take-off and landing. To counteract unplanned flight disruptions and optimize aircraft availability, the study investigates the predictive maintenance technique. The research showcases a case study on the prognostics and health management framework, aiming to enhance the health assessment and prediction of the remaining useful life for in-service aircraft. Utilizing machine learning, a health indicator for landing gear is developed via a data-driven approach, while time-series analysis assists in predicting its degradation. The findings have the potential to benefit fleet operators and streamline aircraft maintenance.

Research Methodology:

- Predictive Maintenance Technique Investigation: The study delves into the predictive maintenance technique, aiming to optimize aircraft availability and reduce unplanned flight disruptions.
- Health Assessment and Prediction: The research presents a case study that implements a health assessment and prediction workflow for the remaining useful life, leveraging the prognostics and health management framework.
- Data-Driven Approach: Machine learning methodologies are employed to develop a health indicator for the landing gear.
- Time-Series Analysis: The research utilizes time-series analysis to predict the degradation of the landing gear.

2.6.2 Machine Learning in *RUL* Prediction

The paper [23] delves into the feasibility of deploying machine learning algorithms to predict loads experienced by landing gears during landing. The primary focus is on the utilization of Gaussian process regression to foresee loads on landing gear components. The study leverages comprehensive measurement data from drop tests, encompassing strain measurements at critical points, acceleration measurements, shock absorber travel, tyre closure, shock absorber pressure, wheel speed, and ground-to-tyre loads.

Research Methodology Overview:

The central methodology of the research revolves around the utilization of machine learning algorithms, with a particular emphasis on Gaussian process regression. This regression is employed to predict loads on various components of the landing gear. The learning process relies heavily on comprehensive measurement data sourced from drop tests. Key data points include:

- Strain measurements at essential spots, like the side-stay and torque link.
- Acceleration metrics of the drop carriage and the gear itself.
- Data regarding shock absorber travel, tyre closure, shock absorber pressure, and wheel speed.
- Ground-to-tyre loads, which are ascertained through measurements made with a drop test ground reaction platform.

The overarching aim is to train the Gaussian process to predict loads at specific locations based on other available measurements.

- The paper's primary objective is to explore the viability of utilizing machine learning algorithms, especially Gaussian process regression, to predict the loads landing gears experience during a landing event.
- The research is grounded in comprehensive measurement data collected from drop tests. These tests provide metrics like strains at crucial locations, accelerations of the gear and drop carriage, shock absorber dynamics, wheel speeds, and ground-to-tyre loads.
- The overarching goal is to train the Gaussian process to predict loads at specific locations using available measurements. If successful, this would allow for the prediction of future load patterns using just these measurements.
- The intention is to develop an accurate model capable of predicting loads across the landing gear using measurements that are readily accessible or simpler to obtain than direct strain measurements on the gear.
- The paper also delves into the dynamics of the Main Landing Gear (MLG) during a landing, describing the forces and behaviors involved.
- The drop test data, crucial for this research, encompasses 21 individual drop tests and covers four distinct test set-ups. The variations in these tests include changes in vertical descent velocity, wheel speed, and ground friction.

2.6.3 Enhancing safety assessments: Validating machine learning in landing gear certification

This research paper [24] delves into the current certification process for landing gear used in the aerospace industry. As the aerospace sector begins to incorporate machine learning into structural health monitoring, challenges arise due to the non-deterministic nature of deep learning algorithms. This nature poses difficulties in obtaining certification and verification for use in the rigorously regulated aerospace domain. The paper outlines regulatory requirements and highlights the budding efforts towards standardization. To validate machine learning for safety-critical applications like landing gear, the safe-life fatigue assessment must be certified, ensuring accurate and reliable predictions of the remaining useful life. The document also offers insights into future certification processes for the integration of machine learning in critical aerospace systems, encompassing risk management and explainability considerations for various stakeholders in the certification procedure.

Research Methodology Overview:

The research primarily centers around the application of machine learning models, particularly offline models, for predicting the remaining useful life of landing gear systems. The approach employed is grounded in the safe-life method, which is a central tenet of the study.

A key facet of the methodology is the integration of certification processes, targeting these machine learning models. This involves examining risk assessments, uncertainties, and ensuring explainability for various end-users involved in the certification process.

The paper also discusses the increasing demand for new aircraft and the rising need for integrating and streamlining maintenance digitization. In this context, avionics systems, a subset of structural health monitoring, play a pivotal role.

Interestingly, outside of the main research focus, the paper states that CS-25 airworthiness certification requirements for large airplanes, the safe-life fatigue analysis that is currently used in the LG certification process utilises Miner's rule for damage accumulation, using S-N

curves. This is a approach similar to the one utilized in the research described in this Dissertation. These curves conform to a certain material coupon, where the material must be the same as that used in the component in question.

Lastly, valuable information is given in the form of expected flight cycles. Expected life cycles are based on industry implemented design lives divided into three categories based on their corresponding cycle ranges:

- 50,000 cycles for short-haul flight aircraft, e.g. A320.
- 25,000 cycles for long-haul aircraft, e.g. A350.
- 10,000 cycles for tactical aircraft.

2.6.4 FE analysis for landing gear testing

The research [25] focuses on the CAD design and static, modal and shock spectrum analysis of the landing gear for an unmanned test air vehicle. The analysis type employed in the document is a combination of static structural analysis for extreme loads and shock spectrum analysis with modal analysis as an initial step. This involved determining maximum stress development under extreme load conditions and identifying resonant conditions through modal frequencies. The primary aim is to assess the structural safety of the landing gear under both static and shock spectrum loads. The objectives of the study are:

- CAD design of the landing gear.
- Static and modal analysis of the landing gear.
- Shock spectrum analysis.

Approach:

Three Dimensional Model: The landing gear's 3D model is developed using Catia software.

Landing Gear Loads: The landing gear is subjected to various loads, including: Lift Load: 1000 N, Drag Load: 450 N, Side Load: 260 N, Torsion Load: 20000 Nmm. The article mentions that the landing gear loads are determined based on a number of load curves specified in FAR (Federal Aviation Regulations) rule books. These regulations provide guidelines for the design of landing gear for various types of aircraft operations such as level landing, one-wheel landing, and level landing with spring back, among others. The article does not contain specific details on the calculation of fatigue life. It discusses various types of analyses performed on the observed unmanned test aircraft landing gear, including static, modal, and shock spectrum analyses. These analyses are used to evaluate the structural safety and performance of the landing gear, particularly in terms of deflection and stress development under different loading conditions

Meshing: Different elements, like Beam elements, are applied for load transfer and connecting members.

Assumptions:

The material is considered elastic and homogeneous. Analyses are within elastic limits. Both solid and shell concepts are applied.

Static Analysis: The conventional material is replaced with a composite material to enhance the landing gear's performance. The results are compared between the composite and conventional materials in terms of displacements and von Mises stresses.

Modal Analysis: This analyses the vibrational characteristics of the landing gear. Different modal frequencies of the system are identified and corresponding mode shapes are analysed.

Shock Spectrum Analysis: The landing gear's deflection and stress responses to spectrum shock are observed.

The paper did not discuss the landing gear remaining useful life.

2.6.5 Nose landing gear dynamics & fatigue

The paper [26] explores the design and analysis of the main landing gear structure for a 737-400 aircraft and a conceptual new design model for a trainer aircraft's nose landing gear. It investigates all the functions, systems, and subsystems associated with the landing gear, such as shock-absorbing equipment, brakes, retraction mechanisms, and more. The paper also delves into the forces and tensions on the landing gear and axle, concluding that these are critical parameters for ensuring safe takeoff, landing, and taxiing.

- In the current work, a conceptual new design model of nose landing gear for a trainer aircraft is analysed under stress and fatigue life of the nose landing gear.
- Design and analysis of the main landing gear structure of a transport aircraft were conducted, along with fatigue life estimation for the critical lug.
- The analysis of the landing gear structure was proposed based on previous works by Horack.

The fatigue life analysis results from this research are as follows:

Table 1. Research results from paper [26].

Reaction, N	Spin up, Ksi	Spring back, Ksi	Number of cycles to failure
879	0.92	16.59	1.1305E6
879	0.92	16.59	1.1305E6
879	0.92	16.59	1.1305E6
1030	1.08	19.44	3.2002E5
1180	1.24	22.28	1.3152E5
1331	1.4	25.13	6.5684E4
1481	1.55	27.96	3.7389E4
1632	1.71	30.81	2.3146E4
1782	1.87	33.64	1.532E4
1933	2.03	36.49	1.062E4

The data in Table 3 is calculated using a fatigue analysis approach, which assesses the damage accumulated on the nose landing gear of an aircraft from the "Spin Up to Spring Back" load case. This analysis aims to estimate the fatigue life of the gear based on the stress experienced during landings and the number of cycles to failure.

2.6.6 Fatigue analysis of light aircraft landing gear

The paper [27] aimed to investigate the fatigue life of a CH 701 Light Sport Aircraft (LSA) landing gear made of different materials like aluminium alloy and carbon fiber-reinforced composites. Utilizing finite element software Ansys/Workbench, the study finds varying results for different composites and manufacturing methods. The paper concludes that the fatigue simulation platform used in this study produced results consistent with data from previous research, highlighting the stress and life cycles under different load conditions. The

methodology of this study was investigated in more detail due to the observed similarities with the research presented in this Dissertation.

Methodology:

Material Selection:

- 6061-T6 aluminium alloy and Carbon/Vinyl Ester composites (UNI 25) were chosen.

3D Model Creation:

- Used Pro-E to establish a 3D model of the observed aircrafts landing gear.
- Simplifications: Ignored the tires, holes, chamfers, and fillets (no such simplifications were implemented in the research described in this study due to the simplicity of the observed struts geometry).
- Created basic fatigue simulation samples of aluminum alloy plates and columns according to ASTM E466.
- Built a basic test sample of composites following ASTM 3039M.

Simulation Using Ansys/Workbench:

- Input boundary conditions:
  - Analysed basic samples of metallic fatigue loads ranging from 1,000 N to 20,000 N.
  - For landing gear loading simulation, used a maximum LSA takeoff mass of 600 kg and a maximum takeoff mass of 450 kg for the CH 701.
  - For fatigue testing, set the stress ratio $R = 0.1$, and $R = 0.1$ for simulating the cyclic loads of landing gear and $R = -1$, and $R = -1$ for the basic sample fatigue simulation.

Next, static and fatigue loads for different landing gear models were determined. Yield stress and maximum stress/strain were used to determine maximum static load limits. The research results fit for comparison with results from the research described in this Dissertation are presented in Table 2. The most relevant data is highlighted.

Table 2. Research results fit for result comparison, [27].

Material	**Weight**	**Landing Gear Shape**	**Max. Alternating Stress (MPa)**	**Life Cycle**
6061-T6 Aluminum Alloy	450 kg	Plate	47.337	>10E8
6061-T6 Aluminum Alloy	450 kg	Column	38.81	>10E8
6061-T6 Aluminum Alloy	600 kg	Plate	64.814	1.926E5

6061-T6 Aluminum Alloy	600 kg	Column	52.694	2.79E6

2.6.7 Landing gear-well beam lifecycle analysis

The paper [28] focuses on the stress analysis of landing gear well beams and the damage calculation due to landing cycles. It employs the Finite Element Method and the Wöhler method for high-cycle fatigue analysis. The study aims to understand the behaviour of the landing gear well beams under various loading conditions and concludes that the maximum stress should be compared with the yield and ultimate stress of the 2024 T351 aluminium alloy used in the landing gear structure. Fatigue damages under variable amplitude were estimated using the Palmgren-Miner rule.

- The study focuses on stress analysis of landing gear well beams and damage calculation due to landing cycles. The finite element method is used for analysis.
- The maximum stress is compared with the yield stress and ultimate stress of the 2024 T351 aluminium alloy used in the landing gear structure.

The fatigue life research paper results are presented in Table 3.

Table 3. Research results from paper [28].

Test number	G range	Cycles
1	0.5 g to 0.75 g	57000
2	0.75 g to 1 g	28000
3	1 g to 1.25 g	24000
4	1.25 g to 1.5 g	18000
5	0 to 1.5 g	50
6	-0.5 g to 1.5 g	100

The above Table 3. presents a load spectrum of a common 13 seater aircraft. The authors state that this data is provided by the designer and other various design teams. This is collected from the existing aircraft during the flight. The table gives various cycles of loading at different range.

2.6.8 Fatigue analysis of main landing gear lug joint

The paper [29] focuses on the design and analysis of a lug joint made from Al T6 7075. Through the use of Finite Element Analysis, the study aims to estimate the maximum local stress, which is crucial for fatigue analysis. The paper concludes that the fatigue analysis is key to predicting the structural life of the lug, and it offers dimensions for the proposed model based on the strength of material approach.

- The dimensions of the proposed model are obtained by the strength of material approach, and stress analysis and fatigue life are estimated.
- The fatigue analysis is carried out to predict the structural life of the lug.
- Stress analysis of the lug is conducted, and the maximum stress is identified around the hole of the lug, which is found to be lower than the yield strength of the material.

The fatigue life research paper results for the lug joint under observed operating conditions was 1.8E7 cycles until fatigue failure.

2.6.9 The role of failure analysis in structural integrity

The paper [30] delves into the failure analysis of an aircraft's strut, focusing on the high level of design stress and limited fracture toughness of the strut alloy. The study employs stress cycle blocks to assess damage and estimates the fatigue life of the redesigned strut to be 3367 flight cycles. The paper suggests that the fatigue life could be further increased with additional simple changes to the material, design, and fabrication processes.

- The study analysed the high level of design stress and the limited fracture toughness of the strut alloy to understand issues related to defect detection in the component before failure.
- Damage was assessed based on the blocks of stress cycles in the stress spectrum experienced by the strut in a typical flight cycle.
- After determining the cause and mechanism of failure, a design review was conducted by the aircraft manufacturer. This review linked fatigue analysis with flight cycle stresses, which were measured using strain gauges at critical points on the landing gear strut.

The fatigue life estimation methodology was examined in more detail due to similarities with this research.

Utilizing the S–N Curve:

- A generalized S–N curve for the strut steel under fully reversed loading is constructed.
- The curve is represented as a straight line on a log–log plot of stress versus life between two defined points. One point corresponds to the ultimate tensile strength (UTS) of the material and a life of 100 cycles. A second point corresponds to the fatigue limit stress and a life of 1,000,000 cycles.

- The fatigue limit strength for steel is estimated as 0.45 times the UTS.

Incorporating Correction Factors:

- Various factors such as surface finish, alloy type, load type, component dimensions, environment, and stress concentration factor are considered.

Damage Accumulation Using the Palmgren–Miner Rule:

- The damage caused by blocks of stress cycles is summed.
- The Palmgren–Miner rule linearly sums the fractional fatigue damage incurred by a component under various loading blocks.
- The damage accumulation rule is expressed as

$$D = \sum_{i=1}^{m} \frac{n_i}{N_i} \qquad (7)$$

Where:

D - Is the damage number;

m - Is a counter for the various stress amplitude blocks;

n_i - Is the number of stress cycles experienced in block i;

N_i - Is the number of load cycles causing failure at stress level i.

Modification Using Liu and Zenner's Approach:

- Liu and Zenner's modification is applied to the S–N curve to make it steeper at the level of the highest stress amplitude in the applied stress spectrum. This modification continues down below the fatigue limit stress.
- The slope of the S–N curve is calculated.
- The reciprocal slope of the S–N curve is used as per the Liu–Zenner modification.

Determining the Damage Number:

- The damage number is determined according to the Palmgren–Miner damage accumulation rule.

Calculating the Fatigue Life:

- Using the linear damage summation, the critical damage number is assumed.
- The fatigue life in flight cycles of the redesigned strut is calculated as the reciprocal of the damage number, resulting in a fatigue life of 3367 flight cycles.

The fatigue life analysis results from this research are presented in Table 4.

Table 4. Research results from [30].

σ (MPa), R = -1	n	N	Damage
828.3	0.25	8801	2.84E−05
776	0.25	12389	2.02E−05
751.7	0.25	14645	1.71E−05

734.1	0.25	16600	1.51E−05
705.4	0.25	20482	1.22E−05
701.3	0.25	21115	1.18E−05
Total damage			2.97E−04

The values in Table 4 are calculated using the Palmgren-Miner rule and the Liu-Zenner modified S-N curve. For each stress amplitude (σ_a):

- Stress amplitudes are known from the stress spectrum of the strut.
- *n* is the number of stress cycles at each σ_a from operational data.
- *N* is the cycles to failure from the modified S-N curve, adjusted for real-world conditions.
- Damage per cycle is *n*/*N*.

Total damage per flight is the sum of individual damages. The component's fatigue life is estimated by inverting the total damage per flight, assuming a damage number of 1 indicates failure.

2.6.10 Failure analysis of a landing gear nose wheel fork

The paper [31] discusses the design and fatigue analysis of a nose wheel fork made of selective laser melted Ti6Al4V(ELI). The study emphasizes the importance of experimentally validated Finite Element Analysis in the design process. The paper also provides data on displacement, von Mises stress, and safety factors for different load cases. It concludes that incorporating experimentally determined material data and the effects of inherent defects of the selective laser melting process can lead to more accurate design models.

- The study conducted fatigue testing on a fork without failure and also measured the number of cycles to failure under specific conditions.
- An experimentally validated Finite Element Analysis was used for designing the nose wheel fork. The material data were determined experimentally, and the effects of inherent defects of the selective laser melting process (like surface roughness) were incorporated into the simulation model.
- The design domain was kept the same as that of the original CAD model of the fork to avoid interference with other parts of the aircraft.

The number of load cycles until fatigue failure was calculated the following way:

- The CAD model of the nose wheel fork was discretized using quadratic tetrahedron elements.
- A plasticity material model with isotropic hardening was applied using experimental data obtained from Ti6Al4V(ELI) specimens with considered surface roughness. This data included the elastic modulus, Poisson's ratio, and plastic stress–strain values.
- The maximum *Z*-load of 8,300 N was divided into 5 equal partitions and applied on the nose wheel fork, along with boundary conditions replicating the experimental setup. The maximum load vas obtained based on previously introduced data which was experimentally obtained from Ti6Al4V(ELI) specimens during a previous research.
- Constraints were applied to various parts like the torque arm, shock strut, and wheel bushes.

Comparison with Experimental Data:

- The nodal strain results from the simulation were compared to those from strain gauges on the experimental prototype.
- Stress values from both simulation load cases were used for subsequent fatigue performance determination.

Fatigue Failure Simulation with fe-safe software:

- To account for the inherent surface roughness from the observed process, the stress vs. number of cycles to failure data of Ti6Al4V(ELI) standard fatigue specimens (with as-built surface roughness and tested at an R value of 0.1) was used as input for the fatigue simulations.
- The Uniform Material Law Method was employed to approximate fatigue material properties. The Uniform Material Law is a methodological approach that allows for the estimation of the fatigue curve of a material based on its tensile strength and hardness. This method is reported to be more suitable for aluminium and titanium alloys.
- Tensile data, crucial for approximating fatigue material properties, were sourced from standard test specimens with as-built surface roughness.
- Fatigue simulations for separate *X*-and *Z*-loads were executed using a stress ratio of $R = -1$ to $R = 1$, consistent with the experimental tests.

Computation of Cycles to Failure:

- The number of cycles to failure for the maximum *X*- and *Z*-load cases were computed using the above methodologies and compared with experimental results.

Research results are presented in Table 5.

Table 5. Research results from [31].

Fatigue load case	Applied load (N)	Frequency (Hz)	Number of cycles
X	6000	3	101609
Z	8300	3	15000

The authors obtained the tabular values presented in Table 5 through force-controlled experimental fatigue testing on a Ti6Al4V nose wheel fork.

2.6.11 Failure analysis of a nose landing gear piston rod

The paper [32] conducts a failure analysis of a fractured piston rod end using various techniques like Scanning Electron Microscopy and Finite Element Analysis. The study aims to identify the cause of fatigue crack initiation and propagation. The paper concludes that the cracks propagated in the direction perpendicular to the highest tensile stress and also delves into the chemical composition of the failed component.

- A finite element analysis was carried out at the failure region of the piston rod end to determine the stress distribution.
- The fractured surfaces of the failed piston rod end were examined with the help of a scanning electron microscope (SEM) to identify the cause of fatigue crack initiation and propagation.

2.6.12 Analysis of landing-gear behaviour

The document titled "Analysis of landing-gear behaviour" [33] is a technical note (No. 2755) published by the National Advisory Committee for Aeronautics. Authored by Benjamin Mllwitzky and Francis E. Cook from the Langley Aeronautical Laboratory. It discusses the mechanics of the landing gear, detailing the dynamics of the system, forces involved in the shock strut, and the forces exerted on the tire. The report then observes motion equations, discussing the motion before and after shock-strut deflection. The note also provides solutions to these equations.

The methodology primarily revolves around the evaluation of landing gear mechanics through mathematical and computational methods. The methodology includes numerical integration procedures such as linear, quadratic and Runge-Kutta for motion equation solving. A significant part of the methodology is the validation of the results produced by the employed motion equation integrations by comparing the calculated results with experimental data.

2.6.13 Light aircraft landing gear damage tolerance

The paper [34] focuses on studying the landing gear of Zenith STOL CH 701 light aircraft. It employs simulation analyses using finite element software FRANC2D and AFGROW. Static analysis and Stress Intensity Factor calculations were performed. The study aims to understand the relationship between crack length and the number of load cycles, as well as the residual strength at various stages of crack propagation. Notably, the research found that the residual strength of Ti-6Al-4V and 4340 materials is higher than that of aluminium alloys at different stages of crack growth.

The landing gear fatigue life was calculated in the following way.

2D Model Creation:

Stress Intensity Factor determination:

- The created model was imported into FEM software (FRANC2D), where parameters for static analysis and Stress Intensity Factor calculation were set up.
- This step determines the relationship between the crack length and the Stress Intensity Factor.

Beta Modification Factor Determination:

- Using FRANC2D, the relationship between the beta modification factor (required for AFGROW) and Stress Intensity Factor was determined.

Landing Gear Life Cycle Calculation:

- The authors used FRANC2D to establish the relationship between the stress intensity factor and the beta modification factor. This factor is necessary for the execution of AFGROW, which is a crack growth analysis software.
- The authors then imported the stress intensity factor and corresponding beta modification factor value into AFGROW to calculate the life cycle of the landing gear.
- The critical stress intensity factor and the β value were used to assess how crack propagation affects the residual strength of various landing gear materials over the load cycles.
- This procedure determined the relationship between crack length and the number of load cycles.

Effect of Crack Propagation on Residual Strength:

- The effect of crack propagation in various landing gear materials on residual strength was determined using the relationships between the crack length, critical stress intensity factor, and beta modification factor.

AFGROW Analysis:

- The authors used the NASGRO equation to define the relationship between crack growth and life cycle within the AFGROW simulation analyses.

Residual Strength Determination:

- The maximum stress sustainable for landing gear without cracks was determined through static load analysis.
- The residual strength of structures containing cracks was calculated in relation to the propagating crack lengths using the residual strength equation.
- Combined with damage tolerance life cycle analysis, changes in the residual strength of the structure in relation to the load numbers or frequencies were determined.

Table 6. Research results from [34].

Material	**Critical Crack Length (mm)**	**Life Cycles**
6061-T6	10.942	4.8E4
6061-T651	10.998	1.62E5
7075-T6	10.990	5.82E4
2024-T3	12.107	1.23E5
AISI 4340	14.637	1.32E6
Ti-6Al-4V	16.246	7.44E5

2.6.14 Analysing large aircraft landing gear dynamics

The paper [35] investigates the impact of active control systems on landing gear performance through simulations for medium and large mass configurations. The study shows that the airframe-gear force with active gears was generally smaller than that with passive gears, leading to reduced cyclic forces during all phases of landing. The paper concludes that the use of active controls could make ground operational loads more important, particularly when reducing aerodynamic manoeuvre and/or gust loads.

- The study conducted landing simulations for medium and large mass configurations and compared airframe-gear-force results.
- For active-gear simulations, hydraulic fluid flow rates and the volume of fluid transferred were analysed to evaluate the operational compatibility of the simulated control hardware and the modified landing-gear shock strut.
- A comparison of the typical airframe-gear-force time histories was made between simulated airplane landings with passive and active gears. The focus was on

understanding the magnitude of the cyclic forces during different phases of the landings.

2.6.15 Small aircraft main landing gear stress analysis

The paper [36] focuses on the stress and impact loads on landing gear, particularly during the landing phase. It emphasizes the importance of understanding two key forces that act upon landing gear: the normal force and the spin-up back force. The paper explores various landing gear models through numerical strength analyses to understand these forces and their impacts better. Forces such as the normal force and the spin-up back force are considered for stress analysis of the landing gear for Cessna 152 during touchdown. Three landing gear models are proposed to reduce stress values while keeping dimensions and materials the same as in the original observed part. The landing gear models involved positive curves on the landing gear strut. The study concludes that making positive curves can reduce the value of stress and deflection on the landing gear, depending on the principle of bending moment in the beams. The paper also cites previous research on UAV aircraft made of composite material, testing axial and uniaxial reinforcements.

- Three models are proposed to reduce stress values while keeping dimensions and materials the same as the original model. The models involve making positive curves on the landing gear strut.
- In one of the suggested models, the landing gear is divided into two parts: the upper part in the vertical direction and the lower part taking a convex shape. The purpose of this division is to reduce the value of the inclined part and to generate initial curvature in the opposite direction of the normal force.
- Two models for the landing gear are considered specifically to reduce the maximum stress. These modifications depend on changing the shape of the landing gear strut, dividing the strut into two parts.

The remaining useful life of the observed landing gear strut resulting from the acting loads was not subject of this research

2.7 Landing Gear Methodology Review Findings

Certain research findings from the papers observed in Chapter 2.6 were selected due to their type and format which made them compatible for comparison with the data generated by the research described in this Dissertation. The research findings are presented in Table 7.

Table 7. Selected research findings fit for comparison.

Research reference	**Object of Observation**	***RUL* indicator**	***RUL* parameter**	***RUL* value**
[22]	The landing gears of an aircraft fleet consisting of 5 airplanes	Vibration signal from the built-in flight control accelerometer	Number of predicted maintenance sorties (PMS), number of actual maintenance sorties (AMS)	PMS - (260, 270, 227, 294, 274) AMS- (271, N/A, 221, 256, 263)
[24]	General aviation certified aircraft landing gears in general	Wheel speed, accelerations in the LG, and similar flight variables, consisting of kinematic approaches related with changes in velocity and displacement, in order to result in load induced on the LG	Industry accepted expectation on the number of flight cycles to failure	50,000 cycles for short-haul flight aircraft, e.g. A320. 25,000 cycles for long-haul aircraft, e.g. A350. 10,000 cycles for tactical aircraft.
[26]	Nose landing gear	Nose landing gear reaction during landing in Kg., spin up force in KSI, spring back force in KSI	Number of operation cycles until fatigue failure	Research findings presented in Table 1
[27]	Landing gear's ability to withstand cyclic stresses	Stresses and strains determined by numerical strength analysis in Ansys fatigue life simulation software	Number of load cycles to failure, each load cycle representing an aircraft operation	Research findings presented in Table 2
[28]	Landing gear beam	Stress determined by numerical strength analysis in Ansys Workbench	Number of load cycles to fatigue failure, each load cycle representing an aircraft operation	Research findings presented in Table 3
[29]	Fatigue strength of a landing gear lug joint	Stresses and strains determined by numerical strength analysis in Ansys fatigue life simulation software	Number of load cycles to fatigue failure, each load cycle representing an aircraft operation	1.8E7
[30]	Main landing gear plate shaped strut made form AISI 5160 steel	Stress induced by load cycling on the observed main landing gear model	Number of load cycles until fatigue failure	Research findings presented in Table 4.
[31]	Material under different conditions of fatigue limit stress	Stress induced by applied cyclic load	Number of load cycles until fatigue failure	Research findings presented in Table 5

[33]	Light aircraft Cessna 210, Joint between the landing gear and the landing gear strut	The crack growth rate according to the NASGRO crack propagation equation	Number of load cycles until fatigue failure	Research findings presented in Table 6

Result comparison was done by comparing the calculated numbers of operations to failure, produced by this research, shown in Table 20, and other research results summarized in Table 7. The comparison is described in Chapter 6.2 of this Thesis.

3 USE OF OPERATION AND MAINTENANCE RECORDS FOR LIGHT AIRCRAFT STRUCTURAL PART *RUL* PROGNOSIS

In this Chapter, various data sources originating from aeronautical regulators, aircraft manufacturers, and operators are explored. These sources hold significant potential for predicting the remaining useful life of light aircraft landing gear structures, using a novel sensor-less approach, and leveraging data that is regularly recorded during aircraft operation. The specific limitations that are faced in data collection for light aircraft are discussed, emphasizing the constraints and opportunities this presents for the subject predictive model.

3.1 The division of general aviation aircraft

The International Civil Aviation Organization (ICAO) characterizes general aviation (GA) as encompassing all operations of civil aviation aircraft, with the exception of those used for commercial air transport or aerial work. Aerial work is specifically described as specialized aviation services carried out for a variety of purposes, [104]. The European Union Aviation Safety Agency (EASA) [105] divides general aviation operations into two main categories: commercial and non-commercial aviation operations. Civil aircraft without a revenue-generating purpose are significant stakeholders in various aeronautical safety-board accident reports. Regardless of the aircraft type, all civil aircraft operations have a common denominator, safety. Aircraft maintenance is a safety issue. The European Aviation Safety Agency consistently identifies aircraft maintenance as one of the safety issues since 2015 for large aircraft used in commercial air transport (CAT) as stated by Insley and Turkoglu [49]. Additionally, from an economic viewpoint, the maintenance definition given by Rodrigues et al. [106] emphasizes that the safe performance of required operations is an adequate replacement for revenue generation. Insley et al. [49] also found that aircraft maintenance costs can contribute to an airline's overall expenditure ranging between 10 to 15 %.

In general, aircraft maintenance approaches can be divided depending on the existence of a present or probable future maintenance requirement (failure). Maintenance performed for an existing reason is commonly called reactive or corrective maintenance, whereas maintenance performed for possible future reasons is called proactive. According to Fei et al. [107], reactive maintenance steps into action after the occurrence of a failure. On the other hand, proactive maintenance consists of preventive and predictive maintenance. Preventive maintenance is performed in predetermined intervals to reduce the probability of failure or performance

degradation according to Guillén et al. [108]. Predictive maintenance involves the replacement or repair of components or systems by predicting their future operational conditions. Predictive maintenance is currently at the cutting edge of aircraft maintenance research, sometimes referred to in a holistic term, "Prognostics and Health Management" (PHM). Goebel et al. [59] define the role of state prediction in aircraft and other technical systems during health management as predicting the required time to realize a future event or condition. Future state prediction determines the observed part or system *RUL*, consequently determining maintenance requirements.

Prognostics and Health Management applied to aircraft maintenance depend on the aircraft type and complexity, as well as the type of intended operation. Various divisions of civil aircraft operations exist depending on the competent regulatory authority.

Regulatory differences between those two categories and their sub-categories are based on risk hierarchy to maintain a proportionate level of safety that correlates with aircraft complexity. Further operations division is provided to ensure proportionality for various aircraft types as shown in Figure 7. Commercial aviation operations branch into Commercial Air Transport operations (CAT) and Special Operations (SPO). Non-commercial aviation operations are even more diverse, including Non-commercial operations with complex aircraft (NCC), Non-commercial operations with non-complex aircraft (NCO), and Special Operations (SPO) with complex and non-complex aircraft.

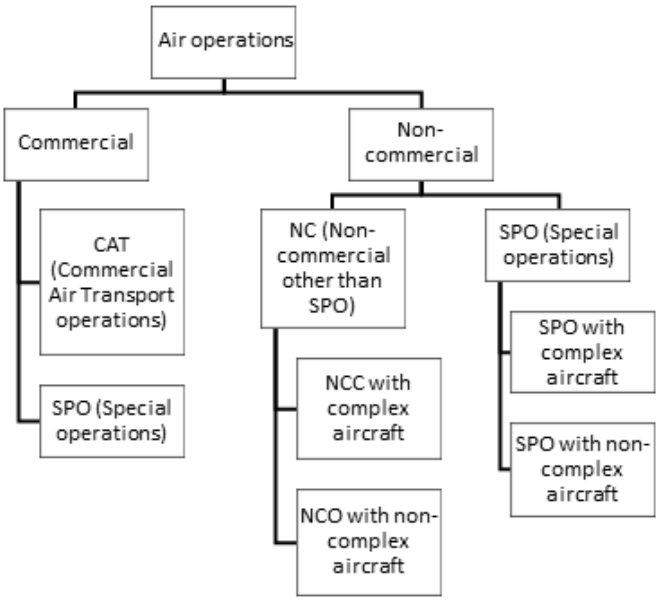

Figure 7. EASA general aviation operation types, [105].

From a regulatory standpoint, NCC and NCO aircraft are differentiated by the complexity of their respective safety rules governing aviation operations. To distinguish between complex

and non-complex aircraft, the European Union Aviation Safety Agency policy (EU) 2018/1139 [109] sets the minimum disjunctive standards for complex aircraft, Figure 8. Complex aircraft are divided into airplanes, helicopters, and tilt-rotor aircraft.

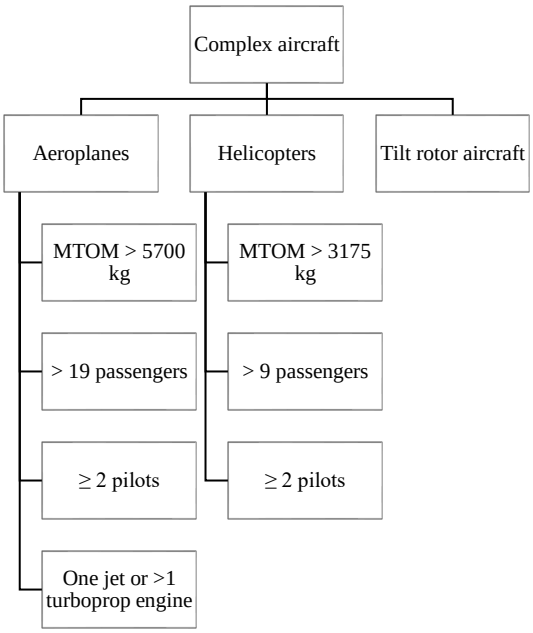

Figure 8. Complex aircraft prerequisites, [109].

Furthermore, non-complex aircraft is defined by Regulation (EU) 800/2013 [110] as manned European Light Aircraft and divided into categories named ELA 1 and ELA 2, Figure 9.

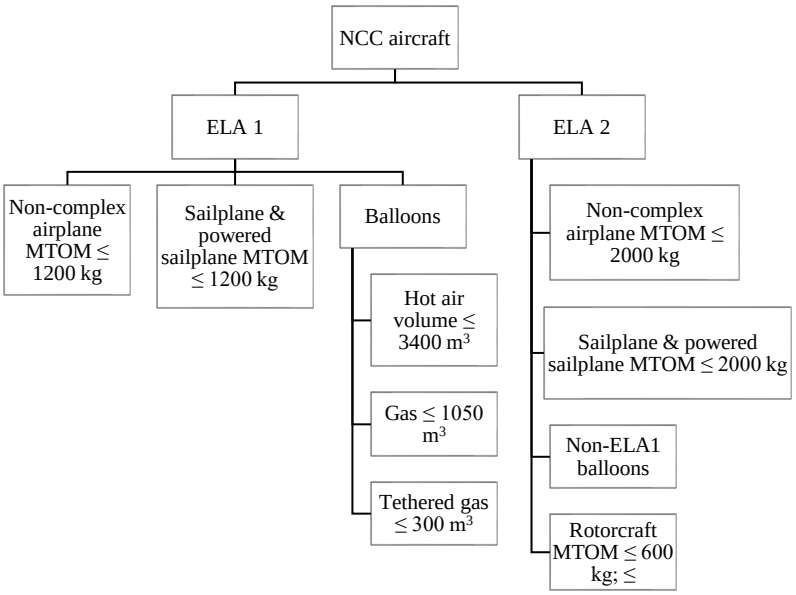

Figure 9. Non-complex aircraft types, [110].

Aircraft named ELA 1 are airplanes, sailplanes, powered sailplanes under 1200 kg maximum take-off mass (*MTOM*), and balloons which are differentiated by their hot air, gas, and tethered gas volume. ELA 2 aircraft are characterized by a higher $MTOM \leq 2000$ kg, which applies to airplanes and sailplanes; they also encompass balloons not classified as ELA1.

Additionally, ELA 2 category includes simple very light rotorcraft (*MTOM* ≤ 600 kilograms) that accommodate no more than two occupants, are not powered by a turbine or rocket engine, and are restricted to operations under visual flight rules.

3.2 Nationally regulated aircraft

The European Parliament declared common rules in civil aviation, establishing a European Union Aviation Safety Agency policy by issuing regulation (EU) 2018/1139 [109]. Regulation (EU) 2018/1139 recognizes the inappropriateness of subjecting all aircraft to the same set of rules; it exempts some types of aircraft and subjects them to the regulatory control of the European Member States where those aircraft operate. Regulation (EU) 2018/1139 recognizes aircraft that are of simple design or operate mainly on a local basis and those which are amateur-built or particularly rare or only exist in a smaller number. Those aircraft are exempt from regulation (EU) 2018/1139, considering their limited risk to civil aviation safety. Additionally, regulation 2018/1139 states that aircraft carrying out military, customs, police, search and rescue, firefighting, border control, and coastguard or similar activities and services undertaken in the public interest should be under national regulations while performing their respective operations.

According to one of the European member state national regulatory bodies, the Croatian Civil Aviation Agency (CCAA), aircraft that are exempt from EU regulations are aircraft performing operations of public interest as stated above, and aircraft such as microlight airplanes and helicopters, gyroplanes, gliders, balloons, former military aircraft, experimental aircraft, scientific aircraft, amateur-built aircraft, historically significant aircraft, and aircraft replicas, [111]. The latter group are all aircraft primarily used for sports and recreational purposes. Authors De Voogt et al. [17] recognize sports and recreational aviation as a general aviation category that includes gliders, balloons and blimps, gyroplanes, and ultralights. For example, ultralight aircraft, as described by Pagán et al. [18], are aircraft that are defined by the Federal Aviation Administration (FAA) Federal Aviation Regulations (FAR) part 103 as lightweight, low-powered, recreational aircraft with one or two seats; pilot certification is not required to fly them and industry self-regulation is mandated. This description corresponds to some degree to microlight aircraft, as stated by the CCAA, [112]. The authors conclude that the FAA operates only in a monitoring capacity, and ultralight aviation is self-regulated under organizations such as the Experimental Aircraft Association (EAA) and United States Ultralight Association (USUA), providing certification for ultralight instructors and pilots under FAA advisory circulars and regulations.

In conclusion, accident reports and the author's personal experience both highlight that the total number of light aircraft is quite significant and should not be underestimated.

3.3 Light aircraft accidents

According to the Statistical Office of the European Union (Eurostat) [19], there were 122 fatalities recorded in 2020 in aviation accidents on the European Union (EU) territory involving EU-registered aircraft. Eurostat states that most air accident fatalities in 2020 (93.5 %) concerned general aviation aircraft. Small airplanes, dirigibles, paragliders, motor-gliders, "microlights", small helicopters, and hot air balloons recorded the highest share of fatalities (91 % of all fatalities in EU aviation accidents) [19]. Relevant aviation accident literature by De Voogt et al. [17] recognizes sport and recreational aviation as a special general aviation category characterized by diverse aircraft types and predominantly recreational flight operations. De Voogt et al. [17] show that the highest number of accidents was found with gliders, but the highest relative number of fatal accidents came from ultralight aircraft (45 %) and gyroplanes (40 %). The fewest number of accidents was found in ballooning, the smallest in glider operations. However, the percentage of fatal accidents in sports aviation was slightly lower (2.3 %) than that found in other general aviation aircraft, as shown by Li et al. [21].

A significant part of sports and recreational aviation is amateur-built aircraft. Research performed by Nelson et al. [20] displayed that between 1983 and 2001 the total number of amateur-built aircraft accidents was 3752, including a 30 % fatality rate, as opposed to 19 % fatalities in other general aviation aircraft flying in the U.S.A. As reported by the Aviation Policy and Plans General Aviation and Air Taxi Activity Survey of 2000 [113], the ratio of the number of accidents and the number of aircraft in operation is much higher when observing amateur-built aircraft compared to other general aviation aircraft. Nelson et al. [20] found that amateur-built aircraft accounted for 3 % of general aviation aircraft but made up 10 % of the accidents. There was a 50 % greater chance of an amateur-built aircraft being destroyed in an accident, having double the probability of a fatal outcome. Nelson et al. [20] conclude that amateur-built aircraft are a particular risk in sports and recreational aviation. The peculiarity of amateur-built aircraft is that one individual often carries out their design, construction, modifications, and maintenance without being required to have a background in aviation.

Another significant part of sport and recreational aviation is ultralight aircraft. The FAA [114] defines an ultralight vehicle as a single-occupancy aircraft intended for sport or recreational purposes only, without a U.S. or foreign airworthiness certificate. If powered, it must weigh less than 254 pounds (115.21 kg) empty, have a fuel capacity not exceeding 5 U.S.

gallons, and have a maximum airspeed of 55 knots at full power in level flight with a power-off stall speed not exceeding 24 knots. If unpowered, it should weigh less than 155 pounds (70.3 kg). Safety devices like parachutes can be excluded from the weight calculation, with up to 24 pounds allowed for parachute systems, and up to 30 pounds per float for float-equipped ultralights. According to the Ministry of Maritime Affairs, Transport and Infrastructure of the Republic of Croatia [111], microlight aircraft, which is equivalent to ultralight, can be airplanes, helicopters, gliders, and motorized gliders, with no more than two seats and a maximum take-off mass of 600 or 650 kilograms, respectively, depending on whether they are intended for operations from land or water. De Voogt et al. [17] compared ultralight accidents in the United States, United Kingdom, and Portugal by their proportionate number of fatal accidents, main causes, and pilot information. The research found a higher ultralight aircraft accident severity when compared to other types of sport aircraft. By analysing ultralight aircraft accident statistics, Pagán et al. [18] observed the operation phase and discerned between active and latent failures. A latent failure cause investigation was not performed on ultralight aircraft before that research. The most common operation phases at which ultralight aircraft accidents happened were approach and landing. The authors suggest a possible reason being their small size and usual unprofessional maintenance since ultralights allow certain maintenance procedures to be performed by the owner and/or pilot. Depending on the observed authority, an ultralight aircraft owner can also be the pilot and the maintenance technician, providing they have the appropriate pilot's license and technical ability according to the respective regulation [111]. Authors Pagán et al. [18] determined a threshold of about 40 hours of flying experience where pilots with less experience had a significantly higher chance to be involved in loss of control-related accidents. In contrast, pilots with more than 40 hours of flying experience had a higher chance of engine failure and other maintenance-related accidents. Pagán et al. [18] found that research assisting ultralight accident prevention is scarce. The authors [18] conclude that the most significant problems causing ultralight aircraft accidents are lack of experience, inadequate maintenance skills, and unfamiliarity with the aircraft.

Research done by De Voogt et al. [17] suggests that no general comparison of aircraft accidents within sports and recreational aviation exists; this is consistent with the findings of this research. Nevertheless, since regulations governing the maintenance of nationally regulated sport and recreational aircraft [111] allow the pilot and/or owner to perform many maintenance actions, having little to no professional maintenance experience, the concern of possible safety issues due to inadequate maintenance is raised.

3.4 The problem with implementing PHM in light aircraft maintenance

Rodrigues et al. [106] emphasize the role of PHM research for aircraft operators; maintenance, repair, and overhaul service providers; aircraft manufacturers; and original equipment manufacturers in achieving reductions in operational costs and increases in fleet reliability. As stated by Qi et al. [115], the major functions of PHM are achieved by data acquisition, data analysis, fault diagnostics, health assessment, life prediction, and maintenance decisions. This then enables better failure prevention, repair planning, and maintenance scheduling. The authors' Qi et al. [115] state that data collection is performed with the help of various transducers; data mining, data transformation, and feature extraction are performed afterward to acquire systematic health state information.

To determine the *RUL* for predictive maintenance decision-making, the identification of degradation-relevant variables is required. Relevance is determined by correlating the observed variable with the degradation. It is possible to consider one or more variables that unambiguously define the current state of the object of observation. Maintenance actions are applied when the observed variable reaches a predetermined value representing a critical value. Critical values of degradation-related variables are defined after applying prognostic methods, giving insight into probable future degradation of the object of observation. Degradation-related variables are usually monitored with various sensors. Sensor data acquisition in large commercial aircraft is common. Gouriveau et al. [1] state that modern large commercial aircraft have many sensors (approximately 300000), creating a flood of information that can be used for state prediction.

Based on the described PHM research and the above examples of PHM application, it can be concluded that prognostics and health management applied to aircraft maintenance increases operational safety and optimizes the maintenance plan based on the projected future condition of the aircraft or some of its components. Current PHM development is concentrated on optimizing prognostic processes according to the observed situation, determination of prognostic uncertainty, and prognostic performance measurement.

The optimization of prognostic processes used in aircraft maintenance depends on the observed aircraft, maintenance personnel, required tools and equipment, and maintenance logistics. Those maintenance predispositions vary substantially when comparing large commercial aircraft and light aircraft, especially aircraft used for sport and recreation [106]. Light aircraft do not have the same sensor technology as large commercial aircraft do.

Approaching PHM implementation in light aircraft maintenance the same way as in large commercial aircraft would significantly raise the cost and complexity of those aircraft and their maintenance. Considering the required steps for PHM implementation in large commercial aircraft regardless of the numerous benefits PHM implementation has demonstrated, the light aircraft owner will likely reject PHM implementation into his aircraft maintenance routine, finding it costly and complicated.

Light aircraft often have a hard-time maintenance schedule that disregards the aircraft's usage conditions. The same aircraft model is often used by a single pilot for recreational purposes, in excellent weather conditions, taking off and landing on a smooth asphalted surface, and for pilot licensing purposes carrying two pilots and taking off and landing on a rough grass runway. Consequently, the *RUL* of affected parts, having the same hard-time maintenance interval, is different. Implementing a simple prognostic and health management system capable of warning the maintainer of the need for early part replacement could increase the safety of light aircraft operations. Implementing prognostics and health management in light aircraft maintenance requires prognostic methods depending on the type and operation of the observed aircraft part, component, or system. Saxena et al. [55] differ between PHM methods used on objects operating on a mechanical Lu et al. [116], Babbar et al. [117], Coppe et al. [85], electronic, Pan et al. [51], Batzel et al. [43], or chemical Saha et al. [96], Calvello et al. [118] basis. The remaining useful life of a light aircraft part, component, or system depends on its most significant *RUL* deterioration factor, such as material fatigue in light aircraft landing gears, [2].

According to Campbell et al. [16], aircraft material fatigue was the direct cause of 2240 deaths, and 1885 plane crashes, respectively, from the start of recording to 1984. Campbell and Lahey identified the two aircraft systems with the highest failure rates due to material fatigue, namely the propulsion system and the landing gear system. The research showed that an average of 100 aircraft accidents occur annually due to material fatigue, of which 18 are a direct consequence of material fatigue of metal parts. Material fatigue is primarily dictated by the amplitude and frequency of the load acting on the observed part and environmental conditions. The amplitude of the load is dictated by the mass of the aircraft and the way the aircraft is used, while the frequency of the load is defined by the way the aircraft is used. While environmental conditions are not always part of light aircraft flight records and the aircraft must perform the operations for which it is intended, aircraft mass and mass displacement remain regularly recorded information relevant to fatigue deterioration. The mass of the light aircraft can be divided into two categories, the mass of the empty aircraft and the operating mass of the aircraft,

including the mass of crew, passengers, luggage (in the case of passenger aircraft), other cargo, and all masses needed to perform operations (technical fluids, fuel, etc.). In doing so, the ratio of aircraft operating mass to empty aircraft mass must be considered, as this ratio gives insight into the load variation to which the aircraft's load-bearing structure is exposed during various operations. Aircraft load variation correlates with the fatigue life of various parts and systems, such as the landing gear. This explains why the landing gear fatigue life (and therefore *RUL*) of two identical aircraft's landing gears can be different. For example, an ultralight aircraft designed to have a maximum take-off mass (*MTOM*) of 473.5 kg (*MTOM* limited by European Commission regulation No 216/2008) can have an empty mass of 280 kg (for example a Pioneer 300 ultralight airplane), meaning approximately 40 % of the total aircraft take-off mass varies from flight to flight. This variability is one of the reasons why light aircraft airframes and systems have a high ratio of hard-time maintenance items to total maintenance items than commercial air transport aircraft. Additionally, the hard-time maintenance approach is preferred in light aircraft because it doesn't require expert knowledge and experience in professional aircraft maintenance, resulting in simplified aircraft maintenance operations.

Fleet databases and advanced sensor technology are not common in light aircraft, consequently inhibiting the first step in prognostics and health management - data acquisition. As stated by Pagán et al. [18], the most significant problem facing light aircraft, especially those used for sport and recreation is that many pilots either lack experience or are unfamiliar with their aircraft's proper maintenance and configuration. The authors recognize that the pilots themselves mostly perform maintenance of light and ultralight aircraft.

Light aircraft and sport and recreational aircraft maintenance personnel do not have the means or knowledge to perform predictive maintenance since those aircraft are not equipped with numerous sensors and supporting systems for collection, storage, and analysis of data that could be used for prognostic purposes. However, even sport and recreational aircraft operations are accompanied by operation records, including parameters that can be used for structural part *RUL* prognosis.

3.5 PHM relevant information in mandatory operation documents

Based on the provided information, it is proposed that data can be collected based on records from aircraft operations and maintenance. For example, the rules on conditions and manner of use of airplanes and helicopters not subject to regulation (EU) 2018/1139 [52], issued by the Ministry of Maritime Affairs Transport and Infrastructure of the Republic of Croatia,

mandates the presence of the following documents on board during each airplane or helicopter flight:

- Aircraft flight manual.
- Certificate of airworthiness or permit to fly.
- Certificate of registration.
- Noise certificate (if applicable).
- Insurance documents.
- Journey logbook.
- Appropriate navigational charts for flown routes or possible route alterations.
- Procedures and visual cues used by intercepting and intercepted aircraft, which must be easily accessible to flight crew members.
- All other documents related to the flight, which may be requested by the countries through which the flight is performed.

Aircraft classified as complex motor-powered aircraft used in non-commercial flight operations and aircraft used in commercial flight operations also have the following documents on each flight:

- Radio station operation license.
- Airplane technical book in accordance with Part-M.
- Information on the completed ATS flight plan (if applicable).
- Information on the search and rescue service for the area in which it is intended to fly.
- A copy of the operator's statement and/or the Authorization of high-risk flight operations from the air.
- Parts of the operations manual related to crew duties.
- A list of minimum equipment or an appropriate document (if applicable).
- Operational flight plan (if applicable).
- Relevant NOTAM / AIS data; appropriate meteorological data.
- Notification of special categories of passengers and special cargo, including dangerous goods, if applicable.
- Mass and balance documentation (if applicable).

Some of the above documents have information directly related to the specific flight. The author of this research proposes that it is possible to extract data relevant for prognostic purposes in light aircraft maintenance, thereby gaining information that can be utilized for better maintenance decision-making.

Regulations applicable to sport and recreational aircraft exist in various countries, such as the rules on conditions and manner of use of sports and recreational aircraft [52], issued by the Ministry of Maritime Affairs Transport and Infrastructure of the Republic of Croatia. According to this regulation sports and recreational aircraft must have the following documents on board:

- Aircraft flight manual.
- Aircraft registration certificate.
- Statement for carrying out commercial operations when applicable.
- Original permit for the use of radiofrequency spectrum on an aircraft when applicable.
- Insurance policy.
- Technical logbook.
- Original airworthiness certificate or flight permit.
- Original airworthiness check certificate.
- Operator's list of permissible malfunctions, when applicable.
- Minimum equipment list, when applicable.
- Flight plan, when required.
- Airline maps suitable for the route of the proposed flight and for all routes that can reasonably be expected to be a flight redirection.
- Appropriate documentation on instructions from Notification of Aircraft Staff (Notam) and Aircraft Service.
- Applicable meteorological information.
- Mass and balance sheets.
- Information on search and rescue services for the area of foreseen flight, which are easily accessible from the pilot's cabin.
- Standard operating procedure, when applicable.
- Checklists and other documentation required for flight operations.
- Pilot license.
- Pilots personal identification document with picture.
- Pilots logbook.
- Pilots health certificate.

Some of the above documents have information directly related to the specific flight, representing an opportunity for PHM application, such as the aircraft technical logbook, its mass and balance sheets, and the pilot's logbook.

According to the Croatian regulation governing the construction, renewal, maintenance, and continuing airworthiness of aircraft not regulated by (EU) 2018/1139 [111], the aircraft technical logbook must include the following information:

- Aircraft manufacturer and type.
- Year of aircraft manufacture.
- Aircraft serial number.
- Aircraft registration.
- Aircraft total flight hours and the number of take-off/landing cycles.
- Observed malfunctions or damage to the aircraft and/or its components.
- Certificates of release to service the aircraft and/or its components.
- Pre-flight inspection information.
- Other information if deemed necessary.

Another regulation, governing the conditions and manner of use of airplanes and helicopters not regulated by (EU) 2018/1139 [52], mandates the required information included in the aircraft mass and balance sheets as follows:

- The dry operating mass and the associated position of the centre of gravity.
- Cargo mass, fuel mass.
- Aircraft mass and centre of gravity position on take-off, landing, and without fuel.
- Aircraft loading information, and cargo distribution.

The third PHM-relevant data source is the pilot's logbook. The Croatian regulation governing the conditions and manner of use of sports and recreational aircraft [52] mandates the following information to be present in the pilot's logbook:

- Personal data on the logbook owner.
- Name and surname and address of the pilot.
- Name and surname of the pilot-in-command.
- Flight date.
- Place and time of take-off/landing.
- Aircraft type.
- Aircraft registration.
- Total flight time.
- The total number of flights.
- Flight time (total pilot flight time, pilot-in-command flight time, instructor flight time), and notes (checklists, etc.).

3.6 Specific data acquisition for PHM

Depending on the prognostic method used, it is possible to consider one or more parameters that unambiguously define the current condition of the observed part and/or component and enable condition prognosis. Maintenance actions are applied when the observed parameter reaches a predetermined threshold representing a critical value, i.e., a favourable moment for applying maintenance procedures. The predetermined critical value of the observed parameter depends on the remaining useful life of the observed part, component, or system. Determining the *RUL* of any aircraft part, component or system requires the application of appropriate prognostic methods. Data acquisition for prognostic method application depends on the relevant *RUL* deterioration mechanism or mechanisms and the availability of deterioration-relevant data. Light aircraft often have more than one *RUL* deterioration mechanism, depending on the observed part, component, or system. When observing *RUL* deterioration of light aircraft landing gears, material fatigue, and impact damage accumulation due to hard landings are the primary cause of *RUL* deterioration. Environmental conditions also influence metal fatigue, although to a lesser degree.

Light aircraft landing gear *RUL* deterioration relevant data can be extracted from:

- The aircraft technical logbook.
- The mass and balance sheets.
- The pilot's logbook.

The relevance of the observed data can be determined by correlating the observed parameter with fatigue degradation and impact damage accumulation.

The aircraft technical logbook contains general information, such as the aircraft's manufacturer and type, the year of manufacture, and the serial number, which are necessary for accurate data management and sorting during data acquisition. The aircraft technical logbook also contains aircraft operation history information like total airframe flight hours, the number of take-off and landing cycles, observed malfunctions, and damage to the aircraft and/or its components. This data is essential when implementing methods to determine fatigue deterioration and impact damage accumulation on an aircraft with operational history.

The aircraft mass and balance sheets contain information on the load distribution acting on the landing gear such as aircraft dry and operating mass with the associated position of the aircraft's centre of gravity; the cargo mass; the fuel mass; the aircraft mass and centre of gravity position on take-off, landing, and without fuel; loading information; and cargo distribution. The

mass and balance sheet information is necessary for determining the approximate load acting on the aircraft during take-off and landing due to mass and mass distribution.

The third suggested information source is the pilot's logbook. The pilot's logbook contains information on the flight date, place of take-off, place of landing, time of take-off, and time of landing. The flight data can be useful in determining meteorological conditions that could have impacted the aircraft's landing gear due to specific runway conditions. The place of take-off and landing is important when considering the differences in runway type impact on the landing gear structure, as is the case when landing on asphalted or grass-covered runways. Finally, the take-off and landing time gives insight into flight operation length since the aircraft's landing gear is not only loaded due to contact surface reaction but also the landing gear's own weight during flight, although to a much smaller degree.

The listed data relevant to the determination of sport and recreational aircraft landing gear material fatigue and impact damage accumulation is sorted according to the source of information in Table 8.

Table 8. PHM-related data acquisition from light aircraft mandatory documents.

Aircraft technical logbook	Mass & balance sheets	Pilot's logbook
Manufacturer & type	Aircraft dry and operating mass with the associated position of the centre of gravity	Flight date
Year of manufacture	Cargo mass	Place of take-off
Serial number	Fuel mass	Place of landing
Total flight hours	Aircraft mass and centre of gravity position on take-off, landing, and without fuel	Time of take-off
Number of take-off & landing cycles	Loading information	Time of landing
Observed malfunctions and damage to aircraft and/or its components	Cargo distribution	

3.7 Data acquisition and PHM implementation steps

The described data extraction process corresponds to the first PHM step, as proposed by Qi et al. [115], data acquisition. The second, third, and fourth steps, are data analysis, fault

diagnostics, and health assessment, relating to the classification of material fatigue relevant data and the application of procedures to determine landing gear deterioration through fatigue and impact damage accumulation. The fifth step, life prediction, estimates the remaining useful life based on the accumulated fatigue damage. The final step, the maintenance decision, can be as simple as deciding whether the landing gear should be replaced. This process can be automated, requiring simple data input and warning the pilot and/or maintainer of a required part or component replacement accounting for past operational conditions.

4 FUNDAMENTAL CONCEPTS IN FATIGUE OF METALS FOR COMPUTATIONAL MODELING

This Thesis Chapter delves into fundamental concepts of metal fatigue for computational modelling. It begins by detailing various fatigue analysis types, followed by an examination of loading types in metal fatigue. The Chapter then explores mean stress effects and the importance of multiaxial stress corrections in fatigue analysis. Finally, it discusses fatigue modifications, bridging the gap between theoretical predictions and practical observations. The Chapter provides a foundation for understanding metal fatigue, enhancing the development of an accurate, reliable computational model.

4.1 Aerospace Material Fatigue: Analysis Approaches and Computational Modelling

According to Mouritz [37], aerospace materials' fatigue properties, such as landing gear structural parts, are determined in a series of fatigue tests. Material properties are first determined by measuring the response of small test coupons with a machine such as the tensile loading machine, displayed by a schematic representation in Figure 10.

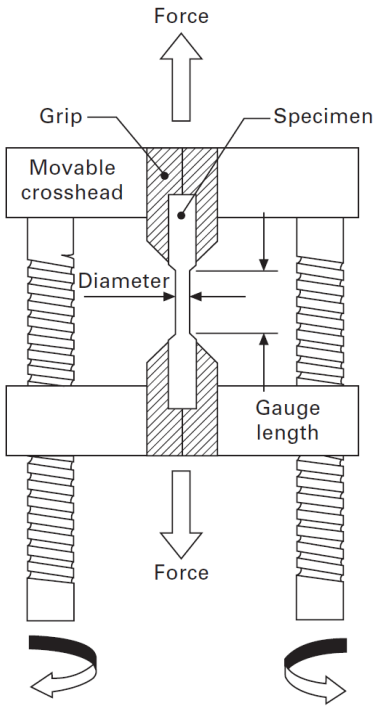

Figure 10. Representation of a tensile loading machine, [109].

Many coupons are observed under constant amplitude loading. This enables fatigue property determination. Since light aircraft landing gear structural parts vary in size and shape compared to test coupons, which do not consider structural details such as bores, stiffeners, etc.,

additional tests are performed. Load conditions causing fatigue damage similar to actual operational conditions are replicated in a computer-aided simulation environment, or on rare occasions, real-life tests, providing information that is usually implemented in the design of large aircraft, as opposed to light aircraft where this is not always the case.

The method subject of this Thesis uses fatigue life data obtained from a computer-aided simulation environment, namely Ansys Workbench 2023 R1 (abbrev. Ansys).

In general, it can be stated that fatigue life analysis has three main approaches, the strain life approach, the stress life approach, and the fracture mechanics' approach.

The strain-life material fatigue analysis, also known as the strain-life method, is a fatigue analysis approach that combines both elastic and plastic strain to predict the fatigue life of a material under cyclical loading. In this method, the total strain experienced by a material during a cycle of loading and unloading is split into elastic strain and plastic strain components. The elastic strain is typically determined by the stress-strain relationship described by Hooke's law, while the plastic strain is derived from the irreversible deformation that occurs beyond the material's yield point. The strain-life curve, a key component of this approach, is obtained from fatigue tests and is typically expressed in a log-log plot of strain amplitude versus the number of cycles to failure. This curve can be divided into three regions: high-cycle fatigue, low-cycle fatigue, and a transition region, as shown by Schjive [48] in Figure 11.

Each of the three regions in Figure 11 may be dominated by different strain components

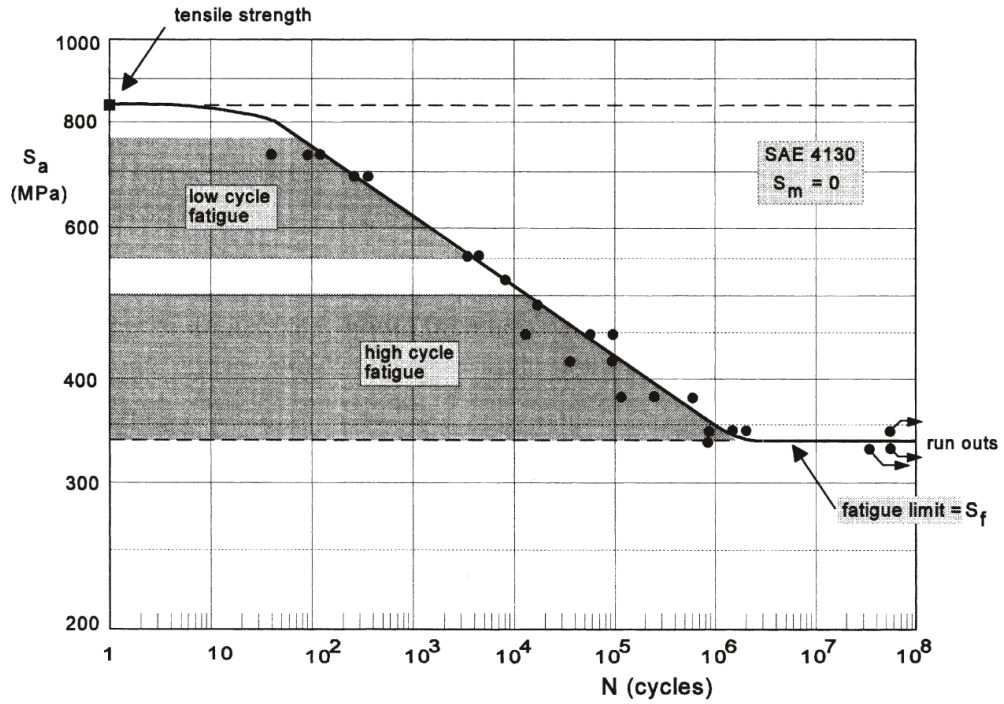

Figure 11. Example of fatigue test results of SAE 4130 low alloy steel, [48].

and have different life-predicting models. By knowing the strain amplitudes, the number of

cycles before failure can be calculated, thus predicting the fatigue life of the object of observation, [119]. This method is particularly useful for materials subjected to high levels of strain and when there is interest in understanding the material's behaviour beyond its elastic region, [120].

In the stress-life material fatigue analysis approach, also known as the S-N method, the stress amplitude experienced by a material during a cycle of loading and unloading is plotted against the number of cycles to failure, as shown in Figure 11, creating what is often referred to as an S-N curve or a Wöhler curve. The data for this curve is typically obtained from fatigue tests under controlled conditions, Schjive [48].

The S-N curve can typically be divided into two distinct regions: a high-cycle fatigue (HCF) region where failure is primarily due to cyclic stress levels below the material's yield strength, and a low-cycle fatigue (LCF) region where failure is due to stress levels above the materials yield strength, [121], [14], [48]. It's important to note that the stress-life method is particularly applicable when the strains are primarily elastic, i.e., the applied stresses are within the elastic limit of the material, [122]. For higher stress levels leading to plastic strains, the strain-life method may be more appropriate.

Fracture mechanics is a fatigue analysis approach that focuses on the growth of pre-existing cracks or defects within a material under cyclic loading conditions. This approach is based on the understanding that the failure of a material often initiates from micro-level defects or cracks and progresses to macroscopic failure as the cracks grow. There are three modes of fracture in this approach: Mode I (opening or tensile mode), Mode II (sliding or in-plane shear mode), and Mode III (tearing or anti-plane shear mode), [123], [124]. The most common mode in fatigue failure is Mode I, where the crack faces move directly apart. The central concept in fracture mechanics is the stress intensity factor, which describes the stress distribution around the tip of a crack. The critical stress intensity factor, or fracture toughness, is a material property that indicates the resistance of a material to the propagation of a crack. Under cyclic loading, a crack can grow each time the load is applied. The rate of this crack growth is described by the Paris Law, which relates the crack growth rate to the range of stress intensity factor experienced during each loading cycle, [125]. Fracture mechanics is particularly useful in safety-critical industries (like the aeronautic industry), where even small cracks can lead to catastrophic failures. By understanding the behaviour of cracks and the conditions under which they propagate, engineers can predict the lifespan of a component and implement necessary maintenance or replacement schedules.

The Ansys Fatigue Module supports the strain life and the stress life fatigue analysis approach, as stated by Browell and Hancq [126]. According to the authors [126], fatigue analysis results depend on five common input factors: the fatigue analysis type (Chapter 4.2), loading type (Chapter 4.2.1), mean stress effects (Chapter 4.2.2), multiaxial stress correction (Chapter 4.2.3), and the fatigue modification factor (Chapter 4.2.4), which are suggested to be resolved consecutively.

4.2 Fatigue Analysis Type

Aircraft landing gear structures are subject to low cycle fatigue (as defined in the continuation of this Chapter); this becomes apparent when considering their high load-to-weight ratio. Substantiating the previous statement are common narrow structural part hard-time replacement intervals. Low cycle fatigue is generally characterized by a fatigue life (described in Chapter 1.1) of less than 10 000 load cycles. It's worth mentioning that the Browell and Hancq [126] state that low cycle fatigue usually refers to less than 10^5 load cycles; they also point out that the approach works well with high cycle fatigue analyses. According to Mouritz [37], peak stresses that can cause general plastic deformation requires a fatigue life analysis that considers the relation between the number of load cycles to failure and plastic strain (e.g., The Coffin-Manson or Basquin-Coffin-Manson relation as explained in Chapter 4.2.2). Li et al. [127] emphasized that low cycle fatigue analysis is conventionally performed with the strain-life analysis approach based on strain parameters; for example, the well-known Coffin-Manson strain-life relationship connects those parameters. Strain can easily be measured and is a good low-cycle fatigue predictor. Strain life is typically associated with crack initiation, which is sufficient for light aircraft landing gear structure fatigue life estimation since structural cracks on those parts are usually not acceptable, [13]. Low cycle fatigue has been successfully estimated solely based on monotonic tensile properties; a link between fundamental low cycle fatigue properties and fatigue crack growth is commonly pointed out, [128]. Troschenko and Khamaza [128] emphasize that the strain-based fatigue analysis approach has been successfully used to analyse and investigate material fatigue. Light aircraft landing gear structures are subject to low cycle fatigue, based on the fact that landing gear structures have mass and material limitations to ensure aircraft operational performance within applicable regulations. The light aircraft landing gear structure is, for this reason, subject to frequent planned and unplanned inspections to ensure no plastic deformation and/or cracks are present, highlighting the manufacturers, operators, and maintainers' awareness of low cycle fatigue probability. For example, the Cessna 172R has a landing gear strut check interval of 100 operation hours [13].

Even smaller airplanes like the Pioneer 200, 230, 300, 300 KITE, 330 and 400 featuring fixed and retractable landing gear systems have visual checks for cracks and corrosion as part of pre-flight inspection, and a hard-time strut replacement interval of 500 operation hours.

For the stated reasons, the strain life fatigue analysis approach was chosen for this research. According to Browell and Hancq [126], the strain life fatigue analysis approach implies additional decisions that need to be made, displayed in Figure 12.

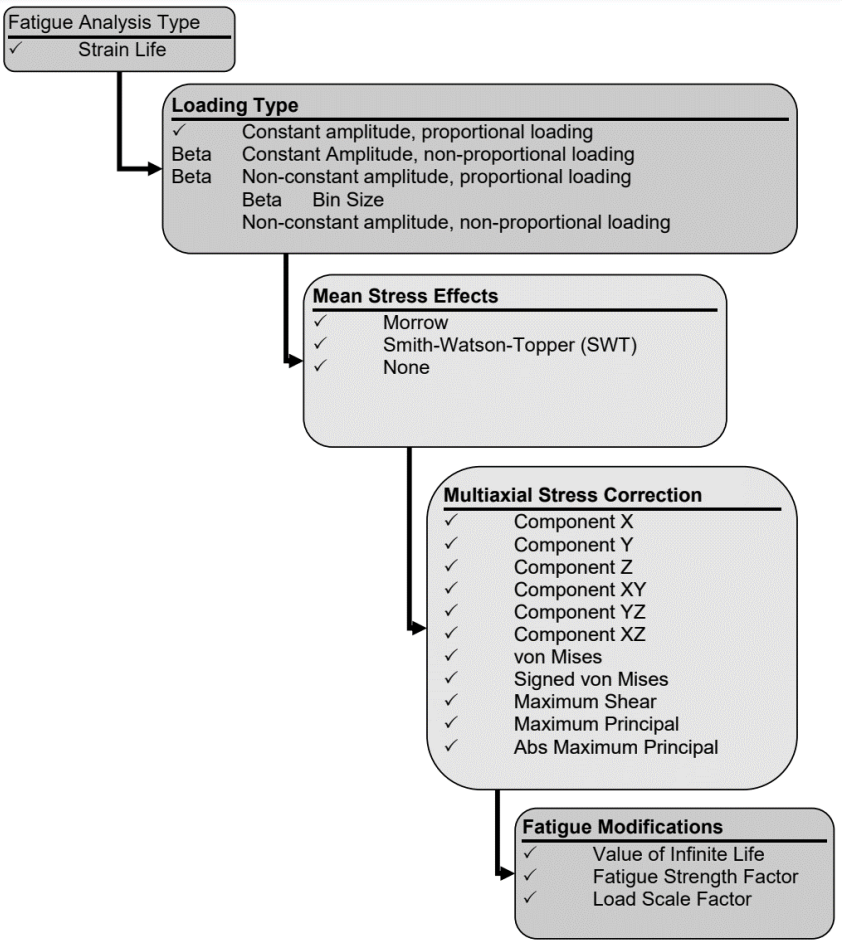

Figure 12. Strain life fatigue analysis decision tree, [126].

4.2.1 Loading Type

According to Le Divenah & Beaufils [128], aircraft design begins by describing the intended mission, attributing a flight duration, altitude, aircraft mass, disturbances, etc. External loads on aircraft structural parts are computed, and stresses in each structural part are calculated. The authors [128] describe the aircraft mission as a series of equilibrium stresses defining an equilibrium structural state, representing loads that slowly change in time, such as weight or pressure. Stresses resulting from disturbances are superimposed on the equilibrium stresses. Load description depends on the type of analysed structure. The aircraft landing gear is primarily sensitive to loads resulting from mission phases where the aircraft is on the ground

(taxi, take-off, landing, etc.), whereas flight phases also have their impact, but usually to a much smaller degree.

The presented loading type options in Figure 12 refer to cyclic loads. Of the ones stated, three are supported by Ansys: constant amplitude proportional loading; constant amplitude non-proportional loading and non-constant amplitude proportional loading, [126]. Coupon tests in laboratory environments are mostly performed with uniaxial loads, whereas the light aircraft landing gear is loaded multiaxially. The reason for uniaxial load tests is the complicated design of multiaxial test machines, additionally considering the landing gear load multiaxiality is variable. Instead, uniaxial test results involving test coupons serve as a means of validation and fatigue property determination for computer-aided fatigue calculations of acceptable accuracy.

Constant amplitude proportional loading can be described with sinusoidal curves of constant amplitude, starting with a load value of 0, Figure 13.

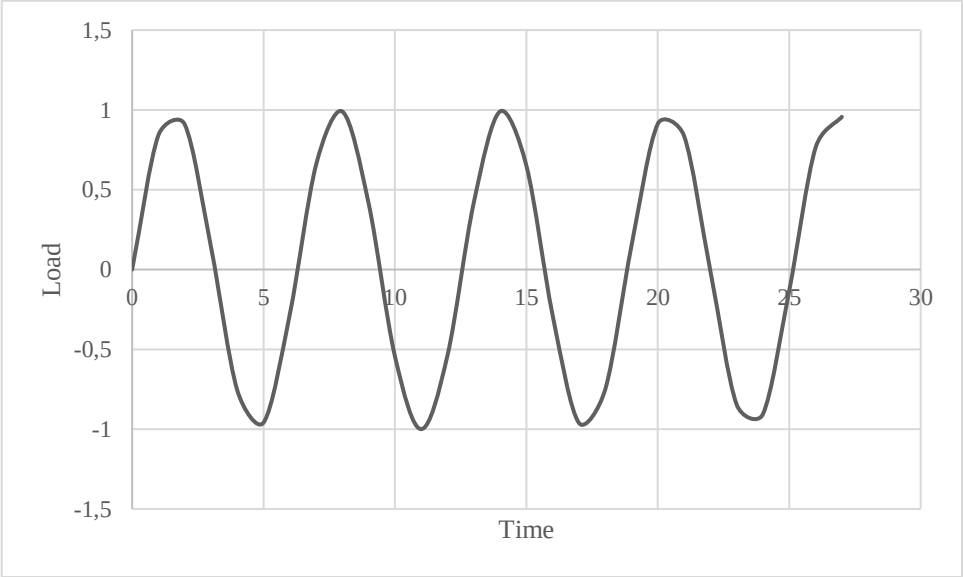

Figure 13. Constant amplitude, proportional relative loading example.

Constant amplitude, non-proportional relative loading can be described by sinusoidal curves of constant amplitude, having a mean value different from zero, Figure 14.

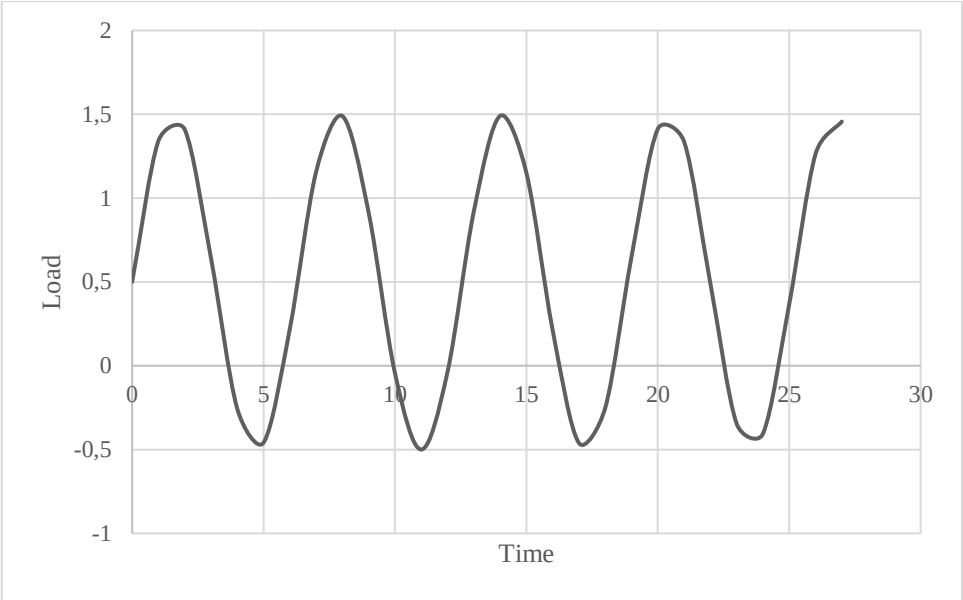

Figure 14. Constant amplitude, non-proportional relative loading example.

Non-constant amplitude, proportional loading can be described by sinusoidal curves of varying amplitudes, starting with a load value of 0, Figure 15.

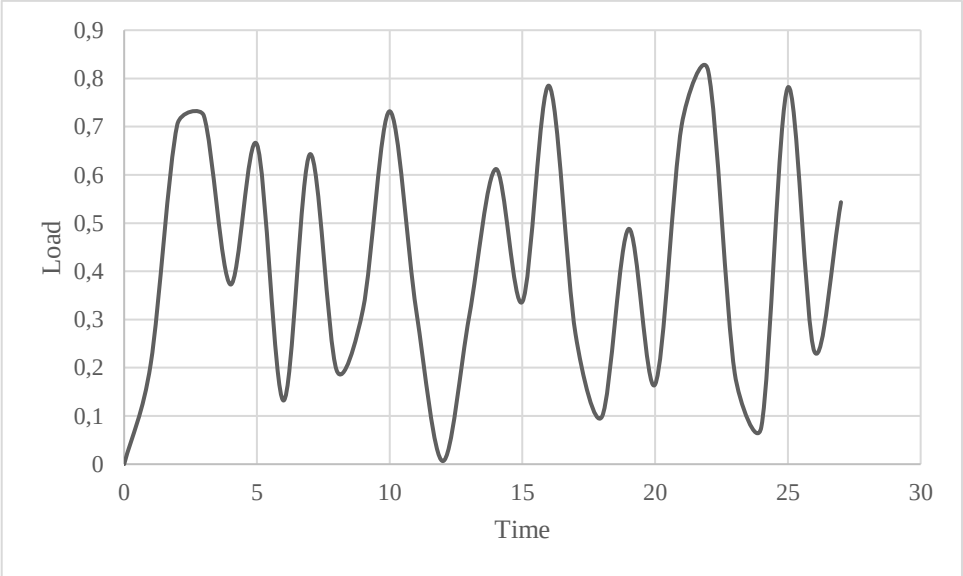

Figure 15. Variable amplitude relative loading example.

From the above, it seems that the variable amplitude proportional loading type corresponds to the methodology generally presented in [128]; however, the varying amplitude intensity acting on the light aircraft landing gear remains unknown since mission loads can drastically vary depending on pilot input and environmental factors. The methodology presented in this Thesis circumvents the unknown mission load intensities by calculating cumulative fatigue life (the remaining useful life considering material fatigue due to experienced load variation) based on the loads that can be expected during regular operation, considering that landing gear overload cases require inspections and parts replacement when overload is detected. Another

unknown is the varying multiaxial nature of loads acting on the light aircraft landing gear during operation. The impact of a variable load multiaxiality on calculated fatigue life accuracy is also mitigated by cumulative fatigue life calculation. The chosen loading type for the method developed in this research is non-constant amplitude proportional loading, based on the load history described later in this document.

According to Browell and Hancq [126], Ansys calculates the total structural response to loads resulting in material fatigue by assuming a nominally elastic response and then relating local stress or strain to nominal stress or strain at a stress concentration location by using the Neuber relation, *(8)*.

$$\varepsilon\sigma = K_t^2 eS \tag{8}$$

Where:

ε – Is the local (total) strain, [m/m].

σ – Is the local stress, [N/m^2].

K_t – Is the Elastic Stress Concentration Factor, [-].

e – Is the Nominal Elastic Strain, [m/m].

S – Is the Nominal Elastic Stress, [N/m^2].

The Elastic Stress Concentration Factor, often denoted as K_t, is a dimensionless factor used in engineering and material science to quantify how concentrated the stress becomes in a material near a geometric discontinuity such as a hole, a notch, a corner or a crack. In the presence of such discontinuities, the stress isn't uniformly distributed but instead gets "concentrated" near these locations. The stress at these points can be significantly higher than the average stress across the material. The Elastic Stress Concentration Factor is defined as the ratio of the highest stress in the element to the reference (or nominal) stress. The reference stress is typically the stress value calculated assuming a uniform stress distribution (i.e., ignoring the discontinuity). The value of K_t can give an idea of how much higher the peak stress is in comparison to the reference stress. In the context of Ansys fatigue analysis, nominal elastic strain and stress refer to the strain or stress calculated under the assumption of a linear elastic material behaviour, which ignores local plastic deformation.

Ansys solves the Neuber and cyclic strain equation, calculating local stress or strain (elastic and plastic response included) based solely on elastic input. Extensive calculations resulting in significant computing capacity occupation are thereby avoided.

4.2.2 Mean Stress Effects

Fully reversed, constant amplitude tests, as shown in Figure 13, are often used to determine cyclic material fatigue properties. Light aircraft landing gears are unlikely to experience such loads; load variability depends on the observed phase of the operation. More significant variability is expected during landing and take-off than taxi or static ground operation (for example, engine warm-up), due to additional dynamic loads being a consequence of the aircraft moving. However, mean stresses can usually be determined and accounted for, [126].

Mean stress adjustments need to be included in strain-based fatigue life prognosis. According to Ince & Glinka [129], there are various methods for mean stress impact prediction on the fatigue behaviour of metals. It is known that tensile mean stress has a diminishing effect on fatigue life, whereas compressive mean stress can even be beneficial. The Goodman, Gerber, Soderberg, Morrow, Walker and Smith-Watson-Topper high-cycle fatigue mean stress correction models were discussed by Ince et al. [129], and Bader et al. [130]. Dowling [131] states that material properties needed for a strain-based fatigue life calculation approach are obtained from controlled strain test conditions to ensure mean stresses are equal or near zero. The target outcome of such tests are cyclic stress-strain and strain-life curves. Strain life can be described by a curve approaching actual elastic strain behaviour in the high cycle region and actual plastic strain behaviour in the low cycle region [132]. Strain life curves considering elastic and plastic strain resistance are defined by the Manson-Hirschberg equation representing a superposition of elastic and plastic strain resistance [46]. The Basquin equation *(9)* describes a linear relationship between applied stress cycles and the number of cycles to failure, representing elastic strain resistance, and is often used for sufficiently accurate high-cycle fatigue prognosis.

$$\sigma_a = \frac{E \cdot \Delta\varepsilon_e}{2} = \sigma_f' \cdot (2N)^b \qquad (9)$$

Where:

σ_a – Is the stress amplitude, [N/m^2].

E – Is the modulus of elasticity, [N/m^2].

$\Delta\varepsilon_e$ – Is the elastic strain, [m/m].

σ_f' – Is the fatigue strength coefficient, [N/m^2].

N – Is the fatigue life, [number of cycles to failure].

b – Is the fatigue strength exponent, [-].

The fatigue strength coefficient, often denoted by σ_f' in fatigue models such as the Basquin's law, typically has the same units as stress because it represents a stress value. Therefore, in the International System of Units (SI), the fatigue strength coefficient is usually measured in Pascals (Pa).

The Coffin-Manson equation, displayed in equation *(8)*, represents plastic strain resistance and is used for general low and high cycle fatigue life calculation, [2].

$$\frac{\Delta\varepsilon_p}{2} = \varepsilon_f' \cdot (2N)^c \qquad (10)$$

Where:

$\Delta\varepsilon_p$ – Is the plastic strain, [m/m].

ε_f' – Is the fatigue ductility coefficient, [m/m].

c – Is the fatigue ductility exponent, [-].

The fatigue ductility coefficient, often represented by ε_f'' in fatigue models like the Coffin-Manson relationship, is a dimensionless quantity. This is because it represents the strain (change in length/original length) which does not have any units. It is a measure of the material's deformation before failure under cyclic loading conditions. This value often helps in determining the material's resistance to fatigue.

The Manson-Hirschberg equation, displayed in equation *(9)* combines the Basquin and Coffin-Manson equations.

$$\varepsilon_{ar} = \frac{\sigma_f'}{E} \cdot (2N)^b + \varepsilon_f' \cdot (2N)^c \qquad (11)$$

Where:

ε_{ar} – Is the combined strain due to its elastic and plastic components, [m/m].

A representation of elastic, plastic, and total strain resistance to fatigue loading is given in Figure 16.

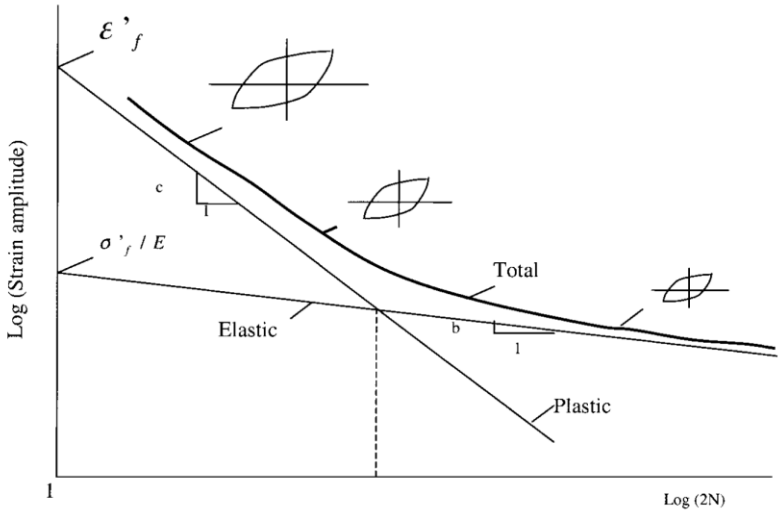

Figure 16. Representation of elastic, plastic, and total strain resistance to fatigue loading, [46].

Ansys offers three mean stress correction approaches for strain life calculation: no stress correction, the Morrow stress correction, and the Smith-Watson-Topper stress correction.

The Morrow mean stress correction *(12*), characterized by the fatigue strength coefficient (σ_f'), produces a good mean stress correction when the observed part material is steel, as is often the case with light aircraft landing gear struts. Browell & Hancq [126] and Ince & Glinka [129] point out that Morrow's mean stress correction modifies the elastic part of the strain life equation, consistent with observations of significant mean stress impact on fatigue life when elastic strain is dominant, and low mean stress significance on fatigue life in situations when plastic strain is dominant. Additionally, Morrow's mean stress correction wrongly assumes the dependency of the elastic and plastic strain ratio on mean stress, [126]. The Morrow mean stress correction for the Manson-Hirschberg equation is displayed in *(12*).

$$\frac{\Delta\varepsilon}{2} = \frac{\sigma_f' - \sigma_m}{E} \cdot (2N)^b + \varepsilon_f' \cdot (2N)^c \qquad (12)$$

Where:

$\frac{\Delta\varepsilon}{2}$ – Is the strain amplitude, [m/m];

σ_m – Is the mean stress, [N/m^2].

The Smith-Watson-Topper mean stress correction *(13)*, on the other hand, suggests a different equation accounting for mean stress influence on fatigue life. The peculiarity of the Smith-Watson-Topper mean stress correction is that it considers the bigger impact of tensile mean stress on fatigue life as opposed to the mean stress being equal to zero [133], [134]. Fatigue testing has shown that tensile mean stress generally produces a shorter fatigue life as opposed to a zero-mean stress, [46]. In the case of light aircraft landing gear structures, tensile

load dominance is primarily expected during the flight phase of aircraft operation, being of lower significance than compressive loads since dominant tensile loads result from inertial and gravitational forces due to the landing gears own mass (while the aircraft is in flight). The Smith-Watson-Topper mean stress correction is displayed in equation *(13)*.

$$\sigma_{max} \cdot \frac{\Delta\varepsilon}{2} = \frac{\left(\sigma_f'\right)^2}{E} \cdot (2N)^{2b} + \sigma_f' \cdot \varepsilon_f' \cdot (2N)^{b+c} \qquad (13)$$

Where:

σ_{max} – is the maximum stress, [N/m^2].

4.2.3 Multiaxial Stress Correction

As Ion et al. [136] stated, many components and different types of equipment are subject to time-variable multiaxial stresses. For example, fatigue life prediction under triaxial time variable loading is an unresolved issue. The light aircraft landing gear is dominantly subject to multiaxial time variable loading during all phases of operation, except in some minor cases where the effects of load variation are negligible (for example, when the aircraft is stationary on the ground). A commonly used method to resolve the problem of multiaxiality consists of replacing time variable multiaxial load with an equivalent uniaxial load, [135]. The reason is a common high complexity of machines able to perform multiaxial testing, as well as the need for major machine modifications for each new test. Coupon testing is, therefore, characteristic of experimental data acquirement. To perform numerical strength calculations resulting in fatigue life, Ansys requires the multiaxial stress state to be observed uniaxially; in other words, a multiaxial stress correction is required. Ansys offers various multiaxial stress correction approaches; the von Mises, max shear, maximum principal stress, component stresses, and other multiaxial stress corrections are available. The "signed von Mises stress" is supposed to be chosen when the von Mises stress takes the sign of the largest absolute principal stress [126]. The „signed von Mises "stress" serves to identify mean compressive stresses since some of the mean stress theories treat positive and negative mean stresses differently.

4.2.4 Fatigue Modifications

Specific cases of constant amplitude loading require modifications to increase the accuracy of calculated results. One such case is when constant amplitude loading results in stresses below the lowest alternating stress on the given fatigue curve, various literature, for example [136], and [50], highlights the importance of making adjustments to increase the accuracy of calculated results in various loading conditions. Fatigue analyses of small-stress variable amplitude loading for many cycles tend to overestimate fatigue damage, as suggested by equation *(12)* in [102]. This however is not a major issue since it enhances safety in the case of

light aircraft landing gear structure fatigue life estimation. Ansys provides the value of infinite life for the last point consideration in such cases since some materials do not have a fatigue endurance limit, [126]. The fatigue endurance limit is the maximum stress level a material can withstand for an infinite number of load cycles without failing due to fatigue. In other words, it's the stress level below which fatigue failure does not occur, even after a very large number of stress cycles, labelled infinite due to the nature of the observed process. Enabling the infinite life value option in Ansys helps mitigate such result deviations. A higher value of infinite life will decrease the calculated damage generated by small stress amplitudes, provided the observed test subject experiences a high number of load cycles.

Another Ansys fatigue modification option is the Fatigue Strength Factor. If the observed subject service conditions differ from the test subject conditions, this modification factor can be applied, [126]. The Fatigue Strength Factor reduces fatigue strength and is less than one, applied only to the alternating stress, not affecting the mean stress. Alternating and mean stress scaling is also possible, provided by the Ansys Loading Scale Factor. The effects of load changes on fatigue life require consecutive calculations, thereby increasing the needed computing resources. This can be avoided by applying a scale factor if consecutive results analysis is needed.

5 DEVELOPMENT OF A METHOD FOR PREDICTING REMAINING USEFUL LIFE

In this Chapter, a sensor-less method for predicting the remaining useful life of light aircraft landing gear structure components is developed, particularly emphasizing parts susceptible to fatigue damage accumulation. The primary objective of this research was to develop an effective method for predicting the *RUL* of critical light aircraft structural parts based on existing aircraft operation records. The focus was on those parts which are vital for flight safety and prone to damage due to regular usage, such as landing gear structural parts, or any other structural part, for example wing and fuselage structural parts, provided their *RUL* for specific loading conditions can be determined.

Fatigue failure has been identified as the primary predictable damage accumulation consequence resulting from regular aircraft use, and various studies have explored the impact of fatigue damage on aircraft parts. For instance, Infante et al. [137] emphasize that material fatigue is crucial for aircraft landing gear as it can lead to component failure, evidenced by the observed nose landing gear failure in a light aircraft.

The proposed method applies to any structural part subject to material fatigue accumulation, considering the fatigue-relevant specifics of the component and its role in the observed system. This method's advantage is particularly apparent when no fatigue-related sensor data is available, as is often the case with light aircraft landing gear structures.

In this research, the landing gear strut is examined as a representative component of light aircraft landing gear structures prone to fatigue damage accumulation. This part is designed to withstand and mitigate loads transferred from the landing gear wheel to the aircraft's fuselage, making it a crucial component within the fixed landing gear structure. The landing gear strut's significance as a load-bearing part is further emphasized by manufacturers' maintenance instructions [13], which state a higher maintenance focus on the landing gear strut compared to other light aircraft landing gear structural components. Additionally, the author of this Thesis can affirm the significance of material fatigue on light aircraft structures, especially the light aircraft landing gear strut based on his aircraft design, production, and accident investigation experience, including several incidents where material fatigue was the primary aircraft structural component failure cause, such as landing gear strut and engine mount fatigue failure.

The method developed in the research leading to this Thesis consists of four main phases, depicted in Figure 17.

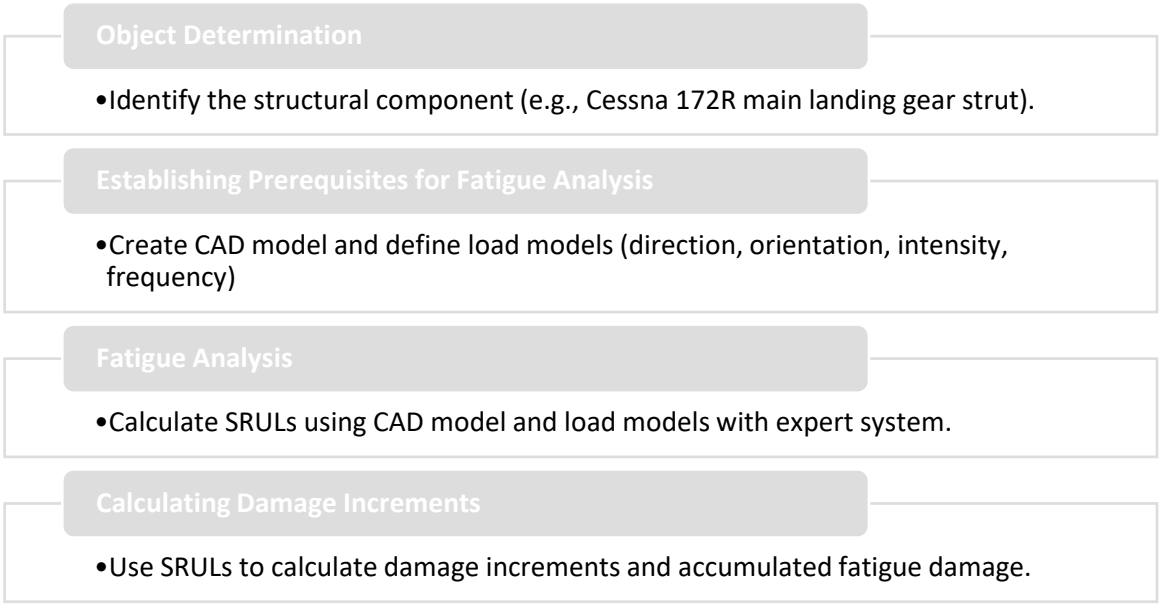

Figure 17. Process for predicting remaining useful life of light aircraft landing gear structural parts.

In the first phase, the object of observation has to be determined. For example, for the purpose of method application this Thesis was focused on a light aircraft landing gear strut. The exact airplane and it's structural part were determined; in the case of this research this was the Cessna 172R main landing gear strut.

In the second phase, the prerequisites for fatigue analysis were established. The first prerequisite was to create a model of the observed part. For example, since the developed method was applied on a light aircraft main landing gear strut, a CAD model was created consisting of the strut's geometry and material fatigue relevant mechanical properties. The second prerequisite was to create models of fatigue relevant loads acting on the observed main landing gear strut model. The load models were defined by several parameters. Those parameters were load direction, orientation, intensity, and frequency. Load model direction and orientation were defined by identifying light aircraft characteristic operation phases, such as taxi before take-off, take-off, flight, landing, and taxi after landing. Load model intensity was determined by calculating the mass acting on the observed part and observed part acceleration relative to the movement of the aircraft. Lastly, load model frequency was determined through measurements taken during research [4] predating the development of this method.

In the third phase, fatigue analysis was performed by calculating specific remaining useful lives of the observed part for various load model parameters. The CAD model of the observed part, along with the fatigue-relevant load models, was employed in the fatigue analysis. This

analysis yielded specific remaining useful lives that corresponded to the variations of fatigue-relevant load models, depending on load model parameter variations. An expert system was created with the purpose of sorting the specific remaining useful lives according to determined operation phases and information crucial for fatigue relevant load model determination, namely the aircraft's mass and mass distribution. Additionally, the expert system included an operator interface enabling mass value and distribution input for several recorded operations and the number of landings input which were performed previous to available mass value and distribution records. The operator interface stored the acquired operational information in the expert systems knowledge acquisition table. After storing the acquired information, the specific remaining useful lives were linked to the corresponding mass value and distribution from the knowledge acquisition table, and the fourth method phase commenced.

In the fourth phase, specific remaining useful lives were used to calculate the resulting damage increments, recorded in the expert systems knowledge base. A single damage increment represents the fatigue damage that was accumulated in the observed part model, due to one of the fatigue relevant load models acting on it. Finally, the accumulated fatigue damage was calculated using the damage increments, thereby representing the part's useful life which was used up due to operating conditions resulting in material fatigue. The accumulated fatigue damage was calculated based on the information recorded in the knowledge acquisition table and its corresponding damage increment from the knowledge base.

5.1 Method phase 1: selecting the structural part for observation

In the initial phase of the developed method, the primary task was to identify and select the object that was the focus of observation. This selection process was important, as it sets the foundation for the subsequent stages of method implementation. For the development and implementation of this method the Cessna 172R airplane was chosen, specifically, the Cessna 172R callsign 9A-DAD. The Cessna 172R is a very common airplane model, various operation and research data are available, helping in the verification of the variables used in the development and implementation of this method.

Additional reasons for choosing the Cessna 172R Skyhawk were:

- The Faculty of Transport and Traffic Sciences owns three Cessna 172 Skyhawk aircraft, two being the variant Cessna 172N Skyhawk, and one being a Cessna 172R

Skyhawk. Ownership of those aircraft conveniently enables access to relevant data, such as landing gear structure geometry, the Aircraft Flight Manual, maintenance manual, logbook, and other parameters relevant to this research and the remaining useful life of a light aircraft landing gear structure.

- Literature review showed the Cessna 172 Skyhawk series is covered relatively well with research papers dealing with subjects relevant to the remaining useful life of structural load-bearing parts. One such document is the "Statistical Loads Data for Cessna 172 Aircraft Using the Aircraft Cumulative Fatigue System ACFS" by Cicero et al. [15].
- The Cessna 172 Skyhawk aircraft has a landing gear load-bearing structure common in many light aircraft landing gear structures where the main landing gear is connected to the fuselage by the landing gear strut. The main landing gear strut of the Cessna 172 Skyhawk aircraft series is the main load-bearing part, simultaneously acting as an elastic shock-absorbing element.

Subject information on the Cessna 172R aircraft can be found in the relevant Aircraft Flight Manual or the Aircraft Information Manual. The Aircraft Flight Manual and the Aircraft Information Manual are inextricably linked to the type and model of the observed aircraft.

The Cessna 172R has an engine with a fuel injection system, and the Cessna 172N has a carburetted engine. Cessna 172R performance parameters such as the maximum take-off and landing mass are less favourable for light aircraft landing gear structure *RUL* than the ones observed in the Cessna 172N (*MTOM*: 2450 lbs. for the Cessna 172R vs. 2300 lbs. for the Cessna 172N). The landing gear structure, and therefore its mechanical integrity, are the same for both aircraft. This is an additional reason why the Cessna 172R landing gear structure was chosen to be the focus of this research. The interior and exterior aircraft dimensions are identical. A three-view aircraft drawing from [3] is depicted in Figure 18.

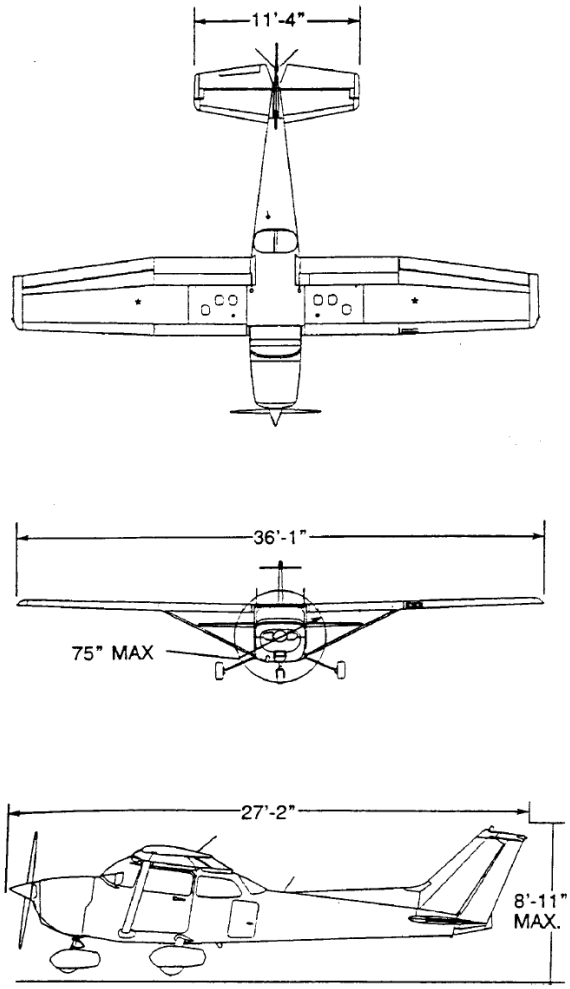

Figure 18. Cessna 172R aircraft three-view drawing, [3].

Interior and exterior aircraft dimensions extracted from [3] are presented in Table 9.

Table 9. Cessna 172R airframe interior and exterior dimensions, [3].

INTERIOR DIMENSIONS (Cabin)	EXTERIOR DIMENSIONS (Overall)
Length: 142 inches	Length: 26 feet, 11 inches
Height: 48 inches	Height: 8 feet, 11 inches
Width: 39.5 inches	Wing Span: 36 feet, 1 inch

The following general performance specifications for normal category Cessna 172R aircraft were considered, [3], as displayed in Table 10 :

Table 10. General performance specifications for normal category Cessna 172R, [3].

Speed	
Maximum at Sea Level	123 KNOTS
Cruise, 80 % Power at 8000 FT	122 KNOTS
CRUISE: Recommended lean mixture with fuel allowance for engine start, taxi, take-off, climb, and 45 minutes reserve.	
80 % Power at 8000 FT - Range	580 nautical miles
53 Gallons Usable Fuel - Time	4.8 hours
Range at 10.000 FT, 60 % power - Range	687 nautical miles

53 Gallons Usable Fuel - Time	6.6 hours
Rate of climb at sea level	720 feet per minute
Service ceiling	13500 feet
Take-off performance	
Ground roll	945 feet
Total distance over 50 feet obstacle	1685 feet
Landing performance	
Ground roll	550 feet
Total distance over 50 feet obstacle	1295 feet
Stall speed	
Flaps up, power off	51 knots calibrated airspeed
Flaps down, power off	47 knots calibrated airspeed
Maximum mass for normal category	
Ramp	2457 pounds
Take-off	2450 pounds
Landing	2450 pounds
Standard empty weight	1639 pounds
Maximum useful load	818 pounds
Baggage allowance: 120 pounds total (the maximum combined mass capacity for baggage area 1 and baggage area 2)	
Performance specifications	
Wing loading	14.1 pounds per square feet
Power loading	15.3 pounds per horsepower
Fuel capacity	56 gallons
Oil capacity	8 quarts
Engine	IO-360-L2A Textron Lycoming
Engine power	160 brake horsepower at 2400 revolutions per minute
Propeller	75-inch, fixed-pitch diameter
Centre of gravity range for normal category	
Forward	35.0 inches aft of datum at 1950 lbs. or less, with straight line variation to 36.5 inches aft of datum at 2100 lbs.
Aft	40.5 inches aft of the datum at all weights
Reference Datum	The lower portion of the front face of the firewall

The Aircraft Information Manual [3] states that speed performance applies to an airplane with installed optional speed fairings which increase the speeds by approximately 2 knots,

corresponding to a difference in range. The Cessna 172 Skyhawk aircraft, owned by the Faculty of Transport and Traffic Sciences, all have the optional speed fairings installed.

The focus of the research leading up to this Thesis was the development of a method for remaining useful life prediction of a light aircraft landing gear structure. In the case of the Cessna 172R, the main parts of the landing gear structure are the main landing gear struts, as they are called in the applicable Aircraft Flight Manual and maintenance manual. The main landing gear struts are most prone to significant *RUL* variation due to regular operational conditions. It is common knowledge that the main landing gear struts are the structural parts exposed to conditions with the biggest potential to reduce the complete landing gear structures *RUL*. The validity of this statement was observed by the author of this research in [2], also referencing other authors having a similar observation. This is because the Cessna 172R landing gear strut not only serves the purpose of attaching the landing gear wheel and braking system parts to the rest of the airplane but also provides the necessary elastic and (to a much lesser degree) damping properties needed to mitigate load impact on the rest of the airplane during taxiing and landing. Furthermore, the main landing gear strut is subject to regular and relatively frequent inspection [13], thereby highlighting the failure expectations of the aircraft manufacturer and operator, based on manufacturer experience, certification mandates, and operator experience. Manufacturer and operator expectations on the significance of fatigue damage initiation and accumulation to the Cessnas main landing gear strut can also be observed in the airplane's maintenance manual (Table 19, [13]), where this is the only structural part scheduled for both crack and corrosion inspection every 100 hours, in addition to mandatory deformation and crack checks after a plausible cause such as a hard landing.

For the stated reasons, the sole focus of developed method implementation is the light aircraft main landing gear strut. The inclusion of additional structural parts would significantly increase workload while having no contribution to the developed method and subsequent operational safety increase.

The Cessna 172R main landing gear assembly is displayed in Figure 19. The main landing gear assembly consists of the inboard landing gear bulkhead, strut, axle, breaking mechanism, fuselage fairing, strut fairing, main wheel speed fairing, and wheel.

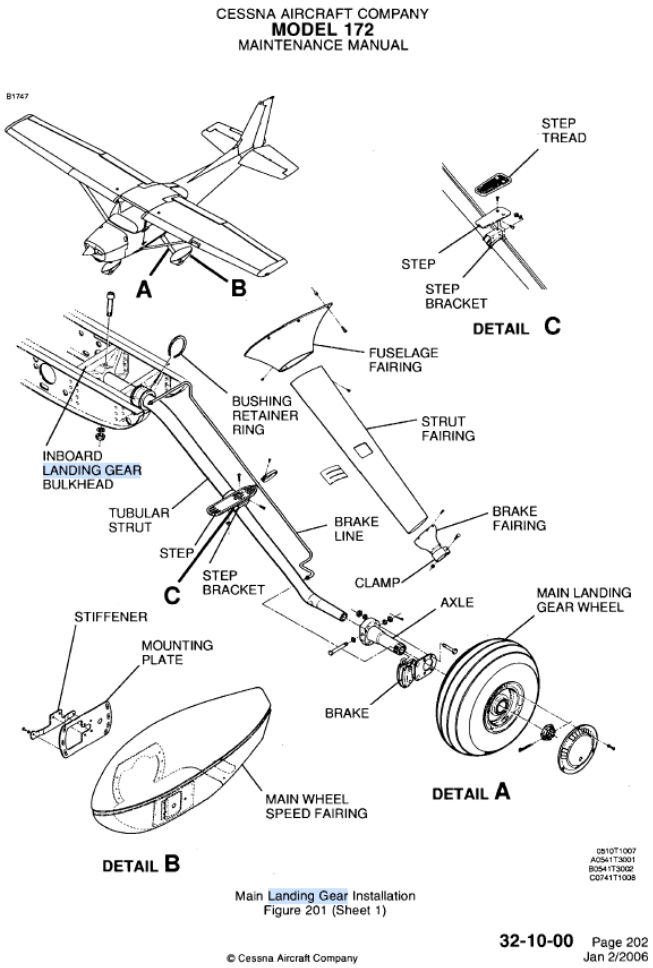

Figure 19. Cessna 172R landing gear assembly, [13].

The selection process, from the aircraft to the landing gear structure to the main landing gear strut ensured a focused and targeted approach to method development, thereby enhancing the effectiveness and applicability of the developed method.

5.2 Method phase 2: creating a model of the observed part

In phase 2, two fatigue analysis prerequisites were established. The first prerequisite was creating a model of the observed part (e.g., CAD model of light aircraft main landing gear strut consisting of strut geometry and material fatigue properties). The second was creating models of fatigue relevant loads, defined by the following parameters: load direction, load orientation, load intensity, and time dependent variability or load frequency. Load direction and orientation were determined by defining characteristic aircraft operation phases (taxi before take-off, take-off, flight landing, taxi after landing). The intensity of the load was determined by calculating the relevant mass for the main landing gear strut of the light aircraft, which includes the mass of the strut itself and the proportion of the overall airplane's mass that is attributed to the strut.

The calculation also considered the acceleration of the specific strut in relation to the entire aircraft's motion, [4]. The load frequency was determined from existing measurements, [4]. The observed part's model was used in later method stages for fatigue life analysis, which was the basis for observed part *RUL* prediction.

5.2.1 Creating the model geometry and defining mechanical properties

The dimensions of the Cessna's main landing gear strut were taken on-site, in between aircraft maintenance operations. The measurements were taken while the strut was still attached to the airplane since a disassembly would cause additional operational delay. Mitigating this suboptimal measuring circumstance were the fairings (displayed in Figure 19, part numbers 32, 34, and 38), which were already removed due to mentioned maintenance activities. The measurements were used to create a CAD model in FUSION 360. The modelled geometry was later imported into Ansys native Space Claim CAD modelling software for preprocessing, from where the geometry was introduced into the Ansys Workbench fatigue analysis project. Figure 20 shows the CAD model and it's dimensions.

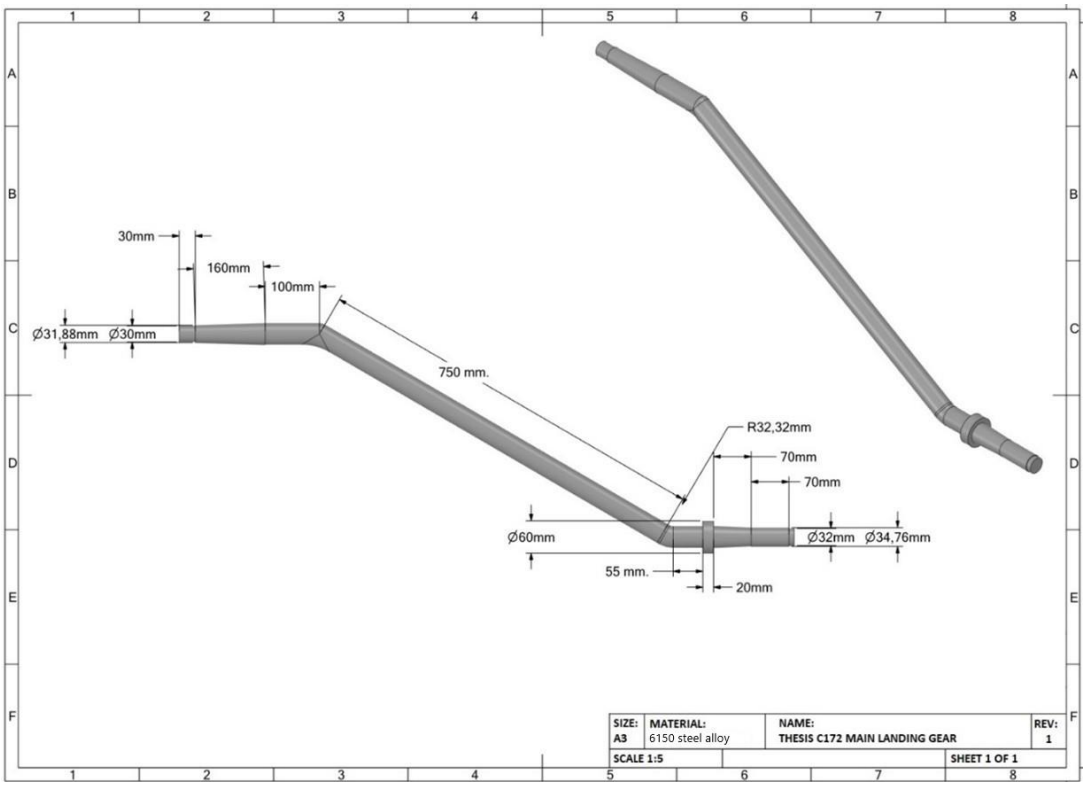

Figure 20. Cessna 172R main landing gear strut CAD model and geometry dimensions.

An additional measurement not displayed in Figure 20, important for determining the load angle acting on the landing gear strut during various operational phases, was the angle between

the strut and vertical line perpendicular to the horizontal surface on which the aircraft stands, as displayed in Figure 21. The angle was assumed to be approximately 15°.

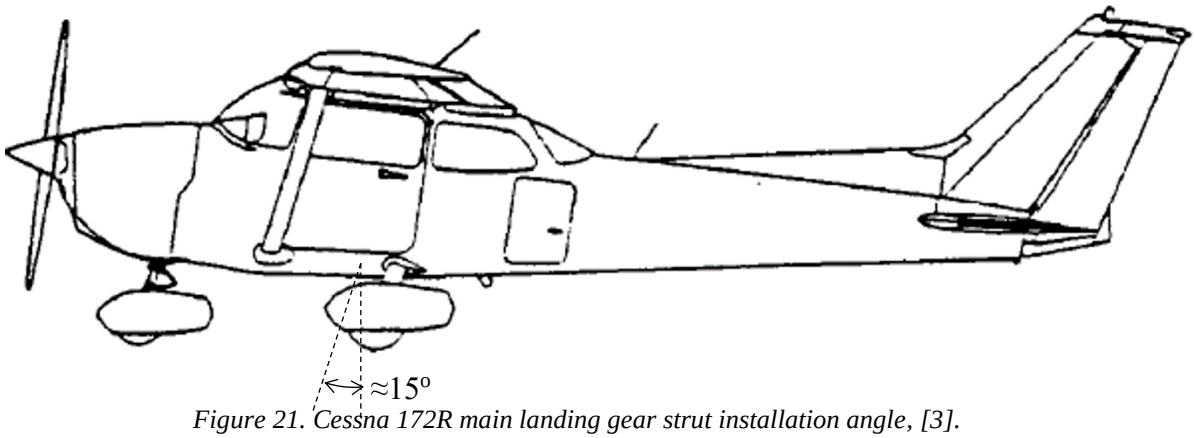

Figure 21. Cessna 172R main landing gear strut installation angle, [3].

After defining the CAD model's geometry, the model's fatigue relevant material properties had to be defined.

In an endeavour to align the results described in this thesis closely with outcomes that could be expected in real-world circumstances, efforts have been made to identify the actual material properties of the observed Cessna 172R landing gear main spar. It was confirmed that the main spar is fabricated from a steel alloy commonly known as 6150 steel, or alternatively 51CrV4 steel alloy, based on information disclosed in the aircraft's maintenance manual, [13].

One crucial aspect that remained elusive, despite extensive research, was the specific heat treatment employed on the material. Heat treatments are used to optimize the mechanical properties of steel alloys, particularly their fatigue durability. Given the lack of precise information on the heat treatment or resulting material fatigue relevant properties, an assumption was made for the purpose of this study. It was assumed that a heat treatment was selected which elevates the fatigue durability of the 6150 or 51CrV4 steel alloy. This assumption is founded on the rationale that a fatigue-critical component like an airplane's landing gear main spar would almost certainly be manufactured from material exhibiting high resistance to fatigue deterioration. This assumption turned into a presumption, based on performed numerical strength calculations for 6150 Steel without appropriate heat treatment which resulted in fatigue lives that are too short based on actual fatigue life observations made on the observed airplane. In simpler terms, if the actual landing gear strut on the Cessna 172R had been made of 6150 Steel without a beneficial heat treatment, it would have already succumbed to fatigue failure, given the number of operational cycles the actual airplane has undergone. This observation was additionally bolstered by performing static structural analysis resulting in von Mises stresses which were above the materials ultimate strength for some of

the relevant load cases. Those stress analysis results were not included in this Thesis, since they were rejected for further observation based on the fact that the actual landing gear strut has a sufficient mechanical integrity to bear the considered loads.

The mechanical and material fatigue-relevant properties chosen for the example displayed in this Thesis are based on extensive literature research. A thorough review of academic journals, industry publications, and technical reports was undertaken to compile all of the relevant properties stated ([5], [6], [7], [8], [9], [10], [11], [12]). The material properties were extracted based on factual data specifically for 6150 steel alloy, otherwise known as 51CrV4 steel alloy, according to Table 11.

Table 11. 6150 Steel alloy material data, ([5], [6], [7], [8], [9], [10], [11], [12]).

Property	Value	Unit
Density	7850	kg/m^3
Young's modulus	2.038E+11	Pa
Poisson's ratio	0.29	-
Bulk modulus	1.6175E+11	Pa
Shear modulus	7.8992E+10	Pa
Strength coefficient	1.1E+9	Pa
Strength exponent	-0.093	-
Ductility coefficient	0.478	-
Ductility exponent	-0.684	-
Cyclic strength coefficient	1.476E+9	Pa
Cyclic strain hardening exponent	0.0651	-
Tensile yield strength	1.042E+9	Pa
Compressive yield strength	1.042E+9	Pa
Tensile ultimate strength	1.2773E+9	Pa

5.2.1 Creating the fatigue relevant load models

Load parameters acting on a light aircraft landing gear strut depend on the fraction of the aircraft's total mass that is relevant to the observed part, acceleration parallel to the load vector, and load vector orientation and direction, depending on the actual operation performed by the aircraft. This research divides aircraft operations into different phases based on variables that affect the *RUL* of the landing gear structure. These phases include taxi or ground manoeuvres, take-off, flight, and landing. Each phase has a specific load distribution, intensity, and direction (referred to as the load profile). The load profile is influenced by the nature of the flight, pilot input, and environmental conditions. To ensure flight safety, it is important to consider environmental conditions which can significantly impact flight planning and pilot input.

However, due to the lack of available sensor data in light aircraft, the aircraft's mass and mass distribution, and available acceleration data are used for the prognosis of maintenance-related issues. For this research, five distinct load profiles were identified, corresponding to the previously mentioned flight phases (Figure 22). The first and fifth load profile (1&5 LP) which are shown in Figure 22 represent the loads acting on the light aircraft landing gear structure during ground manoeuvres, specifically the taxi-out and taxi-in phases of operation. Taxi-out and taxi-in loads are differentiated by the difference in mass resulting from the aircraft's fuel consumption. The second and fourth load profiles (2&4 LP) in Figure 22 show the loads on the landing gear during take-off and landing. Take-off and landing have distinct load intensity and direction differences but can be neatly represented by the same Figure 22.

The third load profile (3LP) shown in Figure 22 illustrates the loads acting on the aircraft during flight, distinctive for its characteristic load being the result of the acting acceleration and masses originating from its own structural and landing gear wheel masses. From the five discerned phases, the fourth load profile (4LP), specifically landing, has by far the greatest potential of inducing loads significant to landing gear structure *RUL* deterioration, as is known from practical experience and shown by numerous research ([138], [139] [140]), one of which was also done by the author of this Thesis, [2].

A load profile is defined in this Thesis through light aircraft landing gear structure load-relevant parameters; those parameters are the aircraft mass relevant to the observed structural part, the load direction relative to the observed structural part (for this research deduced from the lateral and longitudinal airplane angle), the aircraft's acceleration parallel to load direction, and the time the observed part was subject to such conditions. Additional simplifications and assumptions were introduced and explained in the corresponding method development Chapters of this Thesis. The stated *RUL* relevant parameters are operational variables; for example, the aircraft mass changes during flight due to fuel consumption, load direction also changes because of various manoeuvres, such as landing and take-off which cause a change in the lateral aircraft angle.

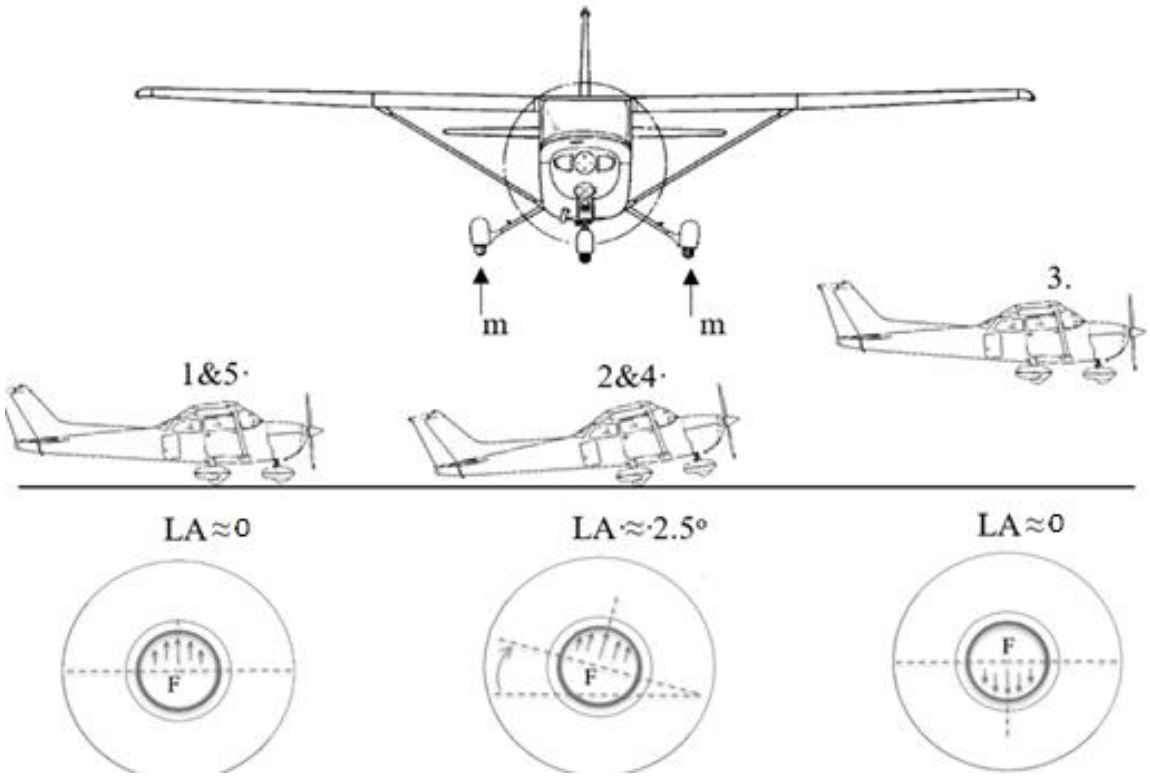

Figure 22. Light aircraft load profiles.

However, considering constant values for various manoeuvres still ensures greater *RUL* precision than disregarding operational conditions altogether, as is the current standard in light aircraft landing gear strut maintenance. Specifically, this research held the aircraft's mass constant for each operational phase, regardless of its variability due to fuel consumption, because of the variabilities' small impact on landing gear strut *RUL*. However, the fuel consumption-related difference in mass was considered when comparing the taxi-out and taxi-in operation phases, as well as landing and take-off. The impact of aircraft total mass variation during flight due to fuel consumption has no significance on aircraft landing gear strut *RUL* and is therefore not considered. Additional landing gear strut *RUL* relevant parameters are, amongst other factors, related to the landing gear type. Suppose the observed light aircraft has a tricycle landing gear layout, as is the observed case with a Cessna 172R. Five *RUL*-related load parameters must be defined. Those parameters are the mass acting on the observed landing gear strut (m_1 or m_2 in the case of this research), the angle of the aircraft around its longitudinal, lateral, and vertical axes (*LA1*, *LA2*, *LA3*), and the acceleration parallel with the acting load on the light aircraft landing gear strut. In this research, only a significant deviation from the neutral position (neutral position being the position when the aircraft is at a standstill on the ground) of the lateral angle was observed for simplicity's sake since *RUL*-significant load angles around the longitudinal and vertical axes derive from landing or take-off conditions often resulting in

part replacement due to strut deformation or detectable crack initiation. Additionally, longitudinal, and vertical axis variable introduction doesn't contribute to method development while simultaneously increasing research complexity, due to reasons stated prior, some of them being unpredictable *RUL* relevant factors. The load profile can be categorized further, depending on the combination of *RUL*-related load parameters collectively labelled load profiles into subcategories LP_1, LP_2, ..., and LP_n. Those subcategories represent the specific flight phase described by the observed landing gear part's load profile. For this research, it was decided to consider five distinctive load profiles.

Load profile LP_1 represents the taxi-out operation phase. The LP_1 load profile is distinguishable by the ground load vector normal to the contact surface patch and the biggest mass for each operation since the aircraft hasn't used up the fuel planned for its operation. The aircraft's angle around its lateral axis is constant and considered zero. Additionally, the LP_1 load profile can be discerned by measured acceleration components, primarily vertical acceleration. The vertical acceleration component, along with the lateral and longitudinal, were measured in [4]. This research methodology considers the calculation of the normal force between the surface and the landing gear by multiplying the value of aircraft mass and the respective component of acceleration. The acceleration measurement samples were taken on asphalt and grass surfaces, whereby the grass surface acceleration values are slightly higher due to higher surface unevenness. It was concluded that the grass surface acceleration values would contribute to a lower structure *RUL*, as opposed to the lower acceleration values measured on an asphalted surface. For this reason, it was decided to use the grass runway acceleration values, since that would result in earlier *RUL* depletion, and thus enhance operation safety. Equation *(14)* is used to calculate the load profile corresponding to the three aircraft axes which are labelled *X* (longitudinal), *Y* (lateral), and Z (vertical).

$$\begin{aligned} F_X &= \begin{bmatrix} a_1 \\ \dots \\ a_n \end{bmatrix} \cdot m \cdot \sin\beta\,; \\ F_Y &= \begin{bmatrix} a_1 \\ \dots \\ a_n \end{bmatrix} \cdot m \cdot \cos\alpha; \\ F_Z &= \begin{bmatrix} a_1 \\ \dots \\ a_n \end{bmatrix} \cdot m \cdot \sin\alpha. \end{aligned} \qquad (14)$$

Where:

F_X – Is the load acting on the observed landing gear structure part in the direction of the longitudinal aircraft axis, [N].

F_Y – Is the load acting on the observed landing gear structure part in the direction of the lateral aircraft axis, [N].

F_Z – Is the load acting on the observed landing gear structure part in the direction of the vertical aircraft axis, [N].

a_1 ... a_n – Are the accelerations measured for the observed load phase, corresponding to the moment in time they were recorded, [m/s^2].

m – Is the part of the aircraft's total mass causing observed part loading, [kg].

α – Is the angle between the vertical aircraft axis and the load direction acting on the observed structural part, [^{o}].

β – Is the angle between the lateral aircraft axis and the load direction acting on the observed structural part, [^{o}].

Load profile LP_2 represents the take-off run and take-off. The load acting on the landing gear strut in this phase is calculated by multiplying the aircraft's starting mass (the mass in the taxi-out phase) and the vertical acceleration component. It is assumed that the aircraft mass is equal to the mass from the previous operation phase because the fuel consumption between those two phases is negligible. Since the Cessna 172R doesn't require a positive angle around the lateral axis for take-off, and this methodology considers the take-off phase finished when lift-off occurs, the lateral angle during take-off is assumed to be equal to the angle in the taxi-out/in phase. The acceleration used to calculate this phase is taken from the research of Juretić et al. [4], measured on the same airplane this method is developed for. To calculate this load profile, equation *(14)* was used.

The load profile LP_3 represents the actual flight. This load profile is distinguishable by a load vector acting in the opposite direction compared to the taxi phase, being a consequence of the landing gear structure and wheel mass. The load angle is assumed constant since there are no mandatory operational records stating them, and the angle change depends on operation specifics and is usually not predictable due to aerodynamic, meteorological, traffic, and other circumstances. It is also worth noting that this phase is expected to have the least landing gear structure *RUL* impact due to obvious reasons (significantly lesser loads). To calculate this load profile, equation *(14)* was used.

Load profile LP_4 represents aircraft landing. This phase is distinguishable because the load angle around the lateral axis is being modulated in the range from a positive angle during touch down, to a zero angle when the aircraft's wheels are simultaneously touching the ground. The mass of the aircraft is lesser than in the taxi-out/in and take-off phases since a significant amount of fuel has been used during operation.

Load profile LP_5 represents the taxi-in phase. This phase is similar to the taxi-out phase, with a key difference which is the lesser mass given the aircraft propulsion system has consumed the fuel required to operate. The aircraft's angle around its lateral axis is constant and considered neutral - zero. The acceleration was again taken from [4], keeping in mind the same assumptions as in the taxi-out phase. To calculate this load profile, again, equation *(14)* was used.

5.2.1.1 Determining aircraft load acting on the observed part

The aircraft's total mass is composed of a variety of masses, variable for each flight, added to the empty aircraft. In the case of the observed Cessna 172R, those masses are the fuel mass, the mass on the front seats (pilot and co-pilot), the masses on the rear seat (passenger/passengers), and the masses stored in two separate baggage compartments. This loading arrangement, applicable to a Cessna 172R, is shown in Figure 23.

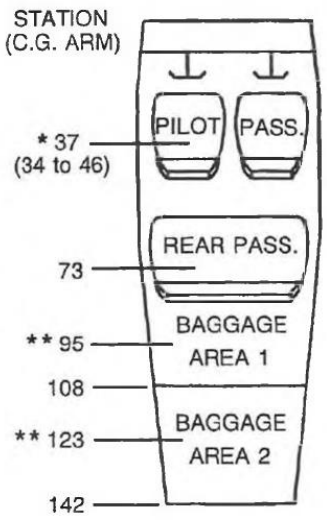

Figure 23. Cessna 172R loading arrangements, [3].

Airplane mass value and distribution validation was performed with Cessna's Maintenance Work Cards for airplane weighing, presented in the Maintenance Manual [13], and used in regular aircraft maintenance actions requiring airplane weighing. An example of a maintenance card used for Cessna 172R weighing is presented in Figure 24.

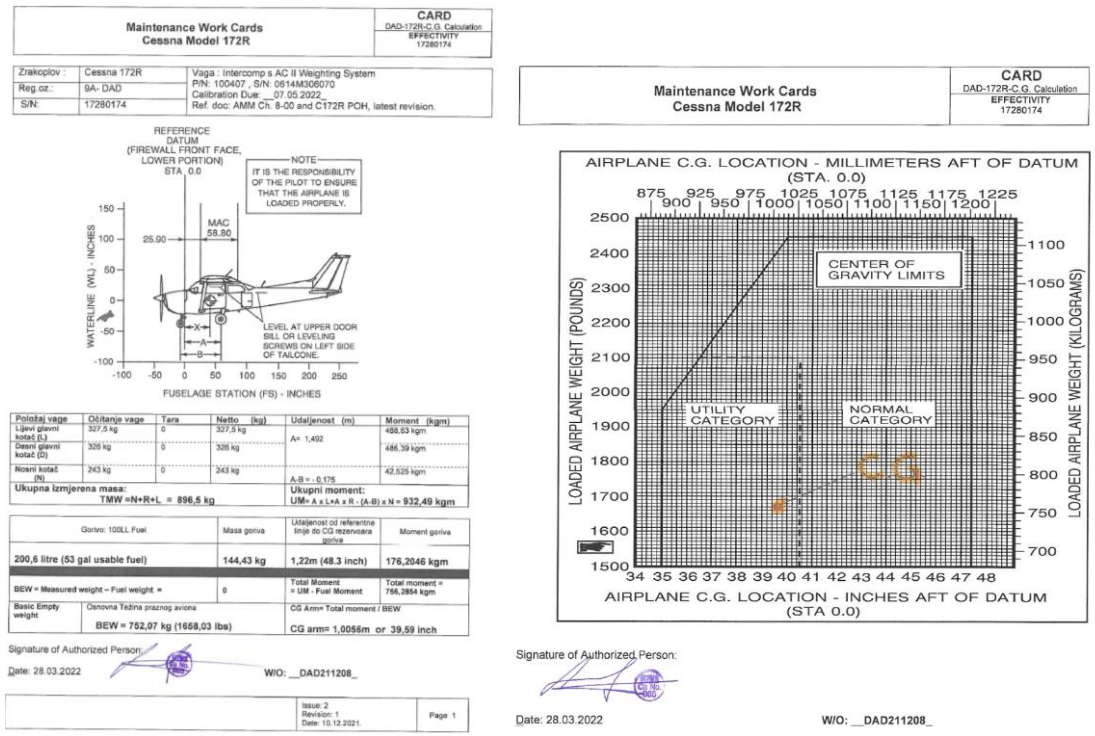

Figure 24. Maintenance card for airplane weighing, used for a Cessna 172R, property of the Faculty of Transport and Traffic Sciences.

Research-relevant documents recording operation data such as aircraft loading are the mass and balance sheets which record the masses positioned according to Figure 23. As stated previously, one essential variable significantly impacting landing gear structure *RUL* is the load intensity. The load intensity acting on the observed structural part is directly related to aircraft mass and acceleration parallel to load orientation. Fuel, crew, passenger, baggage, and empty airplane mass can be extracted from the airplane's mass and balance sheets for the observed Cessna 172R airplane. The airplane operator creates the mass and balance sheet form based on the outlines given by the airplane manufacturer and aligns them with applicable regulations regarding the respective aviation authority. The Mass and balance section in the Cessna 172R Aircraft Flight Manual is labelled “Section 6 Weight & Balance / Equipment List” [3]. An example of the applicable mass and balance sheet used by the Faculty of Transport and Traffic Sciences is displayed in Figure 25.

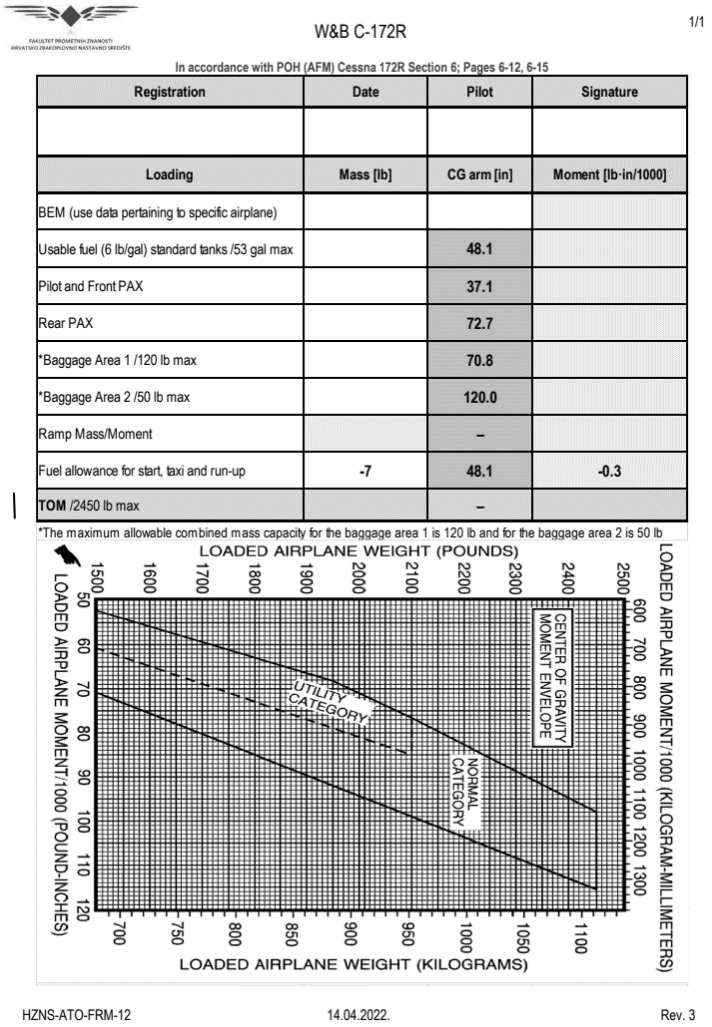

W&B C-172R

1/1

In accordance with POH (AFM) Cessna 172R Section 6; Pages 6-12, 6-15

Registration	Date	Pilot	Signature

Loading	Mass [lb]	CG arm [in]	Moment [lb·in/1000]
BEM (use data pertaining to specific airplane)			
Usable fuel (6 lb/gal) standard tanks /53 gal max		48.1	
Pilot and Front PAX		37.1	
Rear PAX		72.7	
*Baggage Area 1 /120 lb max		70.8	
*Baggage Area 2 /50 lb max		120.0	
Ramp Mass/Moment		–	
Fuel allowance for start, taxi and run-up	-7	48.1	-0.3
TOM /2450 lb max		–	

*The maximum allowable combined mass capacity for the baggage area 1 is 120 lb and for the baggage area 2 is 50 lb

HZNS-ATO-FRM-12 14.04.2022. Rev. 3

Figure 25. Example mass and balance record for the Cessna 172R used by the Faculty of Transport and Traffic Sciences.

Prior to any operation, the mass and balance sheets must be filled out to define the airplane's centre of gravity moment. An example of the centre of gravity moment envelope is displayed in Figure 25. To extract data from the mass and balance sheets, an operator input form was created as explained in Chapter 5.3.4, and displayed in Figure 76.

Fuel, front seat, rear seat, baggage area 1, and baggage area 2 masses, according to Figure 25, proposed for operator input in the operator input form were identified by determining the allowable airplane mass value and distribution (see Table 10.), and mass and balance calculations presented in the aircraft's flight manual [3]. The documents enabled mass boundary determination, meaning the upper and lower mass limits, as well as an acceptable mass distribution. The acceptable mass interval begins with the aircraft's empty mass, which is 1639 pounds or approx. 743 kg (see Table 10.), and ends with the maximum allowable mass, called maximum take-off weight, which is 2450 pounds or approx. 1111 kg (see Figure 24). Decimal

values defining empty and maximum mass for aircraft operations should have no significance to operational safety and research result validity, and they were therefore neglected in the analyses. The Aircraft Flight Manual [3] also defines the aircraft's maximum useful load which represents the cumulative fuel, front seat, rear seat, baggage area 1, and baggage area 2 masses. The aircraft's useful load is 818 pounds or 371 kg. The aircraft's fuel mass is a variable restricted by tank size; the usable fuel volume in a Cessna 172R, according to Table 10., is 53 US gallons or 200.63 litres. The prescribed fuel type, according to the airplane's Aircraft Flight Manual [3] is AVGAS 100LL. The Pilot Operating Handbook ([3], (Figure 1-10)) displays a volume-to-mass conversion chart for fuel mass calculation. The usable fuel mass (litres of Avgas 100LL converted to kilograms) would be 144.45 kg. Having the fuel tanks completely full would leave 227 kg allocated to the front seat, rear seat, baggage area 1, and baggage area 2 in their respective allowable amounts (as restricted by the Aircraft Flight Manual, [3]). On the other side of the spectrum, an empty fuel tank would not enable any kind of operation with the engine running and was therefore not considered. The stated loading boundaries are applicable for any normal category Cessna 172R operation.

Mass value and distribution imply different mass value and distribution combinations, called mass value and distribution scenarios in this Thesis. Every airplane operation has a unique mass value and distribution scenario. Fuel, crew, passenger, and baggage masses change according to the required operation, within the acceptable boundaries, as shown in Figure 25. The predictability of mass value and distribution scenario, which would enable more precise operator input suggestions, would require prediction based on many operations which have to be biased since the Cessna 172 airplane type is one of the most common airplane types in the world, used for operations which vary greatly in parameters relevant to landing gear structure *RUL*. In other words, the generality of the method developed in this research would be compromised by a commitment to a certain operation type implying a certain probable loading intensity and combination. It was therefore decided to neglect to load combination specificity and simply divide the acceptable mass range for any given position into three intensities divided by approximately equal steps. The selected masses are displayed in the operator input form (Figure 76) and the knowledge acquisition table (shown in Table 17.). All possible loading combinations were considered for this research and displayed in the *RUL* matrix presented in Table 20.

According to the Cessna 172R mass and balance sheet displayed in Figure 25 the *RUL* relevant masses are “U. FUEL” which is an abbreviation for usable fuel, *FPAX* which represents

the front seat mass, *RPAX* for the rear sear mass, *BGA1* for baggage area 1 and *BGA2* for baggage area 2. However, not every mass value and distribution scenario is acceptable for operation. Some loading combinations result in unacceptable flight performance and are therefore prohibited. For this research, all loading combinations were considered and checked using the mass and balance calculation procedure presented in [3], and displayed in Figure 25. The validity of acceptable vs non-acceptable loading combinations was checked by creating a simple Excel sheet that calculates mass and balance according to the appropriate procedure (determined by the example document in Figure 25) and warns if the input values result in an overweight airplane. Displayed in Figure 26 is the created mass and balance calculator. The calculator can detect a mass and balance combination leading to an overweight aircraft. If the total weight of the aircraft—comprising its empty mass (*BEM*), usable fuel, *FPAX, RPAX, BGA1, BGA2,* and fuel allowance—exceeds 2450 pounds, the built-in overweight warning in the calculator will be triggered. This is facilitated through a straightforward IF statement that checks if the total mass is above the acceptable limit. The maximum allowable take-off mass reduced by a fuel allowance for take-off predetermined by the operator (in the case of the observed operator -7 pounds) is 2450 pounds.

			Mass [lbs]	CG arm [in]	Moment [lb*
		BEM	1677	39,52	66,27504
FUEL kg.	31	Usable fuel	68,2	48,1	3,28042
FPAX kg.	136	FPAX	299,2	37,1	11,10032
RPAX kg.	150	RPAX	330	72,7	23,991
BGA1 kg.	27	BGA1	59,4	70,8	4,20552
BGA2 kg.	11	BGA2	24,2	120	2,904
		Ramp mass	2137		0
		Fuel allow.	-7	48,1	-0,3367
		TOM	OVERWEIGHT		111,4196

Figure 26. Mass and balance calculator created according to Figure 25.

The lower mass and balance calculator boundary was not considered since the mass and balance calculator's purpose is only to highlight acceptable loading combinations in the process of developing an expert system for the demonstration purposes of this research. Therefore, the lower mass and balance calculator boundary was set to 1500 pounds, which results in a loading that is lower than any possible loading for Cessna 172R operation. However, the calculator issues a warning statement in case of accidental wrong mass input.

After determining the airplane’s mass, the reaction force acting on the observed main landing gear strut had to be calculated. For this purpose, a mass distribution procedure was developed. Light aircraft mass distribution on a tricycle-type landing gear can be calculated based on eight steps.

First, mass distribution information must be acquired. Conveniently, the input of this information into the mass and balance sheets is mandatory prior to any flight operation to ensure airplane dynamic stability and manoeuvrability.

Second, the mass and balance calculation procedure has to be performed. The mass and balance calculation procedure depends on the airplane type and differs with every observed airplane, depending on its geometric, material, and structural specifics. The observed airplane mass and balance procedure is described in the aircrafts' Aircraft Flight Manual, [3].

Third, the value of the centre of gravity arm must be calculated based on mass and balance sheet information. The centre of gravity arm is the distance between the airplane's mass and balance reference line, in the case of the Cessna 172R this line coincides with the airplane's firewall and the centre of gravity. The centre of gravity arm is labelled *X* in Figure 27, and it is measured in parallel with the airplane's longitudinal dimension.

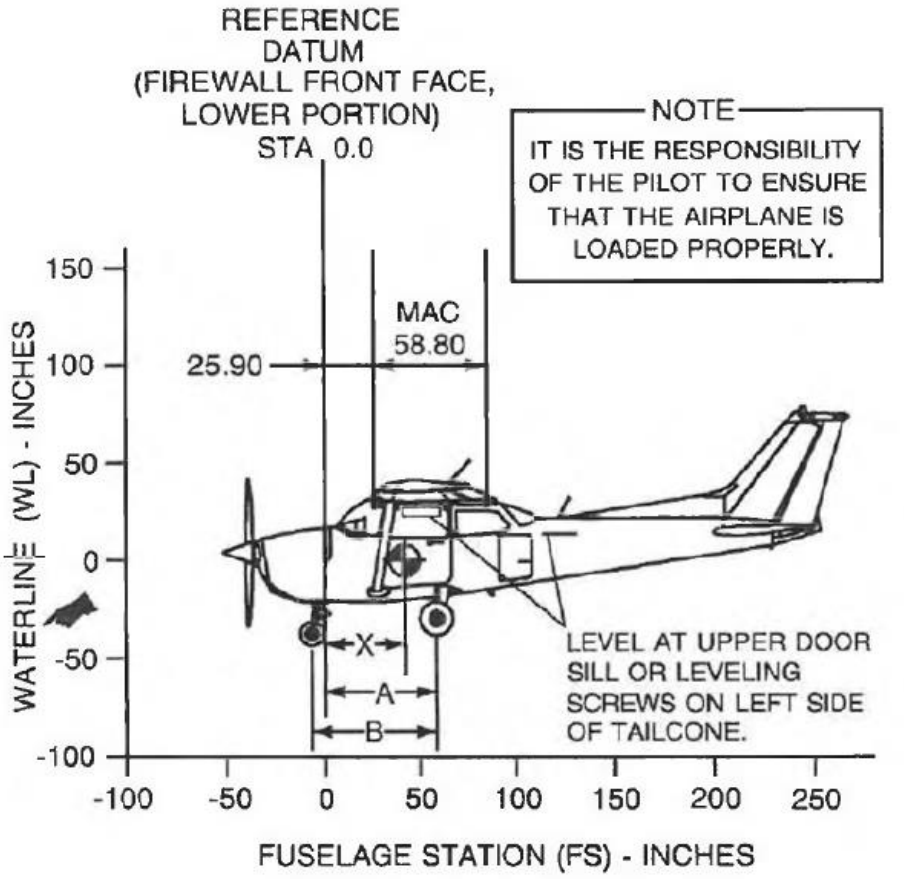

Figure 27. Extract from the Cessna 172R weighing form, [3].

When calculating the airplane's centre of gravity arm, equation *(15*) must be used, according to the airplane weighing procedure, described in [3]:

$$X = A - \frac{mNLG \cdot B}{mNLG + 2mMLG} \quad (15)$$

Where:

X – Is the airplane's centre of gravity arm, [m].

A – Is the distance between the airplane's firewall and its main landing gears, [m].

mNLG –Is the calculated mass that can be measured by placing a scale under the nose landing gear, [kg].

B – Is the longitudinal distance between the airplane's nose and main landing gears, [m].

mMLG – Is the calculated mass that can be measured by placing a scale under one of the main landing gears, [kg].

Fourth, the longitudinal centre of gravity distance from the main landing gear wheels must be calculated. The longitudinal centre of gravity distance from the main wheels is calculated by using equation *(16)*.

$$H = A - X \quad (16)$$

Where:

H – Is the longitudinal centre of gravity distance from the main wheels, [m].

Fifth, the lateral centre of gravity distance from the main landing gear wheels (labelled I) must be calculated. The lateral centre of gravity position is calculated by dividing the airplane's track by two (as displayed in equation *(17)*).

$$I = \frac{track}{2} \quad (17)$$

Where:

I – Is the lateral centre of gravity distance from the main wheels, [m].

track – Is the distance between the aircrafts main landing gear wheels, [m].

Sixth, the distance between the centre of gravity from the main wheels *(E_{CG})* must be calculated. This distance is determined by calculating Pythagoras equation (in equation *(18)*):

$$E_{CG} = \sqrt{H^2 + I^2} \quad (18)$$

Where:

E_{CG} – Is the centre of gravity distance from one of the aircrafts main wheels, [m].

Next, the distance of the centre of gravity from the landing gear nose wheel is calculated by using equation *(19).*

$$D = X + (B - A) \tag{19}$$

Where:

D – Is the distance of the centre of gravity from the landing gear nose wheel, [m].

Seventh, the percentage of the main wheel distance from CoG, against the sum of all wheel distances is calculated by dividing the centre of gravity distance to a main wheel, and the sum of distances of all three wheels from the centre of gravity, equation *(20).*

$$E\% = \frac{E_{CG}}{2 \cdot E + D} \tag{20}$$

Where:

E% – Is the percentage of main wheel distance to the CoG against the sum of all wheel distances to the CoG, [%].

In the eighth and final step, the mass that could be measured by putting a scale under one of the main landing gear wheels is calculated by subtracting the total airplane mass and the product of percentage of main wheel distance to CoG and airplane total mass, equation *(21).*

$$mMLG = \frac{mTOT - E\% \cdot mTOT}{2} \tag{21}$$

Where:

m_{TOT} – Is the total airplane mass, [m].

The calculated value of mass acting on the main landing gear wheel was compared with actual airplane weighing records. The comparison showed a deviation from the expected value by 7.34 %. It was concluded that the reason for this deviation originates from a multitude of factors, such as an expected measurement error of the angle between the landing gear strut and vertical line perpendicular to the horizontal surface (subject angle displayed in Figure 21), and other factors such as the aircraft's variable vertical position of the centre of gravity. To mitigate unwanted result deviations, the procedure for calculating mass distribution had to be adjusted to ensure result credibility.

Result deviation from the actual measured mass was mitigated by subtracting a constant percentage from the calculated percentages of the main wheel distances from CoG against the sum of all wheel distances (*E%*). The required constant percentage was 5.75 %, and the adjusted percentage of main wheel distance against the sum of all wheel distances was calculated according to equation *(22)*:

$$E_A\% = \frac{E_{CG}}{D + E + F} - 5.75\% \quad (22)$$

Where:

$E_A\%$ - Is the adjusted percentage of main wheel distance against the sum of all wheel distances, [%];

F – Is the distance of the main landing gear wheel from the centre of gravity, having the same value as E_{CG}, based on airplane symmetry [m].

After calculating the $E_A\%$ value, the mass on the main landing gear was calculated by using equation *(21*).

The stated mass distribution calculation procedure was validated by comparing measured masses for several Cessna 172 aircraft, recorded in their weighing records, with calculation results for those aircraft. Based on validation findings, it was concluded that the calculated values are satisfactory close to the masses actually measured under each airplane wheel, deviating from the measured values by less than 1 %. Consequently, the mass distribution calculation method was deemed acceptable.

5.2.1.2 Determining acceleration and load frequency

The second source of information used to define landing gear strut *RUL* relevant load intensity is the research done by Juretić et al. [4] presenting acceleration measured on the Cessna 172R during all relevant operation phases, taxi-out, taxi-in, take-off, flight, and landing. The research focused on measuring vibrations on the Cessna 172R main landing gear for modal frequency analysis. The measuring set was comprised of an Arduino UNO board, a tilt sensor SW-420 and an ADXL345 accelerometer. The operating principle of the accelerometer and tilt sensor is based on electromechanical interactions. It features a mass situated between two metal plates, collectively forming two voids between the mass and the plates. The entire assembly is encapsulated in a vacuum, safeguarding it from fluctuating atmospheric parameters to ensure precise measurements. As the mass undergoes movement, the gaps between it and the metal plates correspondingly alter, and this change is directly proportional to the acceleration induced on the system due to the movement of the sensor. Effectively, this setup functions as two capacitors, where the spaces between the mass and the plates symbolize the capacitors. Consequently, the capacity of these capacitors shifts in alignment with the acceleration. This capacity difference is therefore proportional to the acceleration and is interpreted as such. It is crucial to note that time sampling within this system is intrinsically dependent on the registered acceleration, which is dictated by the movement of the components within the sensing device.

The accelerometer was set up in a way that enabled load factor measurement, by dividing the acceleration with the gravitational constant. Variable environmental conditions such as wind, precipitation, temperature, and others all influence airplane movement and consequently the acceleration acting on the landing gear structure, specifically acceleration parallel with load direction. Besides environmental or external conditions, there are also internal factors impacting the movement of the airplane, such as engine vibrations. The impact of all those vibration sources was recorded in the measurement taken by Juretić et al. [4], constituting a representative acceleration (load factor) sample acting on the airplane and consequently the landing gear structure. The ADXL345 accelerometer measures acceleration in three directions, and the orientation of the sensor was coincident with the airplane's three main axes, the vertical, longitudinal, and lateral as described in [4]. The measured data was stored in an Excel sheet, in the format of a single column containing time stamp, *Z*, *X*, and *Y* axis load factor information. For this research, the data was sorted into four columns according to information type (time stamp and three columns stating acceleration along respective axis). Line charts were constructed with the load factor intensity on the vertical and the time stamp on the horizontal axis, displayed in Figure 28. The line charts' purpose was to ease visual identification of the threshold and average load factor values required for this research's result refinement. Data extraction was also performed with built-in Excel functions for minimum and maximum value extraction, and mean value calculation.

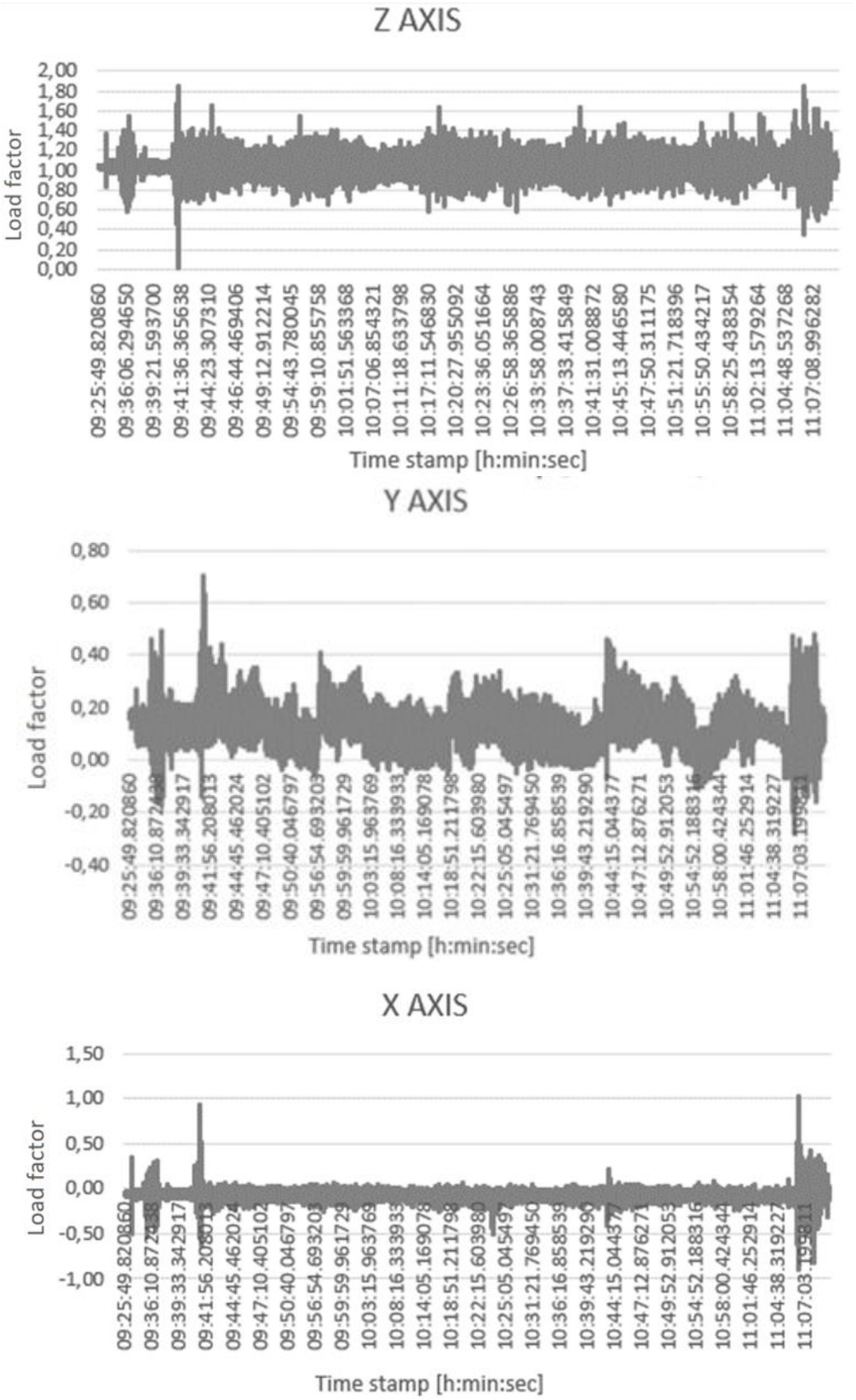

Figure 28. The load factor measured along the vertical, longitudinal, and lateral axis, [4].

As described in [4], the ADXL345 sensor senses acceleration in three directions. The sensor was mounted on the rear seat support structure, as described in [4]. The described placement was considered acceptable to assume that the measurements are representative of the

acceleration acting on the landing gear structure, especially considering the rear seat support structure is in rigid connection with the fuselage and in the immediate vicinity of the Cessna's 172R main landing gear which is also rigidly connected to the fuselage. The measured acceleration was used to refine the simulation results for the methodology developed in this research. Simulation results could have been produced without direct acceleration measurement data. In the absence of actual acceleration data, acceleration threshold values can be extracted from the aircraft's flight manual. These threshold values represent acceleration boundaries. However, to make these values representative of actual flight conditions for total remaining useful life determination, they would need to be adjusted by an estimated coefficient. This coefficient would account for the difference between the ideal conditions represented in the manual and the real-world conditions the aircraft experiences. In this particular case, since acceleration data was available, acceleration measurements were taken from research [4] which was conducted on the exact same aircraft, the Cessna 172R with the callsign 9A-DAD. The airplane's acceleration in three directions relative to airplane axes (parallel, vertical, and lateral) was used in combination with the airplane's total mass to calculate the load acting on the landing gear structure.

To conclude, landing gear strut remaining useful life values can be calculated based on usage information. The remaining useful life calculation for the developed method requires information on the load acting on the observed structure. The specificity of the Cessna 172 aircraft series is the huge number of existing and operating aircraft, having a relatively large body of research and consequently data compared to other light aircraft types and containing useful acceleration measurements for remaining useful life prediction refinement, explained in the continuation of this document.

5.2.1.3 Modelling TAXI-OUT loads

The first phase of operation, discerned as relevant for the light aircraft landing gear strut remaining useful life, was in essence modelled by multiplying the measured load factors, gravitational constant and mass, according to equation *(23)*.

$$F_{X,Y,Z} = n_{X,Y,Z} \cdot m_1 \cdot g \qquad (23)$$

Where:

$F_{X,Y,Z}$ – Is the load acting along the aircraft's respective axis, [N].

$n_{X,Y,Z}$ – Is the load factor measured along the respective aircraft axis, [N].

m_1 – Is the calculated mass on the observed main landing gear wheel, [kg].

g – Is the gravitational constant, [m/s^2].

The mass is calculated based on the explanation given in Chapter 5.2.1.1, and simplifications introduced to establish the specific objective of this research.

The objective is tied to the nature of this research, the development of a new prognostic method. In this context, result refinement is secondary to method feasibility and appropriateness in achieving the desired operational safety improvement. The main landing gear strut relevant mass simplification involves distinguishing three mass values within the prognostic algorithm. If the objective would have been different, such as implementing a commercial prognostic system, precise mass input according to the observed mass and balance record would have been required. The three mass values offered in the operator input form (Figure 76 in Chapter 5.3.4.3) serve a demonstrative purpose and were considered sufficient for this research. Considering the five observed mass stations (fuel, front seat, rear seat, and two baggage areas), in addition to the three offered mass values for each station and the mass and balance procedure for airplane overweight protection, 141 allowable mass combinations were analysed in this research. These allowable mass combinations were determined by performing the respective mass and balance procedure and eliminating any mass combinations that fell outside the allowed boundaries, which could compromise the airplane's dynamic and static stability. The various mass value and distribution combinations are labelled mass value and distribution scenarios in this Thesis.

The measurements in [4] consist of recorded load factors for taxi procedures on asphalt and grass surfaces, flight, approach, take-off, and landing on asphalted and grass surfaces. The recorded measurement had notes, taken by the pilot who was also the person in charge of the measuring procedure, identifying operation phase changes (for example from taxi-out to take-off). Additionally, cumulative frequency data on the incremental vertical load factor during the taxi phase of operation for 395 different flights and recorded for the same aircraft type was available, [15], depicted in Figure 29. The available incremental vertical load factor data [15] was used for load validation. Calculated load value validation was performed because the data measured in [4] was taken for only one single flight. The average values of the available measured vertical acceleration data for the Taxi-in and Taxi-out (displayed as TXOA and TXIA in Figure 29) phase of operation was compared with data from [15]. The validation showed result overlapping in the same order of magnitude, when observing corresponding operation phases, such as data recorded for taxi operations and the taxi load factor values identified by [4]. However, as stated previously, this research considers the impact of the vertical longitudinal and lateral load factor based on measured data during only one flight, which is why information generated by Cicero et al. [15] could only be used to solidify vertical load factor order of

magnitude expectations, regardless of the fact that the data was collected from a much larger sample number.

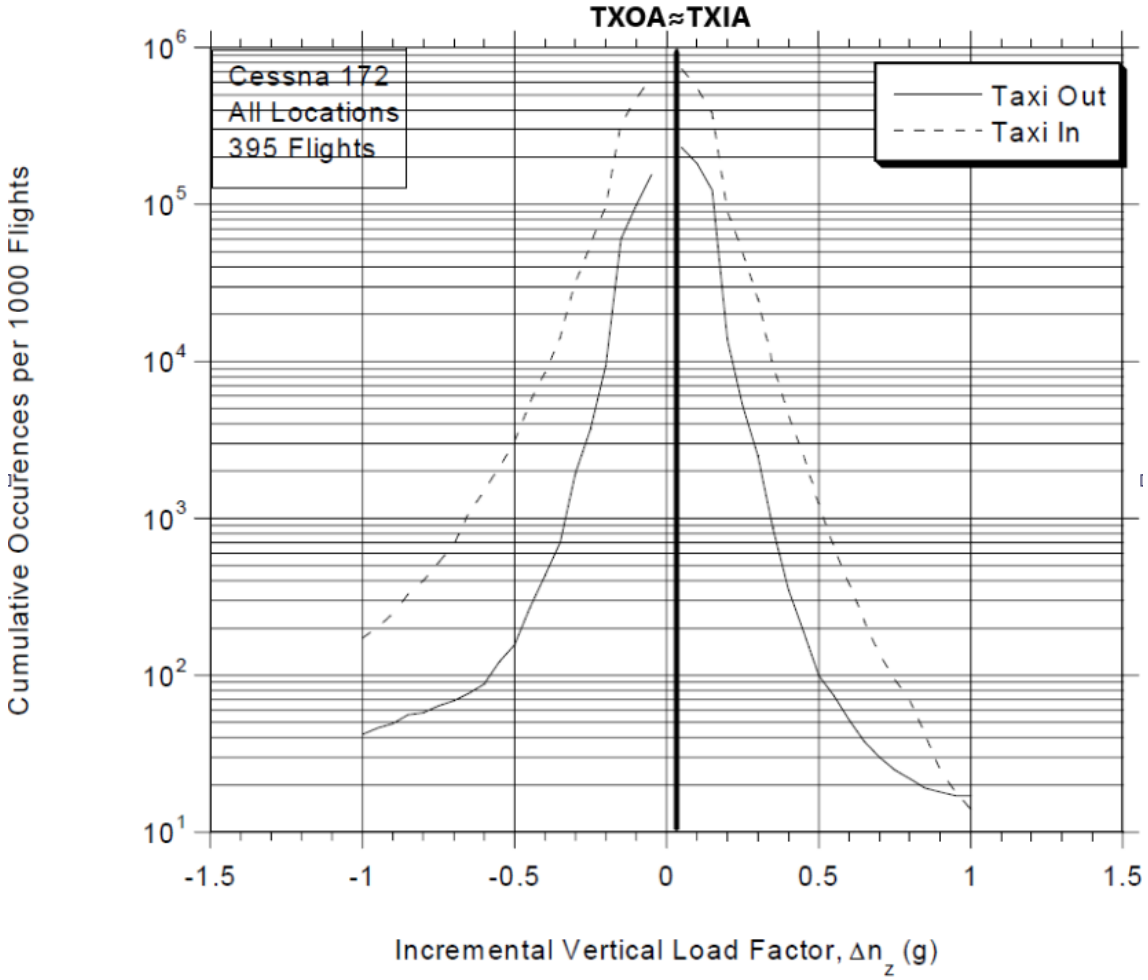

Figure 29. Comparison of the incremental vertical load factor from [15] and [4], for the taxi-out and taxi-in phase of operation.

The taxi-out phase vertical load factor measured by Juretić et al. [4] is displayed in *Figure 30*. Simple statistical analysis reveals the maximum measured load factor was 1.55, the minimum value was 0.58 , the average was 1.03652, the median was 1.04 and the standard deviation was 0.11258. Those values, along with calculated averages and standard deviation confirmed expectations on the vertical load factor value, especially considering the observed taxi-out phase was performed on an uneven grass surface, which can be a reason for result deviation when comparing measurement results in [4] and [15].

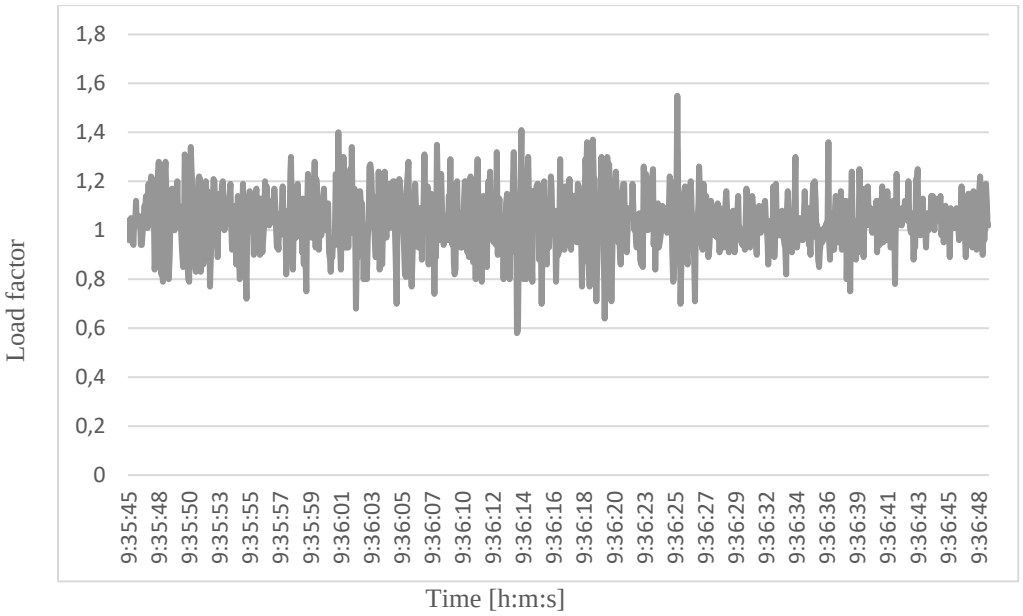

Figure 30. Taxi-out phase vertical load factor data measured in, [4].

The taxi-out phase longitudinal load factor measured by [4] is displayed in Figure 31. Statistical analysis reveals the maximum measured load factor was 0.3, the minimum value was -0.54 , the average was -0.08569, the median was -0.08 and the standard deviation was 0.102994. The longitudinal load factor expectations were confirmed based on those boundaries, calculated averages, and standard deviation. Unlike the previous comparison, expectations were not formed with the help of statistical data based on several hundred recorded flights, since statistical data on the longitudinal load factor was not available. However, the observed values were conforming with pilot subjective experience and engineering judgement.

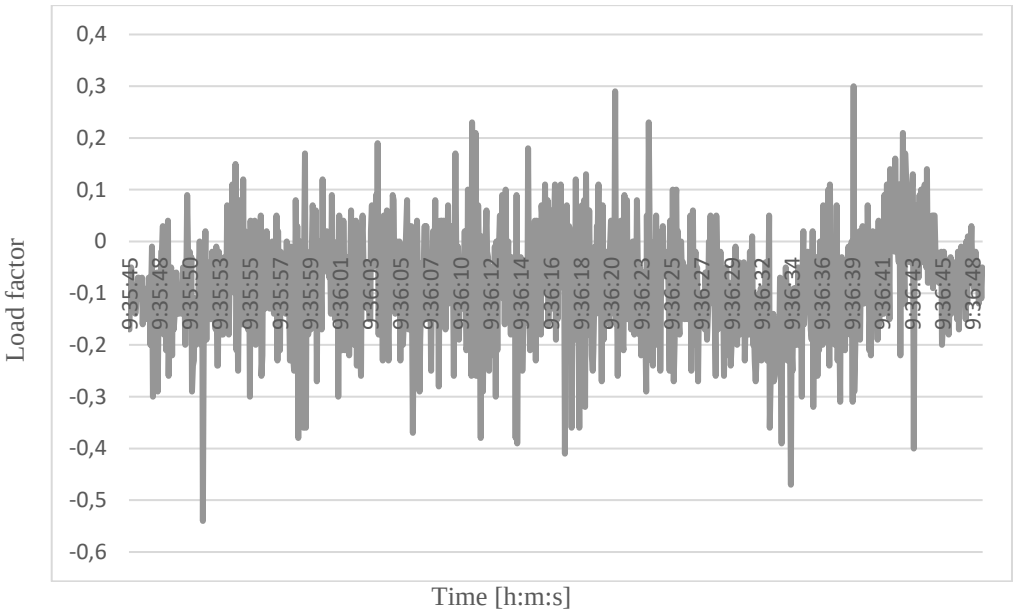

Figure 31. Taxi-out phase longitudinal load factor data measured in, [4].

The taxi-out phase lateral load factor measured by [4] is displayed in Figure 32. Statistical analysis reveals the maximum measured load factor was 0.49, the minimum value was -0.17 , the average was 0.1352, the median was 0.14 and the standard deviation was 0.0749. Those extremes, along with calculated averages and standard deviation confirmed lateral load factor value expectations. Comparison with statistical data was again not performed due to the lack of several measurement sets. However, expected values based on pilot experience and engineering judgement were met by the observed data. An additional affirming point was the fact that longitudinal and lateral acceleration affects fatigue relevant loads to a much lesser degree than vertical acceleration, primarily because of its significantly lower intensity.

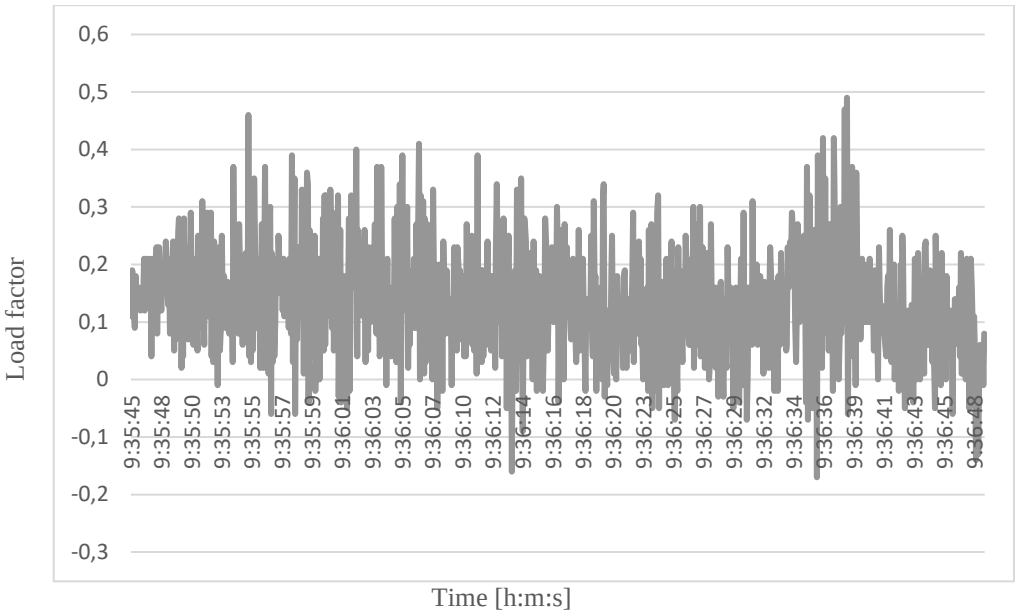

Figure 32. Taxi-out phase lateral load factor data generated by [4].

Calculating the axis loads on the main landing gear strut was performed by a consecutive procedure of mass and load factor input into equation (24). The calculated loads corresponding to the three airplane axes were then used to calculate load vector intensity by using Pythagoras theorem in equation (24).

$$F = \sqrt{F_X^2 + F_Y^2 + F_Z^2} \tag{24}$$

Where:

F – Is the load vector intensity acting on the light aircraft main landing gear strut, [N].

F_X – Is the load vector intensity projection on the aircraft's longitudinal axis, [N].

F_Y – Is the load vector intensity projection on the aircraft's lateral axis, [N].

F_Z – Is the load vector intensity projection on the aircraft's vertical axis, [N].

The resulting load vector intensity was a variable, changing in alignment with load factor variation, according to the measured and recorded values (Figure 30, Figure 31, Figure 32). Load vector intensity values were input into the load history ".dat" file, for fatigue analysis in the computer program Ansys, displayed in Figure 33. The figure illustrates the non-constant amplitude load history data during the taxi phase of a light airplane on a grass surface for a specific mass combination within the aircraft. The horizontal axis represents the time elapsed, while the vertical axis shows the load magnitude experienced by the aircraft's structure. Fluctuations in the load magnitude throughout the taxi phase can be observed, reflecting the uneven grass surface. Peaks in the graph indicate moments of higher and lower stress on the aircraft's structure, respectively. The defined fatigue relevant load vector with variable intensity

and a constant angle is not an accurate representation of the actual load vector since load vector direction changes with acceleration variability. However, it is a good approximation for generating acceptable predictions in a demonstration context, also carrying a significant probability of increasing imminent fatigue failure awareness when compared to existing light aircraft prognostic methods.

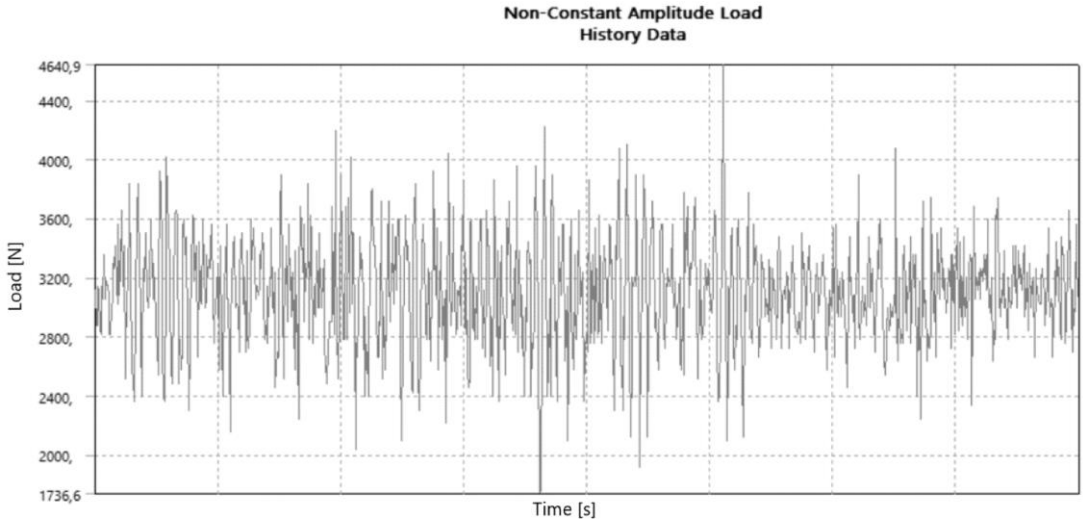

Figure 33. An example of the taxi-out load history for mass value and distribution scenario 31-65-0-0-0.

The last part of defining the taxi-out fatigue analysis relevant load acting on the light aircraft main landing gear strut were the load directions. The only available load vector option for fatigue simulation in the available software was a variable load intensity with a constant orientation and direction (load angles and load direction).

5.2.1.4 Modelling TAKEOFF loads

To determine the load vector acting on an airplane during take-off, the load vector intensity was calculated based on recorded load factor samples taken during this phase of operation, [4]. This intensity is proportional to the acceleration experienced by the airplane and was calculated again by following equation *(23)*. The load vector values were determined by analysing the load factor samples measured during take-off. The load factor samples were aligned with the airplane's vertical, longitudinal, and lateral axes, enabling determination of load vector projections on the three simulation model axes and subsequently load vector intensity for the load history ".dat" file required for Ansys fatigue analysis.

During take-off, the load factor increases as the aircraft accelerates, and the wings generate more lift. However, at a certain point, the lift generated by the wings exceeds the weight of the aircraft, and the aircraft begins to lift off the ground, causing the load factor to significantly drop. Figure 34 clearly displays a drop in load factor values around sample number 655,

continuing with less variability indicating the airplane has taken off. However, additional insight must be gained before deciding on the probable take-off load factor sample set.

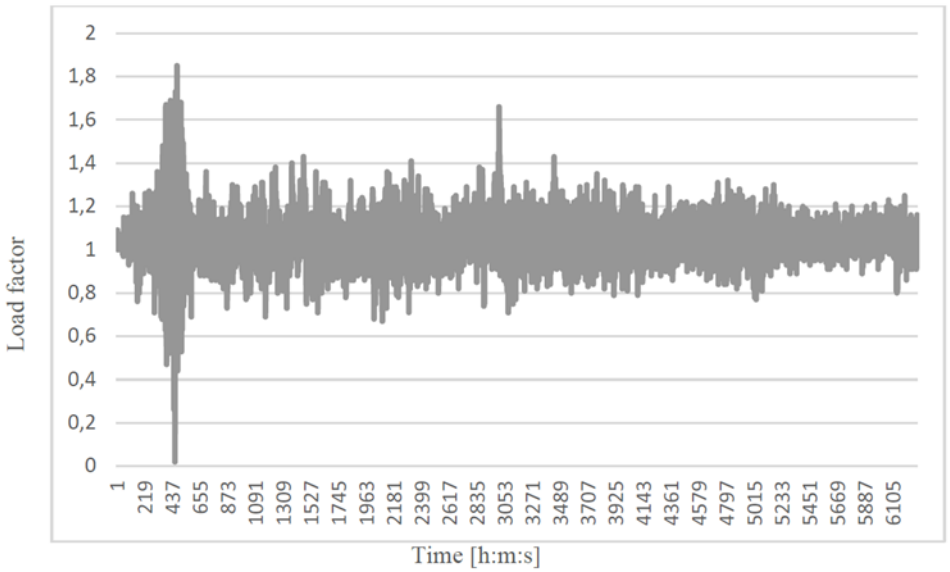

Figure 34. Take-off phase load factor for the vertical airplane axis, [4].

Data comparison of the measured vertical acceleration load factor data from [4], and available data from [15] for the aircrafts take-off phase of operation was done next, Figure 35. The data average from [4] is labelled TOA (take-off vertical acceleration average). This data comparison confirmed the measured data is within acceptable boundaries. At this point it is worth repeating and thereby emphasizing that [15] had only vertical acceleration data, which is why only that data set could be validated.

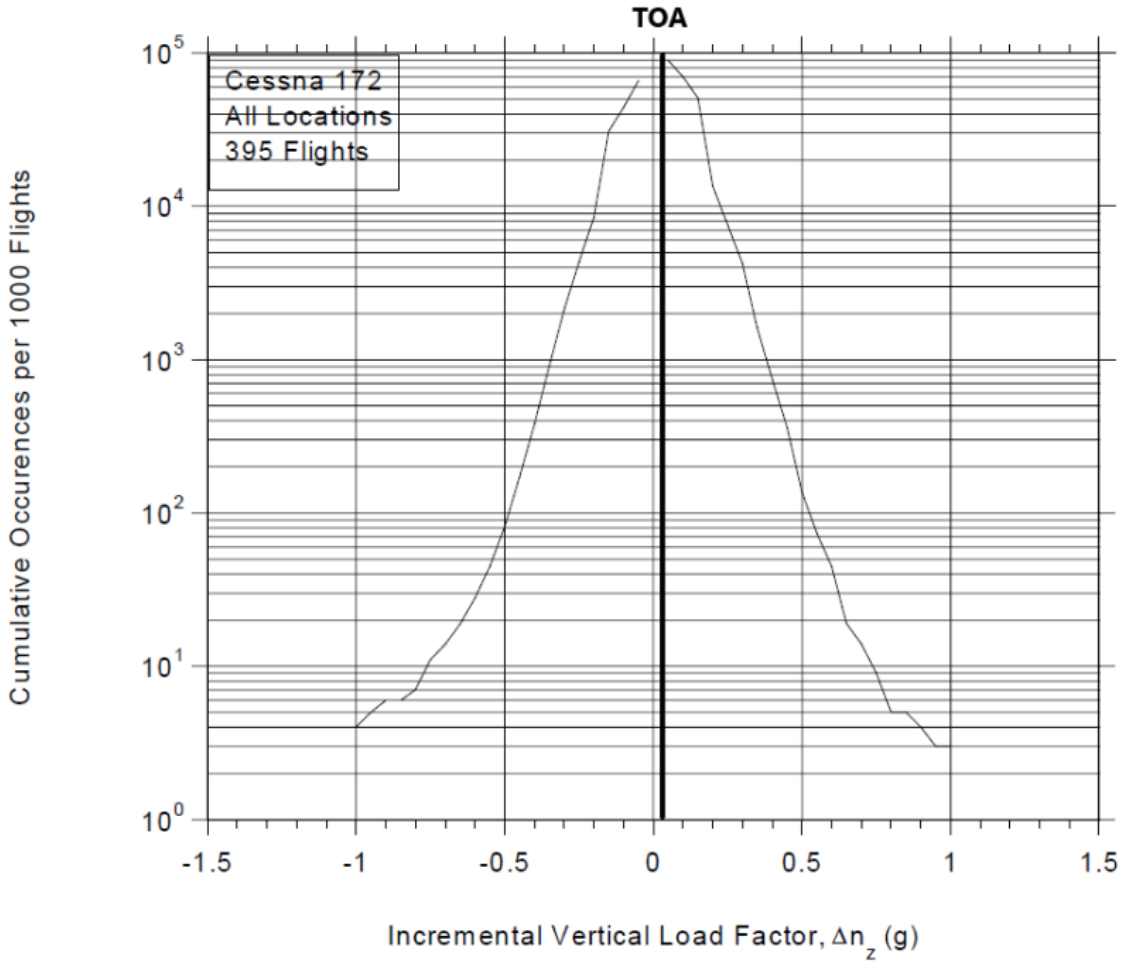

Figure 35. Comparison of the incremental vertical load factor from [15] and [4], for the take-off phase of operation.

Figure 36 illustrates the longitudinal load factor data, during the take-off phase of the observed airplane. It is important to note that the longitudinal load factor is a measure of the force acting on the aircraft in the direction of its motion. The figure shows a significant drop in load factor values, which is indicative of the probable take-off moment. The data presented in the figure is congruent with the previous observation of a similar phenomenon at the same sample number. This consistency in the data reinforces the validity of the findings and provides additional support for the conclusion that the observed drop in load factor values corresponds to the take-off moment.

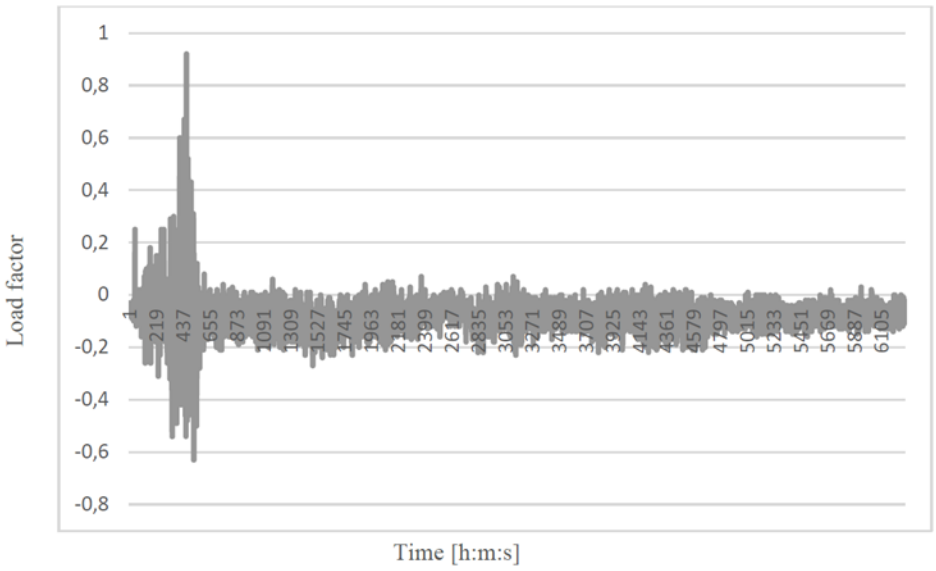

Figure 36. Take-off phase load factor for the longitudinal airplane axis, [4].

Figure 37 presents the lateral load factor data of the observed airplane, recorded during the supposed take-off phase of its operation. The data shows a drop in value intensity, which is congruent with the findings presented in two previous figures displaying vertical and longitudinal load factor data. Additionally, the figure shows significant oscillations after the observed value drop, which indicate that the aircraft is in the climb phase of its operation, with all wheels lifted off the ground. Furthermore, it is worth noting that if the oscillating load factor values were taken while all wheels were still touching the ground, the aircraft would have experienced wheel damage due to lateral movement respective to the direction of movement.

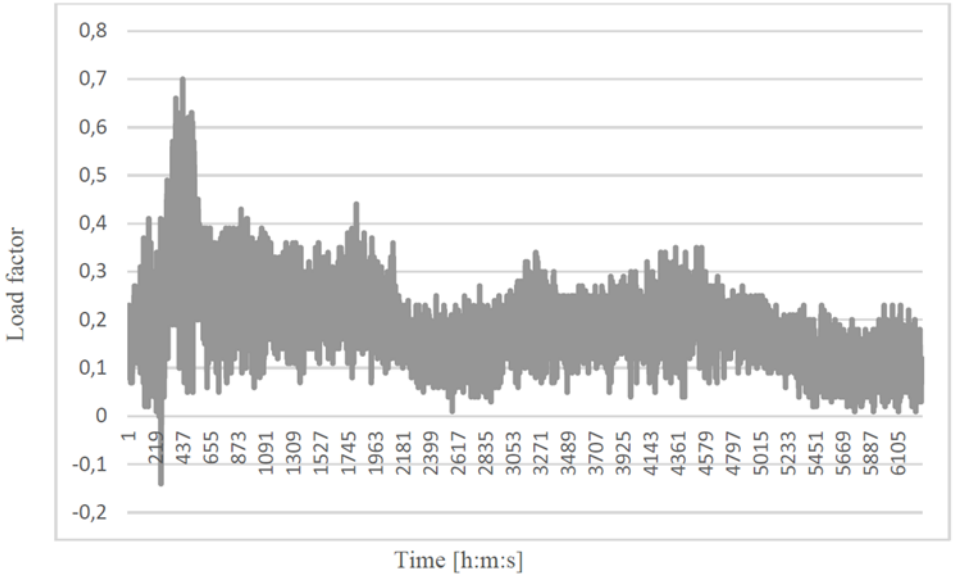

Figure 37. Take-off phase load factor for the lateral airplane axis, [4].

Considering all take-off load factor observations, it was concluded that the chosen interval does not represent the take-off loads in the intended manner. Specifically, this research

considered the observed operational phases according to fatigue life relevant loads, ranging from the expected highest impact during airplane landing, to the lowest impact in the flight phase of operation. The take-off phase fatigue life relevant loads were therefore expected in the immediate vicinity of the observed load factor value drop, in the negative direction of notation. In other words, load factor values with significant relevance for the landing gear structures fatigue life in the take-off phase were observed while the main landing gear wheels still touched the ground. For that reason, a larger dataset of recorded load factor values along the vertical (*Figure 38*), longitudinal (*Figure 39*), and lateral (*Figure 40*) axes was considered. Additionally, the horizontal diagram axis for newly generated figures was chosen to be displayed in units of time, instead of sample number. The observed dataset provided insights into the various phases of the take-off process. The load factor data was categorized into three main parts. The first part is the engine testing phase. During this phase, the airplane's engine is tested while the aircraft remains stationary. The load factor intensity values during this phase were low, indicating that the aircraft was relatively stable and is not subjected to any significant accelerations. The second phase is the idle phase, during which the airplane's engine runs at idle while the aircraft is stationary. The load factor intensity values during this phase were even lower, indicating that the airplane did not move, especially considering the fact of it being on a grass surface. The third part corresponds to the airplane's take-off run on a grass runway. This phase is characterized by a sudden increase in load factor intensity values and variability, indicating that the airplane was subjected to significant loads as it accelerated down the runway, as was expected for such a phase of operation. This phase lasts until the aircraft achieves lift-off speed. Lastly, a small portion of the data shows a drop in the load factor intensity value, indicating that lift-off occurred. This marks the end of the take-off phase and the beginning of the climb phase.

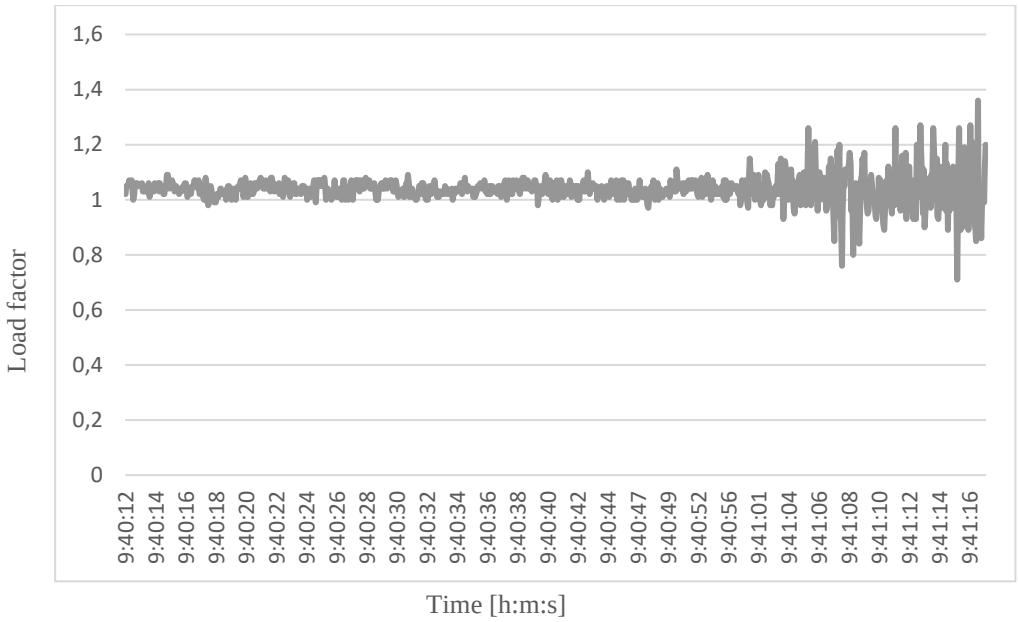

Figure 38. Take-off phase vertical load factor #2, [4].

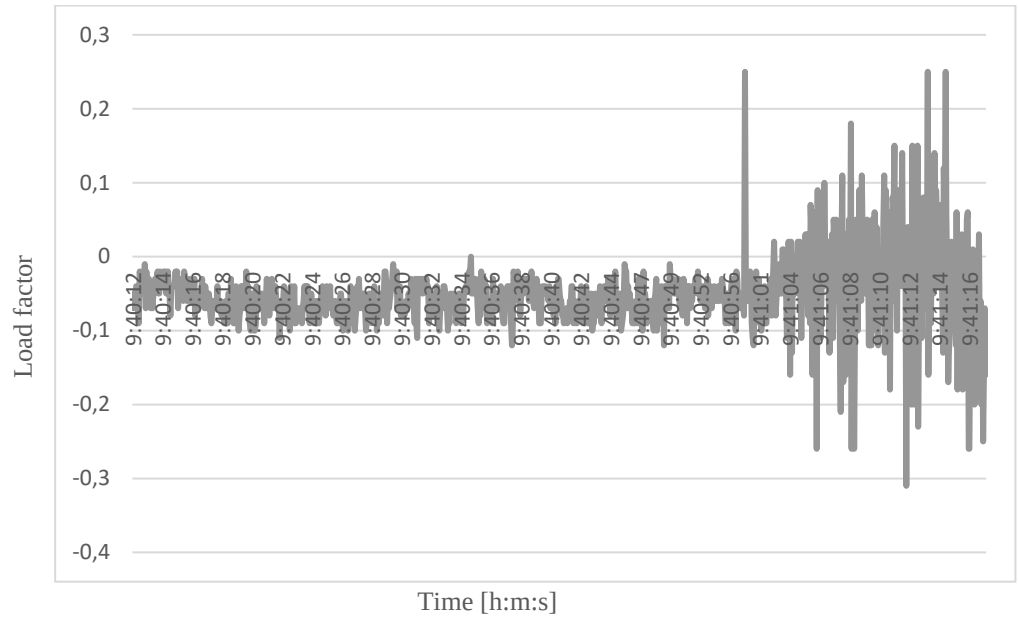

Figure 39. Take-off phase longitudinal load factor #2, [4].

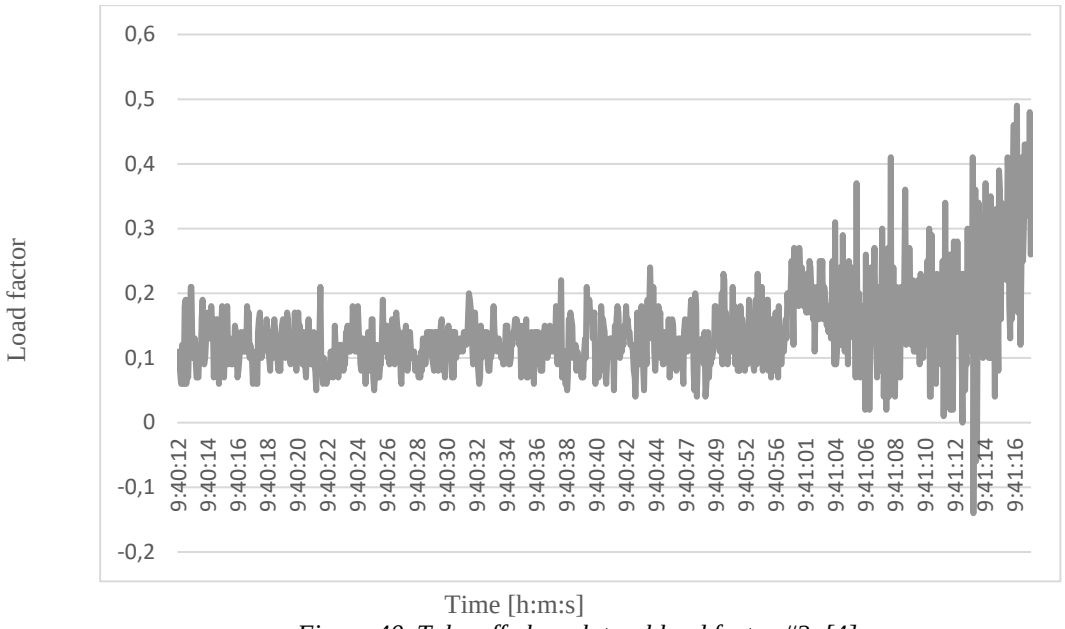

Figure 40. Take-off phase lateral load factor #2, [4].

Upon comparing the data sets Cicero et al. [15] and Juretić et al. [4], it was found that the observed values overlapped in the context of the same order of magnitude. This overlap suggested that the measured load factor data from the single flight is indeed representative of the airplane's take-off phase of operation, despite the smaller sample size. A representation of the load data required for fatigue life analysis in the computer program Ansys is displayed in Figure 41. The figure is representative of the loads acting on the landing gear structure, considering load distribution to one of the two main landing gears struts.

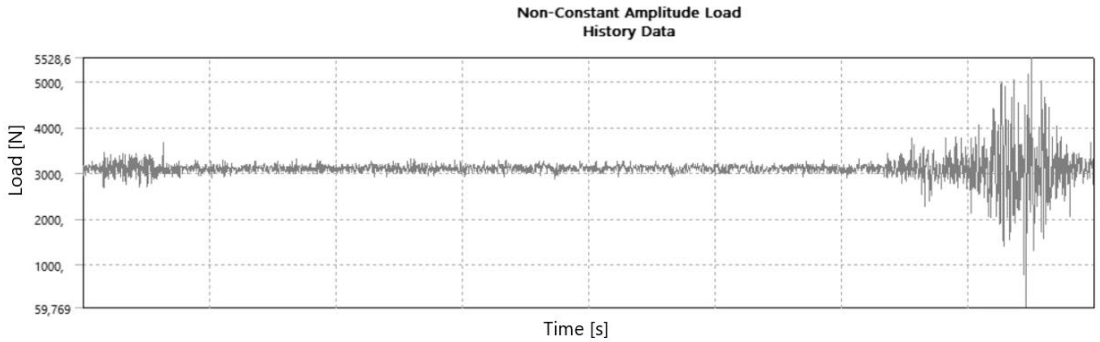

Figure 41. Non-constant amplitude load history data for Ansys fatigue life analysis of the airplane's take-off phase.

After determining the airplane's load vector intensity, the load vector direction and orientation had to be determined. To do so, two assumptions were made. The first assumption was that the take-off phase of operation would be considered with all three wheels of the tricycle type landing gear touching the ground. This assumption ensures that the weight of the airplane is distributed evenly on the landing gear. While this assumption may sometimes deviate from actual conditions, it is still representative for determining the impact of airplane take-off on the

landing gear structural fatigue life. In addition, the Cessna 172 is a type of small aircraft with an interesting aspect that it does not require a positive angle of attack to take-off. Angle of attack in the context of this research refers to the angle between the aircraft's longitudinal axis and the horizontal line parallel to the surface the aircraft is taxiing on. In general, a positive angle of attack is necessary to generate lift and achieve take-off. However, in the case of a Cessna 172R, the design of the aircraft allows it to generate lift even at a zero angle of attack. This is due to several factors, including the shape of the wing and the placement of the main landing gear. The wing of a Cessna 172R is designed with a high-lift aerofoil, which helps to generate lift even at low speeds. Overall, the design of the Cessna 172 allows it to take-off without the need for a positive angle of attack or lifting the nose wheel off the ground. Therefore, the most detrimental take-off circumstance for the landing gear fatigue life was observed when the generated lift can be ignored compared to the weight of the complete airplane. In other words, when the lift generated by the wing is not sufficient to offset the weight of the aircraft. Therefore, the second assumption is that the lift generated by the airplane's wings is significantly smaller than the airplane's weight, enabling the neglect of lift impact. By neglecting the lift impact, the stress on the landing gear parts is caused by the total weight of the airplane, resulting in a shorter estimate of the landing gear's fatigue life. Overall, these assumptions enhance operational safety by reducing the risk of landing gear structural failure due to fatigue. By shortening the calculated fatigue life of the landing gear parts and initiating earlier part inspection, these assumptions help to ensure that any potential issues are identified and addressed before they can become safety hazards.

In the described circumstances, the impact of the take-off phase on the landing gear struts can be significant, particularly if all three wheels are firmly on the ground. This is because the landing gear struts were absorbing the full weight of the aircraft, as well as any additional forces generated by the acceleration. In this sense, immediately after take-off, the landing gear relevant load factor displays a significant drop in value due to the fact that one of the load factor sources changes, from being the airplane's mass to the mass of the landing gear wheels and attached parts. Therefore, the measured load factor data prior to lifting all wheels of the ground was considered in this research.

Given the limitations of the fatigue analysis software, the load vector orientation and direction are considered constant. Based on the previously stated assumptions, the load vector orientation around the lateral axis where all three wheels touch the ground in the take-off phase of operation is used. The other two angles, around the airplane's longitudinal and vertical axes, were considered zero, i.e., the airplane orientation is considered in alignment with the airplane's

direction of movement. If this would not have been the case, the airplane landing gear structure would have been prone to sustain damage based on the fact of consequent unsymmetric weight distribution on the two main landing gear wheels. An extreme example of an existing angle around the airplane's longitudinal axis is when one of the two main landing gear wheels is lifted off the ground. An angle around the vertical axis, on the other hand, would mean the airplane wheel alignment is not parallel to movement direction, causing unnecessary loads to the landing gear wheels and consequently structure. Both circumstances are to be avoided in regular operation conditions, and both circumstances existing simultaneously have a significant probability of inducing landing gear structure overload to the point of requiring unplanned landing gear structural part replacement or even initiating structural failure.

5.2.1.5 Modelling FLIGHT loads

Modelling the flight phase load vector was straight-forward, since the only mass acting on the landing gear strut is that of the landing gear wheel with associated parts as well as parts of the braking mechanism and fairings. The parts adding to the relevant strut mass in the flight phase are displayed in Figure 19, and their masses can easily be determined either by maintenance records, purchase catalogue information or direct measuring with a scale, provided the parts are detached from each other. The observed fatigue relevant parts in the flight phase of operation are:

- Main landing gear wheel.
- Wheel axle.
- Brake callipers.
- Tire.
- Main wheel speed fairing.
- Break fairing.
- Strut fairing.

Various manufacturers produce the listed parts, including differences such as different materials. For that reason, a standard wheel assembly was identified and chosen from the Cessna 172 part catalogue [141]. The standard wheel assembly had a mass of 32 pounds (14.52 kg) for two wheels, meaning one wheel has a mass of 16 lbs. (7.26 kg). Aside from the wheel assembly, the Cessna's fairings had an estimated mass of 1.5 kg that makes a total of 8.76 kg. Based on the expectation of fatigue life being highest for the flight phase, and the fact that wheel assembly mass and fairing usage is a variable, it was concluded to round up the determined mass to 10 kg. The load vector intensity was then calculated by multiplying the

determined mass, measured load factors [4], and the gravitational constant g=9.81 m/s^2. The measured load factors are displayed in Figure 42 (horizontal flight vertical load factor), Figure 44 (horizontal flight lateral load factor), and Figure 45 (horizontal flight phase longitudinal load factor).

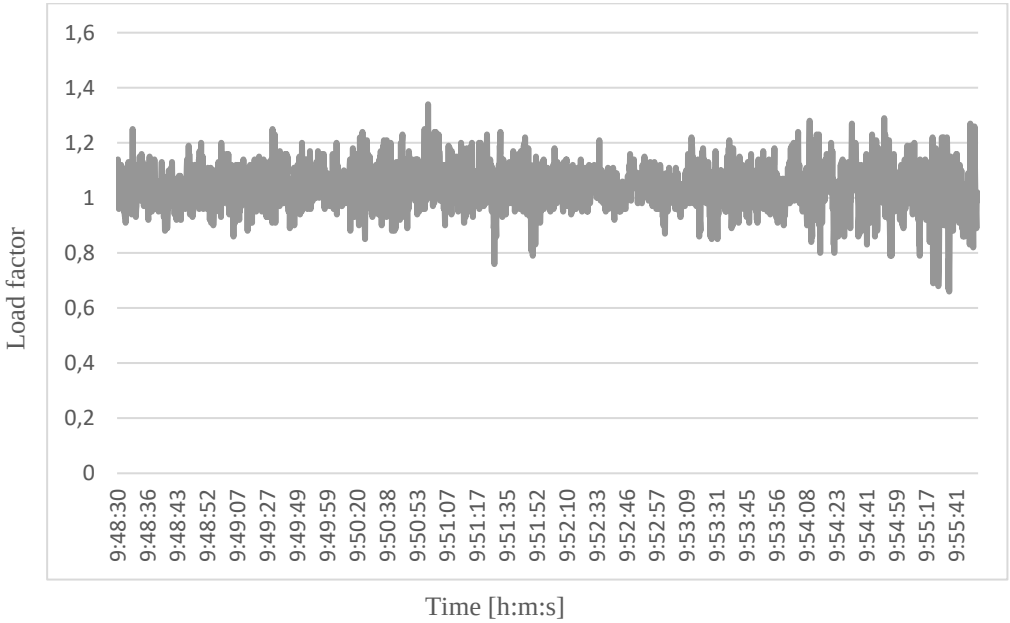

Figure 42. Horizontal flight phase vertical load factor, [4].

Comparison for the aircrafts vertical load factor for flight phase of operation from [4] and [15] was done, and is displayed in Figure 43. This was done regardless of the fact that the flight phase of operation is expected to influence main landing gear strut fatigue life the least, on the brink of being able to neglect it's influence altogether. The data from [4] is labelled FA (flight vertical acceleration average). This data comparison confirmed the measured data is within acceptable boundaries.

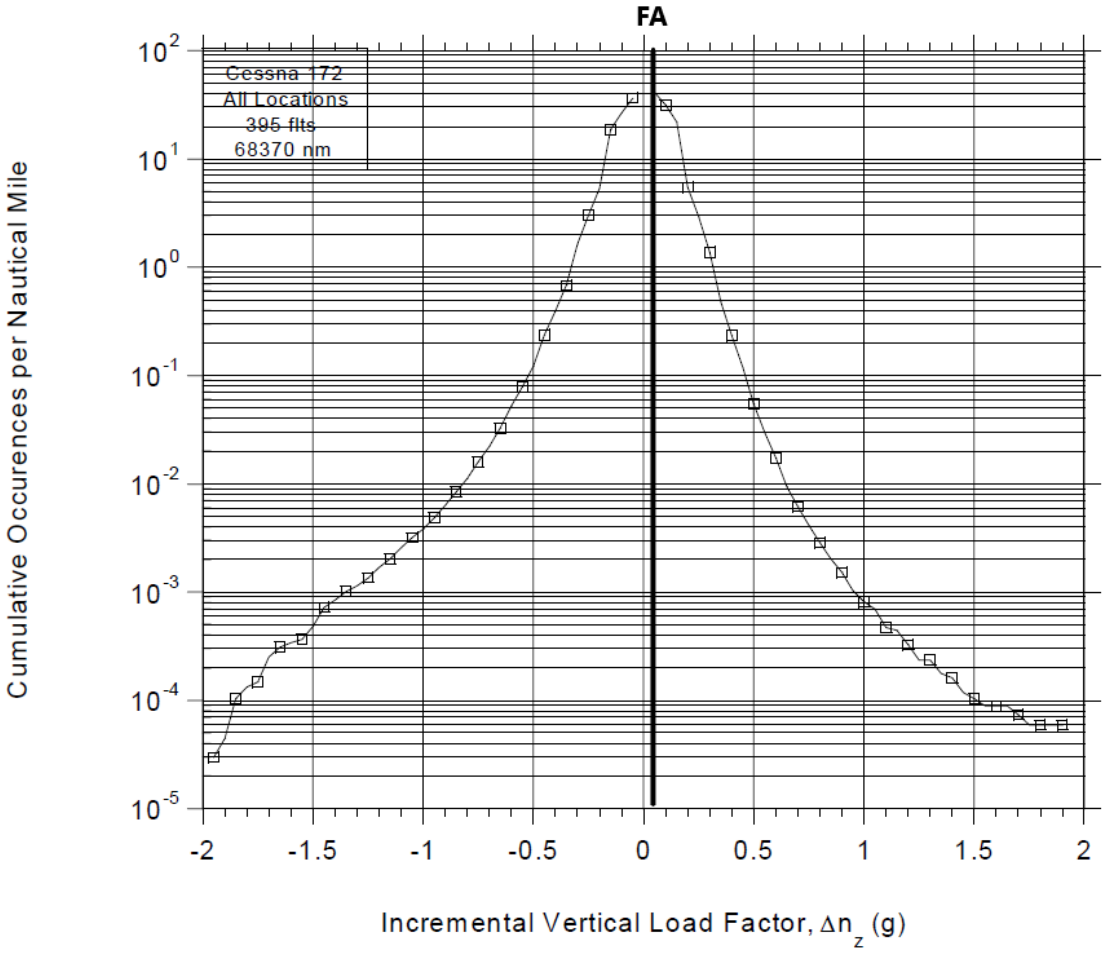

Figure 43. Comparison of the incremental vertical load factor from [15] and [4], for the flight phase of operation.

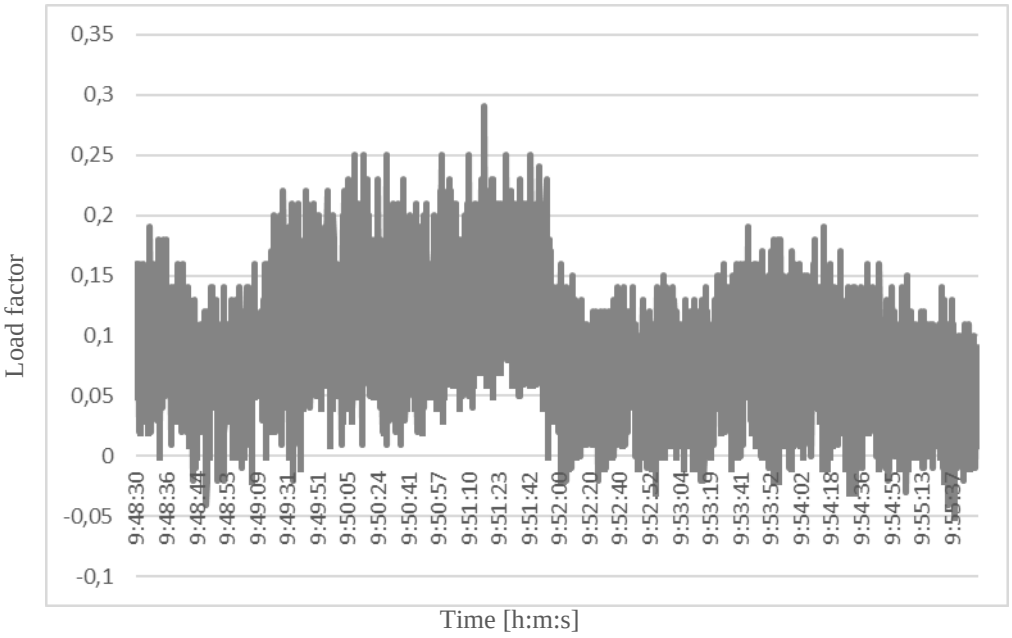

Figure 44.Horizontal flight phase lateral load factor, [4].

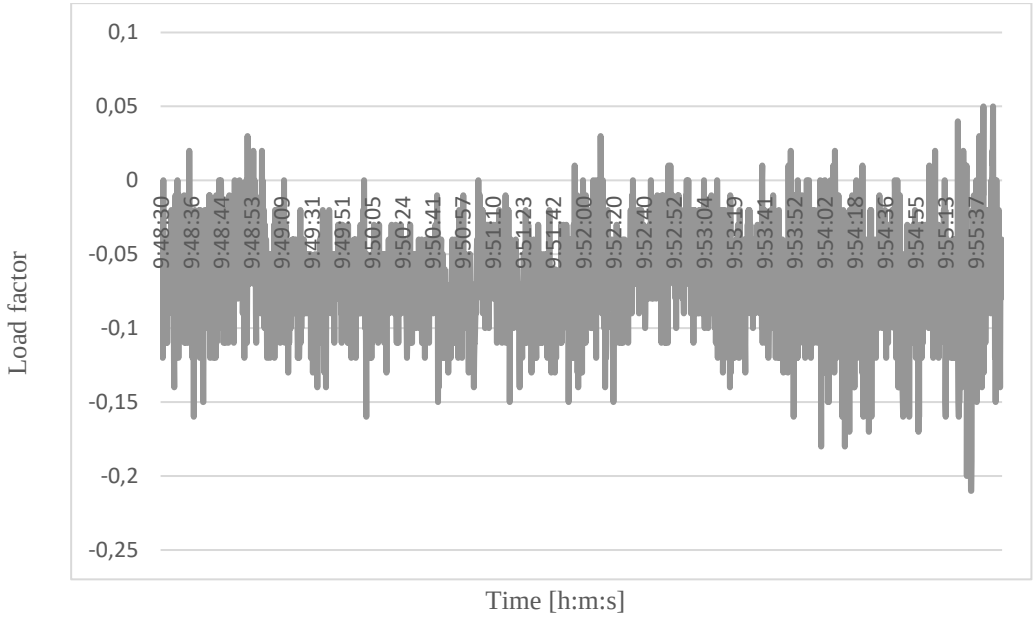

Figure 45. Horizontal flight phase longitudinal load factor, [4].

After determining the mass relative to the landing gear strut, the next step was to determine the load vector orientation and direction. It was decided to simplify load vector direction, to be oriented downwards (in the positive direction of the *Y* axis of the simulation model). The load vector orientation was again decided to be simplified, by assuming it to be parallel to the simulation model *Y* axis, according to Figure 72.

Based on the stated load vector intensity, orientation and direction, the load history ".dat" file required for Ansys fatigue life analysis was calculated by multiplying the recorded values from research [4] during airplane horizontal flight. The required values were obtained by multiplying the recorded data with the stated parameters.

5.2.1.6 Modelling LANDING loads

The load vector's intensity is proportional to the acceleration experienced by the airplane during landing, and it was calculated by multiplying acceleration measurement samples recorded during light airplane landing, the mass acting on the light airplane landing gear structure and the gravitational constant, according to equation *(23)*. The mass acting on the light airplane main landing gear strut in the landing phase is lower than the mass in the previous ground-contact phase considering airplane fuel consumption. Based on oral consultations with pilots, it was concluded that on average, light aircraft consume approximately 20-25 % of their total fuel during take-off, 50-60 % during flight, and 15-20 % during landing and taxiing operations. However, the exact fuel usage can vary depending on the specific aircraft model, operating conditions, and pilot behaviour. In this research, it was decided that a 60 % reduction of fuel mass used during the aircrafts flight phase of operation will result in an acceptable load

vector difference, sufficient for a representable fatigue life prognosis of the light airplane landing gear structure. The landing phase was modelled reducing the fuel mass by 60 %.

The load factor variables were determined by analysing load factor samples measured during airplane landing in research [4]. The three load factor sample sets aligned with the airplane's vertical, longitudinal, and vertical axis were analysed. The airplane's vertical axis load factor during airplane landing is displayed in Figure 46. The values clearly indicate vertical load factors corresponding to usual and expected landing values, according to [15]. The conditions for those load factor values can be encountered during flight, provided relative high gusts are present, however, pilots notes state the recorded load factors correspond to airplane landing. In addition, the recorded longitudinal and lateral load factor values were compared with the vertical values to gain further confidence in the conclusion given in the continuation of this Chapter.

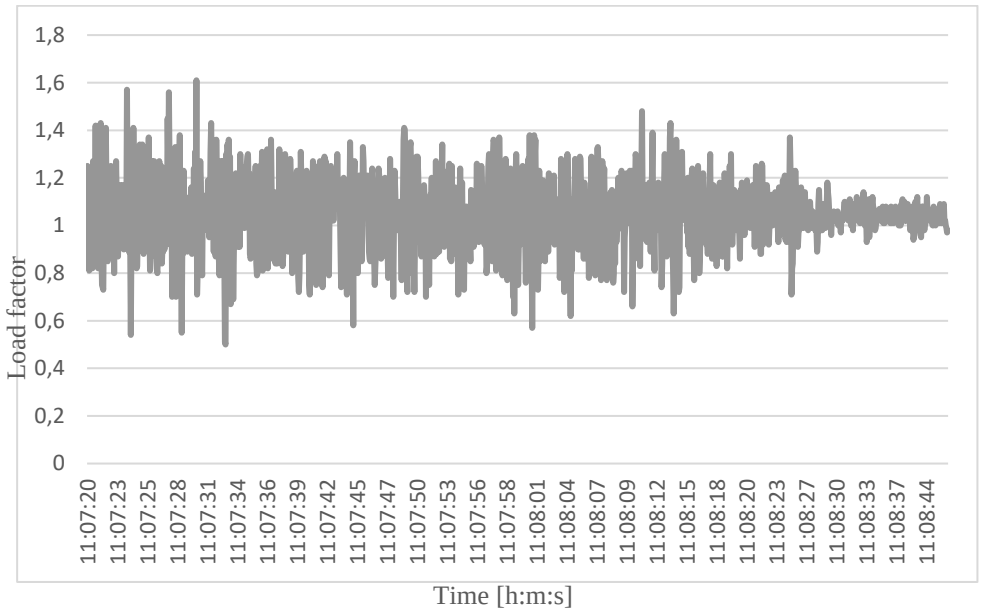

Figure 46. Vertical load factor measurements during airplane landing, [4].

Data comparison of vertical acceleration data from [4] and [15] for the aircrafts landing phase of operation was done next, Figure 47. The data average from [4] is labelled LDGA (landing vertical acceleration average). This data comparison confirmed the measured data is within acceptable boundaries.

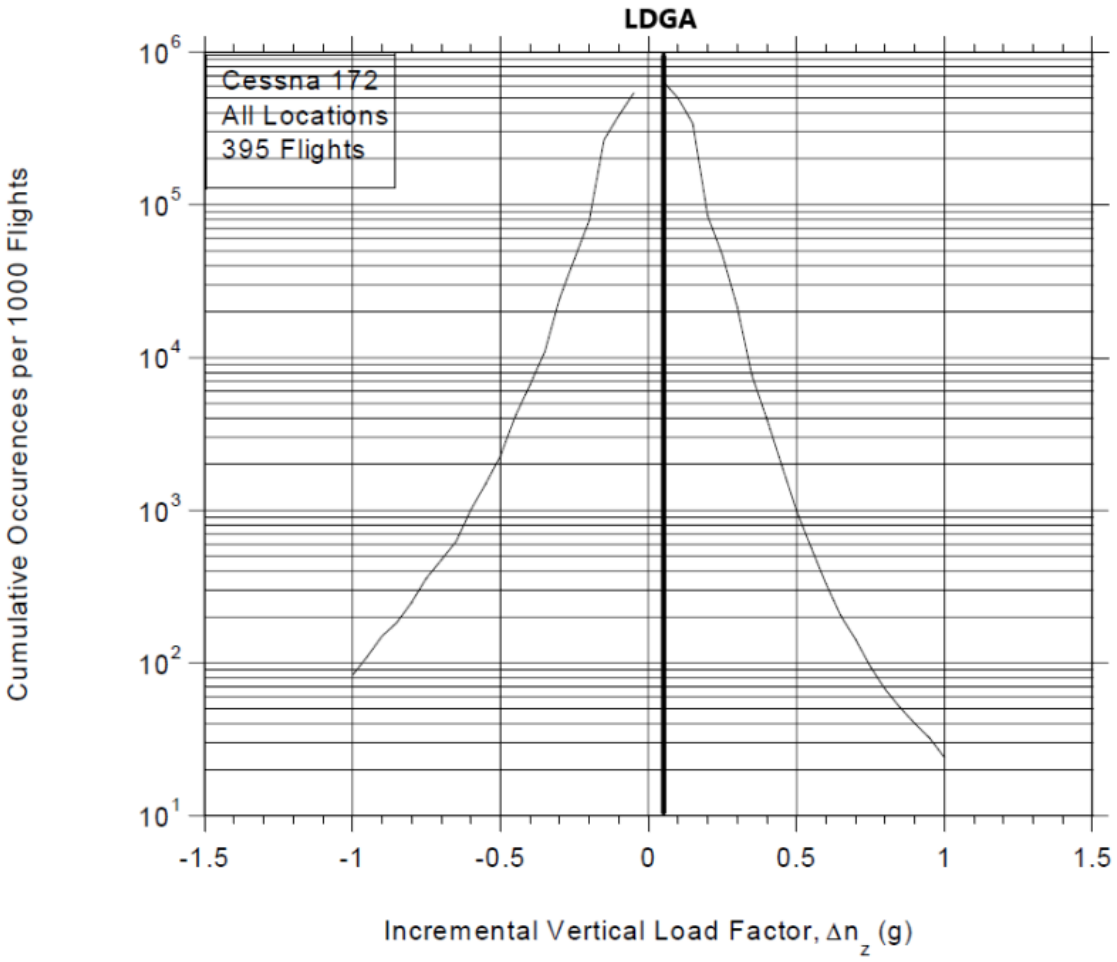

Figure 47. Comparison of the incremental vertical load factor from [15] and [4], for the landing phase of operation.

The airplane's longitudinal load factor values are displayed in Figure 48. The displayed graph represents longitudinal load factor measurements during airplane landing. In this particular graph, negative values can be observed. This indicates that the airplane made touch-down, and the pilot starts to engage the brakes. Continuing the measurement scale, a significantly lower intensity pattern can be observed, representing airplane movement over a grass runway, as was the case in this operation. In the previous figure (Figure 46) displaying the vertical load factor, the values rapidly decreased immediately after touch down. The vertical touch down load factor is clearly visible prior to the observed longitudinal load factor values indicating brake engagement, confirming that the airplane landing gear contacted the runway. Going down further on the longitudinal axis load factor record, a stable decrease of load factor values indicates the airplane is slowing down its movement and coming to a halt, the only measured vibrations being that of the running engine, as could also be observed in the previous figure displaying the vertical load factor intensity.

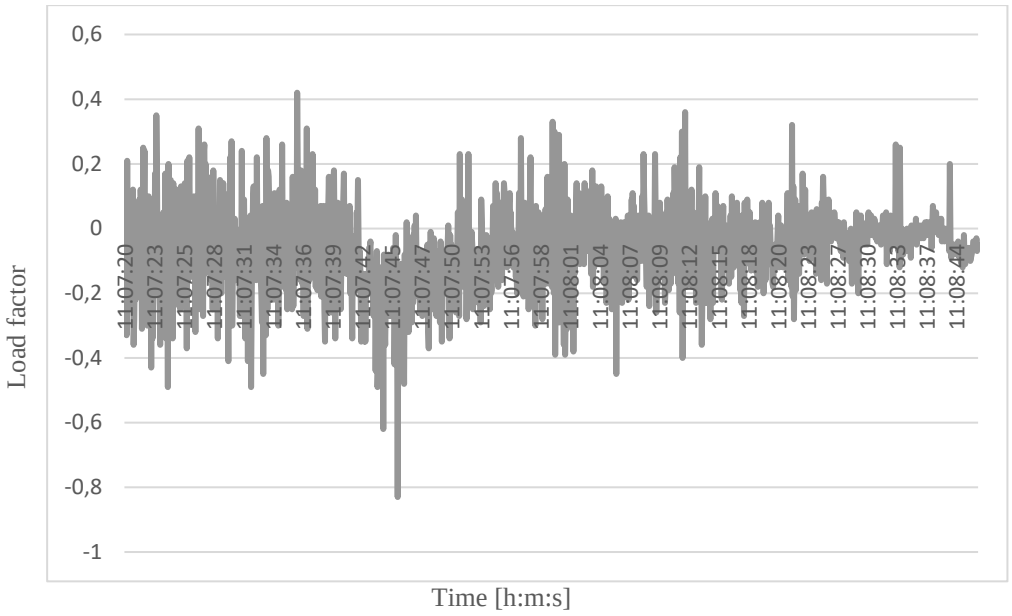

Figure 48. Longitudinal load factor measurements during airplane landing, [4].

The final figure displaying the lateral load factor measurements does not reveal a distinct touch down characteristic. However, the load factor values corresponding to the touch down moment visible in the vertical and longitudinal load factor records is still discernible in the lateral measurements. The touch down indication visible in the lateral load factor record are the peak values around the 0.4 vertical load factor intensity. A decisive conclusion on the touch down moment cannot be made based solely on this observation but having in mind the previous characteristic vertical and longitudinal load factor intensities, an overall conclusion is possible. It was concluded that the observed load factor values corresponding to airplane landing according to pilot notes and observations in this Chapter are representative of airplane landing and was used to determine the airplane's landing load history for fatigue analysis.

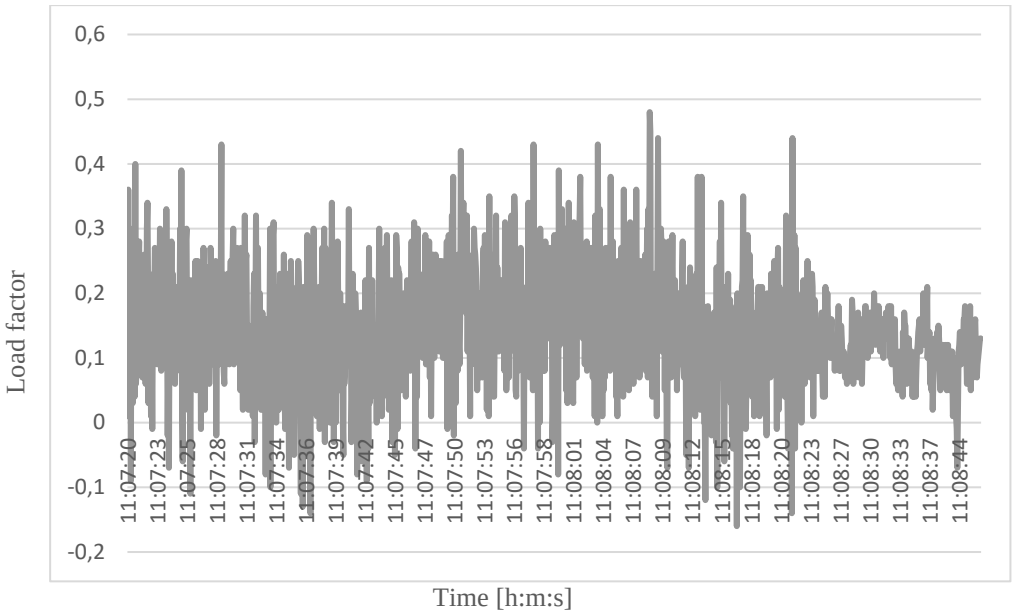

Figure 49. Lateral load factor measurements during airplane landing, [23].

Aside from load vector intensity, the load vector direction and orientation were determined relative to the landing gear strut. The orientation and direction of the load vector were determined based on the airplane's position and angle of descent during landing. To calculate the load vector orientation, the airplane's landing angle must be considered, if only the main landing gear touches the ground until the airplane slows down enough to produce a lower aerodynamically induced moment around its lateral axis. Given the existing Ansys Student license fatigue analysis limitations where fatigue analysis only considers variability of the load vector intensity, while keeping the load vector orientation and direction constant, it was decided to use an average value of load vector orientation for the landing phase of operation of a light airplane. The average value of load vector orientation during the landing phase of operation was determined based on information gathered by consulting with instructor pilots, where instructors stated their instructions on the desired landing angle to pilot trainees. It was concluded that the average light airplane landing angle around its lateral axis can vary depending on the specific type and model of the airplane, as well as the landing conditions such as runway slope, wind, and landing speed. In general, the landing angle around the lateral axis for light airplanes' is typically between 5 to 10 degrees. However, it is important to note that this can vary significantly based on the specific circumstances of the landing. Therefore, a landing angle of 7^{o} was chosen to model the landing phase of light airplane operation. The other two angles, around the airplane's longitudinal and vertical axes, were considered zero i.e., airplane orientation is considered in alignment with the airplane's direction of movement. This means the load vector angle around the *Y* and *Z* axes in the coordinate system of the simulation

model are zero. If those angles were different than zero, considering the impact on the rest of the airplane, a significant probability of landing conditions exist that would lead to an unplanned inspection of the landing gear structure, therefore mitigating the need for prognostic assessment. Lastly, the load vector direction was simplified by assuming that the load vector points upwards or in the negative direction of the *Y* axis in the simulation model coordinate system. This was considered a reasonable assumption for a light airplane, enabling numerical strength analysis with sufficient accuracy respective to unknown remaining useful life circumstances and introduced simplifications.

The comparison between the cumulative frequency data obtained from Cicero et al. [15] and the measured load factor data from the single flight analysed by Juretić et al. [4] showed that the measured values from one single flight ([4]) are representative of the airplane's landing phase of operation. It was concluded that the values coincided in terms of the same order of magnitude when considering corresponding operation phases such as landing operations and landing load factor values.

In summary, to calculate the load vector for a light airplane's landing gear, load vector intensity, orientation, and direction were determined. Load vector intensity was computed by multiplying acceleration samples, mass (factoring in fuel previously used) on landing gear, and the gravitational constant. The load vector orientation was determined based on the airplane's landing angle, considering only the main landing gear touched the ground. The angle around the transverse airplane axis, also known as the roll angle, of a Cessna 172 during landing can vary depending on many factors such as wind conditions, pilot technique, and runway surface. Therefore, it is not possible to provide an average roll angle that would apply to all Cessna 172 landings. However, during a typical landing, the pilot will aim to maintain the wings level and aligned with the runway centreline, which means that the roll angle should be near zero. The roll angle may increase briefly during crosswind landings as the pilot uses a technique called crabbing to maintain the airplane's track along the runway centreline, but the goal is to align the airplane with the runway prior to touchdown and reduce the roll angle to zero. Therefore, it was decided to setup the simulation model load vector orientation the same way as it was setup during take-off. Finally, the load vector direction was assumed to point upwards, as was the case during airplane take-off.

5.2.1.7 Modelling TAXI-IN loads

Modelling the taxi-in loads was equivalent to the process of modelling the taxi-out loads, having in mind the only difference being a lower fuel mass due to fuel consumption. Two of

the three main variables considered for fatigue analysis, namely load vector orientation and direction remained equal to the description in Chapter 5.2.1.3. Load vector intensity was determined by consecutively calculating equation *(23*) for the corresponding measured load factor value and mass value and distribution scenario input form the mass and balance records. To gain additional confidence in calculating with the recorded load factor values, a comparison was conducted between the cumulative frequency data obtained from Cicero et al. [15] and the measured load factor data from the single flight analysed by Juretić et al. [4]. The goal of this comparison was to determine if the observed values from the single flight could be considered representative for the airplane's taxi-out phase of operation. A key difference between Cicero's work and Juretić's measurements of the taxi-in phase of operation was the runway surface. Cicero's data was taken on asphalted surfaces, while Juretić's measurements were obtained on a grass runway. Despite this difference, upon comparing the data sets, it was found that the observed values shared the same order of magnitude. This overlap suggested that the measured load factor data from the single flight is indeed representative of the airplane's taxi-out phase of operation, even though the runway surfaces differed, and the sample size was smaller.

The load vector intensity was calculated with equation *(24*). Load vector orientation and direction were determined next. Equal to the Taxi-out phase, the load vector pointed upwards, aligned with the positive direction of the airplane's vertical axis. The load vector orientation was decided to be equal to the one used in the Taxi-out phase, following the explanation given in Chapter 5.2.1.3. Recorded load factor measurements used for load calculation are displayed in Figure 50 (the vertical load factor of the taxi-in phase of operation), Figure 51 (the longitudinal load factor of the taxi-in phase of operation), and Figure 52 (the lateral load factor of the taxi-in phase of operation).

The taxi-in phase vertical load factor from [4], is displayed in Figure 50. Simple statistical analysis revealed the maximum measured load factor was 1.48, the minimum value was 0.57, the average was 1.0429, the median was 1.04 and the standard deviation was 0.1362. Those values, along with calculated averages and standard deviation confirmed expectations on the vertical load factor value, especially considering the observed taxi-in phase was performed on an uneven grass surface, which can be a reason for result deviation when comparing measurement results in [4] and [15].

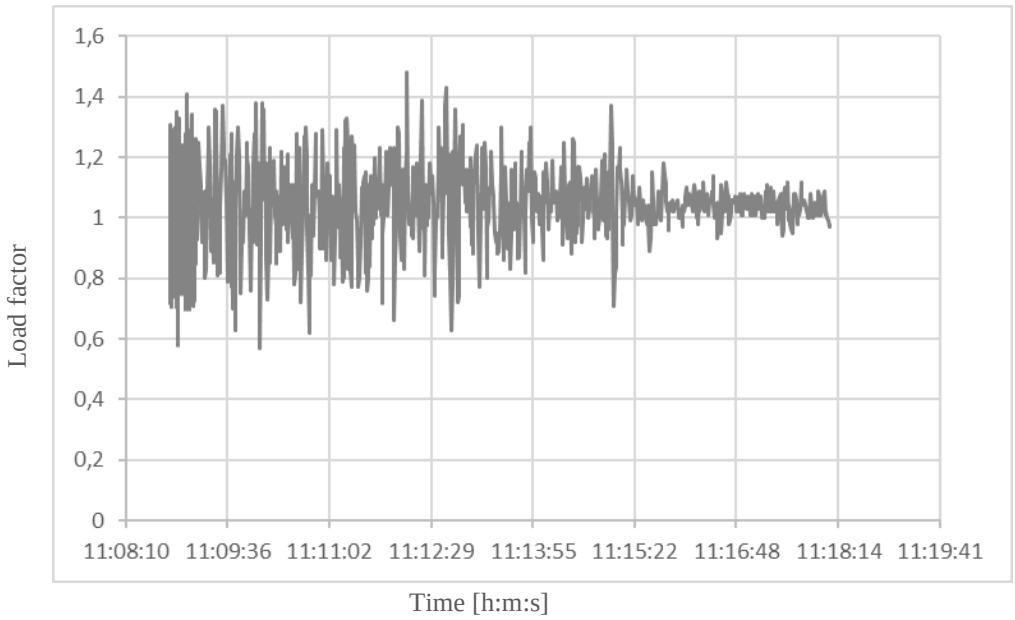

Figure 50. Taxi-in phase vertical load factor, [4].

Data comparison of the measured vertical load factor [4], and the load factors given in [15] was done in Chapter 5.2.1.3, and is displayed in Figure 29.

The taxi-in phase longitudinal load factor measured by [4] is displayed in Figure 51. Statistical analysis revealed the maximum measured load factor was 0.36, the minimum value was -0.83, the average was -0.0676, the median was -0.05 and the standard deviation was 0.1178. The longitudinal load factor expectations were confirmed based on those boundaries, calculated averages and standard deviation. Unlike the previous comparison, expectations were not formed with the help of statistical data based on several hundred recorded flights, since statistical data on the longitudinal load factor was not available. However, the observed values were conforming with pilot subjective experience and engineering judgement.

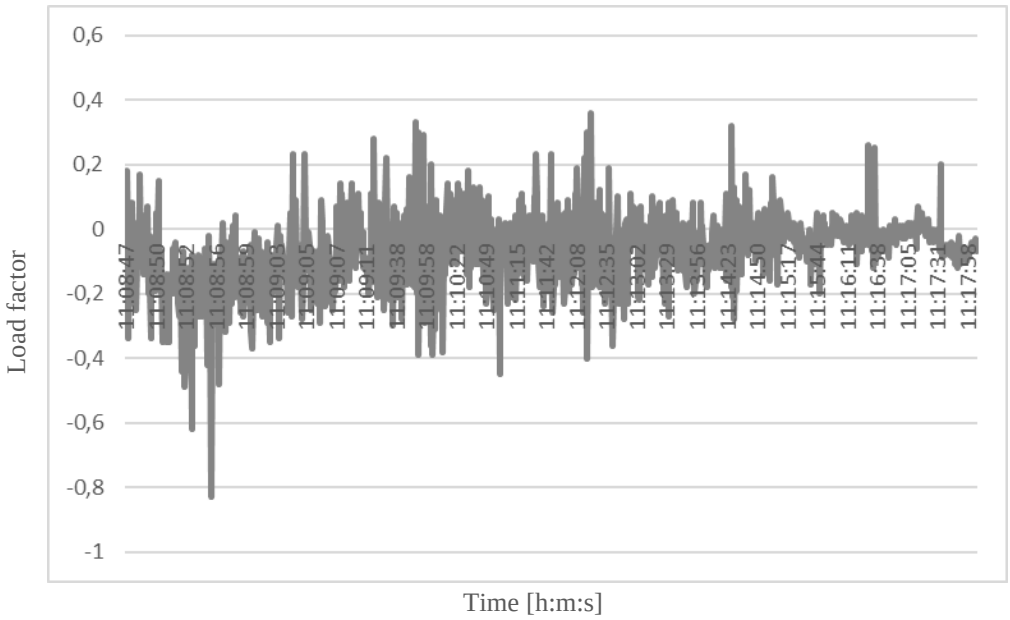

Figure 51. Taxi-in phase longitudinal load factor, [4].

The taxi-in phase lateral load factor measured by [4] is displayed in Figure 52. Statistical analysis revealed the maximum measured load factor was 0.48, the minimum value was -0.16, the average was 0.1403, the median was 0.13 and the standard deviation was 0.0889. Those extremes, along with calculated averages and standard deviation confirmed lateral load factor value expectations. Comparison with statistical data was again not performed due to the lack of several measurement sets. However, expected values based on pilot experience and engineering judgement were met by the observed data. An additional affirming point was the fact that longitudinal and lateral acceleration affects fatigue relevant loads to a much lesser degree than vertical acceleration, primarily because of its significantly lower intensity.

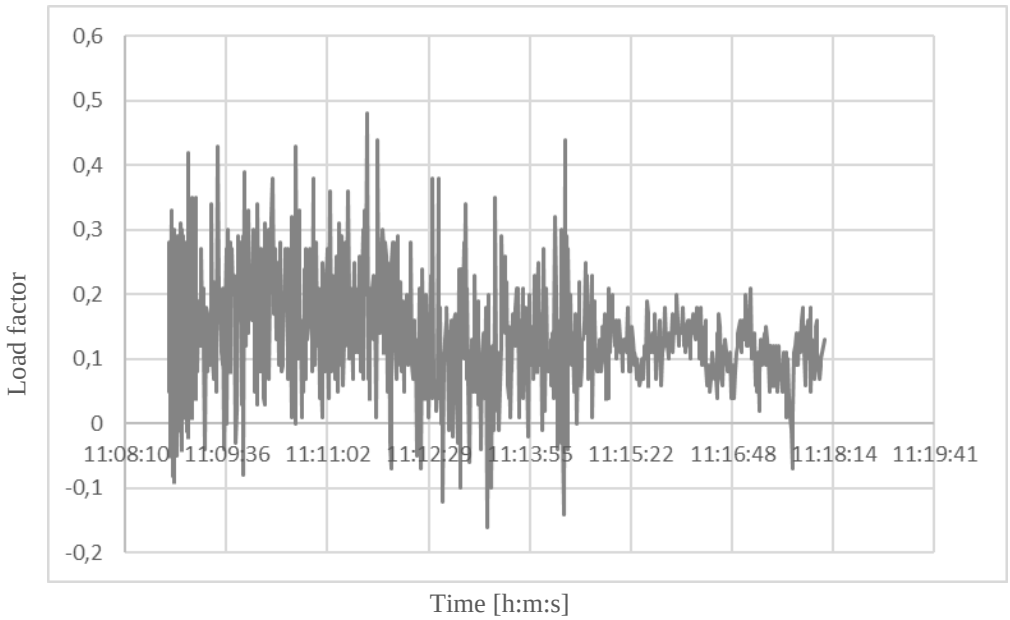

Figure 52. Taxi-in phase lateral load factor, [4].

Considering the taxi-in phase has the same load vector data input (aside from the measured taxi-in load factor values), direction and orientation as was described in the taxi-out phase, the only difference is a lower fuel mass. The average percentage of fuel used in a light aircraft operation can vary widely depending on several factors, including the type of aircraft, the length of the flight, the altitude, and the weather conditions. However, as a rough estimate, light aircraft typically use between 6-12 gallons (22-45 litres) of fuel per hour of flight time. This translates to an average fuel consumption rate of around 5-10 gallons (19-38 litres) per 100 nautical miles, or 9-18 litres per 100 kilometres. In a typical light aircraft operation, fuel consumption plays a significant role in determining the airplane's centre of gravity as fuel is consumed, the mass of the airplane decreases, shifting the centre of gravity position. The position of the centre of gravity is an important factor in determining the remaining useful life of the airplane's landing gear structure. As the centre of gravity moves forward, the loads on the landing gear structure also shift forward, causing increased stress and fatigue on the front landing gear. As the centre of gravity moves rearwards, the load and potential fatigue on the main landing gear increase. Additionally, during the taxi-in phase, the airplane's mass decreases as fuel is burned. This decrease in mass results in a reduction in the load vector intensity, which must be considered when calculating the fatigue life of the landing gear structure. Thus, the combination of the shift in the centre of gravity and the decrease in mass due to fuel consumption during taxi-in impacts the fatigue life of the main landing gear structure in a complex way predetermined for numerical strength analysis.

Based on oral consultations with pilots, it was concluded that on average, light aircraft consume approximately 20-25 % of their total fuel during take-off, 50-60 % during flight, and 15-20 % during landing and taxiing operations. However, the exact fuel usage can vary depending on the specific aircraft model, operating conditions, and pilot behaviour. In this research, it was decided that 60 % reduction of fuel mass used during the aircraft’s flight phase of operation will result in an acceptable load vector difference comparing the taxi-out and taxi-in phase, sufficient for a representable fatigue life prognosis of the light airplane landing gear structure.

Conclusively, the taxi-in phase was modelled by following the exact same algorithm as presented in Chapter 5.2.1.3, with the only differences being a 60 % lower fuel mass, and different load factor values since taxi-in data is available.

5.3 Method phase 3: methodology, validation, and implementation of the fatigue analysis

After determining the loads for each observed load profile, fatigue analysis was performed. It was decided to perform fatigue analysis in Ansys Academic Student 2023 R1 (named Ansys in the continuation of this Thesis). To ensure the reliability of the simulation results, a validation of the fatigue analysis was carried out first. Once that was confirmed, the specifics for the fatigue analysis simulation were established. This included defining the finite element mesh that was used for the main landing gear strut model.

5.3.1 Fatigue analysis validation

The numerical methodology was validated by comparison with specimen tests (tensile and bending), utilizing experimental results from the existing literature due to a lack of data for the examined structure. A dynamic tear test was not available, and such a testing would present significant challenge for subject aircraft part airworthiness. Mouritz [37] outlines the aircraft design process for fatigue failure prevention, with the initial step involving the determination of material properties by measuring test coupon response to constant amplitude loading in a tensile loading machine. To assess the applicability of the Ansys fatigue life estimation tool for this research, a validation process was conducted by comparing the actual fatigue life test results from Nip et al. [14] with the simulation results generated in Ansys for various load types. In this section the reliability of the Ansys fatigue life analysis tool is demonstrated for subsequent use in predicting the remaining useful life of the light aircraft main landing gear strut.

5.3.1.1 Fatigue analysis type for validation

In the research conducted for this Thesis, the strain life analysis type was chosen for the fatigue life analysis, as discussed in Chapter 4.2. According to Li et al. [142], low cycle fatigue analysis is conventionally carried out using the strain life analysis approach, which relies on strain life parameters. Mouritz [37] highlights the importance of adopting a fatigue life analysis approach that accounts for the relationship between the number of load cycles to failure and plastic strain when peak stresses can induce plastic deformation. This is particularly relevant for light aircraft landing gear structures, which often exhibit high load-to-weight ratios due to mass restrictions imposed by corresponding regulations.

Furthermore, Troschenko and Khamaza [128] emphasize the successful application of strain-based fatigue analysis in evaluating both high and low-cycle material fatigue. Consequently, the strain life analysis type is deemed suitable for this research, as it

accommodates the unique characteristics and requirements of light aircraft landing gear structures.

5.3.1.2 Loading type for validation

The loading type for fatigue analysis validation was chosen to replicate the load type applied by Nip et al. [14]. The authors in [14] have applied a uniaxial cyclic constant amplitude non-proportional loading. It was decided to replicate this by applying a constant amplitude, non-proportional loading profile, with the same load intensity as in research [14].

5.3.1.3 Mean stress effects for validation

Since the observed case, which is part of the research used for Ansys fatigue life analysis validation by Nip et al. [14], applies uniaxial fully reversed constant amplitude loading, no mean stress effect adjustment method was necessary. The no mean stress correction option provided by Ansys was chosen, since no multiaxial stress correction (as explained in Chapter 4.2.3), was needed to replicate the test described in the research [14].

5.3.1.4 Multiaxial stress correction for validation

The observed case, part of the research by Nip et al. [14], applies uniaxial loading. Nonetheless, the load-axis-unbiased von Mises stress correction was chosen for simplicity, since several simulation program test runs applying other applicable stress correction methods, such as the component stress correction parallel to the load direction, resulted in very similar fatigue life values.

5.3.1.5 Fatigue modifications for validation

The observed research case by Nip et al. [14], applies constant amplitude loading resulting in stresses above the lowest alternating stress on the subject fatigue curve. The fatigue strength factor modification option for fatigue provided by Ansys was also not necessary since the Ansys simulation for validation replicates actual test coupon testing conditions. The fatigue modification option “infinite life“ was enabled since steel alloys generally do not have fatigue limit, and low-strain fatigue tests would therefore result in infinite fatigue life and unnecessarily burden computing capacity. The number of $1 \cdot 10^9$ cycles was chosen to mark unlimited fatigue life, thus stopping Ansys from further computing and declaring infinite fatigue life.

5.3.1.6 Analysis type for validation

Light aircraft landing gear structural parts are designed with a relatively narrow replacement interval, due to regulatory mass restrictions. The replacement interval is sometimes in the order of 500 flight hours, depending on the type of observed aircraft. Ultralight aircraft, for example, have a landing gear structural part replacement interval which is sometimes less

than 500 flight hours. By analysing a representative light aircraft operational profile, it can be concluded that take-off and landing have the greatest impact on the landing gear structural part's useful life. Previous research [2] has pointed out that fatigue life has the second greatest impact on light aircraft landing gear structure useful life, next to overload situations such as a hard landing which requires visual inspection and part replacement if plastic strain or cracks are detected. Since light aircraft landing gear structures are often made of structural steel such as spring steel, the fatigue limit must be considered. In short, the fatigue limit represents the stress or strain experienced by the observed steel part that is below a fatigue-relevant value. Stresses or strains below the fatigue limit do not cause fatigue damage and are therefore not significant to fatigue life. Landing and the take-off run have the greatest likelihood of resulting in fatigue-relevant stresses and/or strains.

5.3.1.7 Additional considerations

To validate Ansys fatigue life analysis results, fatigue test literature by Nip et al. [14] concerning the analysis of extremely low cycle strain life was examined. The test subject was made from the only material available by the Ansys Academic Student 2023 R1 license, namely structural steel. Coincidentally, spring steel is a common material used in light aircraft landing gear structures and has comparable mechanical properties to structural steel. However, some fatigue life-relevant properties and mechanical properties can be adjusted in Ansys, according to the problem at hand, this feature was used later in this research.

The mechanical and fatigue life properties of the test coupon model created for Ansys fatigue life analysis were set up according to the test subject made from Cold formed carbon steel - S235JRH in [14], as displayed in Table 12. The property values that were not extracted from [14], namely the coefficient of thermal expansion, the strength coefficient, the compressive yield strength, and the compressive ultimate strength were left as standard for Ansys Structural Steel material data. The strength exponent was adjusted following an iterative process of strain calculation for axial test fatigue life values as given by [14]. A comparison of the material mechanical properties used in the validation simulations, and the ones extracted from [14] is presented in Table 12.

Table 12. A comparison of mechanical and fatigue life-relevant properties applied in the validation process and extracted from literature [14].

Mechanical property	Validation	Literature
Density [kg/m^3]	7850	7850
Compressive Ultimate Strength [Pa]	-	-

Compressive Yield Strength [Pa]	$2.5 \cdot 10^8$	$2.5 \cdot 10^8$
Tensile Yield Strength [Pa]	$4.51 \cdot 10^8$	$2.5 \cdot 10^8$
Tensile Ultimate Strength [Pa]	$5.02 \cdot 10^8$	$5.02 \cdot 10^8$
Strength Coefficient [Pa]	$9.2 \cdot 10^8$	$9.2 \cdot 10^8$
Strength Exponent	-0.133	-0.525
Ductility Coefficient	0.3937	0.47
Ductility Exponent	-0.525	-
Cyclic Strength Coefficient [Pa]	$7.64 \cdot 10^8$	$7.64 \cdot 10^8$
Cyclic Strain Hardening Exponent	$5.8 \cdot 10^{-2}$	$5.8 \cdot 10^{-2}$
Young's Modulus [Pa]	$2.1291 \cdot 10^{11}$	$2 \cdot 10^{11}$
Poisson's Ratio	0.29	0.29

The Tensile Yield Strength in the Ansys validation model was set higher than the literature value after several analysis iterations showing this to be the only material property causing result deviation. The impact of this property on the result comparison was therefore noted and considered later on, while performing the fatigue analysis on the landing gear strut observed in this Thesis.

5.3.1.8 Creating the fatigue analysis validation model

The Ansys validation test coupon geometry has been modelled as a three-dimensional geometry, according to [14], the dimensions are displayed in Figure 53. Literature [14] labelled the test coupon „40 × 40 × 3-CS-CF-T" defining the test coupon dimensions, alloy type - carbon steel (abbreviated CS), applied mechanical processing procedure - cold formed (abbreviated CF) and test type – tensile (abbreviated T). Literature [14] lists the results of the cyclic axial material tests performed on various coupons, additionally differentiating the labels by the amount of strain experienced by the coupons during testing. The fatigue life generated by research [14] is given for 1, 3, 5, and 7 % maximum experienced strain in the actual tests.

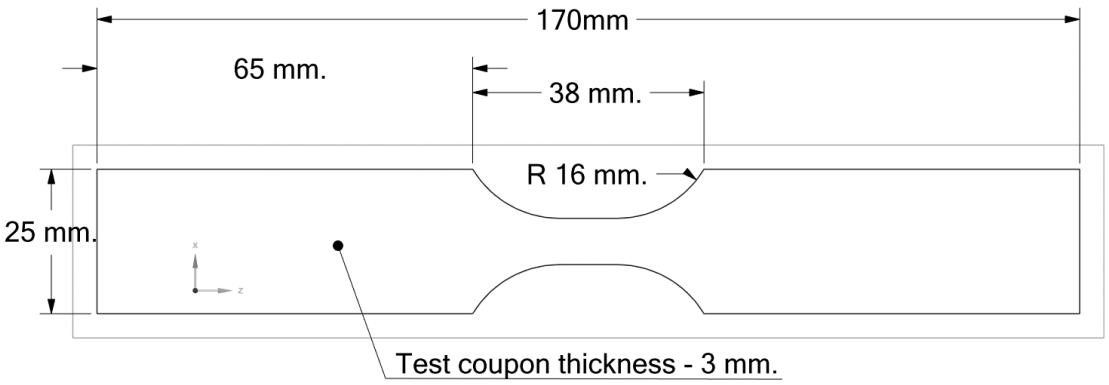

Figure 53. Test coupon from [14], remodelled in Ansys, for fatigue life validation.

After the material properties and geometry were established, a mathematical representation of the test coupon was defined by applying a finite element mesh to the test coupon model as displayed in Figure 54. According to Melchiorre and Duncan [143], Ansys offers two main types of three-dimensional meshing methods, tetrahedral and hexahedral element meshing. The authors [143] state that hexahedral element meshing generally leads to greater result accuracy at a lower element count as compared to tetrahedral element meshing which is usually applied to complex geometries due to a greater number of required mesh elements. It was decided that a hexahedral element mesh would be a good choice, because the observed test coupon is of simple geometry, requiring a relatively low number of mesh elements. Other applied finite element mesh characteristics of the test coupon were element size (1 mm.), number of elements (11115), and number of nodes (57782). Additional meshing characteristics were left at program default, and the applied finite element mesh is shown in Figure 54.

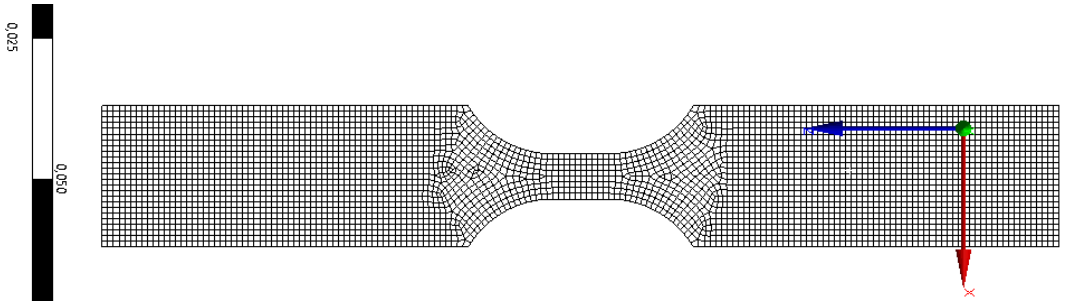

Figure 54. Finite element mesh applied to the test coupon tensile simulation model.

5.3.1.9 Fatigue life analysis for axial loading

The next required step was to set up the test coupon applied loads and constraints. The applied constraint for axial testing was set up at a test coupon surface to restrict its movement fully. It was concluded that this constraint setup replicates the test setup displayed in [14] for axial fatigue life testing. The Ansys simulation model axial fatigue life test constraint is depicted in Figure 55.

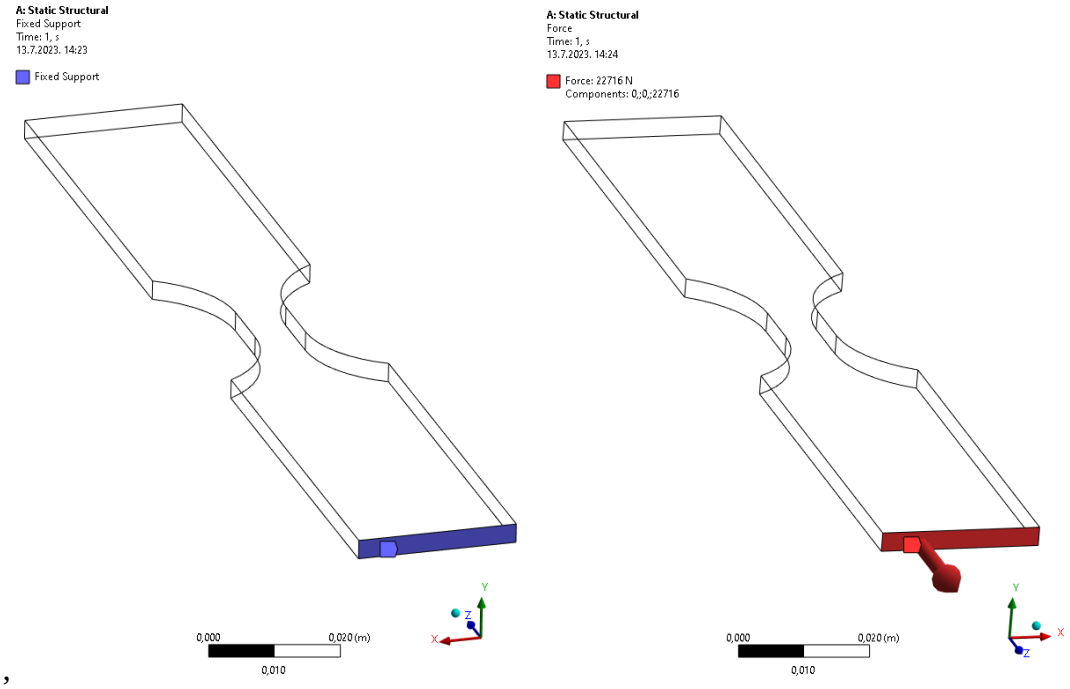

Figure 55. Simulation model axial fatigue life simulation model constraint and load.

Setting up the applied test load in Ansys was required next. The load was set up to be a force vector acting on a surface of the test coupon perpendicular to the *Z* axis and applied to one of its sides. The Ansys simulation model axial fatigue life test load is displayed in Figure 55. The load intensity was incrementally adjusted to result in a 0.5 % test coupon maximum strain, as shown in Figure 56, for result comparison convenience.

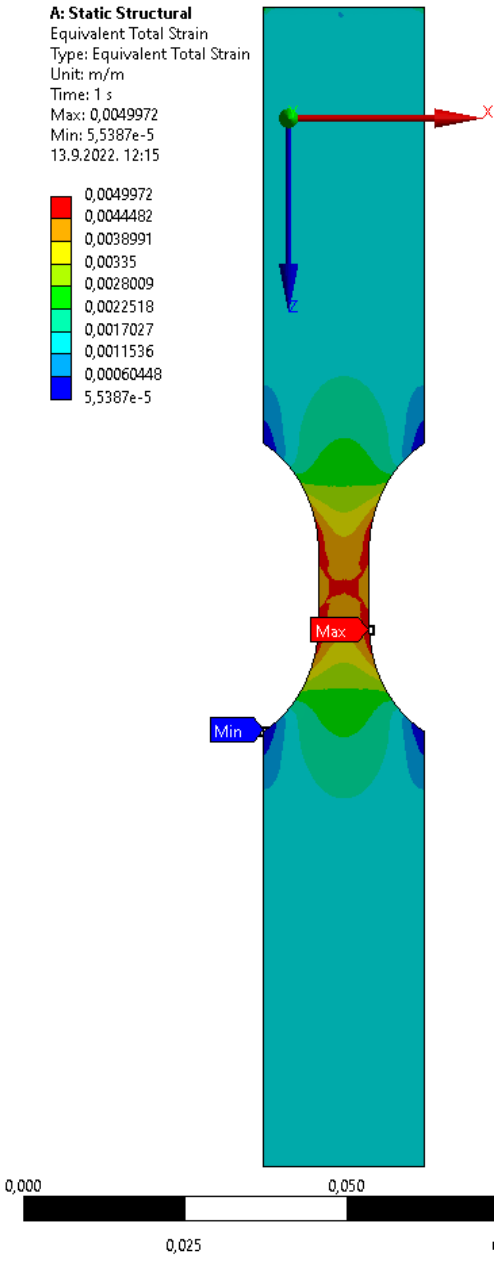

Figure 56. Static structural Equivalent Total Strain [-] tensile simulation results.

A result convergence analysis was performed on the equivalent total strain, a key measure in the static structural analysis, which is shown in Figure 56. In static structural analysis, this equivalent total strain signifies the cumulative strain or deformation that a structure undergoes when subjected to various static loads. This strain includes both elastic and plastic components. According to Higgins [144], Ansys performs an iterative result analysis by using the Newton-Raphson method, where each iteration is in an equilibrium energy state, using an iterative series of linear approximations. As part of this process, Ansys effectively calculates the 'Static Structural Equivalent Total Strain', which provides insight into the behaviour of the analysed structure. The resulting convergence analysis results, based on the program-default

convergence criteria, are displayed in Figure 57. This figure demonstrates the convergence of the calculated static structural equivalent total strain and verifies the stability and accuracy of the simulation.

The default convergence criteria were accepted after inspecting the result convergence, concluding it to have a reasonable ratio of computer processing time and result variability. Figure 57 shows the last two iterative steps, displaying an equivalent total strain deviation of just 0.35254 % by increasing the number of nodes from 57782 to 57920 and of the elements from 11115 to 29277. The increase in the number of nodes compared to the increase in the number of elements could appear contradictory, but it's not necessarily an anomaly. This can happen due to multiple reasons:

- **Element Type**: The increase in the elements compared to the nodes might suggest a switch in element types. For instance, transitioning from linear to quadratic elements, or from lower-order to higher-order elements. Higher-order elements have more nodes associated with them, thereby adding more computational „degrees of freedom“ without significantly increasing the total node count.
- **Mesh refinement**: In FEA, mesh refinement is a common strategy for increasing solution accuracy. This involves increasing the number of elements within a certain area (e.g., a region of interest or a region with high stress gradients). If this region is relatively small compared to the entire model, the number of new nodes can be relatively small, even though the number of elements increases significantly.

In the specific case of the research described in this Thesis, the element type setting is set up to be “Adaptive“, meaning that the software uses an adaptive meshing method. In adaptive meshing, the mesh density is not uniform throughout the model. Rather, it is adjusted based on the needs of the simulation, with denser meshing in areas of higher complexity or where higher precision is needed (for example, in areas with high stress gradients), and sparser meshing elsewhere. The stated settings are the reason for the increase in the number of nodes compared to the increase in the number of elements.

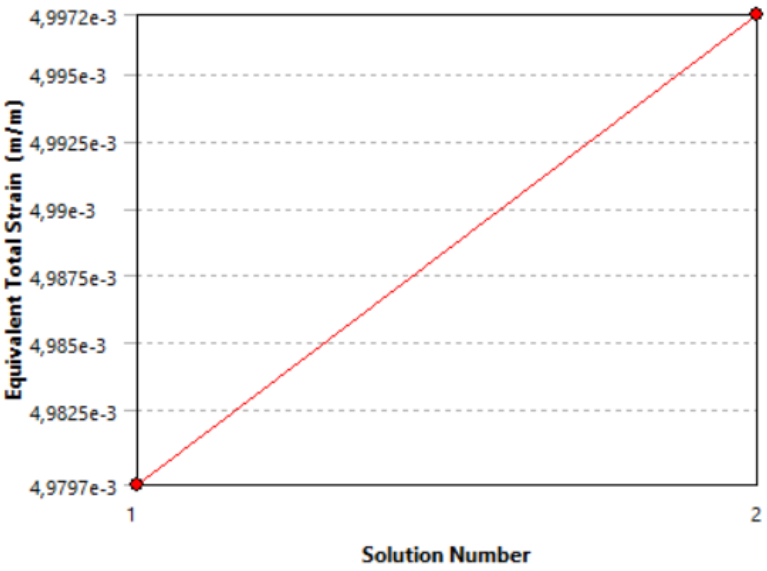

	Equivalent Total Strain (m/m)	Change (%)	Nodes	Elements
1	4,9797e-003		57782	11115
2	4,9972e-003	0,35254	57920	29277

Figure 57. Equivalent total strain convergence analysis.

The Ansys fatigue tool had to be set up next. The fatigue tool was set up the following way, (displayed in Figure 58):

- Domain type – The time domain was applied;
- Fatigue modification option – the fatigue strength factor was left at value 1 since the Ansys simulation for validation replicates actual test coupon testing conditions. The fatigue strength factor serves as a modification factor mitigating differences between actual test conditions and laboratory-controlled material fatigue property tests, as explained in Chapters 4.2.4 and 5.3.1.5.;
- Loading options, loading type, and scale factor – fully reversed loading was applied to replicate test conditions, [14], no scale factor was needed for the reason explained in Chapters 4.2.1 and 5.3.1.2. The time variability of the applied load was defined through the accelerometers time sampling mechanics described in Chapter 5.2.1.2;
- The analysis type – the strain life analysis type was applied for reasons explained in 4.2 and 5.3.1.1;
- The mean stress theory – no mean stress theory was applied for reasons explained in 4.2.2;

- The multiaxial stress correction – the Equivalent (von Mises) multiaxial stress correction was applied for reasons explained in 4.2.3 and 5.3.1.4;
- Fatigue modifications – the infinite life fatigue modification was applied, and the value was set according to the explanation given in 4.2.4 and 5.3.1.5;
- The fatigue life unit name and definition – one loading cycle was defined as the measurable fatigue life dimension.

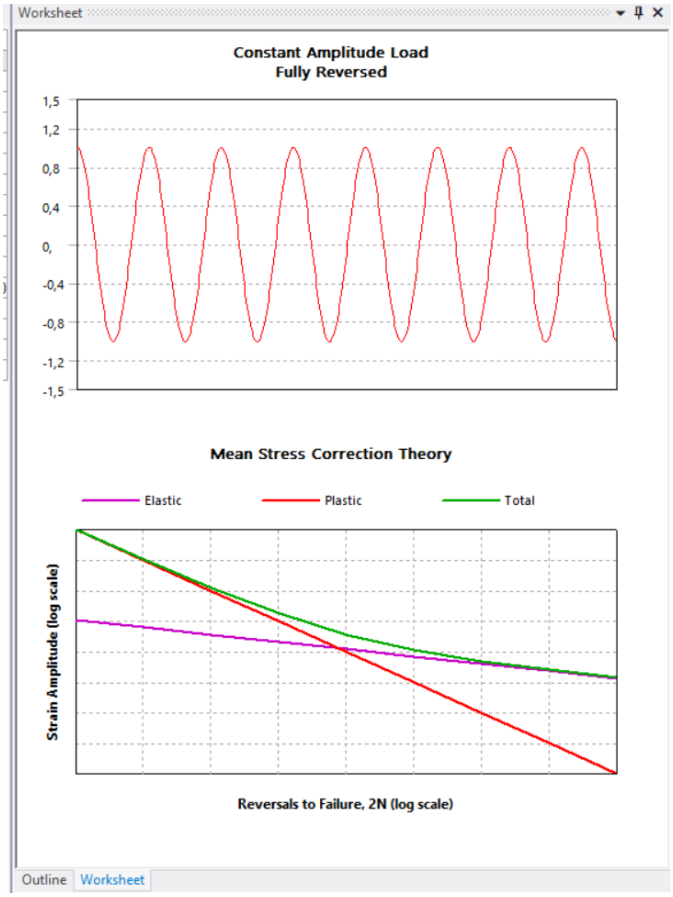

Figure 58. Fatigue tool setup for tensile simulation validation.

5.3.1.10 Comparison of literature and Ansys fatigue analysis results for axial loading

The fatigue life analysis validation was performed by comparing the numerical fatigue life analysis results (Figure 59), having the analysis setup described in the previous Chapter, and the fatigue life test results extracted from [14]. An overview of the literature and the observed research fatigue life test results given in [14] for tensile constant amplitude, and non-proportional loading is displayed in Figure 62.

The low cycle fatigue life test results given in [14] and displayed in Figure 62, which are produced by the very same research ([14]) and gathered from various literature, were matched with Ansys fatigue life analysis results displayed in Figure 59.

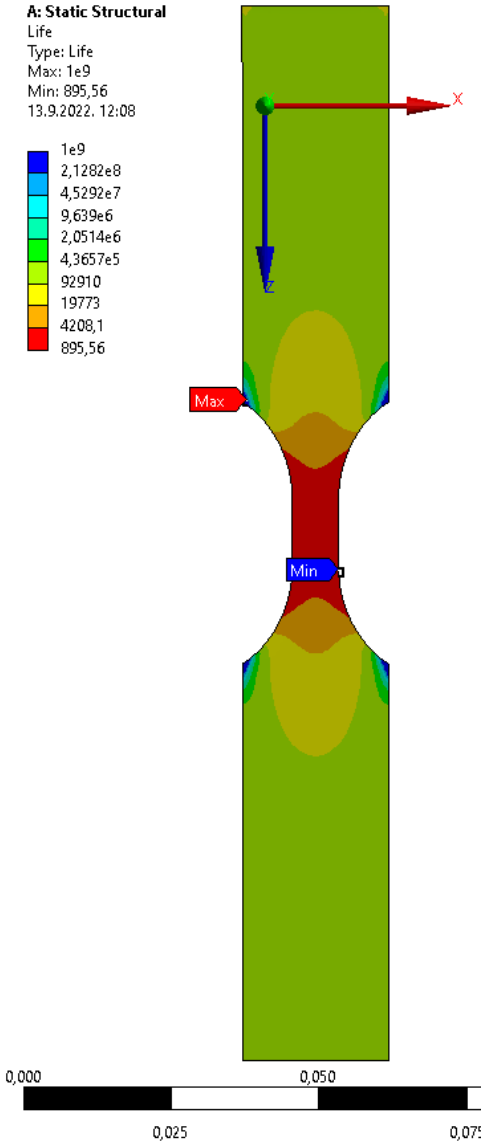

Figure 59. Fatigue life analysis simulation test results for tensile constant amplitude, non-proportional loading.

Literature [14] shows the relationship between the number of strain reversals to failure and the strain amplitude for various test coupons. Since the observed coupon is made from cold-formed carbon steel, the corresponding diagrams were observed. Figure 60 displays the strain life relationship for extremely low fatigue regimes and low cycle fatigue regimes of the observed cold-formed carbon steel test coupon. The diagram displays data for elastic and plastic strain and the Coffin-Manson curve. The Coffin-Manson curve reveals approximately 950 strain reversals to failure for a strain amplitude of 0.5 % (highlighted with the red dotted line).

The plastic strain data show a higher strain amplitude for a similar number of strain reversals to failure (approximately 0.7 %, highlighted with the horizontal purple dotted line). Lastly, the elastic strain data (horizontal blue dotted line) show a lower required strain amplitude for a similar number of strain reversals to failure (approximately 0.27 %). Figure 60 also displays a vertical green dotted line highlighting the number of strain reversals to failure, which corresponds to a strain amplitude of 0.5 % calculated by Ansys (880 strain reversals to failure). The number of strain reversals to failure calculated with Ansys corresponds to plastic and elastic strain fatigue failure results but for various strain amplitudes. Elastic fatigue failure requires a lower strain amplitude (approximately 0.27 %), whereas plastic fatigue failure requires a higher strain amplitude (approximately 0.7 %). Fatigue damage accumulation resulting from pure elastic strain is unlikely in a light aircraft landing gear structure. This is a consequence of the very limited structural safety factors due to regulatory aircraft mass limitations.

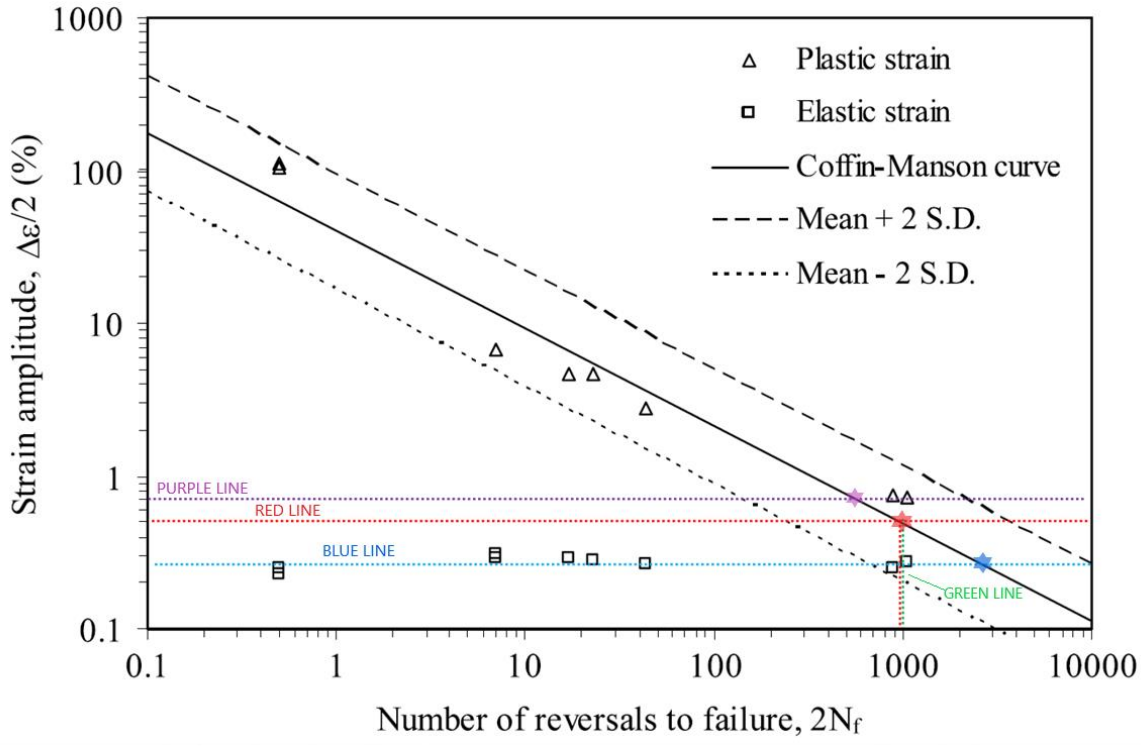

Figure 60. Strain life relationship in extremely low cycle fatigue and low cycle fatigue regimes for cold-formed carbon steel specimens, [14].

Additionally, Nip et al. [14] produced a comparison chart for the strain-life relationship between hot-rolled carbon steel, cold-formed carbon steel, and cold-formed stainless steel for different failure modes, as shown in Figure 61. The Coffin-Manson curve for cold-formed carbon steel corresponds to 1000 strain reversals to failure for a strain amplitude of 0.5 %, indicated by the red vertical line (in Figure 61). The green vertical line indicates 880 strain reversals to failure calculated with Ansys for this research, for the same strain amplitude. By

observing experimental data of cold-formed carbon steel fatigue failure, marked with white triangles and a purple horizontal line in Figure 61, a similar number of strain reversals to failure can be seen (around 1000 reversals), having a strain amplitude of 0.7 %. A mixed or ductile mode landing gear strut fatigue failure would result from one or more hard landings, often having visible part deformation and requiring immediate part replacement. Such cases are often detected before failure and are not the focus of this research.

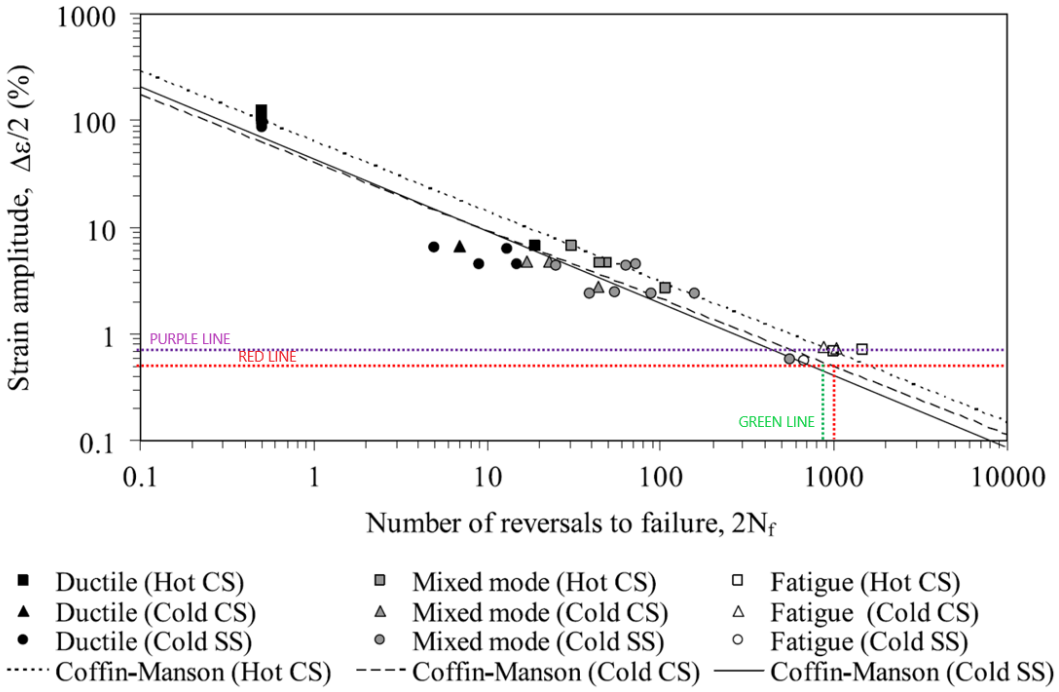

Figure 61. Comparison of the strain-life relationship for hot-rolled carbon steel, cold-formed carbon steel, and cold-formed stainless steel, and their failure modes, [14].

Literature [14] shows one more relevant relationship between the strain amplitude and the number of strain reversals to failure for the observed cold-formed carbon steel test coupon, Figure 62. The vertical red dotted line shows the number of strain reversals to failure (approximately 980) predicted with the Coffin-Manson curve. The green vertical dotted line highlights the number of strain reversals to failure (880) calculated in this research. Additionally, Figure 62 shows cold-formed carbon steel fatigue data the researchers [14] gathered from literature labelled with white triangles. The black triangles show cold-formed carbon steel fatigue failure data originating from research [14]. Literature and research [14] suggest a higher strain is required for the same number of strain reversals to failure as opposed to the results predicted with the Coffin-Manson curve (approximately 980) or calculated for this research with Ansys (880). Both white and black triangles follow a monotonic distribution across the scale of strain reversals to failure, predictably following the Coffin-Manson curve. Since Ansys calculates fatigue life based on the Coffin-Manson relationship, a similar

correlation between Ansys results and literature or research [14] data is expectable. A lower required strain for the same predicted number of strain reversals to failure would result in earlier part replacement of light aircraft landing gear , adding to operational safety. A strain higher than 7 % in a multiaxial load environment requires operational parameters outside the nominal load boundaries that the landing gear structure is designed for, resulting in plastic deformation, immediate part inspection, and eventual part replacement.

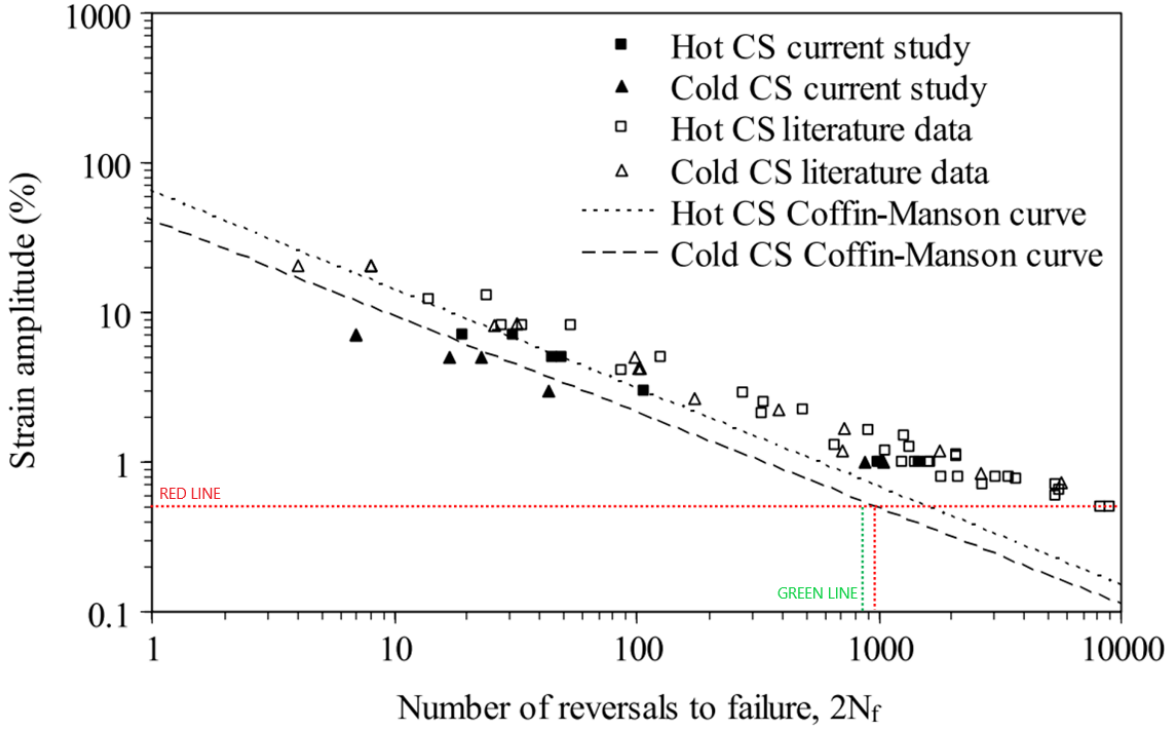

Figure 62. Strain-life relationship of low and high cycle fatigue data, and monotonic tensile data, of carbon steel (CS) material from tests performed in the current research and in the literature [14].

After comparing the Ansys fatigue life analysis results with fatigue life results presented in [14], and displayed in Figure 60, Figure 61, and Figure 62, the following conclusions were made. Literature and research results presented in [14] linearly and reliably exaggerate fatigue life results determined with the Coffin-Manson fatigue life relation and results produced with Ansys in this research. The only exception to the exaggeration is displayed in Figure 60 for pure elastic strain. Numerical verification confirmed the exaggeration amount to be within the limits of 6 % on the strain amplitude scale. This relatively small, predictable, and linear difference between actual fatigue life test data and numerical Coffin-Manson and Ansys results is acceptable for the outcome of this research, especially since numerical results underestimate fatigue life, resulting in earlier part replacement, thereby reducing the risk of sudden fatigue failure.

The stated findings confirm that the Ansys fatigue life analysis results are sufficiently accurate when considering constant amplitude and non-proportional axial loading cases.

5.3.1.11 Fatigue life analysis for bending

The research paper done by Nip et al. [104] states the bending test type is a four-point minor-axis bending test setup backed by research dealing with three-point, four-point, and uniform bending. A four-point bending setup was therefore constructed.

First, additional geometry had to be added. Two cylinders, 25 mm in height, were placed perpendicular to the coupon length, equidistant from each test coupon edge, touching the test coupon constriction intended for primary deformation, displayed in Figure 63. The added cylinder geometry material was selected to be the same as the test coupon since it was estimated that their deformation would be of a lower order of magnitude than the deformation expected from the test coupons. Also, the result deviation due to having the same material as the test coupon was expected to be negligible in this case.

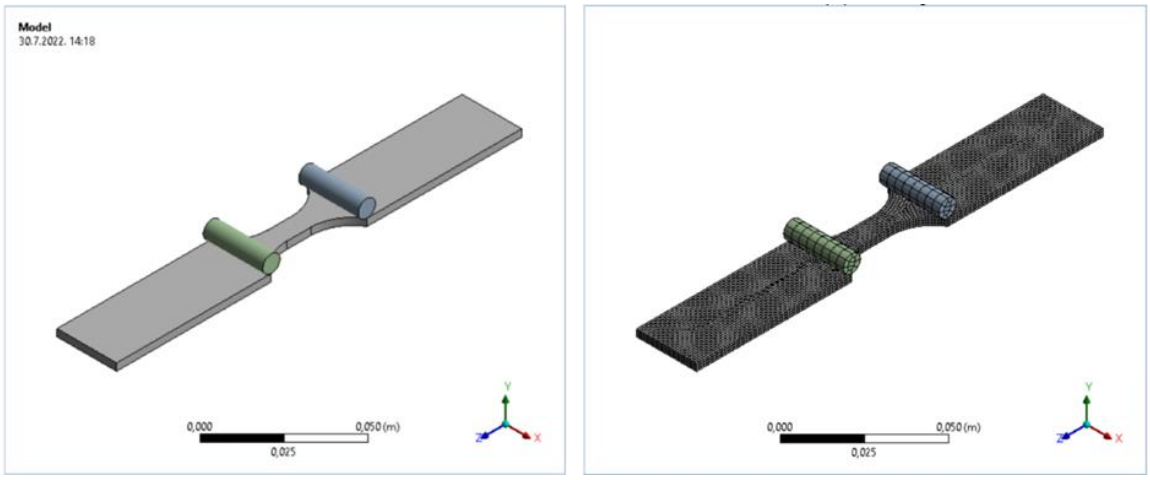

Figure 63. Bending test with added geometry and applied finite element mesh.

Because of the added cylinder-shaped geometry, new geometry meshing had to be done. The cylinders didn't have to have a fine mesh setup since their deformation was not the concern of this research. Therefore, a bigger finite element size was applied to the cylinders instead of the test coupon, as shown in Figure 63 and the setup displayed in Figure 64.

Details of "Mesh"

Display	
Defaults	
Physics Preference	Mechanical
Element Order	Program Controlled
Element Size	1,e-003 m
Sizing	
Use Adaptive Sizing	Yes
Resolution	Default (2)
Mesh Defeaturing	Yes
Defeature Size	Default
Transition	Fast
Span Angle Center	Coarse
Initial Size Seed	Assembly
Bounding Box Diagonal	0,17185 m
Average Surface Area	6,1768e-004 m²
Minimum Edge Length	3,e-003 m
Quality	
Inflation	
Advanced	
Statistics	
Nodes	57782
Elements	11115

Figure 64. Bending test finite element mesh setup.

Next, the contacts between the cylinders and the test coupon had to be defined, the Ansys bonded contact type was chosen, with zero "trim tolerance" and disabled "small sliding" option.

The Ansys analysis settings had to be defined next. The analysis was chosen to be performed in four steps, each step lasting for 1 second. Four displacement structural supports were added, two to define the translatory geometry boundaries and two to define the load acting on the test coupon, displayed in Figure 65. Labels A and B were the representation of the translatory displacement boundaries, acting on the test coupon edges, allowing free rotation around all three axes but disabling translation along the *Y* and *X* axes. Labels C and D represented the load acting on the test coupon; a displacement was added to the cylinders along the *Y* axis, disabling translation along the remaining two axes.

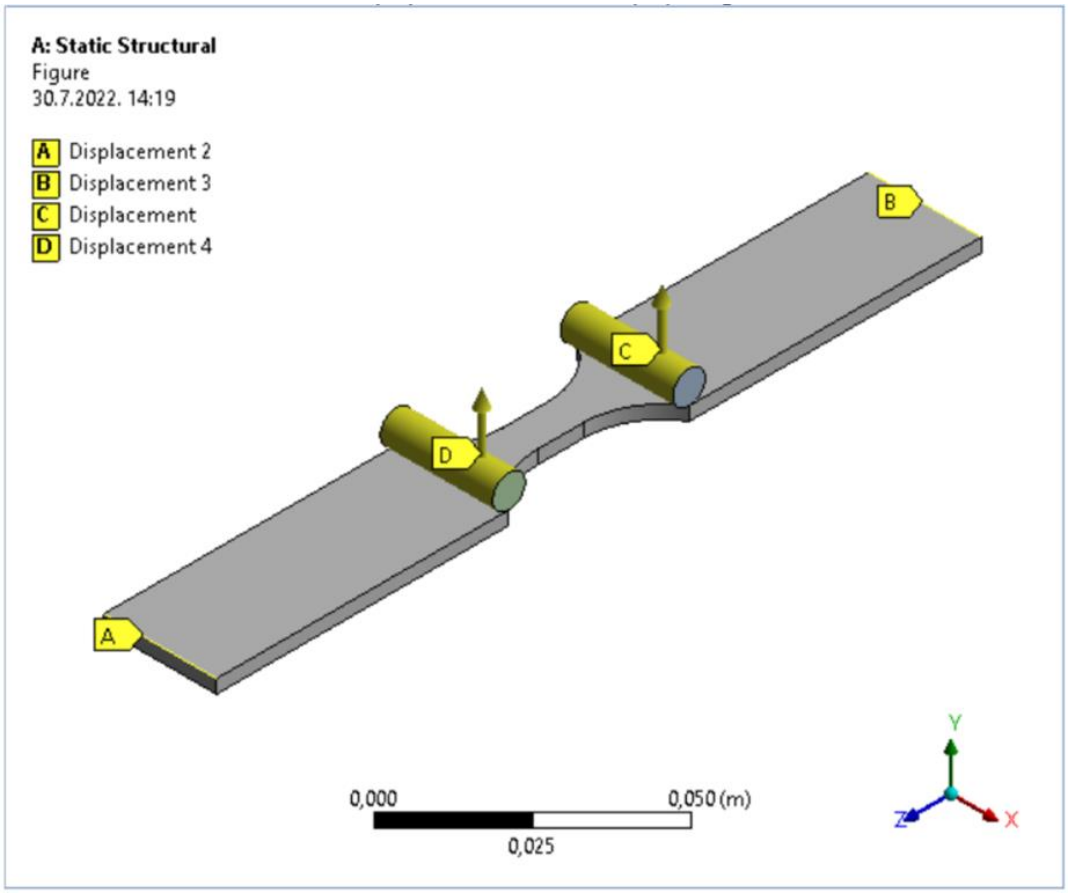

Figure 65. Bending test displacement restriction setup.

The displacements were added to the cylinders labelled C and D in Figure 65 where time is dependent, according to the four steps chosen in the analysis setup. The time-dependent displacements are displayed in Figure 66 and Table 13.

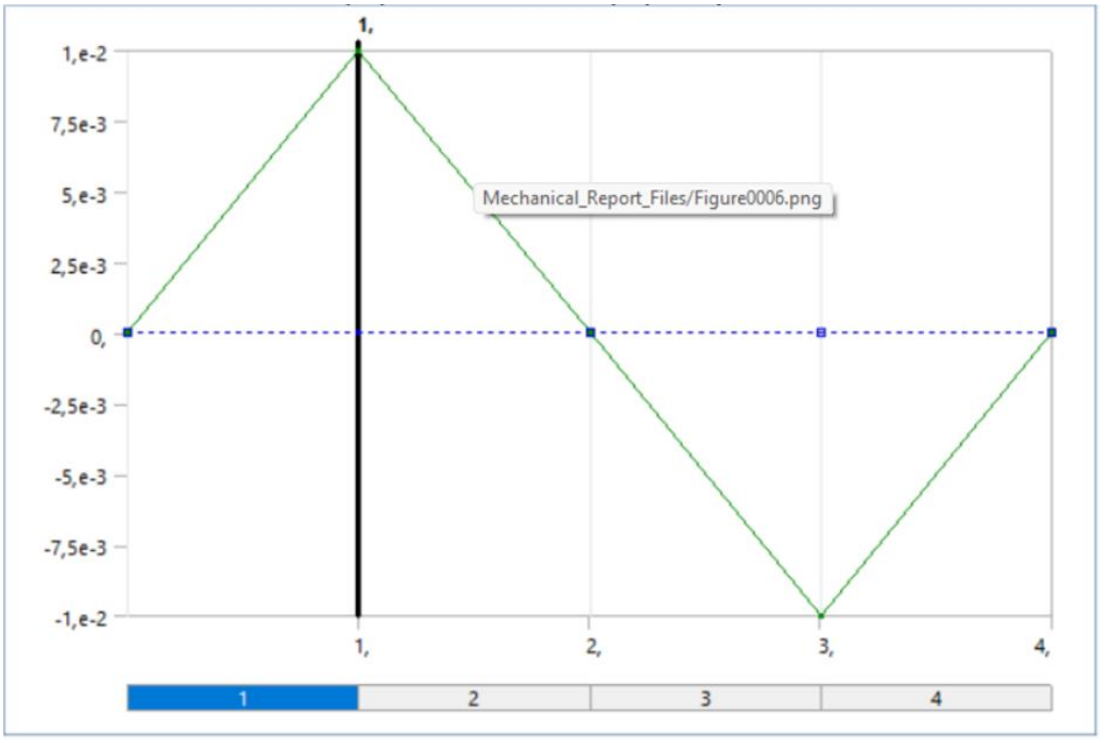

Figure 66. Displacement intensity and time dependency.

Figure 66 describes one load cycle applied throughout the second bend test.

Table 13. Bending test displacement intensity and time dependence.

	Time [s]	*X* [m]	*Y* [m]	*Z* [m]
0	0	0	0	0
1	1	0	1.e-2	0
2	2	0	0	0
3	3	0	-1.e-2	0
4	4	0	0	0

The solution setup was the same as in the previous tests, requiring the equivalent total strain and fatigue life values for the test coupon with applied fully reversed loads. The fatigue life analysis was again chosen to be strain life, as explained in Chapter 5.3.1.1; no mean stress theory was applied for reasons explained in Chapter 5.3.1.3. The observed stress component was chosen to be the von Mises stress, and infinite life was defined to be 10^9 cycles, as this number of cycles is extremely unlikely to be ever experienced by light aircraft landing gear structures.

5.3.1.12 Fatigue life analysis validation results and conclusion for the second bending test.

The second bend test proved to be a much better representation of literature test results according to results displayed by Nip et al. [14]. Five test iterations were done to assess Ansys

fatigue life analysis result accuracy compared to literature results. The five tests were set up identically, with displacement as an exception. The displacement was increased incrementally, according to Table 14.

Table 14. Bend test displacement iterations.

Test iteration	Displacement, *Y* axis [m]	Maximum equivalent total strain [m/m]	Fatigue life analysis results [number of load cycles to failure]
1	± 0.8 e-2	0.016614	751.96
2	± 1 e-2	0.020767	458.77
3	± 1.3 e-2	0.026997	260.61
4	± 1.5 e-2	0.03115	192.3
5	± 1.7 e-2	0.035304	146.64

A visual comparison of the Ansys bending test fatigue life analysis results with literature and test results given in [14] is displayed in Figure 67.

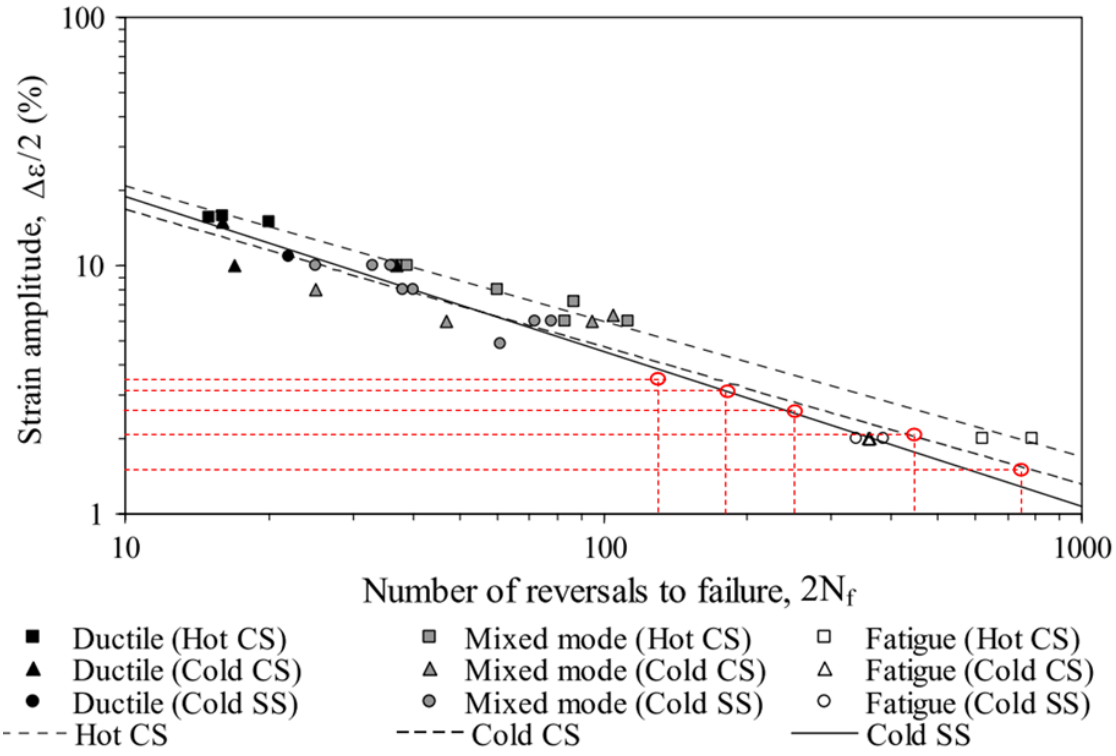

Figure 67. Comparison of bending test fatigue life results calculated with Ansys and fatigue life results given in [14].

Based on comparisons of the bending test fatigue life analysis results in Table 14, and fatigue life tests given in the literature [14], several conclusions were made.

The four-point bending test setup replicated in Ansys gave fatigue life results matching the literature results to a satisfactory level. A slight overestimation of the Ansys fatigue life results can be observed in the pure fatigue failure region in Figure 67 by decreasing the applied load

(through cylinder-shaped geometry displacement) therefore, decreasing the resultant strain and increasing fatigue life. However, the overestimation does not increase significantly with strain decrease, it remains constant. On the other side of the strain spectrum, while increasing its intensity, a slight underestimation can be observed in the mixed mode and ductile fatigue failure regions in Figure 67. This however is not considered to be a concern for two reasons. First, the underestimation is even smaller than it was on lower strain intensities, within expected uncertainty limits due to unpredictable test result variability in actual testing conditions (actual tests which are not computer-aided simulations). Second, as explained in previous Chapters, fatigue life analysis result underestimation is not a safety hazard for light aircraft landing gear structures; it can only have economic implications through maintenance actions.

It was therefore concluded that the bending test gives satisfactory results matching fatigue lives given by literature and the Coffin-Manson curve.

5.3.2 Fatigue analysis finite element mesh setup

To perform fatigue analysis in Ansys, finite element mesh settings had to be set up. The finite element mesh in the Ansys 2023 Student license is limited to a sum of 512000 elements and nodes. Analysis convergence capabilities are thereby limited. Luckily, the main landing gear strut model has a simple geometry, making the limited number of mesh elements and nodes sufficient in the context of a satisfactory convergence criterion. The convergence criteria were set to 15%, meaning fatigue analysis result iterative variability allowance was set to 15 %, based on several fatigue analysis test runs which were limited by the student license finite element boundaries and expected result accuracy. In other words, a higher number of finite elements caused by stricter convergence criteria compromised the result convergence because of license limitations. Based on the fact of numerous unknowns originating from a lack of sensors and sensor data processing, which is characteristic of light aircraft, the chosen convergence criteria were expected to produce satisfactory results in the context of enabling existing operation safety enhancement.

To determine adequate mesh settings for the observed main landing gear structure part, fatigue analysis tests were performed. The tests included setting up a simple finite element mesh with mostly program default settings. The finite element mesh included a linear mechanical analysis preference, program-controlled element order, and element sizes of 5 mm, 7 mm, and 9 mm. The mesh settings for the 7 mm finite element size are displayed in Table 15.

Table 15. Finite element mesh settings for mesh setup analysis.

Element type	Adaptive
Element Size 7.e-003 m	Element Size 7.e-003 m

Nodes 53582	Nodes 48928
Elements 33482	Elements 30451

It was decided to perform mesh setup analysis with loads that resemble airplane operation, while at the same time remaining within allowable boundaries according to airplane mass and balance limitations. Therefore, loads based on acceleration measurements of the Cessna 172R during the taxi-out operation phase on a grass-surface runway were considered. The applied mass combination was 31-65-0-0-0, meaning 31 kg of airplane fuel, 65 kg on the airplane's front seat, and 0 kg on the airplane rear seat with no baggage in the two baggage areas was the mass distribution chosen for finite element mesh-setup analysis.

The correct way to perform fatigue analysis regarding the observed circumstances and available information would be to perform an analysis of the actual loads based on acceleration measurements. Parametrization of fatigue-relevant loads offers the possibility of force vector variability. The parametrized loads would vary in intensity along the three coordinate axes, since total airplane mass changes during operation only regarding used fuel, but the acceleration of the aircraft has significant variability. However, Ansys Student license fatigue analysis capabilities do not include the parametrization of force vector components. In other words, fatigue analysis of a simulation model including a parametrized force vector would result in Ansys calculating fatigue damage only for one load vector, namely the last parametrized force vector, changing vector intensity based on the predefined fatigue analysis loading type. The only way to solve this shortcoming is to enable the variability of force intensity via the Ansys fatigue analysis load history, whereby the direction of the force vector must be set as a constant. It was concluded that the possible approach would yield satisfactory fatigue life results in the context of increasing predictive remaining useful life awareness, especially considering the current hard-time maintenance standard for light aircraft landing gear structural parts. The Ansys fatigue analysis load history requires a “dat“ data file for information input, which in the case of this research consists of a text file containing a column with the calculated load history according to the observed operational phase. The loads have variable amplitudes, based on the measured acceleration variable. An example of the load history applied to the first mesh setup analysis runs is depicted in Figure 68.

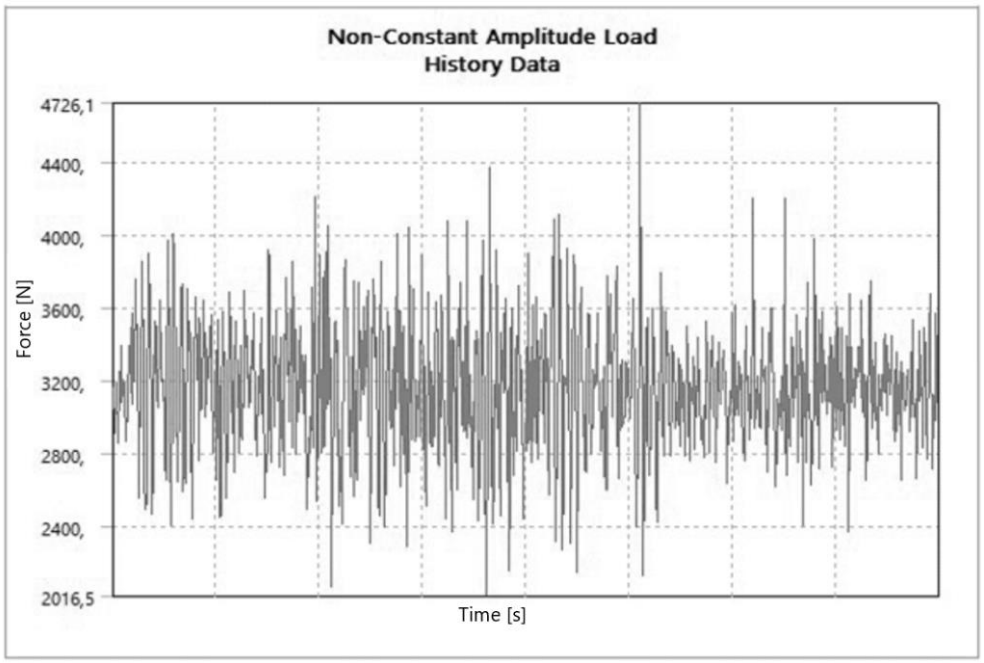

Figure 68. Example of fatigue analysis load intensity history for finite element mesh setup.

It is noteworthy that the load history data acts as a load multiplier, multiplying load intensity applied to the analysed geometry in the static structural force setup part of the project tree. Therefore, base force values directionally aligned with the expected loads acting on the main landing gear strut had to be determined to multiply them with the load history multipliers. The correct and aligned load values, acting on the landing gear strut, would be obtained by multiplying the load history multipliers with the base force values. This was done by determining the angles at which the load is expected to act on the observed main landing gear strut. Before the load vector calculation, the landing gear strut computer model coordinate axes had to be aligned with the coordinate system used for measuring acceleration (load factor). It was stated in [4] that the coordinate axes for acceleration measurement were aligned with the aircraft longitudinal (X axis with its positive oriented towards the aircraft's propeller), vertical (Z axis with its positive oriented towards the sky), and lateral axis (*Y* axis with its positive oriented towards the aircraft's left wing). It is important to note that the base force values only hold true for a levelled airplane, meaning airplane take-off and landing should have different base force values due to a difference in the load angle acting on the main landing gear strut, depending on the type of the aircraft.

Since a cartesian coordinate system was used to set up the simulation model, as well as for load factor measurements, three base force values aligned with the airplane's longitudinal, vertical, and lateral axes had to be determined. The first base force value, aligned with the aircraft's *Y*-axis (coincides with the model's negative *X*-axis), was determined by calculating

the sine value of the cone angle between the landing gear strut axle adapter and the *X*-axis, Figure 69.

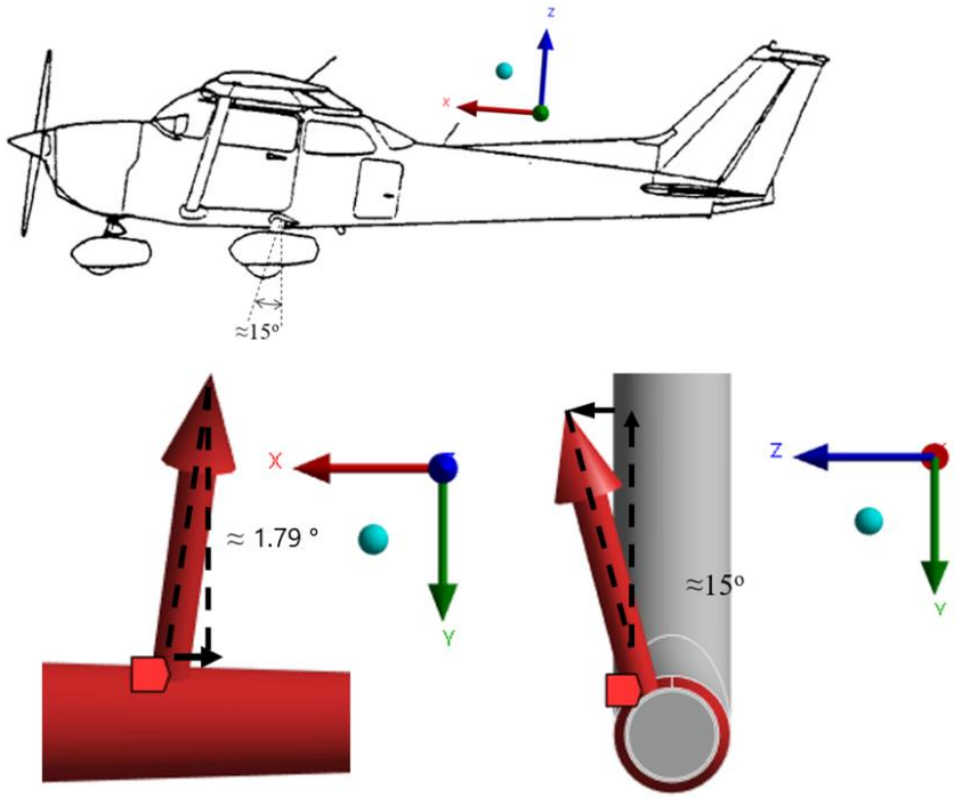

Figure 69. Determining base force direction.

This angle is a consequence of the main landing gear strut geometry in the axle adapter section. The *Y*-axis base force value was determined by calculating the cosine value of the angle between the load vector and the vertical axis. This angle is a consequence of the airplane landing gear installation angle, as depicted in Figure 21. Finally, the longitudinal base force value was determined by calculating the sine value of the same strut installation angle as in the vertical (Y-axis) case. This load intensity and orientation logic was applied to three simulation setups, mimicking operation phases taxi-out, taxi-in, and take-off.

Fatigue analysis model displacement boundaries were applied according to the description given in Chapter 5.3.3.

Fatigue analyses performed to determine acceptable mesh size was performed for three finite element sizes, 5 mm, 7 mm, and 9 mm. The analyses showed that the finest finite element mesh (the one with a 5 mm element size) could not be considered since result convergence could not be achieved because the required number increase of finite elements and nodes exceeded software license limitations. On the other hand, element and node number capacity exceedance was not expected in the case of the coarsest observed finite element mesh (element size of 9 mm). However, convergence analysis showed result divergence due to a lack of finite

element mesh density, not covering the analysed geometry in a sufficient manner. The convergence analysis results feature a 9 mm mesh size is displayed in Figure 70.

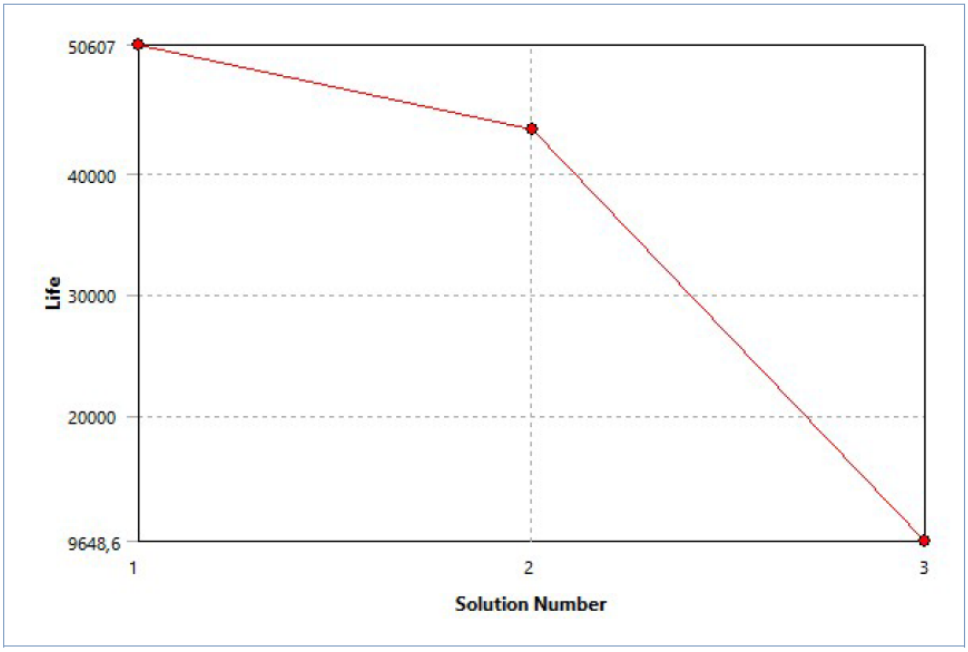

Model (A4) > Static Structural (A5) > Solution (A6) > Fatigue Tool > Life > Convergence

	Life	Change (%)	Nodes	Elements
1	50607		30560	18615
2	43611	-14,85	54163	34760
3	9648,6	-127,54	94378	63065

Figure 70. Result divergence of fatigue analysis for mesh setup with 9 mm element size.

The final test, featuring a finite element size of 7 mm demonstrated clear result convergence. The convergence was achieved with a result variation of -3.9606 %, which is significantly lower than the chosen 15 % convergence criteria, satisfying demonstration purposes, and having a favourable effect on prognostic result accuracy.

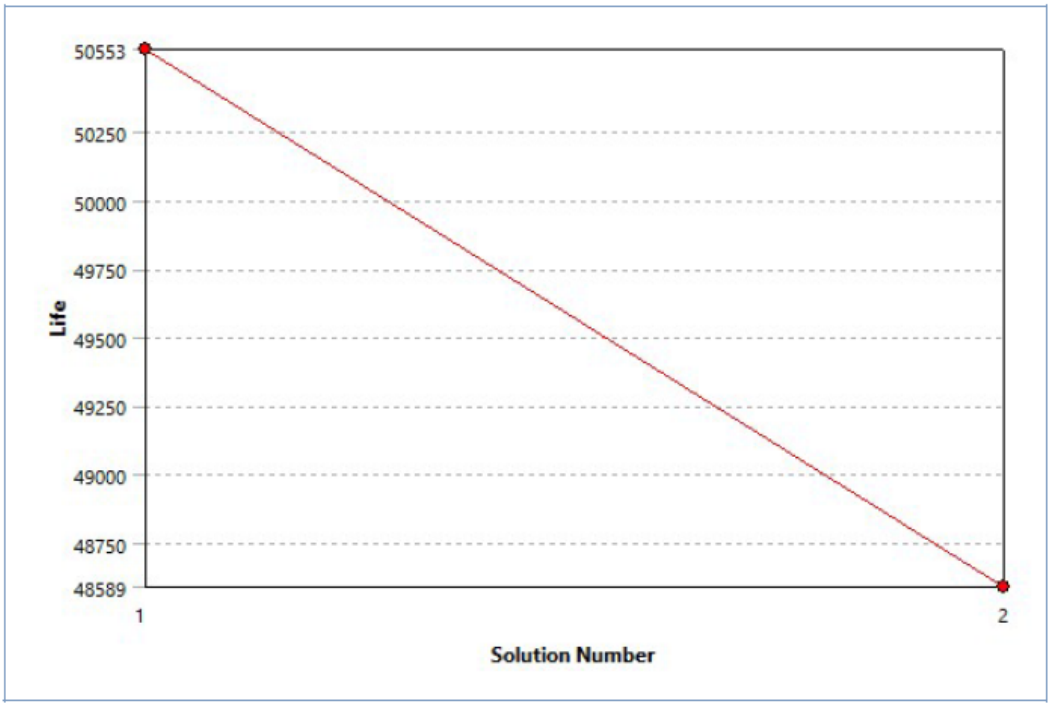

Model (A4) > Static Structural (A5) > Solution (A6) > Fatigue Tool > Life > Convergence

	Life	Change (%)	Nodes	Elements
1	50553		53582	33482
2	48589	-3,9606	86531	56358

Figure 71. Result convergence of fatigue analysis for mesh setup with 7 mm element size.

The 7 mm finite element fatigue result convergence analysis demonstrated a sufficiently small result variation relative to its purpose. Also considering the lack of fatigue analysis standards in light aircraft maintenance, the result has a significant probability of increasing awareness of probable part failure.

5.3.3 Fatigue analysis displacement boundaries

After defining mesh properties, the next step was to define structural displacement boundaries. This was done by applying one support fixed in all directions (A) and one displacement limitation (B – limits displacement in *Y* and *Z* direction) to the main landing gear strut model, displayed in Figure 72.

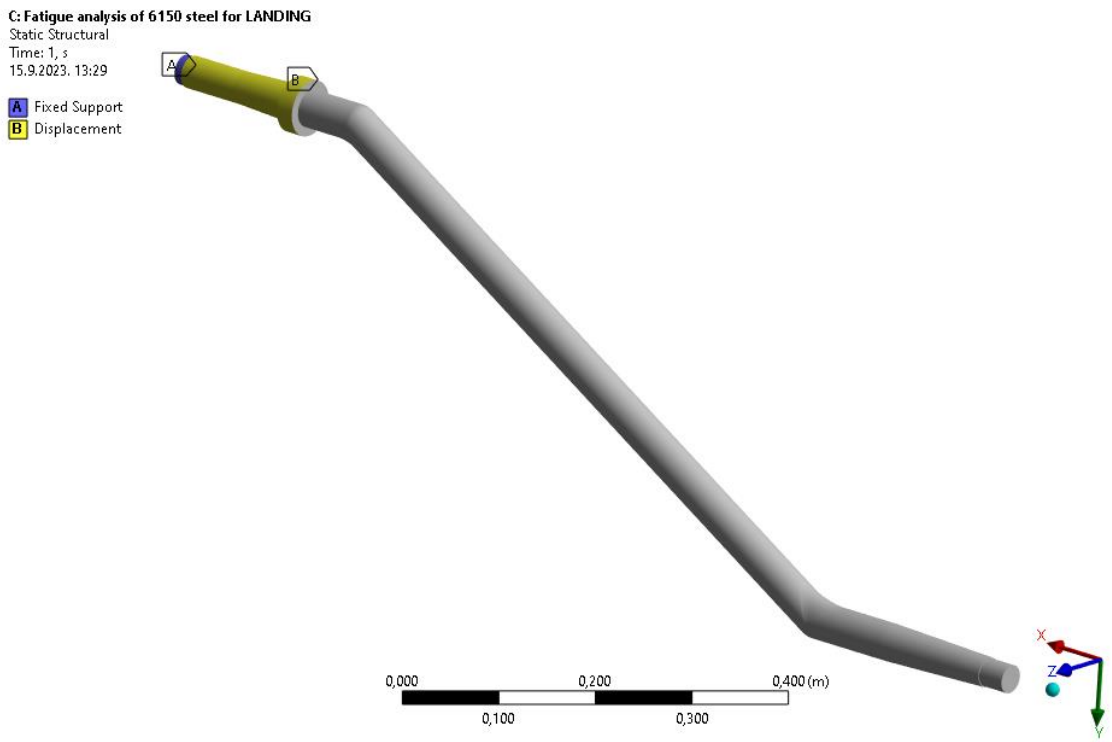

Figure 72. Applied boundary conditions.

This structural displacement boundaries were applied to all simulation runs since they are part of the aircraft landing gear structure and are not operation phase variables in the case of the Cessna 172R.

Finally, fatigue analysis parameters were defined according to Chapter 4.2. The chosen analysis type was strain life, and the mean stress theory was set to none. The chosen stress component for fatigue analysis was Signed von-Mises, to account for the difference in fatigue life in both compressive and tensile-natured loads. Infinite life was declared to be more than $1 \cdot 10^9$ load cycles (equivalent to the part experiencing $1 \cdot 10^9$ load histories). The stated parameters are the same as the ones that were used for fatigue analysis validation in Chapter 5.3.1. Other chosen parameters are displayed in Table 16.

Table 16. Fatigue analysis parameter setup.

Fatigue Strength Factor (*Kf*)	1
Analysis Type	Strain Life
Mean Stress Theory	None
Stress Component	Signed von-Mises
Infinite Life	1.e+009 blocks
Maximum Data Points To Plot	5000

5.3.4 Expert system approach to fatigue analysis result processing

The increasing complexity of the developed method necessitated the need for advanced fatigue analysis result processing given operator input on relevant operation parameters

displayed in Figure 76. One such approach that has proven effective in dealing with complex problems and providing reliable solutions is the expert system. An expert system is a computer-based program used to simulate the judgment and behaviour of a human or an organization with expert knowledge and experience in a particular field. These systems are designed to solve complex problems by reasoning about the knowledge they hold, typically using a rule-based system, or heuristics, to arrive at conclusions or decisions as stated by Shortliffe et al [145]. Reference [145] is stated purposefully to emphasize the generic nature of expert system applicability and relatively long history of implementation. It describes MYCIN, one of the first expert systems, which was developed for diagnostic reasoning in the domain of medicine. This early work paved the way for the development of a wide range of expert systems in various domains. The foundation of the expert system created for the research described in this thesis is explained in the continuation of this Chapter.

In the context of this research, the rationale for employing an expert system can be summarized as follows:

- Flexibility and Adaptability: Expert systems can adapt to different scenarios and accommodate varying inputs, as demonstrated in [146], [147], [148] and other, allowing them to be used in a wide range of applications within the field of light aircraft part remaining useful life prediction. Since the data used in this research is aircraft-specific, adaptability and flexibility are desirable traits.
- Knowledge Representation: Expert systems offer a structured way to represent and store domain-specific knowledge as described by Russel [149]. In this case, the knowledge related to fatigue life prediction of light aircraft parts is to be represented. Expert systems offer easy knowledge updating and expansion, allowing for continuous improvement in the prediction model.
- Reasoning and Inference: Expert systems are designed to perform reasoning and inference based on stored knowledge [149], enabling them to generate predictions and recommendations similar to those made by human experts. In the case of this research, the expert system will calculate the observed parts *RUL* while also enabling maintenance suggestions based on applicable maintenance procedures.
- Enhancing Decision-Making: By incorporating an expert system into the prediction process, decision-makers can benefit from the system's knowledge and reasoning capabilities, resulting in more informed decisions regarding aircraft maintenance scheduling, part replacement, and overall aircraft safety. This was explored by

Tsang [150] and many other, specifically in the field of prognostics and health management of various machinery stated throughout this Thesis and especially in Chapter 2.

In summary, employing an expert system in this research allowed first and foremost for the effective representation and management of domain-specific knowledge, facilitated reasoning and inference, and enhanced decision-making in the field of light aircraft part remaining useful life prediction. This approach can ultimately contribute to improved aircraft safety and more efficient maintenance planning.

5.3.4.1 Generic expert system architecture

The generic expert system architecture, as shown in Figure 73, is a reasonable starting point for expert system development, applicable to light aircraft maintenance. It is comprised of modules, each one having a specific purpose:

- The knowledge acquisition module enables the expert system to gather data from relevant sources and store it in the knowledge base.
- The knowledge base is an accumulation of facts and *RUL*s containing specific knowledge used for domain problem-solving.
- The inference module acquires relevant data for the knowledge base, interprets it, and finds solutions.
- The Explanation module generates an explanation of the achieved solution to the user.

By analysing the requirements for an expert system applicable to light aircraft landing gear maintenance, it was concluded that each module is susceptible to independent functioning based on correct input data of the connected adjacent module. An incremental development methodology was therefore chosen for the development of the expert system at hand, as displayed in Figure 73.

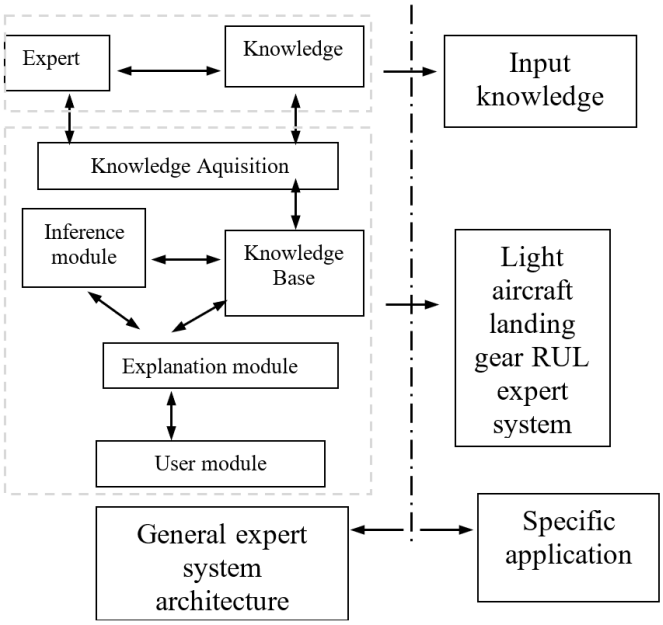

Figure 73. General expert system architecture.

An expert system providing insight into the remaining useful life of a light aircraft landing gear structure should operate based on input knowledge provided by the operator and the aircraft manufacturer. Those sources should be aligned with regulations by the competent national authority and safety guidelines by the relevant international authority dealing with aviation safety.

5.3.4.2 Applied expert system architecture

The parameters primarily influencing light aircraft landing gear strut *RUL* are the load intensity and direction. Load intensity is a direct consequence of the total mass acting on the observed strut, and its associated acceleration component correlating with load direction. The total mass acting on the landing gear strut can be observed as the empty airplane mass, which is relatively constant for various operations, and the mass of the pilot, co-pilot, fuel, and baggage area masses, all of them being variables for various operations, as explained in Chapter 5.3.4.3. The allowable pilot and co-pilot mass, and fuel mass are defined in the aircraft's Aircraft Flight Manual and the Aircraft Information Manual. In the case of the observed Cessna 172R, the Aircraft Flight Manual and the Aircraft Information Manual are presented in the same document named “Pilot's Operating Handbook and FAA Approved Airplane Flight Manual”, [3]. For this research, the relevant mass restrictions are extracted from the Airplane flight manual [3]. The mass distribution on the observed tricycle landing gear is a relevant load factor. Mass distribution on the aircraft landing gear can be extracted from the mass and balance restrictions given in [3], and/or from maintenance work cards documenting actual airplane weighting. Applicable work cards for weighting are displayed in the Cessna 172R maintenance

manual [13]. Aside from mass distribution, load direction also plays a significant role in determining the landing gear *RUL*. The landing gear load direction is a consequence of the airplane's landing gear geometry, and the angle around the airplane's lateral, longitudinal, and vertical axes. The longitudinal and vertical angles are supposed to be approximately zero during taxi, take-off, and landing, meaning the landing gear is aligned with the aircraft's direction of movement. When observing a tricycle-type landing gear, as is the case with the Cessna 172R, loading the landing gear structure asymmetrically regarding the longitudinal and vertical airplane axes can result in landing gear structure overload, requiring a condition check and structural part replacement if needed. Additionally, asymmetrical airplane alignment significantly increases research complexity, without contributing to the method in development. This research will only observe the aircraft rotation around the lateral axis, assuming the vertical and longitudinal angles are aligned with the line of movement during taxi, take-off, and landing. Regarding manoeuvres of lesser impact on the structural integrity of the light aircraft landing gear structure (such as in flight), the Aircraft Information Manual states the applicable limitations [3], highlighting the fact that it is not intended for aerobatics. Depending on the flight phase and nature, various load directions and intensities are acting on the light aircraft landing gear structure, however, while in flight, the load intensity is defined only by the landing gears' own weight and acceleration, including the weight of the landing gear wheels, and mechanisms, such as brakes and a retraction mechanism, if present.

The generalized expert system shown in Figure 73 can be modified for light aircraft landing gear structure *RUL* prognosis. Figure 74 is a schematic representation of the expert system applied to light aircraft landing gear *RUL* prognosis for the purpose of the research described in this Thesis.

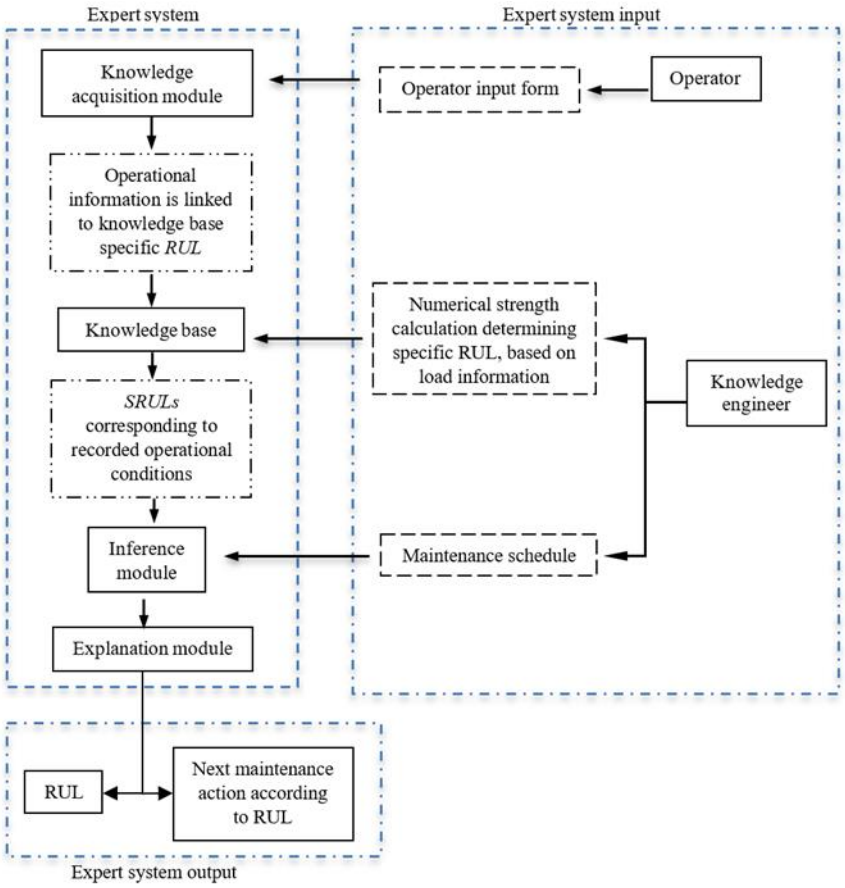

Figure 74. Expert system applicable for light aircraft landing gear RUL prognosis.

The first box labelled "Operator input form" represents information usually recorded for each flight. Additionally, permissible load information used to define operational loads can be extracted from the Aircraft Flight Manual or Aircraft Information Manual. This information is input by the aircraft operator and sent to the knowledge acquisition module, stored for future cumulative *RUL* assessment. The knowledge base is an accumulation of expert knowledge, in the case of this research it consists of specific *RUL*s[1] for specific load profiles[2]. The knowledge base is a matrix that distinguishes specific *RUL*s according to the specific load acting on the aircraft's landing gear structure. Each *RUL* is specific, and valid only for the observed light aircraft landing gear structural part and specific load profile. From the knowledge base, specific *RUL*s are extracted by implementing IF/THEN/ELSE logic, extracting the appropriate operational information recorded in the knowledge acquisition module and linking it to the corresponding *RUL* in the knowledge base. Next in line, the inference module calculates the

[1] Specific *RUL* refers to the *RUL* of a structural part of the light aircraft landing gear structure under a specific load profile.

[2] The specific load profile is defined by load distribution, intensity, direction, and acceleration parallel to load distribution.

total *RUL* of the observed structural part by applying a cumulative damage rule. The explanation module then links this information to the maintenance schedule, finding the appropriate maintenance action for every observed part, displaying the total light aircraft landing gear structure part *RUL* and the appropriate maintenance action.

This research methodology requires data extraction from the mass and balance sheets, numerical strength calculation to determine stresses and strains, fatigue life analysis for *RUL* determination, and *RUL* sorting in a matrix for total *RUL* calculation based on a cumulative damage rule. The information required for knowledge acquisition module input is displayed in Figure 75.

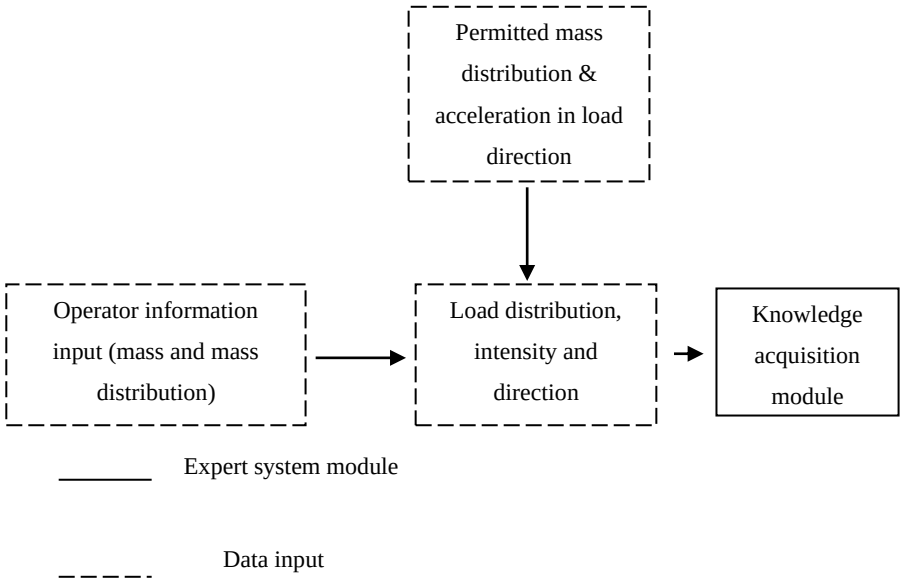

Figure 75. Required information, input into the knowledge acquisition module.

5.3.4.3 The knowledge acquisition module

Operational records are a source of landing gear structure *RUL*-defining information used in this research. The knowledge acquisition module gathers information necessary for determining specific *RUL*s. To do so, the module must accept, sort, and store user information input. An operator input form was created for this purpose, as shown in Figure 76.

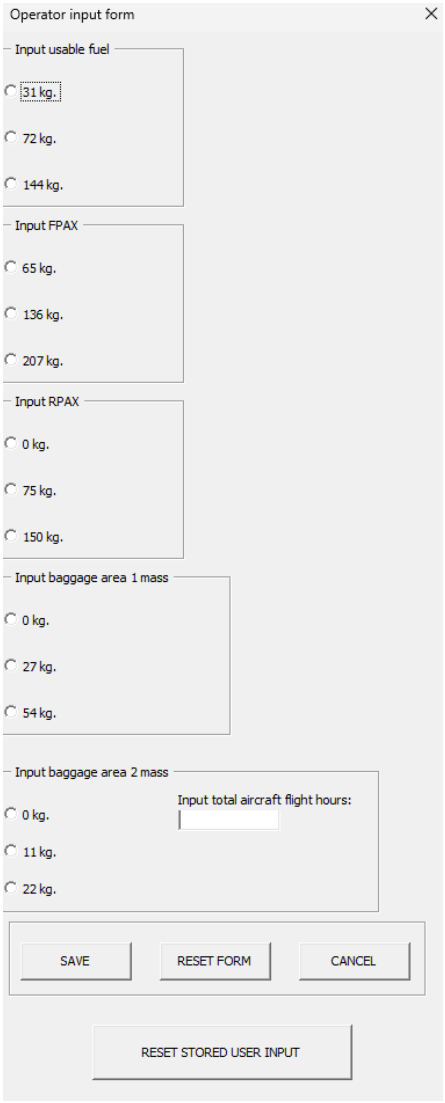

Figure 76. Operator input form.

The operator input form is used to extract airplane operation data. Operation data recording is mandatory for the observed operation category. The expert system developed in this research was simplified by introducing preset conditions. The preset conditions include the option to choose between three fuel, crew, passenger, and baggage area 1 and baggage area 2 masses, respective to the limitations defined by the applicable Cessna's mass and balance sheet. The *RUL* results calculated based on three offered masses are a more precise estimation of the remaining useful life than those usually calculated for this type of aircraft by the manufacturer for maintenance purposes. As previously stated, the current maintenance standard for the observed landing gear structure is hard-time part replacement, regardless of actual operating conditions considering the load profile and acceleration acting on the landing gear structure. A Visual Basic code (VBA code) was created to link the operator input form with a knowledge acquisition table, storing operator mass information input. The created knowledge acquisition table is displayed in Table 17.

Table 17. Example of the Knowledge acquisition table used for this research.

	U. FUEL		FPAX		RPAX		BGA1		BGA2	
$LP_{1,1}$		31 kg		65 kg		0 kg		0 kg		0 kg
$LP_{1,2}$		72 kg		136 kg		75 kg		27 kg		11 kg
$LP_{1,3}$		144 kg		207 kg		150 kg		54 kg		22 kg
$LP_{2,1}$		31 kg		65 kg		0 kg		0 kg		0 kg
$LP_{2,2}$		72 kg		136 kg		75 kg		27 kg		11 kg
$LP_{2,3}$		144 kg		207 kg		150 kg		54 kg		22 kg
$LP_{3,1}$		31 kg		65 kg		0 kg		0 kg		0 kg
$LP_{3,2}$		72 kg		136 kg		75 kg		27 kg		11 kg
$LP_{3,3}$		144 kg		207 kg		150 kg		54 kg		22 kg
$LP_{4,1}$		31 kg		65 kg		0 kg		0 kg		0 kg
$LP_{4,2}$		72 kg		136 kg		75 kg		27 kg		11 kg
$LP_{4,3}$		144 kg		207 kg		150 kg		54 kg		22 kg

The input code linking the operator input form to the knowledge acquisition table was set up for four input iterations, meaning that the operator can input four flight parameter sets, one for each consecutive flight. It was concluded that this number of flight parameter sets was sufficient for explanatory and demonstration purposes of this research. The first column, labelled $LP_{i,i}$ … $LP_{n,}$ represents the various load profiles the observed landing gear part can be subject to, depending on the mass value and distribution that was input into the operator input form displayed in Figure 76. The subsequent columns are labelled according to the position of the input mass, from *U.FUEL* to *BGA2*, as explained in Chapter 5.2.1.1, and displayed in Figure 23. The sorting logic, extracting mass information from the operator input form to the knowledge acquisition table, is based on "IF THEN ELSE" statements, testing the input iteration number first, after which the chosen fuel, front seat, rear seat, baggage area 1 and baggage area 2 are sorted and stored in the knowledge acquisition table. The knowledge acquisition table stores the chosen values as "TRUE" statements, whereas cells linked to values that were not chosen are left empty.

5.3.4.4 The knowledge base

Expert knowledge required for sensor-less prediction of the remaining useful life of light aircraft landing gear structures is stored in the knowledge base in the form of specific *RUL*s. These specific *RUL*s (abbrev. *SRUL*) represent the *RUL* of the observed structural part under specific loading conditions with constant load distribution, intensity, and direction. The knowledge base is a sorting and storage unit that stores previously calculated specific *RUL*s in a *RUL* matrix. These *SRUL*s are calculated using numerical strength analysis, which involves the use of the finite element method in a computer-aided design and testing environment. The knowledge base organizes *SRUL*s according to operator input information on mass and mass distribution, which makes it easier to extract data for cumulative damage calculation. The *SRUL*s are stored in a matrix based on the load profile, with rows labelled by a code representing mass and mass distribution. The columns of the *RUL* matrix are divided by the relevant load

profiles, which are identified as taxi-in, taxi-out, take-off, flight, and landing. Whereas taxi-out is the phase of operation where the aircraft initiates the operation by taxiing to the runway, loaded with the starting fuel amount. The taxi-in phase of operation is when the aircraft has landed and taxis from the runway to its standstill position, loaded by a lesser fuel mass due to fuel consumption during operation. The operator inputs landing gear structure *RUL*-relevant information in the form of mass value and distribution according to the limitations defined in the weight and balance sheets (Figure 25), which is the basis for determining the corresponding critical remaining useful life for the operation at hand. A Visual Basic (VBA) code was written to extract *SRUL*s from the knowledge base *RUL* matrix for use in the expert system's inference module. The VBA code is based on "IF THEN ELSE" statements, which first test the input iteration number, followed by a test of the knowledge acquisition table input (Table 17.) for the validity of the chosen fuel, front seat, rear seat, baggage area 1, and baggage area 2 input masses. Based on the combination of mass input determined from the knowledge acquisition table, the corresponding *SRUL* value is selected from the knowledge base *RUL* matrix. Any given combination of knowledge acquisition table input, considering four input iterations, is linked to the appropriate *SRUL* through the VBA knowledge base code, representing the remaining useful life of the landing gear structure under the corresponding specific loading conditions. An example of the sorting logic for a Cessna 172R is given in Figure 77.

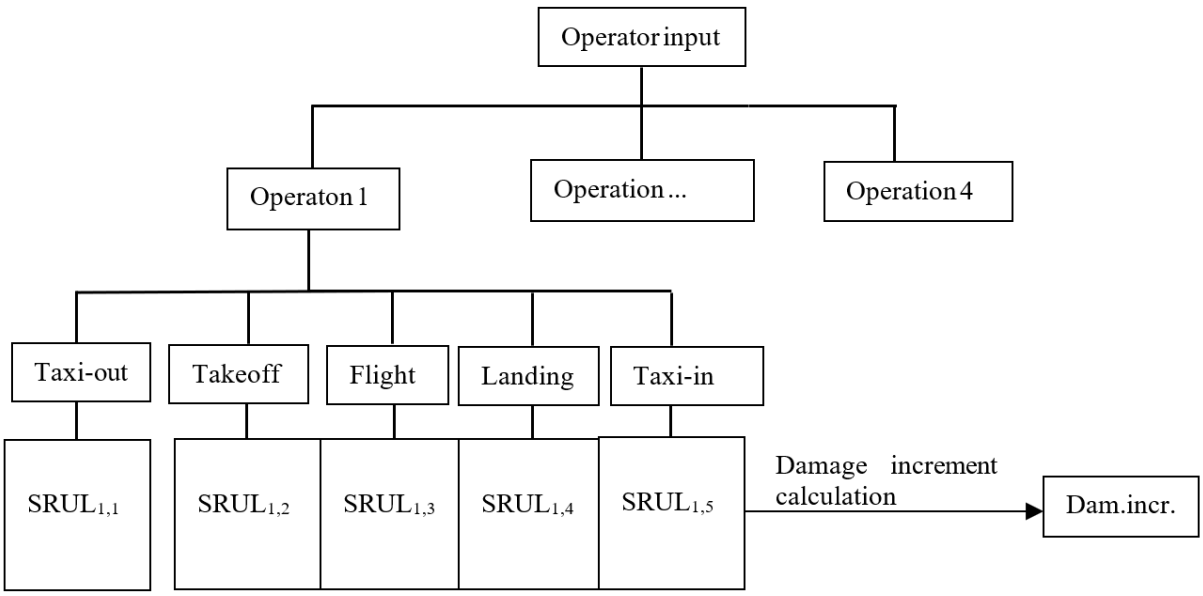

Figure 77. Knowledge base sorting logic.

The damage increment in Figure 77 represents the damage accumulated in the observed landing gear structural part during a single operation consisting of operation phases, each phase causing an *SRUL*. A more thorough explanation and the method of damage increment calculation are presented in Chapter 5.4. The example created for demonstration purposes of

this methodology is limited to four input iterations in the form of mass and mass distribution. The operator extracts this information from the weight and balance sheet corresponding to the observed operation and inputs it into the knowledge base *RUL* matrix. The *RUL* matrix, shown in Figure 78, stores *SRUL*s sorted in rows labelled by mass value and distribution combinations and columns sorted by operation phases, which are explained in more detail later in the document. There are 141 mass value and distribution combinations in the *RUL* matrix, presented in the first matrix column, and based on the observed three masses in each mass position, as explained in Chapter 5.3.4.3. The reason for having exactly 141 mass value and distribution combinations is because a mass and balance check was performed on all possible combinations, by using the mass and balance calculator explained in Chapter 5.2.1.1 and displayed in Figure 26. The mass value and distribution combinations that resulted in an unstable airplane, meaning that the flight would have been prohibited, were excluded from observation. The mass value and distribution combinations are sorted according to the sum of masses in each mass station, from lowest (table top) to highest (table bottom). In addition to the *SRUL*s, the knowledge base *RUL* matrix also enables the determination of the fatigue damage increment and subsequently the accumulated fatigue damage.

KNOWLEDGE BASE	TAXI-OUT	TAKEOFF	FLIGHT	LANDING	TAXI-IN
31-65-0-0-0					
31-65-0-0-11					
31-65-0-0-22					
31-65-0-27-0					
72-207-0-54-11					
144-136-0-54-11					
72-136-75-54-11					
144-65-75-54-11					
31-207-75-27-11					
144-207-0-0-0					
72-65-150-54-11					
72-207-75-0-0					

Figure 78. Expert system knowledge base module RUL matrix.

Where:

TAXI-OUT – Is the remaining useful life of the landing gear when subjected solely to taxi-out phase loads.

TAXI-IN - Is the remaining useful life of the landing gear under only taxi-in phase loads.

TAKEOFF - Is the remaining useful life of the landing gear if exposed exclusively to take-off phase loads.

LANDING - Is the remaining useful life of the landing gear only under landing phase loads.

FLIGHT - Is the remaining useful life of the landing gear when subjected solely to flight phase loads.

Since the subject expert system is focused on prognosing the *RUL* of the light aircraft landing gear structure, expert knowledge includes the *RUL* for various flight conditions that could be encountered during operation. The *RUL* is calculated based on variable load parameters such as load distribution, intensity, and direction. For this purpose, information on the permissible range of mass, distribution, acceleration, and flight nature can be deduced from the Aircraft Flight Manual and/or the Aircraft Information Manual [19], or certification specification compliance documents, issued by EASA [151]. For example, operational restrictions related to the structure's mechanical integrity, such as the vertical acceleration needed to calculate the load acting on the landing gear structure can be found in the aircraft flight manual [3], usually in the limitations section. The observed aircraft's acceleration restrictions are presented in Table 18.

Table 18. Normal category Cessna 172R flight load factor limitations, [3].

Flight load factors for the maximum take-off mass – 2100 pounds	
Flaps up	+3.8 g.....-1.52 g
Flaps down	+3 g
NOTE: the design load factors are 150 % of the above, and in all cases, the structure meets or exceeds the design loads.	
Centre of gravity range	
Forward	35 inches aft of the datum at 1950 pounds or less, with straight line variation to 40 inches aft of the datum at 2450 pounds.
Aft	47.3 inches aft of datum at all masses
Note: reference datum is the lower portion of the firewall front face.	

The extracted information on the permissible range of *RUL* relevant parameters is required for the knowledge base module, as the basis for structure-specific *RUL* determination. In the case of the observed Cessna 172R, two sources of information for specific *RUL* determination were used.

The first information source are the allowable mass combinations considered in the knowledge acquisition module of this method. Derived from those combinations is the total

mass born by the landing gear structure. By filling in the mandatory airplane mass and balance sheets (Figure 25) before any operation, the operator (pilot in charge) determines the correct airplane loading conditions for safe operations. The mass and balance sheets serve as a safety check, warning the pilot in charge if the chosen masses and mass combinations are outside the permissible boundaries, compromising operation feasibility and therefore safety. The mass and balance sheets that are presented in Figure 25 enable input for several masses aligned with the location they would be positioned in the airplane. The total mass acting on the airplane's landing gear is the sum of the masses presented in the mass and balance sheets. Specifically, the total mass is the sum of the mass of the empty airplane, labelled *BEM*, usable fuel mass, pilot and front PAX mass, rear PAX mass, baggage area 1 mass, and baggage area 2 mass. The fuel allowance mass is usually small compared to the airplane's total mass, having a negligible impact on the landing gear's total *RUL*, impacting the *RUL* only in the take-off phase. The fuel allowance mass impact on the landing gear's total *RUL* is therefore not considered since it has a small negative impact on the landing gear structure-specific *RUL* during pre-flight taxi and take-off, and no impact during landing and post-flight taxi, since the fuel is already spent in the take-off phase.

5.3.4.5 The inference module

The purpose of the inference module is to calculate the accumulated fatigue damage of a light aircraft's landing gear structure based on input from the operator. This is achieved by extracting data from the knowledge acquisition table and linking it to the damage increment value determined and stored in the knowledge base. The accumulated fatigue damage is then calculated by following the procedure described in Chapter 5.4. Accumulated fatigue damage represents the accumulated fatigue damage in the observed structural part regarding user input, based on mass and balance information and total flight hours. Accumulated damage is a product of the damage increment, which is the result of fatigue damage accumulation due to the impact of one single mass value and distribution scenario, representing one single aircraft operation. After calculating several damage increments, corresponding to several observed operations, the accumulated fatigue damage can be determined. The method example in this Thesis foresees four input iterations, meaning four aircraft operations that don't have to be in consecutive order. This number of input iterations was deemed to be sufficient for demonstration purposes, as stated and explained earlier. The accumulated fatigue damage unit of measurement is dimensionless, varying between 0 (no useful life left), and 1 (100 % of the useful life is available). For example, if the landing gear structure can withstand 100000 cycles at a given cyclic load before failing, and it has experienced 50000 cycles at that cyclic load, then the

accumulated fatigue damage would be 0.5. This is a direct result of applying the Palmgren-Miner rule, also known as Miner's rule, which suggests that the damage accumulated in a structure due to cyclic stress is the sum of the fractional damages from each loading cycle. In this case, the landing gear has already withstood half of its total tolerance for these load cycles, effectively using up half of its useful lifespan under these conditions. Therefore, its cumulative damage fraction is 0.5, or 50 %. According to Miner's rule, when the cumulative damage reaches 1 (or 100%), the landing gear is expected to fail. This approach to calculating accumulated fatigue damage assumes that the damage fraction is proportional to the fraction of the total life that has been consumed at a given cyclic loading. In other words, if a material or part has experienced 50 % of its life at a given cyclic load, it has also accumulated 50 % of the total damage that it can withstand at that cyclic load. This assumption allows for the calculation of the accumulated damage at each observed cyclic load intensity, which can then be summed up to give the total damage that has accumulated in the landing gear structure. The described approach is linear, which means that it assumes that the accumulation of damage is linearly related to the number of cycles of loading. It is important to note that this approach to calculating accumulated damage is only an approximation and may not accurately predict the fatigue behaviour of an aircraft landing gear structure due to various operational circumstances that were not recorded. Since the method developed in this research predicts the landing gear structure *RUL* without sensory information on operating environmental and structural loading conditions, implementing a more precise method for calculating the accumulated fatigue damage would not serve the purpose of increasing result accuracy while unnecessarily increasing method complexity.

The inference module extracts *SRUL* values from the knowledge base, based on information from the knowledge acquisition table, by choosing the appropriate damage increment according to user input. The inference module stores the chosen damage increment for each input iteration. The number of total operation hours is also stored in the inference module for accumulated damage calculation.

The VBA code created to enable inference module actions is based on “IF THEN ELSE” statements, testing values stored in the knowledge acquisition table. The VBA code extracts the corresponding *SRUL* from the knowledge base for knowledge acquisition table test results labelled “TRUE” and stores the information to be used for total *RUL* calculation. The VBA code does this for four user input cycles.

5.3.4.6 The Explanation module

The purpose of the explanation module is to store information on required maintenance actions, i.e., the maintenance schedule of the observed part, and present this information depending on the calculated total *RUL* of the observed part. It does this by linking the accumulated fatigue damage value to the appropriate required maintenance action according to the aircraft's maintenance manual or program. The maintenance schedule is usually present in the aircraft's maintenance program. The information is sorted into rows and columns, the rows representing the light aircraft landing gear structure part, of which only one is the subject of this Thesis. The columns represent the required maintenance action for the aircraft's total operation time. The prescribed maintenance actions are input into a Macro VBA function, linked to the "VIEW REQUIRED MAINTENANCE ACTION" button in the "USER INPUT SHEET", performing logical tests to determine and present the required maintenance action. An example of the Cessna 172R landing gear maintenance schedule is displayed in Table 19.

Table 19. Cessna 172R callsign 9A-DAD, landing gear structure maintenance schedule, [152].

Reference	Item	Part No.	Period	Requirements	Overhaul period
325001	Nose Gear Steering Mechanism		100 hours 100 hours	Check Lubricate	OC
322001	Nose Gear		100 hours	Inspect, check for corrosion. Check operation	OC
322003	Nose Gear Fork		100 hours 50 hours	Inspect for cracks Lubricate torque link	OC
324004 322002 321001	Tires & Fairings		100 hours	Inspect	OC
324002 324001	Brake, master cylinder & parking brake		100 hours	Inspect Check operation	OC
324003	Brake Lines Wheel Cylinders hoses, Fittings		400 hours / 1 year	Check	5 years rubber hoses OC all other hoses
324005	Wheels, Brake Disc and Lining		100 hours	Inspect	OC

324006	Wheel bearings		100 hours	Inspect & lubricate	OC
321002	Main Landing Gears struts		100 hours	Inspect for crack & corrosion	OC
321003 322004	Main Landing Gears & Nose Gear Attachment Structure		100 hours	Inspect for crack	OC

5.4 Method phase 4: Calculating accumulated fatigue damage

The first step in determining accumulated fatigue damage (abbreviated D_{accFa}) is to count the total number of performed operations (abbreviated *TNO*), which are discerned by the varying mass value and distribution scenarios.

The second step is to calculate the observed parts *SRUL*. The *SRUL* value represents the number of times a specific operational phase can be performed under given load intensity, orientation, and direction, when subject to the loads' cyclic variability originating from the measured or estimated acceleration in the respective direction (measurements were taken for this research, since they were available). The *SRUL* value is determined by performing numerical strength calculations, for this research this was performed through fatigue life analysis in Ansys.

The third step is to count the number of times one specific operation was performed. The number of times one specific mass value and distribution scenario was performed is labelled Counted Number of Operations (abbreviated CNO_i).

Calculating the damage increment is the fourth step in determining accumulated fatigue damage. The damage increment represents the fatigue damage accumulated in the observed part during one of the mass value and distribution scenarios. It is important to mention that equation (25), utilized to calculate the damage increment, was developed based on the Palmgren-Miner linear damage rule. This rule, which was first introduced in the 1940s, states that the total fatigue damage incurred in a system is the sum of the individual damage increments resulting from different load types. Using this rule as a foundation, the equation allows the quantification of fatigue damage for each mass value and distribution scenario, denoted by the variable 'i' which corresponds to the five operation phases observed in this Thesis.

$$\Delta D_i = \sum \frac{CNO_i}{SRUL_i} \qquad (25)$$

Where:

ΔD_i - Is the damage increment for the *i*-th observed mass value and distribution scenario, [-];
CNO_i - Is the number of times the i-th mass value and distribution scenario was performed, [-];
$SRUL_{\mathrm{i}}$ - Is the specific remaining useful life value for one of the five operation phases defined by the observed mass value and distribution scenario, [-].

Lastly, the accumulated fatigue damage can be calculated. This is achieved by adding up all calculated damage increments, according to equation *(26)*, where *i* represents the 141 mass value and distribution scenarios, as explained in Chapter 5.3.4.4.

$$D_{accFa} = \sum \Delta D_i \qquad (26)$$

Where:

D_{accFa} – Is the accumulated fatigue damage for all observed mass value and distribution scenarios, [-].

Step-by-step instructions for determining accumulated fatigue damage (D_{accFa}) are provided as follows:

Step 1: Calculate the specific remaining useful life (S*RUL*) for each operation.

- Use software like Ansys to perform numerical strength calculations and simulate fatigue life for each specific operation.
- Find the S*RUL* value, which represents how many more times the operation can be performed before the part fails.

Step 2: Count the total number of performed operations (*TNO*).

- Identify and count all the different operations that have been performed based on varying mass value and distribution scenarios.

Step 3: Count the number of times each mass value and distribution scenario was performed (*CNO_i*).

- Keep track of the number of times each mass value and distribution scenario was performed.

Step 4: Calculate the damage increment (ΔD_i) for each mass value and distribution scenario:

- For each mass value and distribution scenario, divide the counted number of times it was performed (*CNO_i*) by the specific remaining useful life (*SRUL_i*).
- This will give the damage increment for that specific mass value and distribution scenario (ΔD_i).

Step 5: Calculate the accumulated fatigue damage (D_{accFa}).

- Add up all the damage increments (ΔD_i) from each operation.

- The sum of all these damage increments will give the accumulated fatigue damage (D_{accFa}), which represents the total damage caused by all observed operations.

The stated procedure is presented through a flowchart in Figure 79.

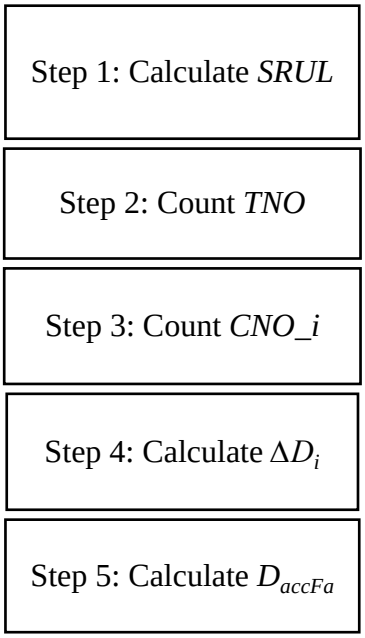

Figure 79. Accumulated damage calculation procedure flowchart.

To carry out this procedure, a fatigue damage accumulation calculator has been created. The accumulated fatigue damage is determined by summing up the damage increments experienced by the landing gear strut during each operation. These operations consist of five distinct phases that encompass every complete airplane operation. By calculating the accumulated fatigue damage, a comprehensive understanding of the remaining useful life of the landing gear strut can be obtained. The calculated accumulated fatigue damage is represented as a variable ranging from 0 to 1. A value of 0 indicates that the landing gear strut is in a like-new condition, while a value of 1 suggests that fatigue failure is imminent, posing a significant risk to the aircraft's safety and integrity.

6 NUMERICAL STRENGTH ANALYSIS RESULTS

This Chapter discusses the results of the numerical strength analysis performed on the main landing gear strut of the observed light aircraft. The primary goal of the analysis results described in this Chapter was to determine the number of times each of the five operational phases (taxi-out, take-off, flight, landing, and taxi-in) can be performed before the observed airplane's strut experiences failure due to material fatigue, given the specific mass value and distribution associated with each phase, according to mandatory mass and balance records.

By considering the mass value and distribution of each operational phase, a comprehensive understanding of the main landing gear strut's performance related to material fatigue can be achieved. To organize the data acquired by numerical strength analysis performed by consecutive simulations for estimating landing gear strut fatigue life, the created Remaining Useful Life Matrix was used, Figure 78. The *RUL* matrix enables analysis of the aircraft's landing gear strut performance and fatigue durability under various mass distribution and intensity scenarios. The matrix consists of 7 columns and 141 rows, with five of the seven rows representing a unique combination of mass distribution and intensity permissible according to the mass and balance calculation.

The columns in the *RUL* matrix are labelled and explained as follows:

- "Mass value and distribution scenario" denotes the mass value and distribution combination applied to the aircraft in accordance with the mass and balance procedure. The mass value and distribution scenarios are sorted from top to bottom according to the sum of masses in each mass station, from lowest to highest.
- "Taxi-out", "Take-off", "Flight", "Landing", and "Taxi-in" represent the number of times each respective phase can be executed before fatigue failure. This is determined by numerical strength calculations under a specific mass value and distribution, measured load factor for the observed phase, and load vector direction and orientation.
- "Dam_incr_i" is the fatigue damage accumulated in the observed part due to specified mass value and distribution, measured load factor corresponding to the observed phase and load vector direction and orientation.
- “Number of cycles to failure” is the number that particular operation with its corresponding fatigue relevant loads according to operation phases can be performed until fatigue failure occurs.

The *RUL* matrix including the specific remaining useful lives and calculated damage increments is presented in *Table 20*.

Table 20. The Remaining Useful Life Matrix.

Mass intensity and distribution scenario	**TAXI-OUT**	**TAKEOFF**	**FLIGHT**	**LANDING**	**TAXI-IN**	ΔD_i	Number of operations to failure
31-65-0-0-0	16430000	814702855	∞	3131200	21226000	4.2857E-07	2333340
31-65-0-0-11	13379000	760920000	∞	2640400	17188000	5.1297E-07	1949436
31-65-0-0-22	10950000	743020000	∞	2078800	13990000	6.4520E-07	1549916
31-65-0-27-0	10682000	616030000	∞	2027600	13639000	6.6175E-07	1511141
31-65-0-27-11	8780100	676980000	∞	1664400	11149000	8.0588E-07	1240876
72-65-0-0-0	9006800	514210000	∞	2445900	16511000	5.8239E-07	1717077
31-65-0-27-22	7254000	660340000	∞	1373700	9160400	9.7650E-07	1024070
72-65-0-0-11	7422100	675930000	∞	1998000	13435000	7.1115E-07	1406183
31-65-0-54-0	7073000	643530000	∞	1339500	8926900	1.0015E-06	998497
72-65-0-0-22	6147600	557710000	∞	1641000	10988000	8.6485E-07	1156268
31-65-0-54-11	5868200	531820000	∞	1110800	7366100	1.2083E-06	827609
72-65-0-27-0	5999400	543970000	∞	1601100	10715000	8.8642E-07	1128134
31-136-0-0-0	6148800	557810000	∞	1164400	7731900	1.1526E-06	867625
31-65-75-0-0	5165100	466710000	∞	977710	6460200	1.3733E-06	728151
31-65-0-54-22	4893900	441630000	∞	926150	6109700	1.4500E-06	689649
72-65-0-27-11	4989900	450510000	∞	1321200	8801400	1.0731E-06	931853
31-136-0-0-11	5100800	460760000	∞	965950	6380300	1.3902E-06	719321
31-65-75-0-11	4318100	388410000	∞	817440	5371600	1.6437E-06	608401
72-65-0-27-22	4171800	374900000	∞	1096200	7266600	1.2922E-06	773856
31-136-0-0-22	4253100	382410000	∞	805660	5291700	1.6679E-06	599545
72-65-0-54-0	4068100	365340000	∞	1069100	7082300	1.3251E-06	754651
31-65-75-0-22	3628600	324810000	∞	687200	4489600	1.9566E-06	511095
31-136-0-27-0	4155100	373360000	∞	787360	5167700	1.7069E-06	585849
31-65-75-27-0	3532800	315980000	∞	669440	4369500	2.0089E-06	497792
72-65-0-54-11	3415100	305140000	∞	891160	5872000	1.5885E-06	629514
31-136-0-27-11	3478700	311000000	∞	659710	4303700	2.0389E-06	490471
72-136-0-0-0	3555500	318070000	∞	931940	6149000	1.5201E-06	657870
31-65-75-27-11	2980900	265200000	∞	565360	3667200	2.3807E-06	420042
144-65-0-0-0	3392400	303050000	∞	1608200	10764000	1.0128E-06	987370
72-65-75-0-0	3027300	269460000	∞	786970	5165000	1.7983E-06	556067
72-65-0-54-22	2881600	256080000	∞	746920	4893700	1.8941E-06	527952
31-136-0-27-22	2927400	260280000	∞	555770	3602600	2.4223E-06	412827
72-136-0-0-11	2983900	265470000	∞	777070	5097900	1.8219E-06	548864
31-65-75-27-22	2528100	223630000	∞	480060	3093600	2.8063E-06	356335
144-65-0-0-11	2853400	253490000	∞	1325800	8833300	1.2219E-06	818415
31-136-0-54-0	2857500	253860000	∞	542840	3515500	2.4805E-06	403142
72-65-75-0-11	2560500	226610000	∞	661380	4315100	2.1387E-06	467575
31-65-75-54-0	2094100	217330000	∞	467390	3008600	2.9541E-06	338518
72-136-0-0-22	2517000	222620000	∞	651460	4248000	2.1722E-06	460361
144-65-0-0-22	2412400	213030000	∞	1099000	7285800	1.4664E-06	681947
31-136-0-54-11	2414400	213220000	∞	459380	2954800	2.9342E-06	340814
72-65-75-0-22	2176700	191460000	∞	558880	3623500	2.5299E-06	395272
72-136-0-27-0	2458700	217280000	∞	636740	4148600	2.2229E-06	449870
31-65-75-54-11	2340850	183920000	∞	398660	2548300	3.3335E-06	299989
144-65-0-27-0	2354200	207700000	∞	1072700	7106800	1.5025E-06	665546
31-207-0-0-0	2510300	222010000	∞	477920	3079200	2.8200E-06	354607
72-65-75-27-0	2119000	186200000	∞	544500	3526700	2.5974E-06	385002
31-136-75-0-0	2149900	195038000	∞	409740	2622400	3.2922E-06	303751
31-136-0-54-22	2050300	179920000	∞	390860	2496200	3.4524E-06	289657
31-65-150-0-0	1869100	163390000	∞	356500	2267100	3.7873E-06	264042
72-136-0-27-11	2082300	182840000	∞	536250	3471200	2.6386E-06	378990
31-65-75-54-22	1792000	156360000	∞	341840	2169400	3.9507E-06	253118
144-65-0-27-11	1998200	175170000	∞	893290	2943200	1.9654E-06	508807
31-207-0-0-11	2120200	186310000	∞	404500	2587400	3.3357E-06	299787
72-65-75-27-11	2078150	157870000	∞	462200	2973800	2.9874E-06	334743
31-136-75-0-11	1830000	159820000	∞	349540	2220700	3.8639E-06	258805
31-65-150-0-11	1603200	139180000	∞	306480	1934500	4.4107E-06	226720
72-136-0-27-22	1772400	154580000	∞	454060	2919200	3.1156E-06	320967
144-65-0-27-22	1704700	148410000	∞	747960	4900700	2.1344E-06	468521
31-207-0-0-22	1799800	157070000	∞	344200	2185200	3.9249E-06	254784

72-65-75-27-22	1551300	134470000	∞	394450	2520300	3.5840E-06	279017
72-136-0-54-0	1729800	150700000	∞	443540	2848600	3.1904E-06	313443
144-65-0-54-0	1662100	144530000	∞	729720	4777200	2.1883E-06	456979
31-136-75-0-22	1565500	135760000	∞	299760	1890000	4.5112E-06	221668
31-207-0-27-0	1759700	153420000	∞	336820	2136000	4.0119E-06	249258
72-65-75-54-0	1508900	130620000	∞	384080	2451000	3.6820E-06	271591
31-65-150-0-22	1381900	119110000	∞	264850	1658900	5.1106E-06	195673
31-136-75-27-0	1525400	132120000	∞	292410	1841300	4.6261E-06	216166
31-65-150-27-0	1342100	115500000	∞	257756	1610800	5.2542E-06	190324
72-136-0-54-11	1478200	127840000	∞	377240	2405400	3.7509E-06	266604
144-65-0-54-11	1423500	122870000	∞	613810	3993800	2.5902E-06	386072
31-207-0-27-11	1499700	129780000	∞	287870	1811200	4.7004E-06	212747
72-65-75-54-11	1299300	111630000	∞	329240	2085600	4.2954E-06	232808
72-207-0-0-0	1526400	132210000	∞	391420	2500000	3.6175E-06	276434
31-136-75-27-11	1310100	112600000	∞	251870	1573300	5.3781E-06	185940
144-136-0-0-0	1464500	126590000	∞	639040	4164100	2.4957E-06	400686
72-136-75-0-0	1325100	113960000	∞	337510	2140700	4.1934E-06	238467
31-65-150-27-11	1161200	99164000	∞	223520	1386800	6.0662E-06	164847
72-136-0-54-22	1269500	108940000	∞	322580	2041400	4.3868E-06	227959
144-65-75-0-0	1276900	109610000	∞	545100	3530800	2.9100E-06	343641
144-65-0-54-22	1225200	104940000	∞	519130	3356000	3.0500E-06	327869
31-207-0-27-22	1284500	110290000	∞	247340	1543500	5.4785E-06	182533
72-65-150-0-0	1167400	99723000	∞	295320	1860500	4.7903E-06	208756
72-65-75-54-22	1124200	95830000	∞	283700	1783600	4.9855E-06	200583
72-207-0-0-11	1303800	112040000	∞	332950	2110300	4.2532E-06	235115
31-136-75-27-22	1130600	96407000	∞	218060	1351000	6.2209E-06	160747
144-136-0-0-11	1253700	107510000	∞	537640	3480600	2.9542E-06	338498
31-207-0-54-0	1254600	107590000	∞	241860	1507400	5.6044E-06	178432
72-136-75-0-11	1140600	97303000	∞	289350	1821000	4.8922E-06	204408
31-65-150-27-22	1009500	85510000	∞	194940	1199600	6.9657E-06	143561
144-65-75-0-11	1101500	93784000	∞	462250	2974100	3.4181E-06	292562
31-136-75-54-0	1100700	93711000	∞	212580	1315000	6.3838E-06	156648
72-65-150-0-11	1012400	85768000	∞	255120	1594800	5.5462E-06	180305
31-65-150-54-0	979660	82833000	∞	189480	1164000	7.1695E-06	139479
72-207-0-0-22	1119200	95381000	∞	284730	1790400	4.9746E-06	201021
144-136-0-0-22	1078600	91727000	∞	454790	2924100	3.4788E-06	287453
31-207-0-54-11	1078800	91737000	∞	208700	1289600	6.5049E-06	153731
72-136-75-0-22	986550	83451000	∞	249370	1556800	5.6781E-06	176116
72-207-0-27-0	1094000	93105000	∞	278620	1750000	5.0854E-06	196643
144-65-75-0-22	954810	80604000	∞	394100	2517900	3.9943E-06	250356
31-136-75-54-11	953560	80492000	∞	184820	1133600	7.3539E-06	135982
144-136-0-27-0	1053200	89441000	∞	444580	2855700	3.5602E-06	280886
72-65-150-0-22	882020	74086000	∞	221520	1373700	6.3895E-06	156507
72-136-75-27-0	961090	81167000	∞	243270	1516600	5.8228E-06	171738
31-65-150-54-11	854800	71653000	∞	165930	1010700	8.1999E-06	121953
144-65-75-27-0	929280	78316000	∞	384030	2450700	4.1009E-06	243850
31-207-75-0-0	971100	82065000	∞	188470	1157400	7.2118E-06	138661
31-207-0-54-22	932120	78571000	∞	181020	1108800	7.5117E-06	133126
72-65-150-27-0	856560	71810000	∞	215450	1333800	6.5726E-06	152147
31-136-150-0-0	860380	72151000	∞	167320	1019700	8.1334E-06	122950
72-207-0-27-11	942710	79519000	∞	239310	1490600	5.9229E-06	168836
31-136-75-54-22	830020	69441000	∞	161490	981920	8.4299E-06	118625
144-136-0-27-11	909630	76556000	∞	377760	2408800	4.1747E-06	239536
72-136-75-27-11	834450	69836000	∞	210550	1301700	6.7304E-06	148579
31-65-150-54-22	749230	62242000	∞	145990	881650	9.3348E-06	107126
144-65-75-27-11	808540	67524000	∞	328877	2083200	4.7723E-06	209543
31-207-75-0-11	840960	70417000	∞	163870	997330	8.3084E-06	120360
72-65-150-27-11	749010	62222000	∞	187850	1153300	7.5416E-06	132597
31-136-150-011	750540	62358000	∞	146540	885230	9.3021E-06	107502
72-207-0-27-22	816350	68220000	∞	206610	1275900	6.8634E-06	145700
144-136-0-27-22	789410	65819000	∞	322690	2042100	4.8706E-06	205313
72-136-75-27-22	727920	60347000	∞	183150	1122700	7.7411E-06	129181
72-207-0-54-0	797120	66506000	∞	202040	1246000	7.0216E-06	142417
144-65-75-27-22	706760	58469000	∞	283120	1779700	5.5260E-06	180964
144-136-0-54-0	770080	64097000	∞	315240	1992700	4.9882E-06	200474
31-207-75-0-22	731750	60688000	∞	143190	863610	9.5247E-06	104990
72-65-150-27-22	657900	54138000	∞	164580	1002000	8.6125E-06	116110
72-136-75-54-0	708520	58625000	∞	178560	1092800	7.9439E-06	125883

144-65-75-54-0	687310	56743000	∞	275720	1730800	5.6772E-06	176143
31-136-150-0-22	657720	54122000	∞	128960	772080	1.0588E-05	94443
31-207-75-27-0	713420	59059000	∞	139830	841910	9.7579E-06	102481
72-65-150-54-0	638480	52420000	∞	159990	972190	8.8643E-06	112812
31-136-150-27-0	639280	52491000	∞	125570	750350	1.0880E-05	91914
72-207-0-54-11	692870	57236000	∞	175170	1070700	8.1035E-06	123404
144-136-0-54-11	670800	55280000	∞	270480	1696100	5.7956E-06	172546
72-136-75-54-11	620330	50816000	∞	155970	946120	9.1002E-06	109888
144-65-75-54-11	602970	49284000	∞	238380	1484400	6.5474E-06	152732
31-207-75-27-11	623070	51058000	∞	122680	731780	1.1142E-05	89748
144-207-0-0-0	684350	56480000	∞	279310	1754500	5.6292E-06	177646
72-65-150-54-11	562790	45745000	∞	140730	847740	1.0084E-05	99166
72-207-75-0-0	627650	51463000	∞	158640	963420	8.9542E-06	111679

By examining information from the *RUL* matrix, researchers and engineers can gain vital insights into the performance and durability of the landing gear strut under different mass value and distribution scenarios. This information is invaluable for assessing the safety and reliability of the light aircraft, as well as for informing maintenance and inspection personnel on estimated fatigue life considering experienced conditions. Some interesting observations on the *RUL* Matrix can be made even at first glance.

The flight phase of operation column has an infinite number of cycles to expected fatigue failure. This is due to several reasons. Fatigue simulation software usually require an “end of life” threshold, which simply stated is a cutoff number of cycles after which the program stops its iterative simulation process, in favour of reducing computational load. This cutoff number is simply a number of cycles that is big enough to conclude that the actual operation will not be compromised due to material fatigue accumulation within the intended usage life of the observed part. Additionally, the observed part is made out of a steel alloy which has a fatigue limit. The fatigue limit is the stress level below which the steel alloy can endure a theoretically infinite number of stress cycles without experiencing fatigue failure. This means that as long as the applied stress remains below the fatigue limit, the steel alloy will not undergo fatigue failure, regardless of the number of cycles it experiences. Since the stresses induced on the observed main landing gear strut are a sole consequence of the main landing gears own weight, it is reasonable to conclude that the stresses during the flight phase of operation are below the fatigue limit. Furthermore, the decreasing trend in the number of operations to failure generally decreases down the rows. This suggests that operations with higher mass and different mass distributions (while moving down the table) are associated with faster fatigue accumulation. As was stated in previous Chapters, the mass value and distribution scenarios are listed according to the sum of their masses. The highest sum of masses is at the bottom of the *RUL* Matrix table, however, contrary to expectation, the minimum number of operations to failure (highlighted in dark grey colour) is not displayed in the last row at the table bottom. This is because mass distribution plays a relevant role as well, as explained later in this Chapter. On the other hand,

the maximum number of operations which is positioned at the top of the *RUL* Matrix table has not only the lowest sum of masses, but the masses are also distributed towards the front of the airplane, away from the main landing gear strut, which is favourable for longer main landing gear strut fatigue life. The ΔD_i values vary across different operations. This suggests that different operations, characterized by their unique mass value and distribution, result in different levels of fatigue damage. Notably, this damage seems to increase (as the number of operations to failure decreases) for operations characterized by higher mass and certain mass distributions, suggesting these factors are correlated.

Additionally, maintenance related conclusions can be made. The impact of the results of this method on the observed light airplane operational safety can be deduced by comparing the maintenance approach and schedule of the observed Cessna 172R and maintenance suggestions resulting from performing the subject method. The maintenance intervals and required actions used to maintain the Cessna 172R callsign 9A-DAD are defined in the airplane's maintenance program [120]. The maintenance program states that the main landing gear struts must be inspected for cracks and corrosion every 100 hours of airplane operation and replaced on condition, meaning that the discovery of any crack or corrosion results in the replacement of that part regardless of the time interval that has passed since its first installation. The observed aircraft, the Cessna 172R callsign 9A-DAD, operated by the Croatian Aviation Training Centre, has its number of landings registered in the airplane's mass and balance sheets, the number is in approximately 20 000 landings at the moment of writing this Thesis. The observed airplane is used for commercial pilot training purposes, meaning the airplane is subject to a relatively broad spectrum of operations. To simplify calculation, it is assumed that one operation lasts for 1 hour. This would mean that the airplane would have 20 000 operation hours, including 200 inspections of the main landing gear struts. The landing gear struts of all of the Cessna 172's owned by the Faculty of Transport and Traffic Sciences did not show material fatigue signs in those 200 inspections.

Now the impact of various mass value and distribution scenarios on the *RUL* of the observed struts can be highlighted, according to the determined *RUL* matrix. If the airplane had been operated exclusively at the mass value and distribution scenario resulting in the minimum calculated fatigue damage increment (31-65-0-0-0) it would have been able to withstand 2333340 operations with such loading before strut fatigue failure, assuming no hard landing or other unpredictable occurrences happened. On the other hand, if the airplane had been operated exclusively at the mass value and distribution scenario resulting in the maximum calculated fatigue damage increment (31-207-75-27-11) it would have been able to endure 89748 of such

loading cycles before strut fatigue failure, which is approximately a 26 times shorter fatigue failure interval.

6.1 Visual representation of *RUL*, deformation, strain, and stress of minimum and maximum fatigue life scenarios

A visual representation of mass value and distribution scenario and measured acceleration effects is presented in this Chapter. It shows the impact of strut loads on the fatigue life of the observed light aircraft's main landing gear strut. This is in relation to the corresponding phase of operation. The focus was on particular scenarios that were found intriguing based on their number of operations to failure. These were scenarios where mass value and distribution lead to the highest and lowest number of operations before the calculated fatigue failure was imminent. Fatigue life scenarios, deformation, strain, and stress results were observed. Since fatigue analysis was performed based on a time-variable load, the deformations, stresses, and strains had to be calculated by applying static structural numerical strength analysis. It was decided to do so by applying average load values for the observed operation values.

Fatigue life analysis results were first observed for the scenario with the greatest calculated number of operations before fatigue failure, namely mass value and distribution scenario 31-65-0-0-0. This scenario resulted in the biggest S*RUL* during the take-off phase of operation, because of its loads which were the smallest from all observed operation phases. However, it was decided to visually present the taxi-in phase of operation because of it having a more pronounced visual profile, due to higher applied loads that enabled a clearer distinction of markers which provide better insight into the physical and engineering validity of the results. Figure 80 shows the distribution of remaining useful life, having a minimum in the expected location of the observed geometry. Program-controlled element order, and adaptive element sizing (explained in Chapter 5.3.1.9), with a maximum element size of 1.4e-2 m, have culminated in an acceptable remaining useful life regarding prediction expectancy, based on airplane load cycle records (recorded number of airplane landings in the airplanes technical logbook).

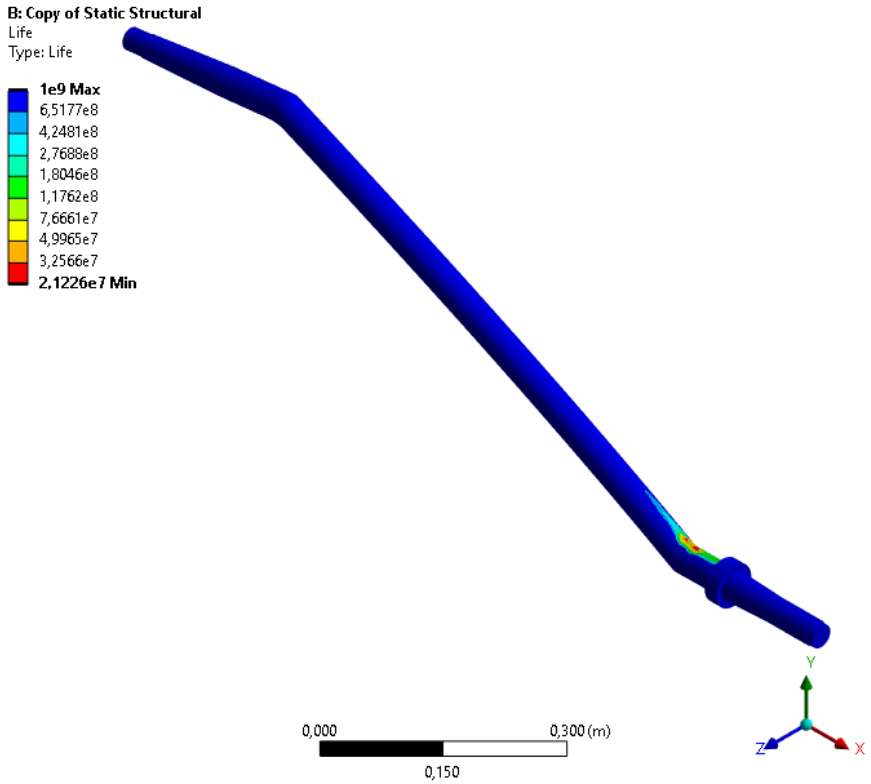

Figure 80. Remaining useful life distribution, for loading resulting from mass value and distribution31-65-0-0-0, and load direction corresponding to taxi-in phase of operation.

Part deformation was observed next, as shown in Figure 81. Total deformation, in the context of this analysis, refers to the maximum displacement a point on a structure experiences due to applied loads. In general, it combines both the translational and rotational displacement into a single scalar quantity, representing the magnitude of displacement in the structure. The observed deformation was within the expected boundaries based on engineering judgment, the strut's part fixed to the airplane's fuselage experienced the largest deformation, as expected.

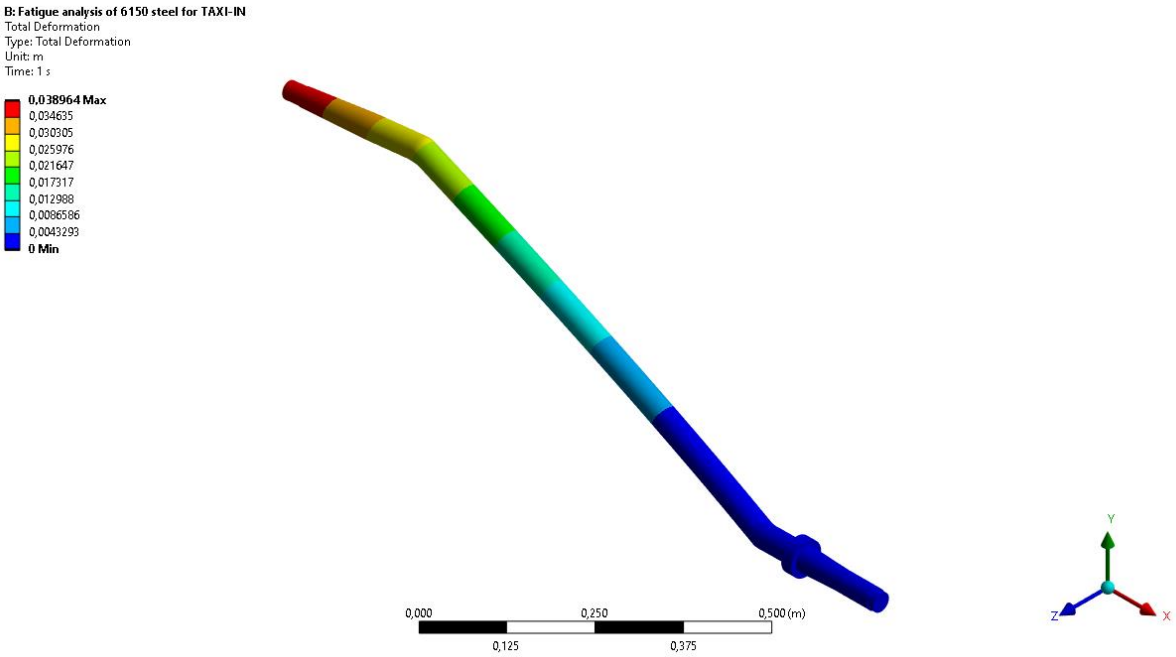

Figure 81. Total deformation, for loading resulting from mass value and distribution31-65-0-0-0 and load corresponding to the taxi-in phase of operation.

The equivalent elastic strain in the subject component was observed next, displayed in Figure 82. Equivalent elastic strain represents a measure of the change in size or shape of an object under applied loads. In an elastic deformation scenario, this strain represents the total amount of deformation, which the material can recover once the load is removed. The strain analysis results were within expected boundaries and position on the observed model.

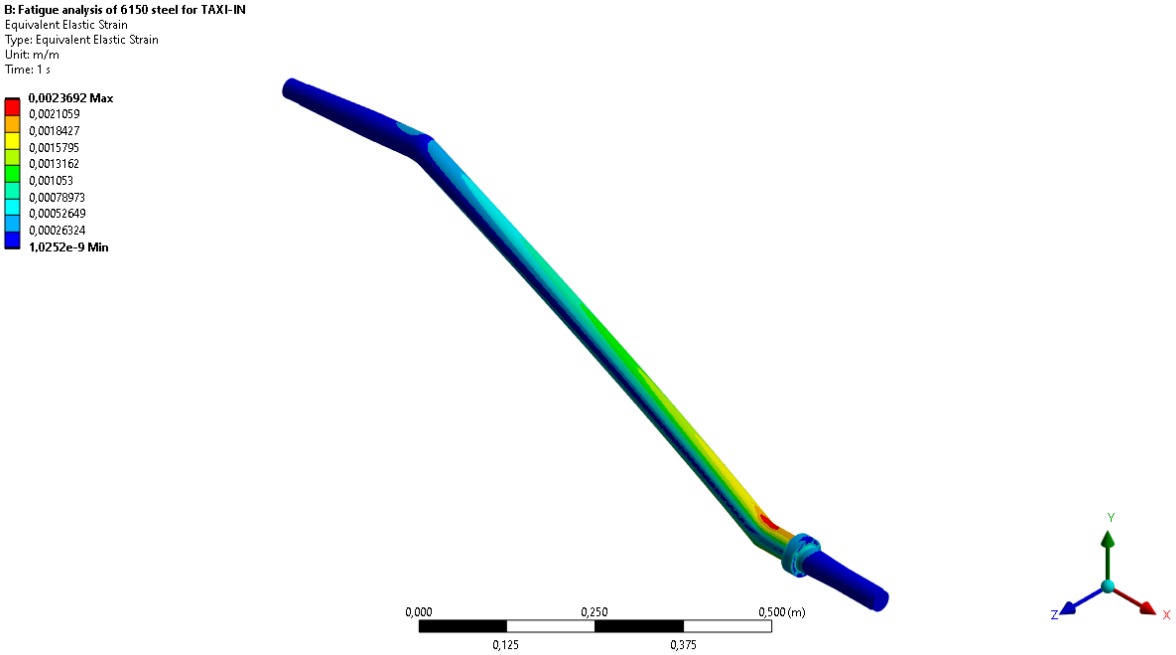

Figure 82. Equivalent elastic strain, for loading resulting from mass value and distribution 31-65-0-0-0, and load corresponding to the taxi-in phase of operation.

Finally, the equivalent von Mises stress was observed, displayed in Figure 83. The equivalent von Mises stress, often simply referred to as the von Mises stress, is a fundamental concept in engineering and materials science. It's a scalar value computed from the three-dimensional stress state within a material to predict yield failure. This stress criterion assumes that failure occurs when the energy of distortion reaches a critical level, irrespective of the individual normal and shear stresses. The results from the von Mises stress analysis were within the expected and acceptable boundaries based on the comparison of the materials yield stress and the calculated maximum stress value.

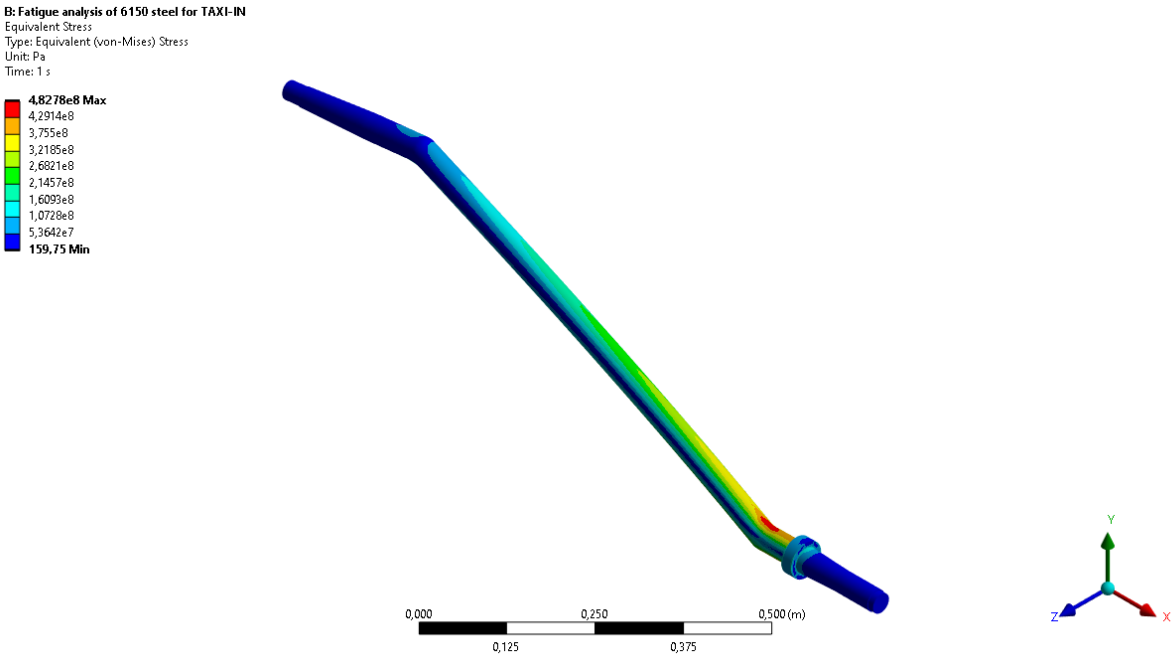

Figure 83. Equivalent von Mises stress, for loading resulting from mass value and distribution31-65-0-0-0, and load corresponding to the taxi-in phase of operation.

The second observed operation phase corresponds to the mass value and distribution scenario 31-207-75-27-11 which resulted in the lowest number of operations until fatigue failure, corresponding to the landing phase of operation. The results showed that the strut could perform only 1.227E+05 landings until fatigue failure. As stated in Chapter 6, the particular airplane this method was applied on, had at the moment of writing this Thesis, little over 20000 registered landing cycles with the same main landing gear strut. Subsequently, had the airplane been operated with the subject mass value and distribution scenario in all of those operations, the main landing gear strut would have been able to perform 1.227E+05 landings before the occurrence of fatigue failure.

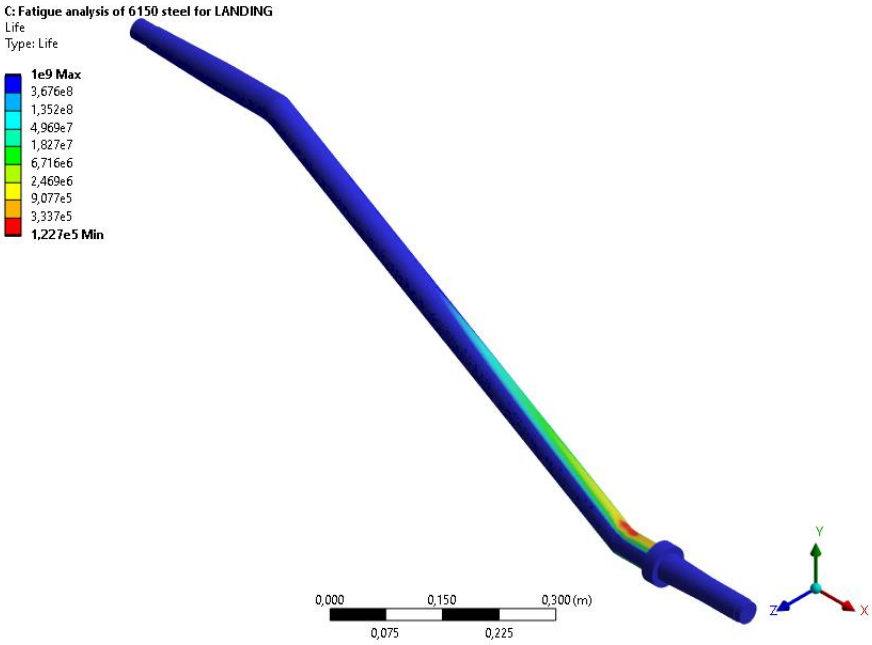

Figure 84. Remaining useful life distribution, for loading resulting from mass value and distribution 31-207-75-27-11, and load corresponding to the landing phase of operation.

The total deformation for the landing phase of operation and mass value and distribution scenario 31-207-75-27-11 is shown in Figure 85. The observed deformation was within expectation, the strut's part fixed to the airplane's fuselage experienced the largest deformation, while the struts wheel bearing attachment had the smallest deformation.

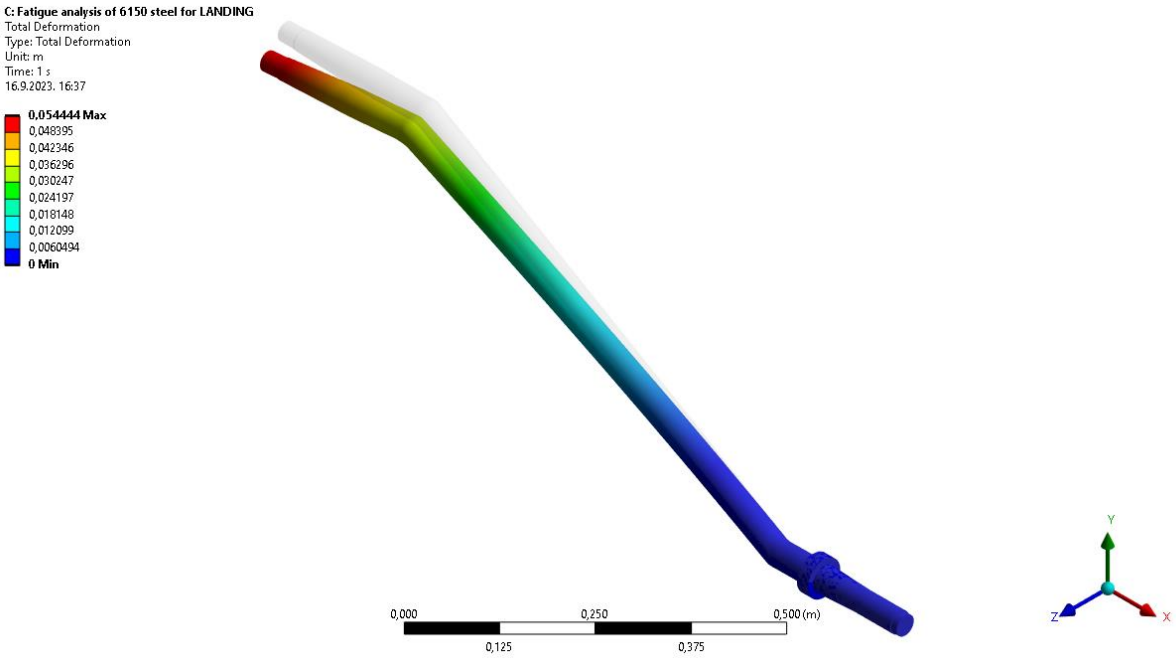

Figure 85. Total deformation distribution, for loading resulting from mass distribution 31-207-75-27-11, and load corresponding to the landing phase of operation.

Equivalent elastic strain and stress were observed lastly, conforming with the expected order of magnitude of their respective strain and stress values.

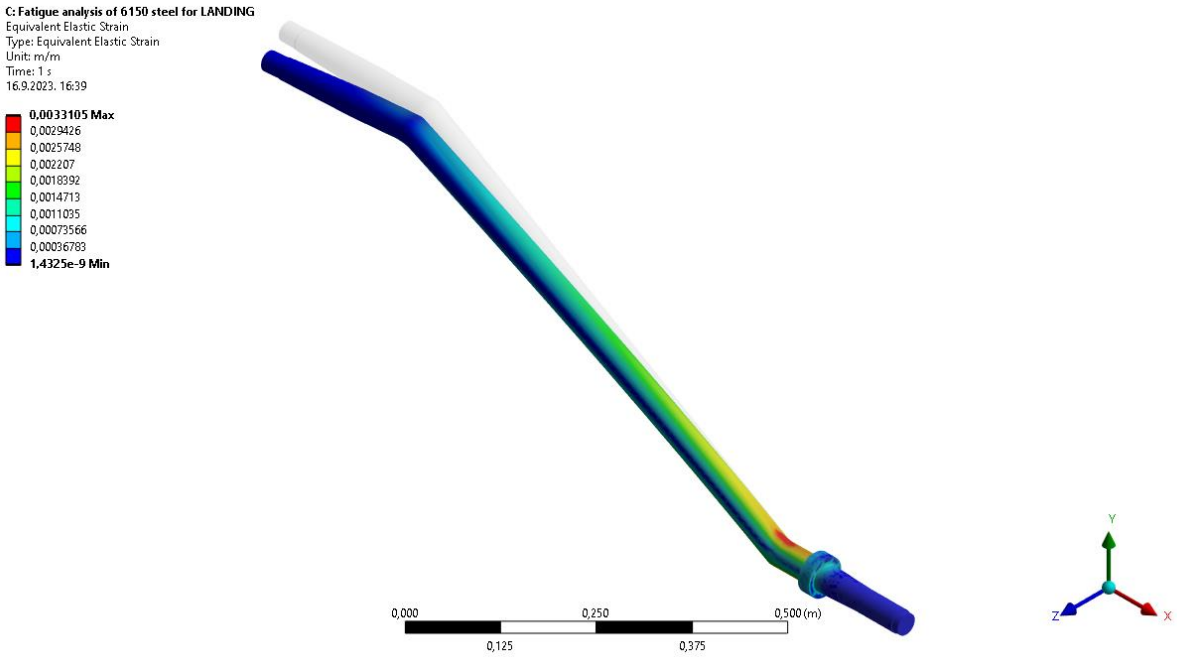

Figure 86. Equivalent elastic strain distribution, for loading resulting from mass value and distribution 32-207-75-27-11, and load corresponding to the landing phase of operation.

The results from the von Mises stress analysis were within the expected and acceptable boundaries based on the comparison of the materials yield stress and the calculated maximum stress value.

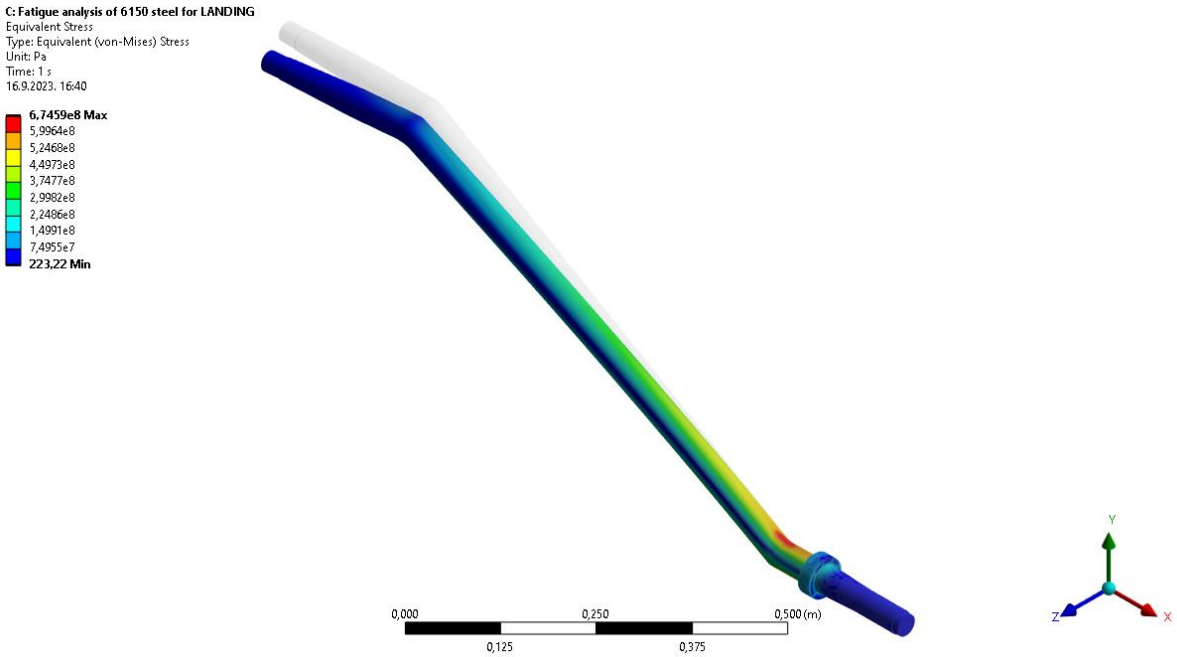

Figure 87. Equivalent von Mises stress distribution, for loading resulting from mass value and distribution 31-207-75-27-11, and load corresponding to the landing phase of operation.

6.2 Result comparison

Based on the findings presented in Chapter 2.6, the minimum and maximum number of cycles to failure of various aircraft landing gears determined in the respective research were extracted and are presented in Table 20. The purpose of this exploration is to bolster confidence in the validity of the results of this research, specifically considering their order of magnitude.

Table 20. Research paper findings from Chapter 2.6.

Research reference and title	**Cycles to Failure (Min - Max)**
[22] Predicting the Remaining Useful Life of Landing Gear with Prognostics and Health Management (PHM)	221 - 294
[24] Certification of machine learning algorithms for safe-life assessment of landing gear	10,000 - 50,000
[26] Linear static and fatigue analysis of nose landing gear for trainer aircraft	10,620 - 1,130,500
[27] Fatigue analysis of light aircraft landing gear	192,600 - 1,000,000,000
[28] Stress Analysis Of The Landing Gear-Well Beams And Damage Calculation Due To Landing Cycles	50 - 57,000
[29] Fatigue analysis of lug joint in the main landing gear	18,000,000
[30] Design of a motor glider landing gear strut–The role of failure analysis in structural integrity	8801 - 21115
[31] Failure analysis of a landing gear nose wheel fork produced in Ti6Al4V (ELI) through selective laser melting	15,000 - 101,609
[34] An analysis of the damage tolerance of light aircraft landing gear	48,000 - 744000

Before comparing the cycle numbers until failure, several comparison-limiting facts have to be considered regarding the methodology developed through the research described in this Thesis. The papers in 2.6 observe various airplane types. Subsequently, various aircraft landing gear systems, their geometry and materials, are considered. The load cases observed by the reviewed research are also different, depending primarily on the observed aircraft type. Not all reviewed research determines the landing gears remaining useful life by performing numerical strength analysis and/or considering material fatigue. Various prognostic methods were applied, which diversifies the capacity for result comparison.

While having in mind the stated differences, a box plot was created (Figure 88) displaying the minimum and maximum numbers of cycles until failure for selected research reviewed in Chapter 2.6, and results from the research described in this Thesis.

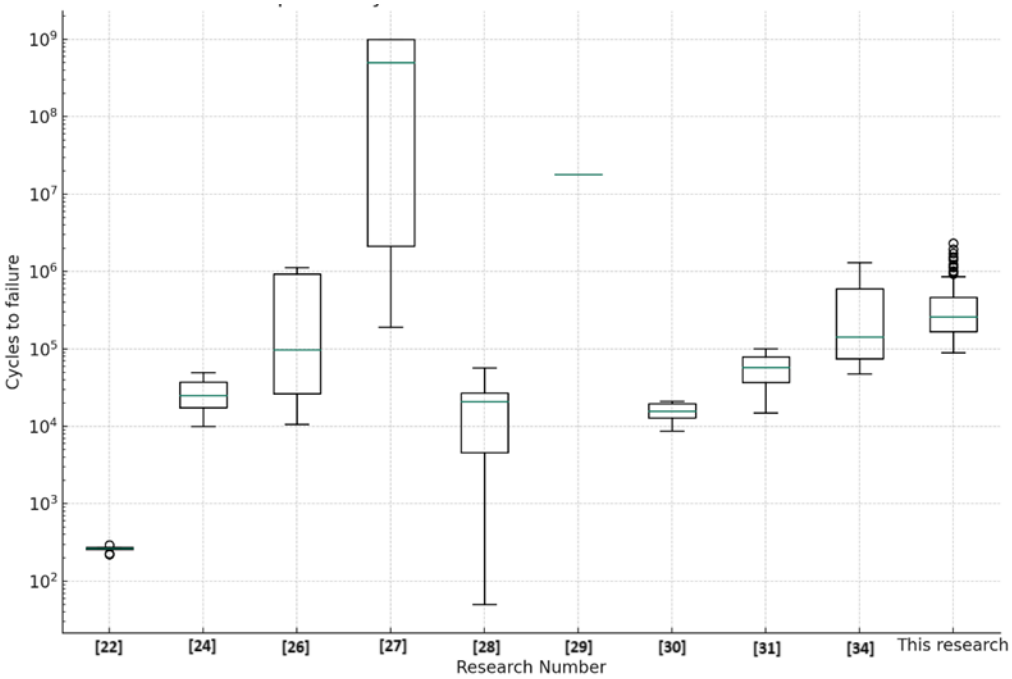

Figure 88. Research result comparison.

The box plot characteristics and their meaning for result comparison are as follows.

X-Axis (Research Number):

- Represents different research reference numbers from Chapter 2.6, with each distinct reference having its own box plot.
- The box plot labelled as "This research" is the data generated by the research described in this Thesis.

Y-Axis (Cycles to Failure):

- Represents the range of "Cycles to Failure" for each research title in a logarithmic scale (due to the wide range of values).

Box Plot Elements:

- **Box**: The main body of the box plot, representing the interquartile range (IQR). The bottom and top of the box signify the 25th (Q1) and 75th (Q3) percentiles, respectively. The range between Q1 and Q3 contains the central 50% of the values.
- **Horizontal Line Inside the Box (Median)**: Represents the median value (50th percentile) of the "Cycles to Failure" for each research title. It gives an idea of the central tendency of the data.

- **Whiskers**: Extend from the box to show the range of the data defined by its minimum and maximum value.

In summary, the findings of this Thesis align with results from other studies. The observation of different aircraft landing gear systems and the application of various methods enhance confidence in these findings. Although direct result validation by comparing actual cycle numbers to failure is not possible, because such data is missing, the comparison detailed in this Chapter is the closest approach to validation the author could do, proving that the calculated minimum and maximum number of cycles until fatigue failure falls within boundaries that can be expected based on results from other research methods including actual tests.

6.3 Result analysis through statistic methods

Descriptive statistical analysis was performed on the damage increments. The purpose of it was to gain an overlook of basic statistical characteristics of the calculated data, as displayed in Table 21.

Table 21. Descriptive statistics analysis of RUL matrix *damage increment data.*

	ΔD_i
Mean	4.29365E-06
Standard Error	2.23444E-07
Median	3.86392E-06
Standard Deviation	2.65325E-06
Sample Variance	7.03974E-12
Kurtosis	-0.461581816
Skewness	0.60857495
Range	1.07138E-05
Minimum	4.2857E-07
Maximum	1.11424E-05
Count	141
Confidence Level(95.0%)	4.41761E-07

The information displayed in Table 21. was first analysed by neglecting engineering experience, based solely on the understanding of basic statistical analysis, thus eliminating engineering bias and improving the likelihood of gaining additional insights:

- Mean: The average incremental damage per flight is approximately 4.29365E-06. This is the central value around which the individual damage increments are distributed.

- Standard Error: The standard error of 2.23444E-07 is a measure of the statistical accuracy of the mean. It indicates the extent to which the mean damage increment might vary if the measurement were repeated multiple times.
- Median: The median incremental fatigue damage per flight is 3.86392E-06. This is the middle value when all damage increments are sorted in order. Since the mean and median are close, it suggests that the data is likely symmetrically distributed.
- Standard Deviation: The standard deviation of 2.65325E-06 measures the dispersion or variability in the damage increments. A higher standard deviation would indicate a wider range of values.
- Sample Variance: The sample variance of 7.03974E-12 is another measure of dispersion in the damage increments. It is the square of the standard deviation.
- Kurtosis: The kurtosis value of -0.461581816 indicates that the distribution of damage increments has lighter tails and a flatter peak than the normal distribution. This means there are fewer extreme values than would be expected in a normal distribution.
- Skewness: The skewness value of 0.60857495 suggests that the distribution of damage increments is slightly skewed to the right, meaning there are a few flights with particularly high damage increments, when compared to mean values.
- Range: The range of 1.07138E-05 indicates the difference between the maximum and minimum damage increments.
- Minimum and Maximum: The smallest damage increment is 4.2857E-07 and the largest is 1.11424E-05. These values represent the extremes of incremental wear and tear experienced by the aircraft.
- Confidence Level (95.0 %): The 95 % confidence interval for the mean damage increment extends 4.41761E-07 on either side of the mean. This means it can be concluded with 95 % confidence that the true average damage increment lies within this range.

Next, by considering the descriptive statistics analysis results through aeronautical engineering comprehension, the following observations were made: The damage increment means, and median values could be misinterpreted as the most likely damage increments due to operation with their respective mass value and distribution scenarios. However, the actual mass value and distribution scenario depends on the kind of operations performed by the subject aircraft. Those operations can include recreational, taxi, panoramic and/or schooling flights for

future licensed pilots (or other). Given the range of operations the subject airplane is used for, information on the mean and median damage increments cannot be considered as the most likely. Statistical analysis of operations performed by the exact observed airplane is therefore needed. Since the focus of this Thesis is on method development, the aspect of operation likelihood through statistical analysis was not considered.

The standard deviation statistic relates to the range in which the damage increments are dispersed for the observed mass value and distribution scenarios. Assessing the standard deviation order of magnitude requires insight of expected values which is not accessible without additional research through either numerical strength analysis or actual recorded data. In general, if the standard deviation is a small fraction of the mean, the data can be considered relatively consistent. If the standard deviation is a large fraction of the mean, the data is considered highly variable. The observed case equates to a ratio of standard deviation vs mean value of 0.6179 which can be considered a relatively large fraction, coinciding with expectation due to relatively high variability of observed scenarios of mass and mass distribution.

The calculated skewness statistic indicates the possibility that a few operations have pronounced fatigue damage accumulation, which was expected because the observed mass value and distribution scenarios closer to the *RUL* matrix bottom are simultaneously closer to the airplane's permitted mass value and distribution limit, according to operational restrictions.

Furthermore, understanding the data presented in appendix Table 20. implies the understanding of general physical principles governing material fatigue life. For example, two of the same material samples, having the same geometry, should experience lessened fatigue lives when subject to the same load orientation and direction, but increasing intensity. This can clearly be seen by observing various mass value and distribution scenarios and their corresponding damage increments, as displayed in Figure 89. It should be pointed out, as stated earlier, that the mass value and distribution scenarios listed in the *RUL* matrix (Table 20) are sorted according to the increase in aircraft total mass. The methodology of this research focuses on one single airplane without significant mass changes other than the masses loaded in the five mass stations.

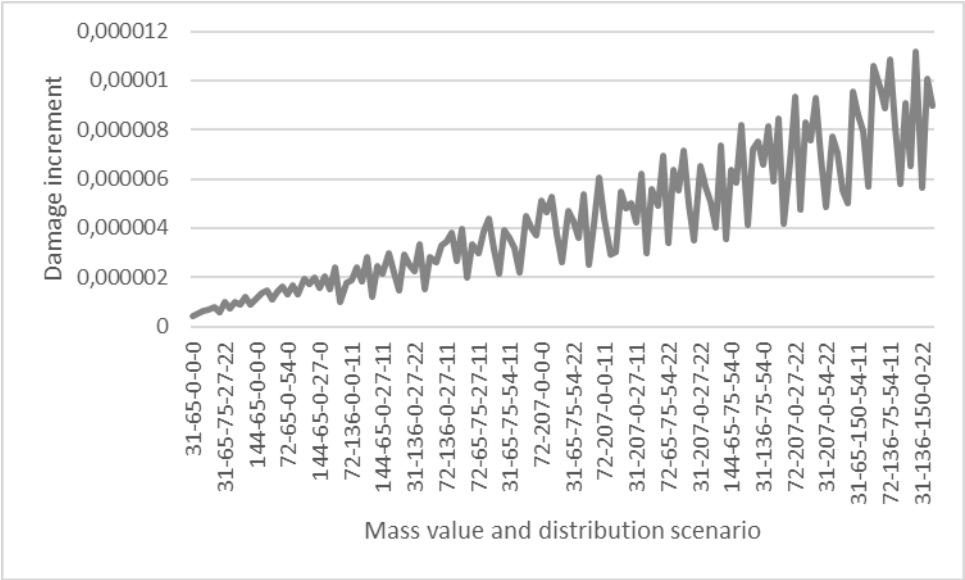

Figure 89. Damage increment variation according to mass value and distribution scenarios, sorted by increasing total mass.

Figure 89 illustrates that as the total mass of the aircraft increases, there is a corresponding rise in damage increments. However, the data also shows periodic fluctuations or oscillations. These oscillations could lead to misinterpretations if one exclusively considers the increase in total aircraft mass as the primary factor affecting damage. A more accurate approach would be to concentrate on the mass that is directly relevant to the mechanical integrity of the specific component under examination, in this case, the main landing gear strut. This relevant mass is influenced by the position of the aircraft's centre of gravity, which in turn is determined by the distribution of mass throughout the aircraft. The mass value and distribution scenarios, as explained in Chapter 5.2.1.1, consist of five values corresponding to airplane mass stations arranged from nose to tail. Since the main landing gear struts are positioned towards the tail of the airplane, an increase of mass in the last three numbers of the mass value and distribution scenario code should have a greater impact on the struts remaining useful life, compared to the masses recorded in the first two numbers (*U.FUEL* and *FPAX*). The relation of the calculated damage increment and an increase in the sum of masses in the mass stations towards the tail of the airplane (*RPAX*, *BGA1* and *BGA2*) is displayed in Figure 90.

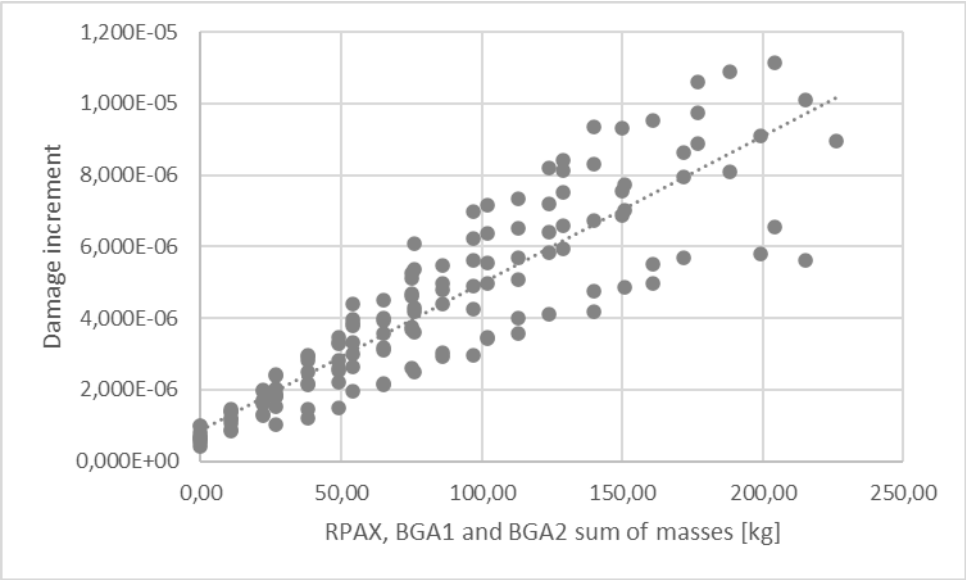

Figure 90. Relation of aircraft rear mass and strut fatigue damage increment.

Figure 90 clearly displays an overall increase of the fatigue damage increment of the light aircraft main landing gear strut as the mass in the rear aircraft mass stations increases. The sum of *RPAX*, *BGA1* and *BGA2* masses increases from 0 to 139, and the relation trend has a positive gradient. The relation trend corresponds to a damage increment range from 5.130E-07 to 1.114E-05. The oscillations of the damage increment with increasing mass in the rear stations is a consequence of main landing gear strut mass variability due to mass distribution. The Pearson correlation coefficient of 0.8898 between the damage increment and rear mass (sum of RPAX, BGA1 and BGA2 masses) is a substantial value that falls within the range of −1 to 1. This coefficient provides insights into both the strength and direction of the relationship between the two variables in question. The value 0.8898 is close to 1, indicating a strong positive linear relationship between the variables. Since the coefficient is positive, it implies that as the mass in the rear of the aircraft increases, the damage increment due to material fatigue also tends to increase. Given the high correlation value, this relationship is likely to be strong.

Figure 91 represents the relation of aircraft front mass increase and strut fatigue damage increment. The aircraft front mass was calculated as the sum of the mass of the usable fuel (U.FUEL) and the mass on the aircrafts front seats (FPAX). Since the U.FEUL masses observed in this research are 31, 72 and 144 kilograms, and the FPAX masses are 65, 136 and 207 kilograms, a simple conclusion can be made that nine mass combinations result in nine different mass sums. Therefore, Figure 91 should clearly display 9 damage increments with the same mass. However, Figure 91 displays just 7 damage increments. This can be explained by calculating the 9 mass front masses, which are 96, 167, 238, 137, 208, 279, 209, 280, and 351

kilograms. At this point it becomes obvious that Figure 91 actually does display 9 damage increments with the same mass, some of these masses are very closely spaced in terms of their mass value, making them less noticeable and seemingly 'invisible'. Figure 90 has 27 possible mass combinations in the rear of the aircraft for the same reason.

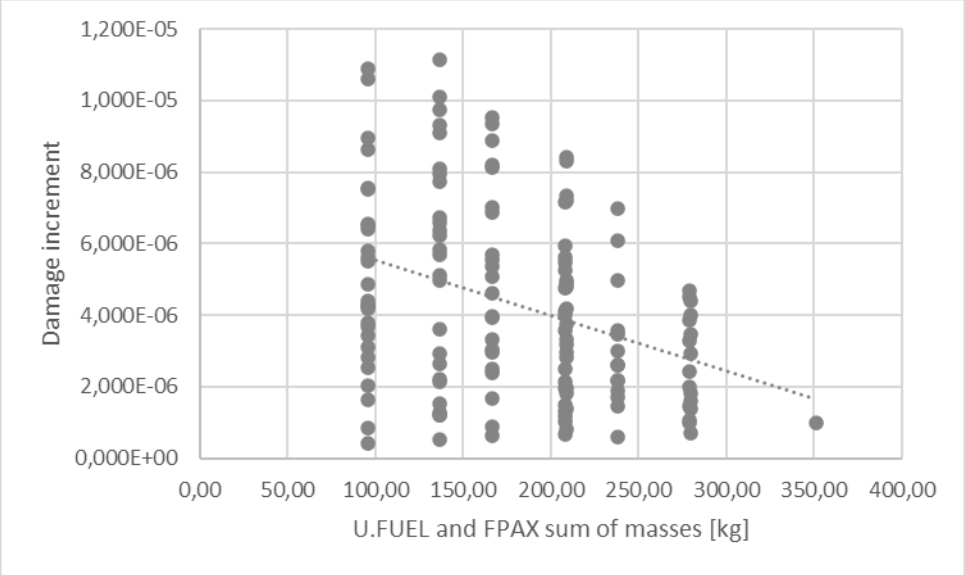

Figure 91. Relation of aircraft front mass increase and strut fatigue damage increment.

Figure 91 displays an overall decrease of the fatigue damage increment of the light aircraft main landing gear strut as the mass in the front aircraft mass stations increases. The relation trend has a negative gradient. The Pearson correlation coefficient of −0.3539 between the damage increment and the mass in the front of the aircraft (sum of U.FUEL and FPAX masses) offers valuable information regarding the strength and direction of the linear relationship between these two continuous variables. The absolute value of the coefficient, |−0.353922255|, indicates a low to moderate negative linear relationship between the variables. The negative sign signifies that as the mass in the front of the aircraft increases, the damage increment tends to decrease, or vice versa. It is crucial to remember that correlation does not imply causation. While there's a negative correlation, this doesn't mean that increasing front mass will cause a decrease in damage increment, although there is an association. From an aeronautical engineering perspective, the negative correlation of −0.3539 could be of interest, albeit not as compelling as a strong correlation. This relationship suggests that different front mass distributions in the Cessna 172R might have a moderate influence on the rate of fatigue damage increment in the main landing gear strut.

In conclusion, Figure 90 and Figure 91 display the impact of mass distribution on the light aircraft main landing gear strut. The damage increment, and therefore accumulated fatigue

damage, has a positive correlation with the masses in the aircraft's rear seats and baggage stations 1 and 2, and a negative correlation between the damage increment and front station masses (*U.FUEL* and *FPAX*). As the trend lines for both relations are indicative of the correlation between the observed variables, a higher significance of the masses in the rear mass stations, compared to the front mass stations on the damage increment can be observed. An increase in aircraft total mass also shows a positive correlation with the damage increment and therefore fatigue damage accumulation. The resulting remaining useful lives should therefore decrease with an increase in aircraft total mass, whereas the masses in the rear mass stations have a significantly higher impact on *RUL* than the front stations, as was expected. Correlation analysis between the calculated damage increments and the airplane's total mass confirmed those observations with a correlation result of 0.4517.

In this Chapter, the influence of mass value and distribution on the remaining useful life of light aircraft landing gear struts was investigated based on the information recorded in the *RUL* matrix. To assess the impact of mass value and distribution variation on light aircraft maintenance and operational safety, sensitivity analysis was performed. Sensitivity analysis is a critical part in the process of modelling relationships between variables. It allows a better understanding of the influence, importance, and uncertainty of different variables and parameters within the created relationship model. Essentially, sensitivity analysis helps to understand the uncertainty inherently included in model results, [153].

There are several statistical methods employed in sensitivity analysis:

1. Local Methods

These methods analyse the change in the model's outcome resulting from small changes in the input parameters. The methods are based on studying one factor at a time.

Derivative-based Local Sensitivity Measures: These measures assess how sensitive a model output is to changes in the values of its parameters. The derivative-based local sensitivity measure is calculated as the partial derivative of the model function with respect to the parameter of interest (Doggett [154], Kurochenko [155]).

One-factor-at-a-time: This is the simplest method of sensitivity analysis. It involves changing one input at a time while keeping others constant to see the effect on the output (Frey et al. [156], Razavi et al. [157], Daniel [158], Czitrom [159]).

2. Global Methods

These methods consider all variables and their interactions at the same time. The methods are based on generating many model outputs by randomly varying all the input factors over their range of variation.

Variance-based Sensitivity Analysis (Sobol Method): This method decomposes the variance of the output of the model into fractions which can be attributed to inputs or sets of inputs. This provides a measure of the relative importance of each input in terms of its contribution to the model output's variance (Saltelli et al. [160], Hekimoğlu et al. [161]).

Monte Carlo Filtering: This method allows us to measure the effect of input factors on parts of the output distribution rather than on its variance (Doggett [154], Kuruchenko et al. [155]).

Elementary Effects (Morris Method): This method measures the effect of small changes in the input parameters on the model output, much like OAT methods, but it does so for multiple parameters at once, providing a more global analysis (Shi et al. [162]).

3. Regression Analysis

This method fits a regression model to the inputs and outputs, and then uses the coefficients of the fitted model as measures of sensitivity (Brown [163], Carlberg [164], Orlov [165], Hu et al. [166]).

Partial Rank Correlation Coefficients (PRCC): PRCCs are used in sensitivity analysis to measure the strength of the relationship between a model parameter and model output.

4. Factorial Analysis

This method involves a systematic combination of changes in all parameters to understand their impact on the output (Holzinger et al. [167], Yong et al. [168].

Fractional Factorial Analysis: This is a method that allows for the analysis of the effect of many factors on a response variable, without requiring the full factorial experimental design (Box et al. [169]).

5. Meta-Modelling

Meta-modelling, also known as surrogate modelling, involves the creation of an approximate model (the surrogate) based on the outputs of the actual model (van de Weerd et al. [170]).

Polynomial Chaos Expansion (PCE): This method uses a series of orthogonal polynomials to construct a surrogate model (Crestaux et al. [171]).

In conclusion, different statistical methods offer different insights and can be used to address different questions. The choice of method depends on the nature of the model and the specific questions being asked.

Regression analysis could be considered a better method for sensitivity analysis than Local Methods, Global Methods, Factorial Analysis, and Meta-Modelling in the specific context of analysing fatigue damage accumulation in relation to loads acting on a light aircraft main

landing gear strut, particularly when considering factors like mass and mass distribution, as well as measured acceleration along the three aircraft axes. The reasons for this are as follows:

- Quantification of Relationships: Regression analysis allows for the quantification of relationships between variables. In the case observed in this research, it can provide numerical measures of how changes in mass value and distribution and acceleration along the three aircraft axes affect fatigue damage accumulation. This is essential in understanding and predicting the effects these factors have on the main landing gear strut.
- Interaction Effects: Regression analysis allows the assessment of interaction between variables, something that many other sensitivity analysis methods do not directly provide. For instance, it could help in the understanding of how the interaction between mass distribution and acceleration along a particular axis influences fatigue damage.
- Efficiency: Regression analysis can efficiently handle multiple input variables at once. This is especially useful in the observed case, where multiple factors are observed, namely mass and mass distribution.
- Correlation Analysis: Regression analysis is usually performed by first applying correlation analysis, which can provide insights into the strength and direction of the relationship between the variables. This can assist in identifying which factors have the strongest association with fatigue damage accumulation.
- Ease of Implementation in Microsoft Excel: Excel has built-in functions for conducting regression and correlation analyses [172], which makes it a convenient tool for this task. This also made the analysis more accessible to the author of this research since his experience in statistic sensitivity analysis methods is limited.
- Predictive Power: Regression models can provide a mathematical formula that can be used to predict future outcomes. This can be particularly useful for predicting fatigue damage accumulation under different scenarios of mass value and distribution and acceleration, which is a probable direction of future research based on the findings described in this Thesis.

While regression analysis has these advantages, it's important to keep in mind that it assumes a specific functional form (linear, unless otherwise specified) for the relationship between variables, and it requires that certain conditions are met regarding the distribution and independence of the residuals.

Having in mind the stated reasoning, it was concluded that correlation analysis was performed on several light aircraft landing gear strut remaining useful lives estimated using the established linear relationship. The expected outcome of this approach is an enhanced understanding of the influence of mass value and distribution variation on the safety and maintenance requirements of light aircraft landing gear systems.

Next, linear regression analysis was performed on the *RUL* matrix data. The dependent variable in the analysis is the calculated accumulated fatigue damage, while the independent variables are the various masses in the mass value and distribution codes.

By undertaking sensitivity analysis in the described manner, the findings are anticipated to contribute to the comprehension of the complex relationships between mass, mass distribution, and the *RUL* of light aircraft landing gear structures, specifically the landing gear strut.

6.3.1 Correlation analysis

The performed correlation analysis results, displayed in Table 22., deviated from initial expectations in the *U.FUEL* and *FPAX* correlation coefficient. The *U.FUEL* numbers in the *RUL* matrix (Table 20.) represent the fuel mass stationed in the airplane's fuel tanks, as stated earlier. Initially it was expected that all the correlation coefficients would be positive, based on a false hypothesis that an increase in mass has a significantly higher impact on the calculated damage increment compared with the impact of mass distribution. However, the findings of this research revealed that the mass distribution significance on the damage increment should not be underestimated.

The correlation analysis results in Table 22. show the correlation coefficients between different variables and the damage increment (ΔD_i). The variables include *U.FUEL*, *FPAX*, *RPAX*, *BGA1*, *BGA2*, and *Tot_mass*, explained in previous Chapters. The correlation coefficient measures the strength and direction of a linear relationship between two variables. It ranges from -1 to 1, where -1 indicates a perfect negative correlation, 1 indicates a perfect positive correlation, and 0 indicates no correlation. In the context of this analysis, a positive correlation coefficient, for example, means that if *RUL* of any calculated flight phase increases, so the damage increment. Conversely, a negative correlation coefficient means that if any flight phase *RUL* increases, the damage increment decreases, as is the case with *U.FUEL* and *FPAX*.

Table 22. Correlation analysis results.

	U.FUEL	***FPAX***	***RPAX***	***BGA1***	***BGA2***	***Tot_mass***
ΔD_i	-0.13664	-0.29685	0.82326	0.28673	0.03957	0.4517

By observing the correlation coefficients presented in Table 22., the following conclusions were made:

U.FUEL: As mentioned before, this variable represents the fuel mass stationed in the airplane's fuel tanks. The correlation coefficient of -0.13664 indicates a weak negative correlation with the damage increment. This is contrary to initial expectations. It was initially assumed that all correlation coefficients would be positive, given the assumption that an increase in mass would have a significantly higher impact on the calculated damage increment compared to the impact of mass distribution. However, by increasing the mass in the airplane's front mass stations, such as the *U.FUEL*, a decrease of fatigue damage accumulation in the landing gear strut was determined. This is a probable consequence of the centre of gravity arm, which shortens by increasing the mass in the airplane *U.FUEL* mass station. A shorter centre of gravity arm results in a smaller momentum acting around the centre of gravity and decreasing the load on the main landing gear strut. However, another fact should also be considered as the reason for this negative correlation. Namely, since the total mass value and distribution are limited, it is reasonable to conclude that an increase in mass in the *U.FUEL* mass station leads to a lower mass value that can be distributed on the remaining mass stations. Consequently, the mass value in mass stations with a significantly higher impact on the observed main landing gear strut are left with less distributable mass. Hence, the calculated correlation coefficient shows that a larger fuel mass can be associated with a slight decrease in the damage increment for the mass value and distribution scenarios observed in this research based on the stated reasoning. Of course, this observation highly depends on the position of the observed mass station, being different for different aircraft.

FPAX: The impact of the mass stationed in the aircrafts front seat on the main landing gear strut damage increment is similar to the *U.FUEL* and ΔD_i observation. The same reasoning and conclusions are valid, having in mind the main difference being that the correlation coefficient is nearly two times greater, Table 22. The expected impact of mass increase in this mass station on the main landing gear strut damage increment is therefore significantly higher than in the previous case.

RPAX: Correlation analysis revealed the impact of the mass in the rear aircraft seat on the main landing gear strut, it is the highest of all the mass stations. This is congruent with expectation, since the rear seat is positioned directly above the observed landing gear structural part, having therefore the biggest impact on the calculated mass relevant to the observed strut. In other words, a variation in mass of the *RPAX* mass station has the most significant impact on the calculated mass relevant to the observed strut, as can be concluded from the strut relevant mass calculation procedure in Chapter 5.2.1.1.

BGA1* and *BGA2: These variables represent baggage mass stations in the airplane. The correlation coefficients are 0.28673 and 0.03957 respectively, indicating weak positive correlations with the damage increment. The *BGA1* correlation coefficient is significantly higher than the correlation coefficient for *BGA2*, this can be explained by observing the positional relation of the baggage areas compared to the position of the observed main landing gear strut. The *BGA1* mass station is in closer proximity to the observed landing gear strut, compared to *BGA2*, both being behind the strut along the longitudinal airplane axis. This observation can lead to the conclusion that the longitudinal distance between the observed landing gear strut and the observed mass station is a significant fatigue damage accumulation predictor, which is congruent with expectation prior to analysis based on engineering judgment. Also, the order of magnitude of the correlation coefficients being a consequence of the masses loaded in *BGA1* and *BGA2* suggests that increases in those variables leads to minor increases in the damage increment, which is due to the mass restrictions on *BGA1* and *BGA2* given by the manufacturer and considered in this research.

Tot_mass: This variable represents the total mass of the airplane. The correlation coefficient is 0.4517, indicating a positive correlation with the damage increment. This suggests that as the total mass of the airplane increases, the damage increment increases, although with lesser impact compared to mass station *RPAX*.

In conclusion, the results of the correlation analysis suggest that both mass value and distribution have significant impacts on the damage increment. Additionally, the position of the observed mass station has a significant role in fatigue damage accumulation, depending on the distance from the observed landing gear structural part. The unexpected negative correlation coefficient for U.FUEL and FPAX underscores the importance of considering all these factors in aeronautical engineering analyses. Be it because of the centre of gravity arm or the simple fact that an increase in mass in those mass stations leaves less mass for mass stations with more impact on the observed main landing gear strut *RUL*. This illustrates that simplistic assumptions about the relationships between variables can be misleading, highlighting the need for a nuanced understanding of these relationships. Additionally, it can be concluded that the total variable airplane mass consisting of the masses in the five mass stations has the second highest impact on the calculated damage increment, after RPAX which is positioned directly above the observed strut. However, the division of the significance of masses in the mass stations on the damage increment from highest to lowest holds a greater informative value. This is because literature research did not result in research findings dealing with the relation between light

aircraft landing gear structure remaining useful life and relevant loads partially but also significantly resulting from the masses in the five mass stations.

A correlation matrix heatmap with displayed correlation coefficients was created, Figure 92.

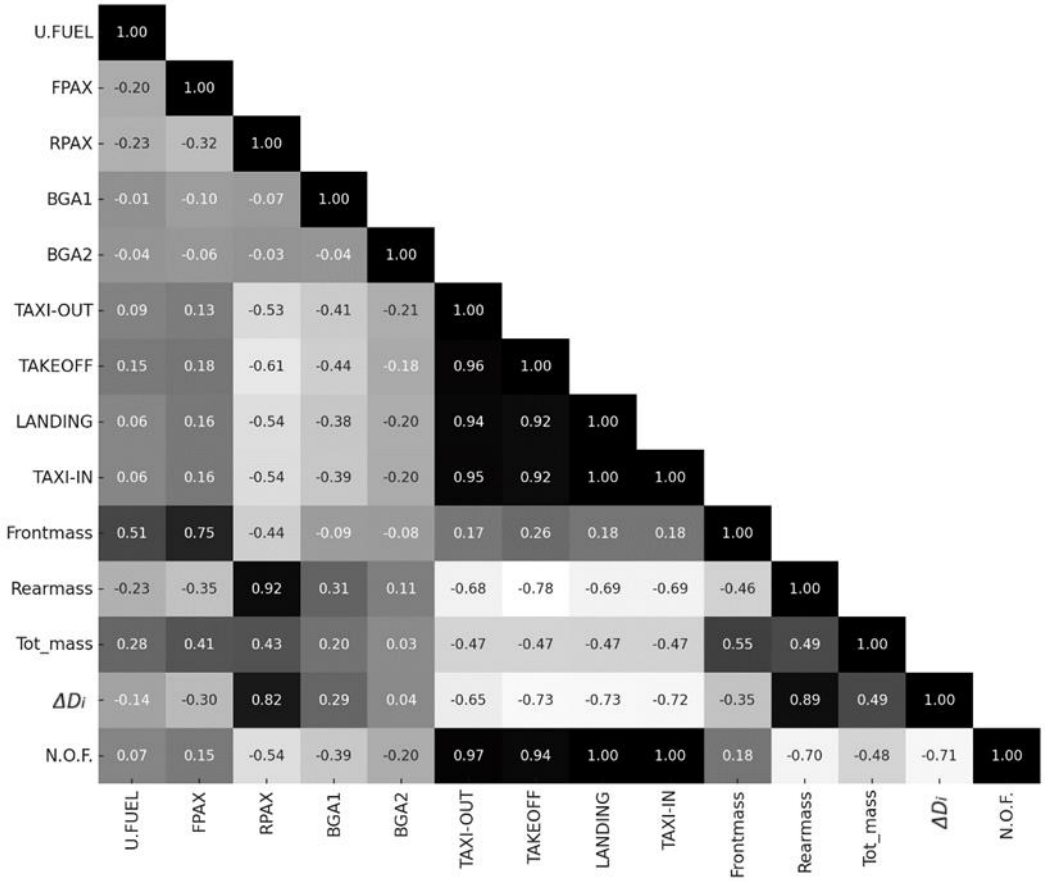

Figure 92. Correlation matrix heatmap with correlation coefficients of RUL relevant variables.

The heatmap of the correlation matrix provides a source of potentially valuable insights. Strong positive correlations were observed between the:

- **Rearmass and damage increment**: The *Rearmass* variable represents the sum of the masses in three mass stations, namely the *RPAX*, *BGA1* and *BGA2*. A strong positive correlation between the *Rearmass* and the calculated damage increment bolsters the conclusion that the distribution of mass at the rear of the aircraft has a significant impact on the fatigue damage accumulation.

Moderate Negative Correlations were observed between the:

- **Frontmass and damage increment**: The *Frontmass* variable represents the sum of the masses in two mass stations, namely *U.FUEL* and *RPAX*. The moderate negative correlation between the *Frontmass* and the damage increment highlights

the inverse relationship between these variables. Further research could be done on how redistributing mass towards the front might mitigate damage accumulation, and thus, extend the observed parts *RUL*.

6.3.2 Regression analysis

To perform regression analysis, the dependent variable and independent variables had to be determined first. It was decided they were as follows:

Dependent variable – Damage increment

Independent variables – Mass and mass distribution, according to the predetermined mass intensities described in Chapter 5.3.4.3, and mass distribution determined by the airplane manufacturer.

Table 23. Regression analysis statistics.

Regression Statistics	
Multiple R	0.87233
R Square	0.76096
Adjusted R Square	0.7521
Standard Error	1.3E-6
Observations	141

The regression analysis statistics represent the following:

Multiple R: This is the correlation coefficient. It measures the strength and direction of the linear relationship between the dependent variable and the independent variables. It ranges from -1 to 1. A value of 0.87233 indicates a very strong positive correlation. This was expected since the dependent variable was determined by applying numerical strength calculation on load vector values based on the independent variables (U.FUEL, FPAX, RPAX, BGA1 and BGA2).

R Square: This is the coefficient of determination. It measures the proportion of the variance in the dependent variable that can be predicted from the independent variable(s). A value of 0.76096 means that approximately 76 % of the variance in the dependent variable can be explained by the independent variables in the model. This is a very high value, suggesting a good fit of the model, which is congruent with expectations since the dependent variable was determined by numerical strength analysis based on impact of the independent variables on the load acting on the landing gear strut.

Adjusted R Square: This is a modified version of R-squared that has been adjusted for the number of predictors in the model. It incorporates the model's degrees of freedom. The adjusted R-squared increases only if the new term improves the model more than would be expected by chance. It decreases when a predictor improves the model by less than expected by

chance. The adjusted R-squared can be negative, but it's usually not. It is always lower than the R-squared. In the case of the observed data, the value is 0.7521.

Standard Error: This measures the accuracy of predictions. In regression analysis, the standard error of the model is the standard deviation of the residuals (the difference between the observed and predicted values). A lower standard error indicates a better fit of the model. In the case of the observed data, the standard error is very small (1.3E-6), suggesting that the model's predictions are quite accurate, again this was expected since the dependent and independent variables have a direct numerical co-dependence.

Observations: This is the number of data points used in the regression analysis. In the case of this research, there were 564 observations used (not counting 141 observations made for the Flight phase, which were not included in observation since they all have a *RUL* above the observed threshold).

Overall, these statistics suggest that the regression model has a very good fit to the data, with the independent variables explaining a large proportion of the variance in the dependent variable, and the model's predictions being quite accurate.

Next, analysis of variance was performed. The purpose of the analysis was to understand the existence and overall effect of mass value and distribution on the accumulated fatigue damage in the light airplane landing gear strut, and which specific levels of these factors have the highest impact. The ANOVA (Analysis of Variance) table (Table 24) is used in regression analysis to determine the significance of the model.

Table 24. Analysis of variance results.

ANOVA					
	df	*SS*	*MS*	*F*	*Significance F*
Regression	5	7.49971E-10	1.49994E-10	85.95	3.19536E-40
Residual	135	2.35593E-10	1.74513E-12		
Total	140	9.85563E-10			

df (Degrees of Freedom): This is the number of values in the final calculation of a statistic that are free to vary. In the subject table, the regression has 5 degrees of freedom, which likely corresponds to the number of predictors in the regression model. The residuals have 135 degrees of freedom, which is the number of observations (141) minus the number of predictors (5) minus 1. The total degrees of freedom are 141, which is the number of observations minus 1.

SS (Sum of Squares): This is the sum of the squared differences between each observation and its group's mean. It can be thought of as the spread of the observed data around the mean. The regression sum of squares (7.49971E-10) is the sum of the squared differences between the

predicted values and the mean of the dependent variable. The residual sum of squares (2.35593E-10) is the sum of the squared differences between the observed and predicted values. The total sum of squares (9.85563E-10) is the sum of the regression and residual sums of squares.

MS (Mean Square): This is the average of the sum of squares. The regression mean square is the regression sum of squares divided by its degrees of freedom (1.49994E-10). The residual mean square is the residual sum of squares divided by its degrees of freedom (1.74513E-12).

F (F-statistic): This statistic is used to compare the model fit of the model to that of a model with no predictors. It is calculated as the ratio of the regression mean square to the residual mean square (85.95). A larger F-statistic indicates a more significant model.

Significance F (p-value): This is the probability that the null hypothesis (that the model with no predictors fits the data as well as the model) is true. A smaller p-value indicates a more significant model. In the case of the observed data, the p-value is extremely small (3.19536E-40), indicating that the regression model is highly significant.

Overall, the ANOVA table suggests that the regression model is highly significant and explains a large portion of the variance in the dependent variable. Thus, it was concluded that the created regression model is a viable candidate for *RUL* prediction.

6.3.3 Sensitivity analysis and impact on maintenance and operational safety

The performed sensitivity analysis revealed the impact of loads partially resulting from masses in the airplane's mass stations. Two main impact variables were determined, mass and mass distance from the observed structural part. Based on the stated impact variables, impact hierarchies were created, as presented in Figure 93 and Figure 94.

From Figure 92 the impact of mass value and distribution on the observed main landing gear strut *RUL* becomes evident for various flight phases and mass distribution scenarios. An impact hierarchy of the influence of mass distribution on strut *RUL* can be established based on correlation coefficient values, given in Figure 92, and , Table 22.

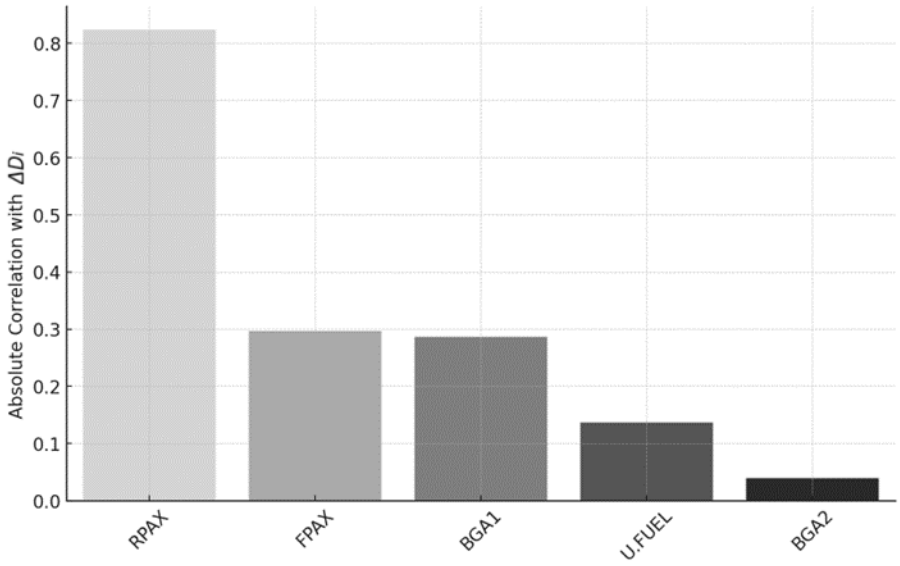

Figure 93. U.FUEL, FPAX, RPAX, BGA1 and BGA2 impact on main landing gear strut fatigue damage accumulation.

Figure 93 displays the impact of mass distribution on fatigue damage accumulation in the main landing gear strut.

- The *RPAX* variable has the greatest impact on the observed main landing gear strut fatigue life, as expected.

- *FPAX* has the second highest impact on fatigue damage accumulation, this was also expected since the mass loaded in this mass station is similar to *RPAX* (actually even higher), however *FPAX* is farther away from the observed landing gear strut, thus highlighting the importance of the distance from the observed part. It is also noteworthy that *FPAX* has a negative correlation coefficient, meaning that an increase in mass in this mass station has a beneficial effect on strut *RUL*, due to reasons related to the distance of this mass station from the observed strut, and mass station restrictions, as discussed in Chapter 6.3.1.

- *BGA1* has the third greatest impact due to the small mass allowed in this station and its distance form the observed strut.

- *U.FUEL* is the second variable having a negative correlation coefficient with *Dam_incr_i*, for reasons related to its distance from the observed strut, as discussed in more detail in Chapter 6.3.1. Additionally, it is worth noting that the position of this mass station is in vicinity of the front landing gear, thereby additionally reducing its impact on main landing gear strut fatigue life and creating a momentum

around the airplane's centre of gravity which has an impact on the load acting on the observed main strut.

- *BGA2* has the smallest impact on main landing gear strut damage accumulation, again due to the small mass allowed in this station, as well as its distance form the strut.

Another hierarchy can be observed based on the correlation coefficients of the flight phases and the ΔD_i,

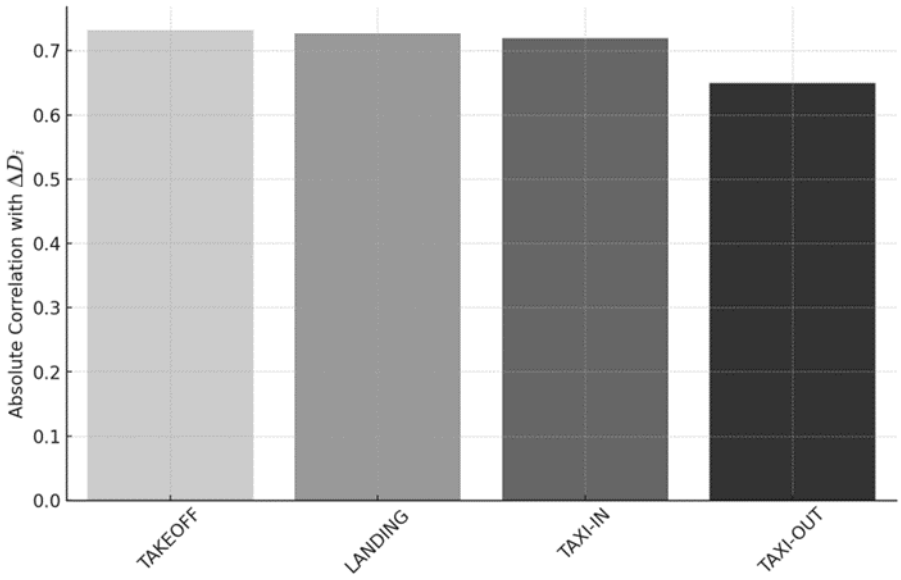

Figure 94. TAXI-OUT, TAKEOFF, LANDING and TAXI-IN impact on main landing gear strut fatigue damage accumulation.

Figure 94 shows that the absolute correlation with the damage increment decreases progressively from TAKEOFF to TAXI-OUT. The damage increment is least correlated with the TAXI-OUT phase and most correlated with the TAKEOFF phase. This suggests that the TAKEOFF phase has the least number of unconsidered factors influencing fatigue life. On the other hand, the TAXI-OUT phase has the most unconsidered factors influencing fatigue life.

A visualization of the relation between the calculated damage increments for various mass value and distribution scenarios is presented in Figure 95. The damage increments were sorted from lowest to highest. A redistribution of the mass value and distribution scenarios had to be undertaken to create the figure, the reason as mentioned prior is because the scenarios were initially sorted from lowest to highest airplane total mass. However, numerical strength analysis and subsequent sensitivity analysis revealed the degree to which the resulting damage increment depends on mass distribution as well.

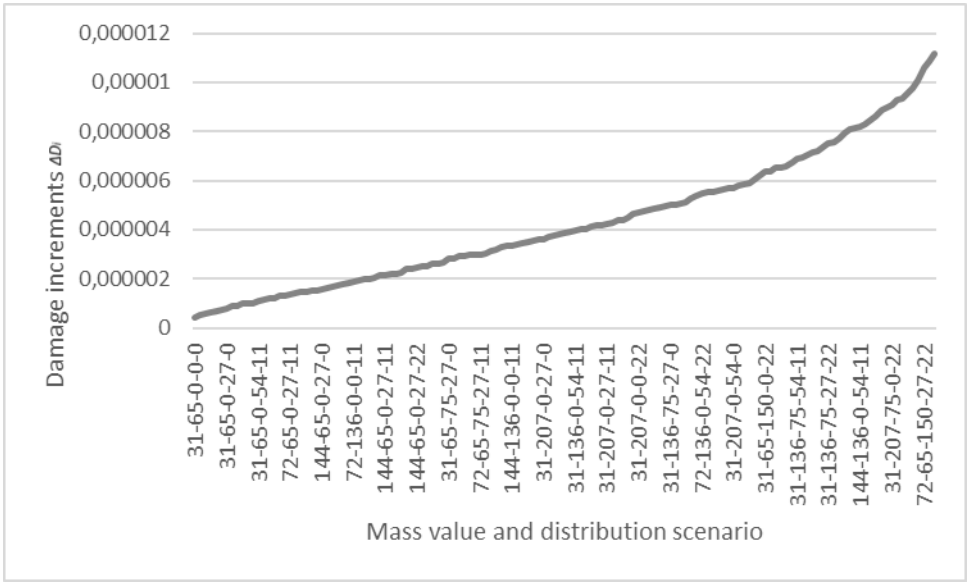

Figure 95. The relation between the damage increment and mass value and distribution scenario, sorted by increasing the damage increment.

The number of operations until fatigue failure was also observed. Here, as expected, the number of operations decrease with an increase in aircraft total mass (variable *Tot_mass).* Deviations from this observation are visible and they are a consequence of mass distribution or, in other words, the position of the airplanes centre of gravity relative to the position of the main landing gear strut.

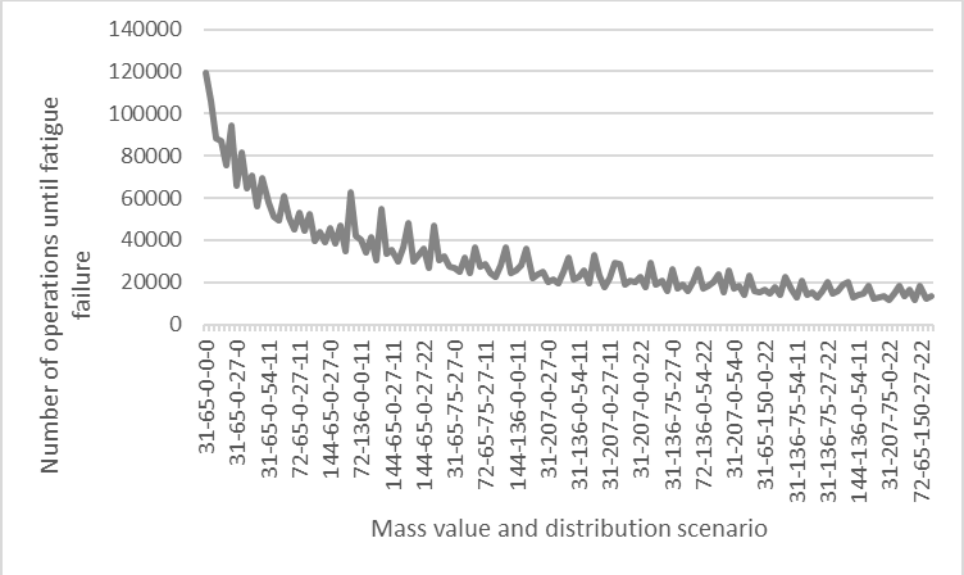

Figure 96. The relation between the number of operations until fatigue failure, and mass intensity and distribution scenarios.

In Figure 96 the relation between the number of operations until fatigue failure, and various mass intensity and distribution scenarios is presented. It can be seen that the decrease of number of operations is exponential towards mass value and distribution scenarios with ta higher total

mass. Again, oscillations can be observed, highlighting the importance of the distance between the centre of gravity and the observed main landing gear strut.

Figure 95 displays a non-linear relationship between the mass value and distribution scenarios and the resulting damage increments. However, given the stated uncertainties affecting *RUL* prediction, a linear relationship assumption by applying the created linear regression model has a significant probability of producing acceptable results. The following conclusions can be made based on the displayed data relation alone:

- Increasing mass: The data shows a clear trend of increasing fatigue damage increment with increasing mass acting on the light airplane landing gear strut. For the same mass distribution scenario, a larger mass generally leads to a higher fatigue damage increment. This suggests that as the mass acting on the observed strut increases so does stress, leading to higher rates of fatigue damage.
- Impact of distribution scenarios: Different distribution scenarios present varying levels of fatigue damage increments. The trend shows that as the complexity of the distribution increases (i.e., more numbers in the distribution scenario are non-zero), the fatigue damage increment tends to increase. This suggests that a more even distribution of mass may lead to less fatigue, while a highly concentrated mass distribution tends to increase the rate of fatigue damage. More precisely, by decreasing the mass in the last three numbers of the mass value and distribution scenario, the fatigue damage increment accumulated in the observed strut decreases due to mass distribution. However, taking a binary-perspective of this occurrence by reducing the first two numbers to zero (*U.FUEL* and *FPAX*) would make no sense, since this would indicate there is no pilot and no fuel in the airplane.
- Scenario impact on *RUL*: The impact of different scenarios on the Remaining Useful Life of the landing gear struts is noticeable. Scenarios with lower mass and mass simpler mass distributions have significantly higher *RUL*s than those with higher mass and mass more complex distributions. For instance, the scenario with the minimum calculated fatigue damage increment (31-65-0-0-0) results in a significantly higher *RUL* than the scenario with the maximum calculated fatigue damage increment (31-207-75-27-11). This trend highlights the importance of careful planning and management of mass value and distribution not only to ensure airplane stability during operation but also to maximize the *RUL* of the landing gear struts, both contributing to operation safety.

Now that the impact of mass value and distribution on fatigue damage accumulation has been discussed, it becomes clear that the generally accepted simplistic maintenance standard for light aircraft landing gear structural parts neglects the relation of fatigue damage accumulation and airplane mass and mass distribution. As shown, various operations lead to vastly different part fatigue lives, strongly influencing the observed part remaining useful life as the established primary mechanical integrity deterioration mechanism.

6.4 Prediction uncertainty

To identify parameters affecting light aircraft landing gear structure remaining useful life prediction uncertainty, the landing gear structure deterioration mechanism must be determined first. Based on literature review findings presented in Chapter 2 of this research, material fatigue was concluded not only to be the primary deterioration mechanism, but also the primary accident cause originating from light aircraft landing gear failure, provided the observed case was not caused by structural overload, such as a hard landing. Generally, fatigue life affecting parameters for light aircraft metal landing gear parts are:

- **Material properties**: The material properties of the landing gear such as strength, hardness, toughness, and ductility can significantly influence fatigue life. Different metals and alloys have different resistance to fatigue. As explained in Chapter 5.2.1, differences between the mechanical properties of the model, being a consequence of unknown heat treatment, are existent but mitigated. The differences were deemed acceptable based on the expected result deviation from actual landing gear fatigue failure, based on other uncertainty relevant factors described in this Chapter.
- **Loading conditions**: Cyclic loads experienced by the landing gear, such as those due to take-off, landing, and taxiing, can lead to material fatigue accumulation. The magnitude, frequency, and type of these loads (tensile, compressive, or shear) can affect the fatigue life of the observed part or structure and are a consequence of unpredictable operation conditions. The loads applied in the numerical strength analysis were simplified to enable fatigue life analyses. The simplifications related to fatigue relevant load intensity, direction, orientation, and variability were described in the respective Chapter, 5.2.1.
- **Surface conditions**: The surface condition affecting the landing gear, including surface roughness, type such as asphalt or grass, and other can influence fatigue damage accumulation. Those surface conditions were applied in the Analyses

described in this Thesis through measured acceleration in each operation phase, as described in Chapter 5.2.1.

- **Corrosion**: Corrosion can significantly reduce the fatigue life of landing gear parts, especially when the aircraft operates in a corrosive environment such as near the sea. Corrosion can lead to pitting, which can act as a stress concentrator initiating fatigue cracks. Corrosion impact on fatigue life was not observed in the research leading up to this Thesis.
- **Temperature**: High or low temperatures can affect the material properties and thereby influence the landing gear structures fatigue life. The impact of temperature variability on fatigue life was not observed in the research leading up to this Thesis.
- **Maintenance practices**: Proper maintenance, including regular inspection for cracks and other signs of fatigue can significantly impact operation safety. Part replacement in the observed Cessna 172R is mandatory if corrosion or cracks are detected by pre-flight or planned inspection.
- **Design factors**: The design of the landing gear, including its geometry and the thickness of different parts, can affect the stress distribution and hence the fatigue life. For example, sharp corners or notches can act as stress concentrators and reduce the fatigue life of the light aircraft landing gear structure.
- **Manufacturing processes**: The manufacturing processes used to produce the landing gear structure, including forging, machining, welding, and heat treating (depending on the specific structure under observation) can introduce residual stresses or defects that can influence structural fatigue life.
- **Aircraft operation**: The way the aircraft is operated can also affect the fatigue life of the landing gear structure. Hard landings or rapid manoeuvres can introduce high loads that lead to accelerated fatigue damage accumulation. Aircraft operation variations were not considered in this research, due to a lack of data.
- **Environmental factors**: Environmental conditions such as humidity, temperature, and air pressure can also influence the fatigue life by affecting material properties and corrosion rates, although the scale of this influence is usually lesser than previous influence sources. Oscillations in environmental conditions were not observed in the research leading up to this Thesis.

The listed factors can interact in complex ways, thereby influencing the fatigue life of light aircraft landing gear structure and/or its parts.

The correlation between these factors affecting the fatigue life of a light aircraft's landing gear structures can be quite complex, as they can interact with each other in numerous ways, and their impacts can be cumulative or multiplicative. The following can be considered an attempt to describe some of these interactions:

- **Material properties and loading conditions**: The response of a material to loading conditions depends on its properties. Materials with beneficial properties for fatigue resistance might resist the initiation of cracks better, but once cracks start, they could propagate rapidly due to lower ductility.
- **Material properties and temperature**: Material properties can change with temperature. For example, metals can become more brittle at low temperatures, which can increase their susceptibility to fatigue.
- **Surface conditions and loading conditions**: Rough surfaces or surfaces with defects can concentrate stress, and the effect is more pronounced under high loads. Surface treatments can improve fatigue life by introducing beneficial residual stresses that counteract the applied loads.
- **Corrosion and environmental factors**: Environmental factors like humidity, temperature, and the presence of corrosive substances can accelerate corrosion, which can in turn increase the susceptibility of the material to fatigue.
- **Maintenance practices and all factors**: Proper maintenance can mitigate the effects of all the other factors on landing gear structure remaining useful life in general. For example, regular inspections can detect cracks or corrosion early, and corrective actions can be taken before they lead to failure.
- **Design factors and loading conditions**: The design of the landing gear structure affects how loads are distributed. If the design leads to stress concentrations, it can increase the susceptibility of the landing gear structure to fatigue damage accumulation.
- **Manufacturing processes and material properties**: The manufacturing processes can affect the material properties. For example, heat treating can increase the strength and hardness of the material, but it might also make it more brittle.
- **Aircraft operation and loading conditions**: The way the aircraft is operated affects the loading conditions. Hard landings or rapid manoeuvres can introduce high loads, significantly impacting fatigue damage accumulation, or even lead to structural overload and immediate failure.

Predicting the remaining useful life of light aircraft landing gear structural parts is a complex process, dependent on various factors and the specific situation. To ensure high prediction accuracy, detailed analysis and advanced methods that account for all these factors are necessary. However, acquiring the necessary information can be a challenge, especially for light aircraft. This difficulty could arise due to various reasons, including manufacturing policies or a lack of necessary sensors common in light aircraft. Additionally, it's often not feasible to predict how these factors correlate with the part's lifespan using available methods. Given these constraints, compromises become inevitable. This research is based on one such compromise: the hypothesis that remaining useful life of landing gear structural parts can be predicted without relying on sensor data. The objective is to reach a satisfactory level of prediction accuracy that would contribute to operational safety enhancement.

After highlighting the parameters that could affect the determined light aircraft landing gear structure remaining useful life, the reasons affecting those parameters, being *RUL* prediction uncertainty sources, can be identified. The following parameters could potentially contribute to the uncertainty in predicting the remaining useful life of a light aircraft's landing gear structure:

- **Measurement errors**: Any inaccuracies or variability in measurements of factors such as stress levels, temperatures, load frequencies, and other operational parameters can introduce uncertainty. Errors in detecting and measuring any existing damage or fatigue cracks can also contribute to uncertainty.
- **Material property variations**: Variations in material properties can introduce significant uncertainty. These can include variations in the inherent material properties (strength, ductility, toughness, etc.) due to manufacturing variability or changes in these properties over time due to factors such as corrosion, wear, or exposure to high temperatures. For example, the *RUL* prediction method described in this Thesis was applied to the same material (6150 steel), but with a less beneficial heat treatment resulting in calculated *RUL*'s that were an order of magnitude smaller than the ones displayed in this Thesis. For some loading cases the resulting stresses were higher than the materials ultimate strength, which was the main reason why a material was chosen that had a heat treatment with significant beneficial effects on material properties.
- **Uncertainties in operational conditions**: Variability in how the aircraft is operated introduces uncertainty. This can include variability in loadings (due to variations in

flight conditions, landing conditions, etc.), environmental conditions (temperature, humidity, etc.), and maintenance practices.

- **Modelling deviations**: Simplifications in the models used to predict fatigue life can contribute to *RUL* prediction uncertainty. These can include simplifications in the stress analysis, assumptions about the fatigue crack propagation mechanisms, and assumptions about the loading conditions.
- **Uncertainty in damage initiation and propagation**: The initiation and propagation of fatigue damage can be influenced by many factors and can be somewhat random. This can introduce uncertainty in the predictions of light aircraft landing gear structure remaining useful lives.
- **Maintenance and inspection data**: The accuracy and completeness of maintenance and inspection data can impact the prediction of remaining useful life. Missing or inaccurate data can introduce uncertainty.
- **Manufacturing inconsistencies**: Differences between individual parts due to manufacturing processes can introduce variability in the actual performance of the parts, leading to uncertainty in life prediction.
- **Unexpected events**: Unforeseen events like hard landings or environmental extremes can introduce additional stresses that are not accounted for in the prediction models, increasing uncertainty.

Each of these uncertainty sources can contribute to the overall *RUL* prediction error, of the landing gear structure. Identifying and quantifying their impacts can help improve the reliability and accuracy of the predictions. This could be one of the directions of future research as a continuation of subject method development, by including some of the stated influences in *RUL* prediction.

7 CONCLUSION AND FUTURE WORK

The findings, contributions, implications, limitations, and potential future research directions are highlighted and discussed in this Chapter. The prime focus of this Thesis was to document the innovation of a methodology for predicting the Remaining Useful Life of light aircraft landing gear structures, specifically, under recorded operational circumstances. In this thesis, the existing *RUL* prediction methods were evaluated, vital data on light aircraft usage was collected, and the representative load profiles were determined. In this concluding Chapter, a review of main research outcomes, broader implications for the current maintenance standard, potential limitations, and prospective directions for future research are assessed.

7.1 Summary of Research Findings

The main objective of this research was to develop a method for predicting the remaining useful life of light aircraft landing gear structures based on actual operating conditions. The research identified a significant gap in current light aircraft landing gear structural part maintenance standard, being condition monitoring and part replacement on condition, and actual structure deterioration due to regular use. Remaining useful life prediction was established as a developmental focal point for operation safety increase. In this light, a critical review of current *RUL* prediction methods was conducted, highlighting their relation to aircraft maintenance and applicable regulations. Data on light aircraft usage was collected, and characteristic load profiles were identified. A computational model was created for numerical strength analysis of the part under research, and a method for predicting the remaining useful life was developed. A method application example was performed revealing its significance for light aircraft landing gear structure maintenance.

7.2 Main Contributions

The expected contributions of this research were:

- Defining the parameters that describe the type of aeronautical operation and affect the prediction of the remaining useful life of a light aircraft's landing gear structure.

This doctoral Thesis has successfully accomplished its expected scientific contribution of defining the parameters that characterize different aeronautical operations and influence the prediction of the remaining useful life of a light aircraft's landing gear main load bearing structural part and therefore structure. It has identified and quantified various factors, including but not limited to the observed parts remaining useful life relevant load intensity, direction, and

orientation, as well as light aircraft operational phases that contribute to part failure. By characterizing these parameters, this Thesis has deepened the understanding of the light aircraft's landing gear structure remaining useful life under fatigue relevant loads.

- Developing a method for predicting the remaining useful life of a light aircraft's landing gear structure according to the types of aeronautical operations.

This scientific contribution has been successfully met through the developed method for remaining useful life prediction of a light aircraft's landing gear structure, contingent on the various types of aeronautical operations. This method draws on the parameters defined in the first contribution and integrates them into a computational model using software tools. As a result of this approach, a method for estimating the remaining useful life of a light aircraft's landing gear structures without the input of additional operational conditions, for example through sensor measurements, was established. This development marks the introduction of a preventative maintenance possibility into light aircraft maintenance planning, since at the moment of writing this Thesis light aircraft maintenance does not include any kind of remaining useful life prediction procedures.

- Identifying the parameters that affect the uncertainty of predicting the remaining useful life of a light aircraft's landing gear structure.

The anticipated scientific contribution of identifying the parameters that contribute to the uncertainty in predicting the remaining useful life of a light aircraft's landing gear structure has been effectively achieved within this Thesis. These parameters, potentially encompassing measurement errors, variations in material properties, and uncertainties within operational conditions, were examined and their impact on prediction uncertainty was quantified.

Additionally, this Thesis displays applicative contributions of the developed method. The applicative contributions are:

- The possibility of predicting the remaining useful life of any Cessna 172R or Cessna 172N main landing gear strut, provided the strut has the same geometry and mechanical properties, and the main deterioration mechanism is material fatigue.
- The possibility of method application to any structural part, be it of aeronautical or other origin, provided the part CAD model and load model for fatigue analysis are created, and the main deterioration mechanism of the observed part is metal material fatigue.

7.3 Implications for the current standard in light aircraft landing gear structure maintenance

The current standard in light aircraft structural part maintenance is based on a reactive maintenance strategy, applying maintenance actions after certain conditions are met. The method proposed in this research could be the first step in advancing current light aircraft maintenance from a reactive to a proactive maintenance approach, namely predictive maintenance. The developed method has significant implications on aeronautical operation safety, by providing a more accurate and reliable approach to light aircraft landing gear structure maintenance. It does this by predicting the remaining useful life of structural parts, as opposed to the current maintenance standard consisting of regular visual inspection and part replacement. This method can result in improved safety and reduced maintenance costs, as it accounts for the specific usage conditions of individual aircraft. The method can also enhance the understanding of the degradation of aircraft parts and inform the design of future aircraft systems.

7.4 Limitations and Future Research Directions

This research has some limitations that could be addressed in future research. The developed method was tested using a single light aircraft landing gear structure part as an example. This fact implies the need for testing on other structural parts and other aircraft. Future studies should consider validating the developed method using other aircraft landing gear structural types and parts. In addition, method testing revealed a validation problem, being the lack of fatigue failure data. The subject data should consist of the number of operational hours, or at least the number of operations the observed part experienced before fatigue failure. Since this analysis found the observed part can perform a relatively large number of operations, the likelihood of premature fatigue failure due to damage accumulation resulting from non-recorded structural overloads increases. In the observed case, records of part failure due to regular use were not available, not only for the observed airplane, but also for two other Cessna 172N airplane's operated by the Croatian Aviation Training Centre, having the same landing gear structure. Literature research also did not result in such findings. Additionally, the impact of uncertainty sources could be mitigated by introducing damage increment impact factors, which could be applied according to additional data from the mandatory recorded operational information. For example, different damage increment impact factors could be considered for airplane operated in various environmental conditions, benefiting or mitigating material

corrosion, for example. Temperature influence could also be considered by expanding the knowledge base *RUL* matrix with various numerical strength analysis results performed for various environmental conditions. Additional acceleration samples, consisting of operational records on asphalted or other surface types, could be included in the method knowledge base, thereby permitting the prediction of *RUL*'s which vary depending on the surface conditions of arrival and departure landing strips.

One of the anticipated directions of future research is utilizing the created regression model for damage increment predictions that are not observed in the *RUL* matrix. The upper and lower boundaries for this are defined by the mass value and distribution scenarios permitted by mass and balance calculations.

Future research directions can include the development of more advanced computational models that can simulate the degradation of aircraft parts under more complex loading conditions. Future studies can also investigate the integration of the developed method into existing maintenance practices and further evaluate its impact on maintenance costs and safety.

REFERENCES

[1] R. Gouriveau, M. Kamal and Z. Noureddine , From prognostics and health systems management to predictive maintenance 1: Monitoring and prognostics, John Wiley & Sons, 2016.

[2] D. Gerhardinger, A. Domitrovic and E. Bazijanac, "Fatigue Life Prognosis of a Light Aircraft Landing Gear Leg," in *Prognostics and Health Management Annual Conference,* Nashville, 2020.

[3] Cessna Aircraft Company, 172R Pilot's operating handbook, Wichita, Kansas: Cessna Aircraft Company, 1996.

[4] F. Juretić, D. Gerhardinger, A. Domitrović and J. Ivošević, "Small Piston Engine Aircraft Vibration Measurement and Analysis," in *43th International Convention on Information, Communication and Electronic Technology (MIPRO)*, 2020.

[5] A. Abazarpoor, M. Maarefvand, S. K. Sadrnezhad and M. G. Bahrami, "Effect of thickness and heat treatment on the toughness of AISI 1045 and AISI 6150 sheet steels," Materials science and Engineering Department, Sharif university of technology, Tehran.

[6] T. Alp and A. Wazzan, "The influence of microstructure on the tensile and fatigue behavior of SAE 6150 steel," *Journal of materials engineering and performance,* pp. 351-9, 2002 Aug.

[7] R. Fragoudakis and A. Saigal , "Predicting the fatigue life in steel and glass fiber reinforced plastics using damage models," *Materials Sciences and Applications,* vol. 2, no. 6, p. 596, 2011.

[8] V. M. Gomes, S. Eck and A. De Jesus, "Cyclic Hardening and Fatigue Damage Features of 51CrV4 Steel for the Crossing Nose Design," *Applied Sciences,* vol. 13, no. 14, p. 8308, 2023.

[9] A. Kubit, M. Bucior, W. Zielecki and F. Stachowicz, "The impact of heat treatment and shot peening on the fatigue strength of 51CrV4 steel," *Procedia Structural Integrity*, vol. 2, pp. 3330-6, 2016.

[10] "AZO Materials - AISI 6150 Alloy Steel (UNS G61500)," 2012. [Online]. Available: https://www.azom.com/article.aspx?ArticleID=6744. [Accessed June 2023].

[11] "Titanium - Alloy Steel AISI 6150 | UNS# G61500," [Online]. Available: https://titanium.com/alloys/alloy-steels/alloy-steel-aisi-6150/. [Accessed July 2023].

[12] "ASTM STEEL - AISI 6150 Steel | 1.8159 | 51CrV4 | Sup10 Spring Steel," [Online]. Available: https://www.astmsteel.com/product/aisi-6150-steel/. [Accessed July 2023].

[13] Cessna Aircraft Company, *Cessna Maintenance Manual, model 172 Series, 1996 & on,* 15 ed., Wichita, Kansas: Cessna Aircraft Company, 2007.

[14] K. H. Nip , L. Gardner , C. M. Gardner and A. Y. Elghazouli , " Extremely low cycle fatigue tests on structural carbon steel and stainless steel," *Journal of constructional steel research,* vol. 66, no. 1, pp. 96-110, 2010.

[15] J. A. Cicero, F. L. Feiter and J. Mohammadi, "Statistical loads data for Cessna 172 aircraft using the Aircraft Cumulative Fatigue System (ACFS)," United States , 2001.

[16] G. S. Campbell and R. Lahey, "A survey of serious aircraft accidents involving fatigue fracture," *International Journal of Fatigue,* vol. 6, no. 1, pp. 25-3, 1984.

[17] A. J. De Voogt and R. R. van Doorn, "Sports aviation accidents - Fatality and aircraft specificity," *Aviation, space, and environmental medicine,* pp. 81(11):1033-6., 2010 November 1.

[18] B. J. Pagán , A. J. De Voogt and R. R. Van Doorn, "Ultralight aviation accident factors and latent failures: a 66-case study," *Aviation, space, and environmental medicine.,* pp. 1;77(9):950-2., 2006. September 1..

[19] Statistical Office of the European Union, “Air safety statistics in the EU,” Eurostat, [Online]. Available: https://ec.europa.eu/eurostat/statistics-explained/index.php?title=Air_safety_statistics_in_the_EU#Most_of_the_air_accident_fatalities_concerned_general_aviation. [Accessed 8 February 2022].

[20] N. L. Nelson and S. M. Goldman, “Maintenance-Related Accidents - A Comparison of Amateur-Built Aircraft to all Other General Aviation,” in *SAGE Publications*, Los Angeles, 2003.

[21] G. Li and S. P. Baker, “Correlates of pilot fatality in general aviation,” *Aviation, space, and environmental medicine,* pp. 1;70(4):305-9, 1999.

[22] T. Hsu, Y. Chang, H. Hsu, T. Chen and P. Hwang, “Predicting the remaining useful life of landing gear with prognostics and health management (PHM),” *Aerospace,* vol. 9, no. 8, p. 462, 20 Aug 2022.

[23] G. Holmes, P. Sartor, S. Reed, P. Southern, WOrden K and E. Cross, “Prediction of landing gear loads using machine learning techniques,” *Structural Health Monitoring,* vol. 15, no. 5, pp. 568-82, Sep 2016.

[24] H. El Mir and S. Perinpanayagam, “Certification of machine learning algorithms for safe-life assessment of landing gear,” *Frontiers in Astronomy and Space Sciences,* vol. 9, 15 Nov 2022.

[25] M. Imran, R. Ahmed and M. Haneef, “FE analysis for landing gear of test aircraft,” *Materials Today: Proceedings,* vol. 2, no. 4-5, pp. 2170-8, 1 Jan 2015.

[26] A. C. Gowda and N. Basha, “Linear Static and Fatigue Analysis of Nose Landing Gear for Trainer Aircraft,” *Measurement 2,* 2014.

[27] P. W. Chen, Q. Y. Sheen, H. W. Tan and T. S. Sun, “Fatigue analysis of light aircraft landing gear,” *Advanced Materials Research,* vol. 550, pp. 3092-3098, 2012.

[28] K. RV, “Stress Analysis Of The Landing Gear-Well Beams And Damage Calculation Due To Landing Cycles,” Visvesvaraya Technological University, Belgaum, 2014.

[29] J. Florance and S. Balaji, “Fatigue analysis of lug joint in the main landing gear,” *International Journal of Engineering Research,* vol. 5, no. 5, May 2016.

[30] D. Erasmus, D. Hattingh, A. Young, A. Els-Botes and M. James, “Design of a motor glider landing gear strut–The role of failure analysis in structural integrity,” *Engineering Failure Analysis,* vol. 41, pp. 30-8, 2014.

[31] L. Monaheng, W. du Preez and C. Polese, “Failure analysis of a landing gear nose wheel fork produced in Ti6Al4V (ELI) through selective laser melting,” *Engineering Failure Analysis,* vol. 153, no. 11, 2023.

[32] A. Osman and Y. Onder, “ Failure analysis of an aircraft nose landing gear piston rod end,” *Engineering Failure Analysis,* vol. 32, pp. 283-91, 2013.

[33] B. Milwitzky and F. Cook, “Analysis of landing-gear behavior,” NACA, 1952.

[34] P. Chen, S. Chang and J. SIao, “An analysis of the damage tolerance of light aircraft landing gear,” *Transactions of the Canadian Society for Mechanical Engineering,* vol. 37, no. 4, pp. 1147-59, 2013.

[35] J. McGehee and H. Carden, “Analytical investigation of the landing dynamics of a large airplane with a load-control system in the main landing gear,” NASA, 1979.

[36] R. Pires, S. Ali and A. Al-banaa, “Stress analysis on main landing gear for small aircraft,” *Al-Rafidain Engineering Journal (AREJ),* vol. 22, no. 1, 2014.

[37] A. P. Mouritz, Introduction to aerospace materials, Elsevier, Ed., Woodhead Publishing Limited, 2012 May 23..

[38] H. M. Elattar , H. K. Elminir and A. M. Riad , “Prognostics: A literature review,” *Complex & Intelligent Systems,* vol. 2, no. 2, pp. 125-154, 30 June 2016.

[39] P. C. Paris, “A rational analytic theory of fatigue,” *The Trend in Engineering,* vol. 13, pp. 9-14, 1961.

[40] P. C. Paris and F. Erdogan, "A critical analysis of crack propagation laws," *Journal of Basic Engineering,* vol. 85, no. 4, pp. 528-533, 1963.

[41] J. Gu , M. H. Azarian and M. G. Pecht, "Failure prognostics of multilayer ceramic capacitors in temperature-humidity-bias conditions," in *International conference on prognostics and health management*, Denver, 2008.

[42] J. Gu, D. Barker and M. Pecht, "Prognostics implementation of electronics under vibration loading," *Microelectronics reliability,* vol. 47, no. 12, pp. 1849-1856, 2007.

[43] T. D. Batzel and D. C. Swanson, "Prognostic health management of aircraft power generators," *IEEE Transactions on Aerospace and electronic systems,* pp. 473-482, 2009.

[44] K. S. Lok, M. J. Paul and V. Upendranath, "Prescience life of landing gear using multiaxial fatigue numerical analysis," *Procedia Engineering ,* vol. 86, pp. 775-779, 2014.

[45] A. Hess, G. Calvello and T. Dabney, "PHM a key enabler for the JSF autonomic logistics support concept," in *IEEE Aerospace Conference Proceedings (IEEE Cat. No. 04TH8720)*, 2004.

[46] W. Cui, "A state-of-the-art review on fatigue life prediction methods for metal structures," *Journal of marine science and technology,* vol. 1, no. 7, pp. 43-56, 2002 Jun.

[47] F. G. Yuan, Ed., Structural health monitoring (SHM) in aerospace structures, Woodhead Publishing, 2016.

[48] J. Schijve , "Fatigue of structures and materials in the 20th century and the state of the art," *International Journal of fatigue,* pp. 679-702, 2003.

[49] J. Insley and C. Turkoglu, "A contemporary analysis of aircraft maintenance-related accidents and serious incidents," *Aerospace,* vol. 7, no. 6, p. 81, 2020.

[50] K. Reza Kashyzadeh, K. Souri, A. Gharehsheikh Bayat , R. Safavi Jabalbarez and M. Ahmad , "Fatigue life analysis of automotive cast iron knuckle under

constant and variable amplitude loading conditions," *Applied Mechanics,* vol. 3, no. 2, pp. 517-32, 25 April 2022.

[51] H. Pan, E. Dong, Y. Jiang and P. Zhang, "Prognostic and health management for aircraft electrical power supply system," in *Proceedings of the IEEE 2012 Prognostics and System Health Management Conference*, Beijing, 2012.

[52] Ministry of Maritime Affairs, Transport and Infrastructure of the Republic of Croatia, "Narodne Novine - Pravilnik o uvjetim i načinu upotrebe sportsko rekreativnih zrakoplova," 18 March 2014. [Online]. Available: https://narodne-novine.nn.hr/clanci/sluzbeni/2014_03_34_611.html. [Accessed 9 February 2022].

[53] T. Tinga and R. Loendersloot, "Aligning PHM, SHM and CBM by understanding the physical system failure behaviour," in *European Conference on the Prognostics and Health Management Society,* 2014.

[54] V. Fornlöf , D. Galar , A. Syberfeldt and T. Almgren , "Aircraft engines: A maintenance trade-off in a complex system," in *International Conference on Quality, Reliability and Infocom Technology*, 2015.

[55] A. Saxena, J. Celaya, B. Saha , S. Saha and K. Goebel, "Metrics for offline evaluation of prognostic performance," *International Journal of Prognostics and Health Management,* vol. 1, no. 1, pp. 4-23, 2010.

[56] K. M. Janasak and R. R. Beshears, "Diagnostics to Prognostics-A product availability technology evolution," *2007 Annual Reliability and Maintainability Symposium,* pp. 113-118, 22 Jannuary 2007.

[57] Department of Defense, "Operation of the Defense Acquisition System," Department of Defense, 2013.

[58] N. H. Kim, D. An and J. H. Choi, Prognostics and Health Management of Engineering Systems, Cham: Springer, 2017.

[59] K. Goebel, D. Matthew , A. Saxena, S. Sankararaman, I. Roychoudhury and J. Celaya, Prognostics: The science of making predictions, 2017.

[60] K. Chakraborty , K. Mehrotra , C.-K. Mohan and S. Ranka , “Forecasting the behavior of multivariate time series using neural networks,” School of Computer and Information Science Syracuse University, Syracuse, 1992 Nov 1.

[61] F. Ahmadzadeh and J. Lundberg , “Remaining useful life prediction of grinding mill liners using,” *Minerals Engineering,* vol. 53, pp. 1-8, 2013 Nov.

[62] D. Li, W. Wang and F. Ismail, “Enhanced fuzzy-filtered neural networks for material fatigue prognosis,” *Applied Soft Computing,* vol. 13, no. 1, pp. 283-291, 2013 January.

[63] E. Zio and F. Di Maio, “A data-driven fuzzy approach for predicting the remaining useful life in dynamic failure scenarios of a nuclear system,” *Reliability Engineering & System Safety,* vol. 95, no. 1, pp. 49-57, 2010.

[64] R. E. Silva, R. Gouriveau, S. Jemei, D. Hissel, L. Boulon, K. Agbossou and N. Y. Steiner, “Proton exchange membrane fuel cell degradation prediction based on adaptive neuro-fuzzy inference systems,” *International Journal of Hydrogen Energy,* vol. 39, no. 21, pp. 11128-11144, 2014 July.

[65] D. J. MacKay, “Introduction to Gaussian processes,” NATO ASI Series F Computer and Systems Sciences, Cambridge, 1998 June.

[66] M. Seeger, “Gaussian processes for machine learning,” *International Journal of Neural Systems,* vol. 14, no. 2, pp. 69-106, 2004 April.

[67] M. E. Tipping, “Sparse Bayesian learning and the relevance vector machine,” *Journal of machine learning research,* pp. 211-244, 2001.

[68] T. Benkedjouh , K. Medjaher , N. Zerhouni and S. Rechak , “Health assessment and life prediction of cutting tools based on support vector regression,” *Journal of Intelligent Manufacturing,* vol. 26, no. 2, pp. 213-223, 2015 April.

[69] O. Bretscher , Linear algebra with applications, New Jersey: Prentice Hall, 1995.

[70] A. Coppe , R.-T. Haftka and N.-H. Kim , "Uncertainty identification of damage growth parameters using nonlinear regression," *AIAA Journal,* vol. 12, pp. 2818-2821, 2011 December.

[71] M. D. Pandey and J. M. Noortwijk, "Gamma process model for time-dependent structural," in *Paper presented at the second international conference on bridge maintenance, safety and management*, Kyoto, 2004.

[72] X. S. Si, W. Wang and C. H. Hu, "A Wiener process-based degradation model with a recursive," *Mech Syst Signal Process,* vol. 35, pp. 219-237, 2013.

[73] A. Liu, M. Dong and Y. Peng, "A novel method for online health prognosis of equipment based on," *Mech Syst Signal Process,* pp. 331-348, 2012.

[74] X. S. Si, W. Wang and C. H. Hu, "Remaining useful life estimation—a review on the statistical," *Eur J Oper Res,* pp. 1-14, 2011.

[75] P. Zhang , "Model selection via multifold cross validation," *The Annals of Statistics,* pp. 299-313, 1993.

[76] D. M. Hawkins, "The problem of overfitting," *J Chem Inf Comput Sci,* vol. 44, no. 1, pp. 1-12, 2004.

[77] M. Daigle , I. Roychoudhury , S. Narasimhan , S. Saha , B. Saha and K. Goebel , "Investigating the effect of damage progression model choice on prognostics performance," in *Annual Conference of the Prognostics and Health Society*, Montreal, 2011.

[78] B. P. Zeigler, T. G. Kim and H. Praehofer, Theory of modeling and simulation, Academic press, 2000.

[79] F. K. Frantz , "A taxonomy of model abstraction techniques," in *Proceedings of the 27th conference on Winter simulation,* 1995.

[80] K. Lee and P. A. Fishwick, "Dynamic model abstraction," in *Proceedings Winter Simulation Conference*, 1995.

[81] J. T. Oden, E. E. Prudencio and P. T. Bauman, "Virtual model validation of complex multiscale systems: Applications to nonlinear elastostatics," *Computer Methods in Applied Mechanics and Engineering,* vol. 266, pp. 162-184, 2013 Nov.

[82] R. Rebba, S. Mahadevan and S. Huang, "Validation and error estimation of computational models," *Reliability Engineering & System Safety,* vol. 91, no. 10-11, pp. 1390-1397, 2006.

[83] R. G. Sargent, "Verification and validation of simulation models," in *2010 Winter Simulation Conference,* 2010.

[84] Y. Ling and S. Mahadevan , "Quantitative model validation techniques: New insights," *Reliability Engineering & System Safety,* vol. 111, pp. 217-231, 2013.

[85] A. Coppe, M. J. Pais, R. T. Haftka and N. H. Kim, "Using a simple crack growth model in predicting remaining useful life," *Journal of Aircraft,* vol. 6, no. 49, pp. 1965-1973, 2012.

[86] H. Hanachi , J. Liu , A. Banerjee , Y. Chen and A. Koul , "A physics-based modeling approach for performance monitoring in gas turbine engines," *IEEE Transactions on Reliability,* vol. 64, no. 1, pp. 197-205, March 2015.

[87] T. Shen, F. Wan, W. Cui and B. Song, "Application of prognostic and health management technology on aircraft fuel system," *2010 Prognostics and System Health Management Conference,* pp. 1-7, 12 January 2010.

[88] J. N. Rozak and J. P. Cycon, "Aircraft health and usage monitoring system with comparative fleet statistics". United States Patent US 7,984,146., 19 July 2011.

[89] E.-R. Brown , N.-N. McCollom , E.-E. Moore and A. Hess , "Prognostics and health management a data-driven approach to supporting the F-35 lightning II," in *2007 IEEE Aerospace Conference,* 2007.

[90] P. H. Barton, "Prognostics for combat systems of the future," *IEEE Instrumentation & Measurement Magazine,* vol. 10, no. 4, pp. 10-14, 2007.

[91] N.-N. McCollom and E.-R. Brown , "PHM on the F-35 fighter," in *2011 IEEE Conference on Prognostics and Health Management*, Montreal, 2011.

[92] Y. G. Li and P. Nilkitsaranont, "Gas path prognostic analysis for an industrial gas turbine," *Insight - Non-Destructive Testing and Condition Monitoring*, vol. 50, no. 8, pp. 428-435(8), 2008.

[93] J. S. Gupta , C. Trinquier , K. Medjaher and N. Zerhouni , "Continuous validation of the PHM function in aircraft industry," in *2015 First International Conference on Reliability Systems Engineering (ICRSE)*, Beijing, 2015.

[94] B. Sun, S. Zeng, R. Kang and M. G. Pecht, "Benefits and challenges of system prognostics," *IEEE Transactions on Reliability*, vol. 61, no. 2, pp. 323-335, 2012.

[95] S. Marble and D. Tow , "Bearing health monitoring and life extension in satellite momentum/reaction wheels," in *2006 IEEE Aerospace Conference 2006*, Big Sky, 2006.

[96] B. Saha, S. Poll, K. Goebel and J. Christophersen, "An integrated approach to battery health monitoring using Bayesian regression and state estimation," in *2007 IEEE Autotestcon*, Baltimore, 2007.

[97] D. G. Luchinsky, V. V. Osipov, V. N. Smelyanskiy, D. A. Timucin and S. Uckun, "Model based IVHM system for the solid rocket booster," in *2008 IEEE Aerospace Conference*, Big Sky, 2008.

[98] A. Coppe , R.-T. Haftka , N.-H. Kim and F.-G. Yuan , "Reducing uncertainty in damage growth properties by structural health monitoring," in *Conference of the Prognostics and Health Management Society*, 2009.

[99] X. Guan , Y. Liu , A. Saxena , J. Celaya and K. Goebel, "Entropy-based probabilistic fatigue damage prognosis and algorithmic performance comparison," in *Conference of the Prognostics and Health Management Society*, 2009.

[100] B. Zhang, T. Khawaja , R. Patrick, G. Vachtsevanos, M. E. Orchard and A. Saxena, "Application of blind deconvolution denoising in failure prognosis,"

Transactions on Instrumentation and Measurement, vol. 58, no. 2, pp. 303-310, 2008.

[101] A. Grbović and B. Rašuo, "FEM based fatigue crack growth predictions for spar of light aircraft under variable amplitude loading," *Engineering Failure Analysis,* pp. 50-64, 2012.

[102] A. Grbović, G. Kastratović, A. Sedmak, K. Eldweib and S. Kirin, "Determination of optimum wing spar cross section for maximum fatigue life," *International Journal of Fatigue* , pp. 305-311, 2019.

[103] J. X. Tao, S. Smith and A. Duff, "The effect of overloading sequences on landing gear fatigue damage," *International journal of fatigue,* vol. 31, no. 11-12, pp. 1837-1847, 2009.

[104] International Civil Aviation Organization (ICAO), "Annex 6, Operation of Aircraft Part I, International Commercial Air Transport – Aeroplanes," 2010.

[105] European Union Aviation Safety Agency, "Operations in General Aviaiton," EASA, [Online]. Available: https://www.easa.europa.eu/domains/general-aviation/operations-general-aviation. [Accessed 8 February 2022].

[106] L. R. Rodrigues, J. P. Gomes, F. A. Ferri, I. P. Medeiros, R. K. Galvao and J. Cairo L Nascimento, "Use of PHM information and system architecture for optimized aircraft maintenance planning," *IEEE Systems Journal,* vol. 9, no. 4, pp. 1197-1207, 2014.

[107] X. Fei, B. Chen, J. Chi and S. Hu, "Literature review: Framework of prognostic health management for airline predictive maintenance," in *2020 Chinese Control And Decision Conference (CCDC),* 2020.

[108] Guillén, Antonio J, Crespo, Adolfo, Macchi, Marco, Gómez and Juan, "On the role of Prognostics and Health Management in advanced maintenance systems," *Production Planning & Control,* vol. 27, no. 12, pp. 991-1004, 2016.

[109] The Euroipean Parliament and of the council of 4 July 2018, "Eur-Lex Europe," [Online]. Available: https://eur-lex.europa.eu/legal-

content/EN/TXT/PDF/?uri=CELEX:32018R1139&from=EN. [Accessed 22 January 2022].

[110] European Union Aviation Safety Agency, "Commision Regulation (EU) No 800/2013," EASA, [Online]. Available: https://www.easa.europa.eu/document-library/regulations/commission-regulation-eu-no-8002013. [Accessed 8 February 2022].

[111] Ministry of Maritime Affairs, Transport and Infrastructure of the Republic of Croatia, "Pravilnik o gradnji, obnovi, održavanju i kontinuiranoj plovidbenosti zrakoplova na koje se ne primjenjuje uredba (EU) 2018/1139.," 4 12 2020. [Online]. Available: https://narodne-novine.nn.hr/clanci/sluzbeni/2020_12_134_2570.html. [Accessed 17 1 2022].

[112] Croatian Civil Aviation Agency, "Definition and types of aircraft," [Online]. Available: https://www.ccaa.hr/zrakoplov-32468. [Accessed 21 February 2022].

[113] Federal Aviation Administration Washington DC Office of Aviation Policy and Plans, "General Aviation and Air Taxi Activity Survey," 1 2 2002. [Online]. Available: https://apps.dtic.mil/sti/pdfs/ADA401777.pdf. [Accessed 14 3 2022].

[114] Federal Aviation Administration (FAA), "FAA Advisory Circular - The Ultralight Vehicle," Federal Aviation Administration, 1984.

[115] S. QI and W. ZHANG, "Prognostic and health management system based on flight data," in *The 32nd Chinese Control Conference*, 2013 Jul 26.

[116] Y. Lu, Q. Li and S. Y. Liang, "Physics-based intelligent prognosis for rolling bearing with fault feature extraction," *The International Journal of Advanced Manufacturing Technology*, no. 1, pp. 611-620, 2018.

[117] A. Babbar, V. L. Syrmos, E. M. Ortiz and M. M. Arita, "Advanced diagnostics and prognostics for engine health monitoring," in *2009 IEEE Aerospace conference*, 2009.

[118] G. Calvello, S. Olin, A. Hess and P. Frith, "PHM and corrosion control on the joint strike fighter," *Corrosion Reviews*, no. 25, pp. 5-80, 2007.

[119] Reliability - A Python library for reliability engineering, “Reliability 0.8.10 documentation,” Reliability, [Online]. Available: https://reliability.readthedocs.io/en/latest/Stress-strain%20and%20strain-life.html. [Accessed 20 June 2023].

[120] L. Zhang , B. Jiang, P. Zhang, H. Yan, X. Xu, R. Liu, J. Tang and C. Ren, “Methods for fatigue-life estimation: A review of the current status and future trends,” *Nanotechnology and Precision Engineering (NPE),* vol. 6, no. 2, 1 June 2023.

[121] S. Farfan, C. Rubio-Gonzalez, T. Cervantes-Hernandez and G. Mesmacque, “High cycle fatigue, low cycle fatigue and failure modes of a carburized steel,” *International Journal of Fatigue,* vol. 26, no. 6, pp. 673-8, June 2004.

[122] Altair Engineering Inc. , “Stress-life (SN) Approach - Altair,” 2021 . [Online]. Available: https://2021.help.altair.com/2021.1/ss/topics/simsolid/analysis/fatigue_sn_curve_r.htm.

[123] J. F. Knott , Fundamentals of fracture mechanics, Gruppo Italiano Frattura, 1973.

[124] C. H. Wang, “Introduction to fracture mechanics,” Melbourne, Australia, 1996.

[125] D. Roylance, “Introduction to fracture mechanics,” 2001.

[126] R. Browell and A. Hancq, “Calculating and displaying fatigue results,” Ansys Inc, 2006 March 29.

[127] D. M. Li, W. J. Nam and C. S. Lee, “A Strain Energy–Based Approach to the Low-Cycle Fatigue Damage Mechanism in a High-Strength Spring Steel,” *METALLURGICAL AND MATERIALS TRANSACTIONS A,* vol. 29A, pp. 1431-1439, 1998.

[128] V. T. Troshchenko and L. A. Khamaza, "Strain-life curves of steel and methods for determining the curve parameters. Part 1 conventional methods," *Strenght of Materials,* vol. 42, no. 6, pp. 647-659, 2010 December.

[129] L. Le Divenah and J. Y. Beaufils , "Large commercial aircraft loading spectra: Overview and state of the art," in *Fatigue Testing and Analysis Under Variable Amplitude Loading Conditions,* ASTM International, 2002, pp. 127-39.

[130] A. Ince and G. Glinka, "A modification of Morrow and Smith–Watson–Topper mean stress correction models," *Fatigue & Fracture of Engineering Materials & Structures,* vol. 34, no. 11, pp. 854-67, 2011.

[131] Q. Bader and E. Kadum, "Mean stress correction effects on the fatigue life behavior of steel alloys by using stress life approach theories," *International Journal of Engineering & Technology IJET-IJENS,* vol. 14, no. 4, pp. 50-58, 2014.

[132] N. E. Dowling , "Mean stress effects in stress-life and strain-life fatigue," SAE technical paper, 2004.

[133] Matthew Reid Revision, "Reliability (A Python library for reliability engineering)," Copyright 2019-2023, Matthew Reid Revision , 2020. [Online]. Available: https://reliability.readthedocs.io/en/latest/Stress-strain%20and%20strain-life.html. [Accessed 2023].

[134] Altair Engineering Inc., "Altair Engineering," Altair Engineering, 2020. [Online]. Available: https://2020.help.altair.com/2020.1/hwdesktop/altair_help/topics/solvers/os/analysis_fatigue_multiaxial_strain_life_damage_models_r.htm. [Accessed 2023].

[135] T. Łagoda, S. Vantadori, K. Głowacka, M. Kurek and K. Kluger, "Using the Smith-Watson-Topper Parameter and Its Modifications to Calculate the Fatigue Life of Metals: The State-of-the-Art," *Materials,* vol. 15, no. 10, p. 3481, 12 May 2022.

[136] D. Ion, K. Lorand, D. Mircea and M. Karoly, "The equivalent stress concept in multiaxial fatigue," *Journal of Engineering Studies and Research,* vol. 17, no. 2, pp. 53-62, 2011.

[137] S. Krscanski and J. Brnic , "Prediction of Fatigue Crack Growth in Metallic Specimens under Constant Amplitude Loading Using Virtual Crack Closure and Forman Model," *Metals,* vol. 10, no. 7, p. 977, 20 July 2020.

[138] V. Infante, L. Fernandes, M. Freitas and R. Baptista, "Failure analysis of a nose landing gear fork," *Engineering failure analysis,* no. 82, pp. 554-565, 2017 Dec. 1. .

[139] A. Rajesh and B. T. Abhay , "Design and analysis aircraft nose and nose landing gear," *Journal of Aeronautics & Aerospace Engineering,* vol. 4, no. 2, pp. 74-80, 2015.

[140] J. Wong, L. Ryan and I. Y. Kim, "Design optimization of aircraft landing gear assembly under dynamic loading," *Structural and Multidisciplinary Optimization,* vol. 57, pp. 1357-1375, 2018.

[141] A. Iadicicco , D. Natale, P. Di Palma, F. Spinaci, A. Apicella and S. Campopiano , "Strain monitoring of a composite drag strut in aircraft landing gear by fiber bragg grating sensors," *Sensors,* vol. 19, no. 10, pp. 22-39, 2019.

[142] Cleveland Wheels & Brakes, "Skyshop," Cleveland Wheels & Brakes, 2010. [Online]. Available: https://www.skyshop.com.au/landing.pdf. [Accessed 17 3 2023].

[143] M. Melchiorre and T. Duncan, "The Fundamentals of FEA Meshing for Structural Analysis," Ansys, 28 April 2021. [Online]. Available: https://www.ansys.com/blog/fundamentals-of-fea-meshing-for-structural-analysis. [Accessed 13 9 2022].

[144] Higgins, John;, "Obtaining and Optimizing Structural Analysis Convergence," 9 August 2012. [Online]. Available: https://www.researchgate.net/profile/Deeptea-M/post/In_ANSYS_Workbench_I_am_facing_problems_in_solving_a_transien

t_structural_model_Any_suggestions/attachment/59d624b679197b8077983069/AS%3A314483291951104%401451990068232/download/obtaining-and-optimizing-. [Accessed 14 9 2022].

[145] E. H. Shortliffe and B. G. Buchanan, "A Model of Inexact Reasoning in Medicine," *Mathematical Biosciences*, vol. 23, no. 3-4, pp. 351-379, 1975.

[146] J. Lee, F. Wu, W. Zhao, M. Ghaffari, L. Liao and D. Siegel, "Prognostics and health management design for rotary machinery systems—Reviews, methodology and applications," *Mechanical systems and signal processing*, vol. 42, no. 1-2, pp. 314-334, 2014.

[147] A. K. Jardine, D. Lin and D. Banjevic, "A review on machinery diagnostics and prognostics implementing condition-based maintenance," *Mechanical systems and signal processing*, vol. 20, no. 7, pp. 1483-1510, 2006.

[148] Y. Zhi-Ling, W. Bin, D. Xing-Hui and L. Hao, "Expert system of fault diagnosis for gear box in wind turbine," *Systems Engineering Procedia*, vol. 1, no. 4, pp. 189-195, 2012.

[149] S. J. Russel, Artificial Intelligence: A Modern Approach, Pearson Education, Inc. , 2010.

[150] A. H. Tsang, "Condition-based maintenance: tools and decision making," *Journal of quality in maintenance engineering*, vol. 1, no. 3, pp. 3-17, 1995.

[151] European Aviation Safety Agency, "Easy Access Rules for Normal, Utility, Aerobatic and Commuter Category Aeroplanes (CS-23) (Initial issue) Subpart C - Structure - Ground Loads," Jun 2018. [Online]. Available: https://www.easa.europa.eu/sites/default/files/dfu/CS-23%20Initial%20issue.pdf. [Accessed 22 October 2022].

[152] Croatian Aviation Training Centre (HZNS), *Aircraft Maintenance Programme Cessna 172R S/N 17280174 9A-DAD*, Zagreb: Faculty of Transport and Traffic Sciences, 2018.

[153] Z. Mingliang , “Robust Global Sensitivity Analysis for Robust Design under Parameter Uncertainty,” *Journal of Modern Mechanical Engineering and Technology,* vol. 9, pp. 50-54, 2022.

[154] R. J. Doggett, “On simple aerodynamic sensitivity derivatives for use in interdisciplinary optimization,” NASA-TM-104145, 1991 August 1. .

[155] S. Kucherenko and B. Iooss, “Derivative based global sensitivity measures,” *arXiv preprint arXiv:1412.2619,* 2014, December 8..

[156] D. D. Frey, N. Sudarsanam and J. B. Persons, “An adaptive one-factor-at-a-time method for robust parameter design: comparison with crossed arrays via case studies,” in *International Design Engineering Technical Conferences and Computers and Information in Engineering Conference*, 2006 January 1.

[157] S. Razavi and H. V. Gupta, “What do we mean by sensitivity analysis? The need for comprehensive characterization of "global" sensitivity in Earth and Environmental systems models,” *Water Resources Research,* vol. 51, no. 5, pp. 3070-92, 2015 May.

[158] C. Daniel, “One-at-a-time plans,” *Journal of the American Statistical Association,* vol. 68, no. 342, pp. 353-60, 1973 June 1.

[159] V. Czitrom, “One-factor-at-a-time versus designed experiments,” *The American Statistician,* vol. 53, no. 2, pp. 126-31, 1999 May 1.

[160] A. Saltelli, M. Ratto, T. Andres, F. Campolongo, J. Cariboni, D. Gatelli, M. Saisana and S. Tarantola, “Global sensitivity analysis: the primer,” 2008 February.

[161] M. Hekimoğlu and Y. Barlas, “Sensitivity analysis of system dynamics models by behavior pattern measures,” *Retrieved on March,* vol. 18, 2010 July.

[162] W. Shi, X. Chen and J. Shang, “An efficient Morris method-based framework for simulation factor screening,” *INFORMS Journal on Computing,* vol. 31, no. 4, pp. 745-70, 2019 October.

[163] A. M. Brown, “A step-by-step guide to non-linear regression analysis of experimental data using a Microsoft Excel spreadsheet,” *Computer Methods and Programs in Biomedicine,* vol. 65, no. 3, pp. 191-200, 2001 June 1.

[164] C. Carlberg, “Regression analysis Microsoft Excel,” Que Publishing, 2016 May 2.

[165] M. L. Orlov, “Multiple linear regression analysis using Microsoft Excel,” Chemistry Department, 1996.

[166] W. Hu, X. Jing, W. C. Henry and C. S. Bing, “Evaluation of parameter uncertainties in nonlinear regression using Microsoft Excel Spreadsheet,” *Environmental Systems Research,* vol. 4, pp. 1-12, 2015.

[167] K. J. Holzinger and H. H. Harman, “Holzinger KJ, Harman HH. Factor analysis; a synthesis of factorial methods,” 1941.

[168] A. G. Yong and S. Pearce, “A beginner’s guide to factor analysis: Focusing on exploratory factor analysis,” in *Tutorials in quantitative methods for psychology*, 2013, pp. 79-94.

[169] G. E. Box and R. D. Meyer, “An analysis for unreplicated fractional factorials,” *Technometrics,* vol. 28, no. 1, pp. 11-8, 1986 February 1.

[170] I. van de Weerd and S. Brinkkemper, “Meta-modeling for situational analysis and design methods,” in *Handbook of research on modern systems analysis and design technologies and applications*, IGI Global, 2009, pp. 35-54.

[171] T. Crestaux, O. Le Maitre and J. M. Martinez, “Polynomial chaos expansion for sensitivity analysis,” *Reliability Engineering & System Safety,* vol. 94, no. 7, pp. 1161-72, 2009 July 1.

[172] W. H. Laverty and I. W. Kelly , “Exploring the effects of assumption violations on simple linear regression and correlation using excel,” *American Journal of Theoretical and Applied Statistics,* vol. 10, no. 4, pp. 194-201, 2021.

AUTHOR BIOGRAPHY

David Gerhardinger, born on October 18, 1986, in Zagreb, has dedicated his career to aeronautics since 2001. A distinguished graduate of the Aeronautical Technical School in Zagreb in 2005, he went on to earn a Bachelor of Science degree (2012) and a Master of Science degree in Aeronautical Engineering (2014) from the Faculty of Mechanical Engineering and Naval Architecture at the University of Zagreb. He is the first Croatian Citizen to be approved by the Croatian Civil Aviation Agency as an aviation expert & work controller for oversight, support, and certification of aircraft construction, testing, modification, repair, and restoration of aircraft compliant with the Ordinance on building, restoration, maintenance, and continued airworthiness of aircraft for which Regulation (EU) 2018/1139 is not applicable. His work experience involves three years as a production manager and R&D engineer, where he managed the production of 51 two- and four-seater, retractable and fixed landing gear, fixed and variable pitch propeller airplanes. He was also responsible for the assembly of 16 turbine engine powered helicopter composite bodies, as well as several light aircraft modifications and overhaul procedures. At present, he is a teaching and research assistant and head of the Laboratory for Testing in Aeronautical Engineering at the Department for Aeronautics at the Faculty of Transport and Traffic Sciences at the University of Zagreb. Additionally, he serves as a coordinator of court expertise, where he successfully completed several court expert evaluations, at the Department for Technical-Traffic Assessment at the same Faculty. His main research interest is prognostics and health management in the maintenance of light aircraft, he published several scientific papers on the subject.